Integrin Expression in the Mouse Vestibular System

Nicole Jennie Stanley

Ear Institute

University College London

A thesis submitted for the degree of

Doctor of Philosophy

April 2013

Declaration

I, Nicole Stanley, confirm that the work presented in this thesis is my own. Where information or assistance has been derived from other sources, I confirm that this has been indicated in the thesis.

Acknowledgements

I would like to begin by thanking my supervisors Ruth and Andy for everything they have done for me as their PhD student which has culminated in the completion of this thesis. You have each always been ready to offer assistance and advice throughout my research, in so many different ways I couldn't possibly describe them all here. Ruth has been instrumental in helping me learn all I needed to know about culturing utricles. I am very grateful to have had the support of your experience during this PhD. I have also appreciated Andy's enthusiasm and encouragement – it is always good to have someone to remind you of what you have achieved, particularly when experiments are not going your way. I will miss working with you both very much indeed (and Andy is going to have to find somebody else with good hearing to test the click box on!). I wish you both, and the rest of the research group (especially Kiran who is going to carry 'integrin torch' once I have left), every success for the future. I would also like to thank Sally for her invaluable assistance with the molecular aspects of my project, since I had no real experience of this kind of lab work. Thank you for being patient and listening to all my many, many questions. An additional thank you must go to Deafness Research UK for the funding of my PhD studentship.

The faces at the Ear Institute have been ever changing throughout my time as a PhD student. I would like to thank the back office crew, especially John and Elena, for making me feel welcome right from the start. I will miss the 'in-jokes,' Capital-FM Friday dancing and carving pumpkins at Halloween a lot. Thank you to Elena for all the 'guy/relationships' talk and for accommodating me on your sofa so I could be a part of after-work fun when I wasn't living in London. John, who is forever in my debt since it was me that contained the cockroach that invaded the bathroom on our Californian adventure (although we did leave it there for the cleaners to deal with, oops!), I will miss having someone to keep me occupied during solution changes etc in the lab, and our attempts to communicate about our experiments only in bad GCSE French. I hope you have forgiven me for my less than perfect navigational skills in the US; I don't think I can blame the map for my intermittent inability to get left and right correct! There are so many other people, too many to mention individually in case I forget someone, at the institute who have been around in the lab to ask questions or a share a friendly word, plus there was never a shortage of friendly faces to sit in the atrium with for lunch or have a tea-break to commiserate another failed cloning experiment. I can

safely say that the friendliness and social nature of the people who have worked at the Ear Institute have made it the most enjoyable place to have worked at for the past 5 years.

I couldn't write these acknowledgements without thanking my incredible girls; the best group of friends that anyone could ask for. It is amazing that having met each other at secondary school (or infant school in some cases!) that we have stuck it out together through whatever personal trials and tribulations we each have had to face in our lives, as well as the good fun times – there's been 2 gorgeous weddings already during the time I've been a PhD student and I don't doubt that there's plenty more scary grown-up ness to come! Having friends like you girls has been so important in keeping me going throughout this PhD. Love you all lots.

My family have always supported me in everything I have done, this PhD being no exception. Thank you to my parents for everything you have done for me and for listening to me talk about my research successes and woes even when you really didn't have a clue what I was babbling on about. Thanks also to, 'the other one,' otherwise known as my brother, Anton – I think we have looked after each other pretty well in the last few years. Whenever I have been home and visiting family, I have always appreciated their taking an interest and asking me how my PhD was going; thank you and lots of love to you all. I hope I have made you, and those who are no longer with us and missed greatly, proud of all my achievements.

Nicole Stanley

September 2012

Abstract

The mammalian utricle has shown limited capacity for spontaneous regeneration of hair cells within a damaged sensory epithelium. *In vivo* and *in vitro* exposure of the tissue to ototoxic aminoglycosides has been utilised to induce hair cell loss, in order to study these regenerative events. The mammalian utricle is believed to regenerate hair cells by the direct transdifferentiation of supporting cells without a mitotic event. The cellular and molecular mechanisms behind this regenerative capability continue to be the subject of inner ear research.

The integrin family of cell surface receptors are known for their key role in cellular adhesion, both to the extracellular matrix and to neighbouring cells. Studies of integrins have shown that they are also involved in numerous cellular processes including proliferation, differentiation and migration. They are therefore a likely candidate for involvement in the cellular events which underlie the regenerative ability demonstrated by the mammalian utricle.

This study has identified a subset of the mammalian integrin subunits as being present in the normal adult mouse utricle. The identification of these integrins was achieved by both degenerate PCR and qPCR screening of utricular cDNA. Through immunohistochemistry, β1 and α6 have been shown to localise at the basement membrane of normal utricular tissue. Integrins β3 and β5 appear to be expressed within vestibular hair cells. Integrins β1, αV, β5, β3 and α6 are also present within the mesenchyme.

The utricular macula of adult mice was utilised as an *in vitro* model in order to induce hair cell loss by gentamicin treatment and investigate integrin expression in the utricle during this process and subsequent regeneration. Relative quantification of qPCR data has indicated that a number of integrins including β1, αV and β3 show an increase in expression level at 4 days post treatment. Immunohistochemistry shows some changes in integrin localisation between 4 and 21 days post-gentamicin.

Table of Contents

List of Figures

List of Tables

Chapter 1: Introduction

1.1 Integrins

Integrins are a family of cell-surface glycoproteins which are widely expressed in many different cell types. They are heterodimeric proteins, consisting of a non-covalently associated alpha subunit and beta subunit. The integrins and their homologs are well conserved across a broad range of organisms, both vertebrate and invertebrate; in Drosophila, homologs to the vertebrate integrins called position specific antigens exist as two 'alpha' subunits (PS1 and PS2) and just a single 'beta' subunit (PS3) which can associate with either of the alphas, resulting in two functional heterodimers (Marcantonio et al, 1988). In vertebrate species such as humans and mice, there are currently 18 known α subunits and 8 β subunits, however, not every α subunit possesses the ability to form a functional association with every β subunit (van der Flier et al, 2001). At present, 24 different heterodimers are known to exist; some subunits, such as integrin αV (*Itgav*) and integrin β1 (*Itgb1*) are considered the most 'prolific' and are able to form numerous heterodimers, whereas most of the other known subunits are only present in one or two functional integrin proteins.

This section of this chapter introduces the integrin family in terms of their structure and function. This thesis aims to investigate the presence of integrins in the murine vestibular system, a tissue known to be capable of a limited degree of spontaneous regeneration in response to damage induced by ototoxic aminoglycosides. The cellular mechanisms, signalling pathways and proteins which initiate and regulate this regenerative capacity, an ability which is lacking in the mammalian auditory epithelium, are the subject of ongoing research. As established from previous studies, the integrin family are known to be involved in numerous cellular processes including signalling, differentiation and cell adhesion, in addition to having been identified as playing a role in tissue repair and regeneration in other organ systems. The work carried out during this study is based upon the hypothesis that integrins could be considered, based upon this knowledge of their capabilities, as potentially being important molecules in the regeneration which occurs in the mouse utricular epithelium.

1.1.1 Integrin Structure and Ligand Binding

Nomenclature

The integrin family of cell adhesion molecules was so named due to their critical role in maintaining the 'integrity' of the adhesion of cells to the extracellular matrix (ECM) and the interaction of this ECM with the intracellular cytoskeleton (Hynes, 2004). Although linked by certain conserved DNA sequences in key functional areas, the integrins are a diverse protein family; many have previously been known by other names as they were first studied and categorised as separate groups of cell surface molecules by scientists working independently, before eventually being brought together under the integrin family.

The names, including synonyms and previous names under alternative classification systems, of the currently known vertebrate integrin subunits are summarised in table 1-1 and table 1-2. Many of the integrin subunits have also been named under the 'cluster of differentiation/determinants' or 'CD' classification system.

Protein Name	Gene Name	Synonyms
Integrin α1	*ITGA1*	VLA1, CD49a
Integrin α2	*ITGA2*	CD49b
Integrin α2b	*ITGA2b*	CD41B, CD41
Integrin α3	*ITGA3*	CD49c, VLA3a, VCA-2, GAP-B3
Integrin α4	*ITGA4*	CD49d
Integrin α5	*ITGA5*	CD49e
Integrin α6	*ITGA6*	CD49f
Integrin α7	*ITGA7*	
Integrin α8	*ITGA8*	
Integrin α9	*ITGA9*	RLC, ITGA4L, ALPHA-RLC
Integrin α10	*ITGA10*	
Integrin α11	*ITGA11*	HsT18964
Integrin αD	*ITGAD*	CD11d, αDβ2
Integrin αE	*ITGAE*	CD103, HUMINAE
Integrin αL	*ITGAL*	LFA-1
Integrin αM	*ITGAM*	CD51
Integrin αV	*ITGAV*	
Integrin αX	*ITGAX*	CD11c

Table 1-1 Nomenclature of Mammalian α Integrins

This table summarises the 18 known mammalian integrin α subunits in terms of their protein name and abbreviated gene name. Many integrin subunits have been previously known by alternative names or synonyms, including different family classification systems. VLA = Very late activation antigen, CD = Cluster of differentiation/determinants antigen, VCA = Very common antigen, GAP = galactoprotein, RLC = regulatory light chain, LFA = lymphocyte function-associated antigen.

Protein Name	Gene Name	Synonyms
Integrin β1	*ITGB1*	CD29, GPIIA
Integrin β2	*ITGB2*	LFA-1, MAC-1
Integrin β3	*ITGB3*	CD61, GPIIIa
Integrin β4	*ITGB4*	CD104
Integrin β5	*ITGB5*	
Integrin β6	*ITGB6*	
Integrin β7	*ITGB7*	
Integrin β8	*ITGB8*	

Table 1-2 Nomenclature of Mammalian Integrin β Subunits

This table summarises the 8 known mammalian integrin β subunits in terms of their protein name and abbreviated gene name. GP = Glycoprotein, CD = Cluster of differentiation/determinants antigen, MAC = Macrophage antigen, LFA = lymphocyte function-associated antigen.

Structure and Ligand Binding

The 24 different combinations of α and β subunits (illustrated in figure 1-1) which produce a functional protein heterodimer confer ligand binding specificity to each individual integrin. Current work suggests that ligand specificity is highly dependent upon which α subunit is present (Mould et al., 2000), and that on this basis, the integrins can be divided into four main groups (as shown in figure 1-1), based upon their major ligand binding specificity and function; the laminin receptor integrins (those containing α3, α6 and α7), the collagen receptor integrins (those with an α1, α2, α10 or α11 subunit) and the integrins which recognise a particular amino acid sequence known as RGD (Arg-Gly-Asp) found in ECM proteins such as fibronectin (Ruoslahti and Pierschbacher, 1987) i.e. those possessing an αIIb, α5, α8 or αV subunit. The remaining integrins (those which have an αL, αM, αX, αD, αE, α9 or α4 subunit) are those which are specifically expressed on cells of the haematopoietic system. Leucocyte-specific integrins are frequently involved in cell-cell adhesion, through molecules such as ICAMs and proteins found in blood plasma (van der Flier and Sonnenberg, 2001).

The association of an α and β subunit creates an integrin heterodimer with a globular head domain; this is the region which binds ligands i.e. ECM components or cell surface molecules. The individual structural regions of a typical integrin heterodimer are shown in figure 1-2. Some of the integrin α subunits (α1, α2, α10, α11, αE, αD, αX, αM and αL) contain an additional insert within their extracellular head consisting of 200 amino acids, which is not present in the other α integrins. This insert is known as the 'I domain'(Colombatti et al., 1993), and it has been shown to contain a MIDAS motif (metal ion dependent adhesion site) which is able to bind Mg^{2+} ions (Lee et al., 1995). The I domain has been determined as having a key role in the ligand binding of those integrin heterodimers which include an I domain containing α subunit (Kanazashi et al., 1997). All of the known mammalian integrin β subunits also contain a similar 'I-like domain' which features metal ion binding sites (Huang et al., 2000a) and is known to be an important part of the extracellular region of the heterodimer in terms of regulation of integrin activity (Takagi et al., 2002).

The intracellular region of an integrin consists of a cytoplasmic tail. In most subunits, this region is relatively short (up to 50 AAs long), and it is through this that integrins are able to interact with the intracellular actin cytoskeleton via various β integrin

cytosplasmic-domain binding proteins (Liu et al., 2000) e.g. actin binding proteins such as talin or signalling molecules like FAK (focal adhesion kinase). The integrin β4 subunit has a cytoplasmic tail which is considerably longer than that of other integrins, consisting of around 1000 AA (Tamura et al., 1990) . Integrin β4 is the only integrin subunit which interacts with intermediate filaments of the cytoskeleton, as opposed to actin filaments, and it is this longer tail region which allows this integrin subunit to interact with intermediate filaments at hemidesmosomes (Spinardi et al., 1993) as part of the α6β4 heterodimer.

Figure 1-1 Mammalian Integrin Heterodimers and their Ligand Binding Properties

Adapted from (Barczyk et al., 2010) The 24 known integrin heterodimers organised according to their ligand binding specificity. The integrin subunits which have previously been found in the mammalian inner ear are highlighted with references to these earlier studies.

Figure 1-2 Integrin Structure

Adapted from (Barczyk et al., 2010). Schematic diagram of an integrin heterodimer showing the different domains within each of the subunits. The alpha subunit has a β-propeller at the top of the 'thigh' and 'calf' domains – together with the β subunit hybrid (H) domain, PSI domain and four EGF repeats, these features of integrin structure make up the extracellular head region which binds ligands. The αI domain present in some, but not all, alpha subunits, is inserted between two of the blades of the β-propeller. Both the α and β subunits also have a short cytoplasmic tail region which intracts with intracellular integrin-binding proteins.

1.1.2 Integrin Activation: 'Inside-Out' Signalling

The ability of a given integrin heterodimer to bind with a known ligand is dependent on several factors, including whether the integrin is active and its current affinity state for that particular ligand. Integrins can be both activated and deactivated according to the adhesive requirements of a cell at a particular time. The most well-known example of integrin activation is of integrin αIIbβ3 on blood platelets (Kieffer and Phillips, 1990).This integrin is critical for the process of forming blood clots following vascular injury; deficiency in either integrin αIIb or β3 in humans due to genetic mutation results in a bleeding disorder called Glanzmann thrombasthenia (Hodivala-Dilke et al., 1999) . Under normal conditions, αIIbβ3 is present at the cell surface in an inactivated form and it is therefore unable to bind its usual soluble ligands in this state. This inactive state prevents platelet aggregation and the potential for thrombosis which would occur if this integrin were to be constitutively active. Only when blood platelets are stimulated i.e. in response to wounding, is integrin αIIbβ3 activated and then able to bind ligands such as fibrinogen in order for platelets to aggregate and form a clot at the site of the injury (Phillips et al., 1991). Activation of integrins is believed to be achieved through a conformational change which takes place in the extracellular region of the protein. This shape change results in the exposition of integrin ligand binding sites (O'Toole et al., 1994). This activation is triggered intracellularly (as shown in figure 1-3); a process widely described as 'inside-out' integrin signalling.

The affinity of an integrin for its ligand binding partners also represents a key way in which integrin adhesion and signalling may be regulated. Signals via other cell surface receptors are able to alter the affinity state of integrins for their respective ligands through the induction of a conformational change in the extracellular domain of the heterodimer. This so called 'inside-out signalling' is the primary method via which integrins are activated. Inside-out signalling of integrins represents a vital method of regulating integrin activity, preventing pathologies which could arise from unwanted binding of integrins to their ligands.

The extracellular shape change exhibited by integrins on activation, has been determined as being induced by an initial alteration in the intracellular region of the integrin heterodimer. In the integrin receptor low-affinity state, the cytoplasmic tails of the α and β subunits are 'clasped' together (Vinogradova et al., 2002). Disruption of this

association, leads to ‘unclasping’ of the cytoplasmic tails which then become embedded in the plasma membrane (Kim et al., 2003; Vinogradova et al., 2004), and it is this intracellular event which is believed to be the trigger for the change in conformation exhibited by the extracellular head region.

The extracellular head of an integrin has been shown to exist in one of three possible conformational states (Takagi et al., 2002) which are shown in figure 1-3. The low-affinity state for inactive integrins on the cell surface is a bent state, where the globular head is in close proximity to the cell membrane (Xiong et al., 2002), a position which is not conducive to ligand binding. Inside-out and outside-in integrin signalling pathways are able to trigger a conformational change, resulting in both the extension of the head-piece and also an ‘opening’ of the globular head domain to reveal ligand binding and recognition sites (Takagi et al., 2002). This structural rearrangement from a low to a high-affinity state is referred to as the ‘switchblade model’ of integrin activation (Xiong et al., 2003).

The key intracellular integrin-binding protein which is involved in triggering these conformational changes is talin. In its active form, talin is able to bind the cytoplasmic tail of β integrins through its F3 domain (as shown in figure 1-3), and acts as the final molecule of intracellular signalling cascades which are responsible for the activation of integrins (Wegener et al., 2007). More recently, additional integrin binding proteins known as kindlins have also been shown to be able to interact with integrin cytoplasmic tails in a similar manner to talin (Ma et al., 2008). Kindlins promote the effects of talin binding in the integrin activation process; the presence of talin alone is not sufficient to alter the extracellular conformation to that of the high affinity state (Moser et al., 2008). The changes observed in integrin affinity-state have been shown to be reversible; conformational changes in the extracellular structure of integrins therefore represent a key method for the regulation of their activity and ligand binding properties.

Figure 1-3 Integrin Conformational States: Inside-Out Activation

Adapted from (Al-Jamal and Harrison, 2008; Wang, 2012). When an integrin heterodimer is in its 'inactive' state, the extracellular head region is in a closed, 'bent' conformation; the integrin in this state has a low affinity for its ligand binding partners (Xiong et al., 2002). On delivery of an intracellular activation signal, the protein talin is able to bind to the cytoplasmic tail region of the integrin β subunit (Wegener et al., 2007). Talin binding causes the integrin α and β tails to move further apart at the membrane and results in a conformation change in the integrin extracellular head. Activation of an integrin results in a 'switchblade' like extension of the head region which also opens and exposes ligand binding sites (Xiong et al., 2003). In this conformational state, the integrin is said to be 'active' and has a high affinity for its ligand binding partners.

Outside-in signalling, whereby integrin ligand binding brings about changes in the intracellular environment of a cell, is involved in the remodelling of the cytoskeleton and formation of intracellular protein complexes. Integrins play a role in numerous cellular processes through this method of signal transduction; they are able to influence the cell cycle, modify cell morphology and alter the location of a cell through migration. For the purpose of this thesis, the intracellular responses induced by ligand binding are described in terms of the formation of cellular adhesion structures and cell shape changes, since these are of particular interest with regards to the potential role of integrins in the vestibular epithelium.

1.1.4 Integrins and Cell Adhesion

The integrin family of proteins is best known as being a group of cell adhesion molecules. Spanning the plasma membrane, integrins constitute a direct linkage between the extracellular environment e.g. the ECM or adjacent cells within a tissue, and the intracellular cytoskeleton, in particular actin filaments. The binding of integrins to ligands which are ECM components, such as collagens and laminins, triggers the formation of specialised adhesive structures known as focal adhesions.

Focal Adhesions

Focal adhesions are complex structures which provide a linkage between the extracellular matrix and the intracellular actin cytoskeleton, mediated by members of the integrin receptor family. In addition to acting as anchoring junctions, adhering cells to the ECM, focal adhesions are also linked to integrin-mediated 'outside-in' signalling pathways. The assembly of focal adhesions is shown in figure 1-4.

At focal adhesions, integrin heterodimers which are bound to ECM ligands cluster at the plasma membrane (Cluzel et al., 2005). As described in 1.2, the cytoplasmic tail regions of integrins are able to associate with numerous intracellular integrin binding proteins such as talin (which may act as an inside-out activator of integrins); particular integrin α subunit tail regions associate with another integrin-binding protein, paxillin (Liu et al., 1999). The linkage of the actin cytoskeleton to integrins may be directly mediated by some integrin-binding proteins which are also able to associate with actin filaments e.g. tensin (Lo et al., 1994; Miyamoto et al., 1995a).

Focal adhesion kinase (FAK) is another key constituent of focal adhesions – it is a tyrosine kinase which is recruited to the focal adhesion by associating with talin, and is thought to be activated via integrins (Chen et al., 1995). Clustering and activation of FAK triggers the recruitment of other downstream signalling molecules (Hanks and Polte, 1997)such as Src (Fincham et al., 2000), vinculin and α-actinin. This phosphorylation cascade leads to the activation of multiple signalling pathways i.e. ERK and JNK (Miyamoto et al., 1995b), in addition to interaction with the actin cytoskeleton. It is this integrin-dependent signalling cascade (illustrated in figure 1-5) which results in cytoskeletal remodelling and translocation of signalling molecules to the nucleus to effect further downstream changes within a cell – focal adhesion are thus able to act as an anchorage junction between a cell and the extracellular matrix, but are also important for in integrin-mediated 'outside-in' signalling pathways. Focal adhesions are highly dynamic structures, with as many as 50 proteins known to associate with the intracellular protein complex; they undergo constant changes of the downstream protein constituents. The dynamic nature of these adhesions is particularly important for cell migration, where new adhesive contacts are formed at the leading edge of the migrating cell, whilst the old anchorages dissociate, in addition to re-modelling of the actin cytoskeleton.

Figure 1-4 Assembly of Focal Adhesions

Adapted from (Mitra et al., 2005). This figure summarises some of the key constituents of focal adhesion complexes. (A) Binding of integrins to extracellular matrix ligands leads to clustering of integrin heterodimers. (B) Integrin binding proteins such as paxillin and talin (Chen et al., 1995) are able to associate with integrin cytoplasmic tails; these proteins are able to recruit focal adhesion kinase (FAK) (Hildebrand et al., 1995) . (C) FAK is a tyrosine kinase and its recruitment to focal adhesions initiates a phosphorylation cascade which in turn recruits further downstream proteins such as Src, vinculin and α-actinin. (D) Proteins such as α-actinin are able to bind actin filaments, thus forming a linkage between the ECM and the intracellular cytoskeleton via integrin receptors.

Hemidesmosomes

The α6β4 integrin heterodimer is unique amongst the integrin receptors, since it interacts with intermediate filaments, as opposed to the actin cytoskeleton. This integrin is a key component of hemidesmosomes, specialised adhesive complexes (shown in figure 1-5), which are found in epithelial tissues such as the skin epidermis (Stepp et al., 1990). The integrin β4 subunit, which binds extracellularly to laminin-5, is crucial for the initiation of hemidesmosome formation (Schaapveld et al., 1998), with plectin, BP230 and BP180 accessory proteins forming the link between the integrin heterodimer and intermediate filaments (Koster et al., 2003); the structure of hemidesmosomes is illustrated in figure 1-5. The skin blistering disorder junctional epidermolysis bullosa, which causes separation of the dermal and epidermal layers of the skin, has been linked to mutation and deficiency in the integrin β4 (Jonkman et al., 2002; Niessen et al., 1996) and α6 (Pulkkinen et al., 1997) subunits in humans, emphasising the importance of integrin α6β4 in hemidesmosome structure and function.

Figure 1-5 Structure of Hemidesmosomes in the Skin Epidermis

From (Zahreddine et al., 2010)**.** Hemidesmosomes are specialised adhesive complexes which are critical for maintaining the integrity of skin epidermis. Hemidesmosomes link laminin-5-containing extracellular matrix with intracellular intermediate filaments. Integrin α6β4 is the key transmembrane protein which binds laminin-5 extracellularly, and through recruitment of the accessory proteins plectin, BP180 and BP230, forms an intracellular linkage with the intermediate filaments of the cell cytoskeleton.

Integrin Adhesion: Proliferation and Cell Death

Binding of the extracellular matrix by integrins has the ability to influence numerous cellular events by way of the downstream signalling pathways integrins are linked to i.e. proliferation, cell death, migration and phagocytosis. Proliferation of cells is a process which must be tightly regulated; many tumours result as a consequence of proliferation control defects. One way in which this event may be regulated is through cellular adhesion to the extracellular matrix. Ligand binding by numerous integrins has been described as activating a number of proliferative signalling pathways. They are known to act cooperatively with receptor tyrosine kinases (RTKs) to control signalling pathways that regulate G1 cell cycle phase cyclin-dependent kinases (CDKs) – loss of cell adhesion is known to halt the cell cycle at the G1 phase (Schwartz and Assoian, 2001). Integrins are also believed to trigger activation of the PI-3K and MAPK cascades (Montcouquiol and Corwin, 2001). In addition to being involved in proliferation, integrins are also now thought to play a role in cell death, a process known as integrin-mediated death (IMD). This process occurs as a result of un-ligated integrins being able to recruit and activate caspase-8 to induce apoptotic cell death (Stupack et al., 2001).

1.1.5 Integrins in Repair, Regeneration and Wound Healing

Due to their involvement in numerous cellular events such as proliferation, migration and adhesion, integrins have been shown to be important in numerous organ systems for the repair and regeneration of damaged tissue.

Wound healing of lesions in the skin has been shown to involve several different integrin heterodimers in the process of wound closure. After initial blood clot formation and deposition of a provisional matrix rich in the protein fibronectin within the wound site (Clark, 1990), skin lesions undergo reepithelialisation, whereby keratinocytes migrate into the wound space. In order achieve this, basal keratinocytes at the periphery of the wound must dissolve their linkages with the adhesive structures which anchor them to the basal lamina e.g. hemidesmosomes (Litjens et al., 2006; Mercurio et al., 2001). The mechanisms involved in this disassembly are not fully understood, but are thought to involve phosphorylation of integrin β4, the integrin β subunit constituent of hemidesmosomes (Germain et al., 2009; Kashyap et al., 2011). Several integrins are known to be expressed in normal skin tissue by keratinocytes, including α2β1, α3β1 and αVβ5 (Marchisio et al., 1991; Peltonen et al., 1989), in addition to the hemidesmosomal

integrin α6β4 as described in 1.1.2. The cellular mechanisms which underlie the migration of cells in the wounded region are complex and not fully understood, however studies have shown that integrin β1 is particularly crucial for proper migration of both keratinocytes and fibroblasts (Grose et al., 2002; Liu et al., 2010). Fibroblast migration into the wound site is important for wound contractility, a process which brings the wound edges closer together, facilitating the reepithelialisation process (Grinnell, 1994).

Previous studies have shown that keratinocytes which lack the integrin β1 subunit show reduced migratory capability, believed to be the result of their inability to bind dermal matrix ligands deposited in the wound site. The function of integrin β1 in this process is believed to be dependent upon the TGF-β signalling pathway; TGF-β1 has been shown to be involved in the regulation of the reepithelialisation stage of cutaneous wound healing (Singer and Clark, 1999).The phenotype of mice with a fibroblast-specific deletion of integrin β1 – these mice showed delayed reepithelialisation of skin wounds, was found to be rescued by the addition of exogenous active TGFβ1 (Liu et al., 2010). Epithelial integrins of the skin have also been shown to alter their expression and localisation during cutaneous wound healing. Integrins α2, α3, α6 and β1 are localised to the basal layer of the skin in normal tissue, however, following injury, these integrins become detectable in the suprabasal layers of the epidermis during wound healing (Cavani et al., 1993; Hertle et al., 1992). It is this alteration in both the type of integrins expressed on basal keratinocytes and of their cellular localisation, which allows these cells to become migratory and to utilise fibronectin within the temporarily deposited wound site matrix to 'crawl' and reepithelialise the lesion (Cavani et al., 1993; Martin, 1997).

The epithelia of the cornea express a similar cohort of integrins as shown by the epithelial layers of the skin (Stepp et al., 1993) i.e. α2, α3 and β1. Wounding of the corneal epithelium is repaired in a similar way to that observed in skin lesions, and integrins such as α5β1 (Murakami et al., 1992) and α9 (Stepp and Zhu, 1997) have been shown to have increased expression in migrating corneal epithelial cells as they move into the lesion.

These findings support the idea that members of the integrin family are involved in this type of tissue repair involving proliferation and migration of cells into a lesion in

several epithelial tissues. Based upon this knowledge of the behaviour and capabilities of integrins in the regeneration of other epithelia, the work carried out in this thesis set out to investigate the expression of members of the integrin family within the vestibular epithelium of the mouse inner ear.

1.2 The Mammalian Inner Ear

Responsible for the detection of sound and movement, the specialised auditory and vestibular systems within the mammalian ear are capable of transmitting the information received through sound and motion stimuli as electrical impulses to the centres of the brain dedicated to the processing of such signals. This chapter will introduce and summarise the structure and function of the mammalian organ of Corti – the auditory epithelium, and will subsequently focus upon the vestibular sensory epithelium, principally the mammalian utricle and its capacity for hair cell regeneration, as the model tissue studied throughout this project.

Both the auditory and vestibular structures of the ear utilise mechanosensory hair cells within a specialised sensory epithelium. Hair cells are present within the organ of Corti, the utricle and saccule (the two otolith organs of the vestibular system) and the cristae ampullaris located with the semi-circular canals of the labyrinth.

1.2.1 The Mammalian Auditory System

The mammalian auditory system is divided into three distinct regions; the outer ear, middle ear and inner ear. The outer ear consists of the ear canal and the external pinna or auricle which directs sound stimuli into the ear canal. Many mammalian species are able to manipulate the position of their pinnae, moving them independently of one another e.g. horses, cats and mice among others, in order to locate the source of the auditory stimulus. On reaching the ear drum, also known as the tympanic membrane, sound waves enter the structures of the middle ear. Oscillation of the tympanic membrane triggered by sound waves is conducted through the three tiny ear bones, the malleus, incus and stapes, to the fluid which fills the cochlea via the oval window. The inner ear constitutes both the auditory and vestibular organs. The organ of Corti, the specialised auditory epithelium, is found within the cochlea, a coiled, fluid-filled bony tube, which is divided by membranes into three separate compartments.

The organ of Corti is supported by the basilar membrane which lies beneath it; the organ of Corti is located within the central compartment of the cochlear duct – the scala media, which is situated between the scala vestibuli and the scala tympani as shown in figure 1-6. There are two types of mechanosensory hair cells within the auditory epithelium, known as inner and outer hair cells. They exist in the organ of Corti as a single row of inner hair cells and three rows of outer hair cells (as illustrated in figure 1-7), surrounded by several types of supporting cells; such as the inner and outer pillar cells and Deiters' cells (Lim, 1986). It is these supporting cells which are in direct contact at their basal surface with the basilar membrane. Both inner and outer hair cells possess structures known as stereocilia on their apical surfaces. Stereocilia are constructed of parallel arrays of actin filaments (Flock and Cheung, 1977; Tilney et al., 1980), which are cross-linked to provide structural integrity by actin-bundling proteins such as fimbrin (Tilney et al., 1989) and espin (Sekerkova et al., 2011). Stereocilia are anchored at the hair cell apical surface within an actin-dense region known as the cuticular plate. In the organ of Corti, stereocilia are arranged in ordered rows on the apices of hair cells, forming a staircase-like arrangement whereby the rows of stereocilia are of increasing height; adjacent rows are connected by structures known as tip-links (Pickles et al., 1984). Outer hair cell stereocilia rows are highly organised into a 'V' or 'W' shape on the apical surface, whilst inner hair cell stereocilia form rows which are straighter and appear less organised, exhibiting a gently curved, open 'V' or 'W'-shaped arrangement. (Hackney and Furness, 1995). Detection of auditory stimuli is conducted by inner hair cells; the function of outer hair cells lies with sound amplification (Ashmore, 1987) .

The tectorial membrane, a structure which is made up of several types of collagen and other extracellular matrix proteins (Richardson et al., 1987) lies above the auditory epithelium and this plays a crucial role in the mechanosensory function of the organ of Corti; the tallest stereocilia of outer hair cells are embedded in the tectorial membrane at their tips (Kimura, 1966; Lim, 1972). When acoustic stimulation occurs, the propagation of sound waves by fluid motion through to the inner ear, causes oscillation of the basilar membrane upon which the organ of Corti sits. This oscillatory movement at the basilar membrane results in a shearing motion of the apical hair bundles against the tectorial membrane, and causes deflection of the stereocilia towards the tallest row in the staircase. Deflection of hair bundles results in the opening of mechanosensitive

ion transduction channels, allowing an influx of cations – primarily K^+ ions of the endolymphatic fluid which bathes the hair cell apices. This influx is driven by the endocochlear potential of the endolymph – which has a high positive charge of around -80 to 100mV in comparison to the potential of the perilymph. The high concentration of K^+ ions within the endolymphatic fluid is actively maintained by the stria vascularis (Tasaki and Spyropoulos, 1959) through the presence of tight junctions and the K+ ion channel $K_{ir}4.1$ (Marcus et al., 2002; Takeuchi et al., 2000). The cation influx driven by this ion concentration gradient results in a depolarisation of the hair cell membrane, which in turn, triggers the opening of baso-lateral voltage dependent Ca^{2+} channels. The opening of these channels leads to an influx of calcium into the hair cell, and results ultimately in the release of glutamate, a neurotransmitter at the base of the hair cell which is in contact with afferent auditory neurons. Action potentials are relayed via these nerve fibres to the auditory cortex of the brain for processing of the stimulus. The mechanotransductive capabilities of auditory hair cells are reviewed in depth by (Hudspeth, 2001)

Figure 1-6 Location of the Organ of Corti within the Cochlea

The mammalian auditory epithelium, the organ of Corti, is found within the coiled cochlea of the inner ear. The cochlear duct is divided by membranes into three compartments (bold typeface); the scala vestibuli, the scala media and the scala tympani. The organ of Corti is situated on top of the basilar membrane within the scala media.

Figure 1-7 Structure of the Organ of Corti

The organ of Corti lies on top of the basilar membrane and consists of one row of inner hair cells and three rows of outer hair cells. Both types of hair cell, which have a mechanosensory function, have hair-like projections on their apical surface called stereocilia. Hair cells are surrounded by several different types of supporting cell e.g. Dieters' cells, which provide structural support, as well as having a key homeostatic function to maintain the optimum physiological environment for hair cells. Overlying the auditory hair cells is the tectorial membrane which is involved in the creation of mechanical shearing and deflection of stereocilia. The coloured regions highlight areas of the auditory epithelium where integrin proteins might be expected to be present e.g. blood capillaries (red), the basement membrane of the basilar membrane (green) and the interface with the base of supporting cells (yellow). Integrin αV was localised to supporting cell regions in contact with the basement membrane of the basilar membrane in the chinchilla cochlea (Tsuprun and Santi, 1999).

The mechanosensory hair cells of the mammalian inner ear are susceptible to damage, which may be induced by numerous factors including ototoxic drugs i.e. aminoglycoside antibiotics, in addition to ageing and noise exposure, resulting in both hearing and balance impairments. There are also numerous genetic mutations of proteins which are critical for the development and function of the inner ear which are the cause of many congenital hearing disorders e.g. mutations of multiple genes including cadherin 23 (Bolz et al., 2001) and myosin Viia (Weil et al., 1995) are known to underlie the deaf-blind disorder known as Usher's syndrome. Unlike the auditory systems of birds and amphibians, the mammalian auditory epithelium is unable to regenerate lost hair cells and therefore humans and other mammalian species, are subject to permanent hearing loss. The mammalian vestibular epithelium has been shown to be capable of a limited degree of spontaneous hair cell regeneration, raising the question of what are the differences between auditory and vestibular hair cells and the epithelia within which they exists which allows vestibular hair cells to regenerate where auditory hair cells cannot.

1.2.2 The Mammalian Vestibular System

The mammalian vestibular system (illustrated in figure 1-8) consists of two main anatomical features; a system of semi-circular canals and several otolith organs. There are three semi-circular canals, the anterior, posterior and horizontal canals, each filled with endolymphatic fluid – they are involved in the detection of rotational movement. Each canal has a crista ampullaris at its base; cristae are covered in sensory hair cells, over which lies a structure known as the cupula. Sensory function is achieved as the movement of endolymph fluid within the semi-circular canal pushes on the cupula, which acts in a similar manner to the tectorial membrane in the organ of Corti, generating a mechanical shearing motion which results in the deflection of hair bundles of the cristae (Dohlman, 1969; Dohlman, 1981; Takumida, 2001).

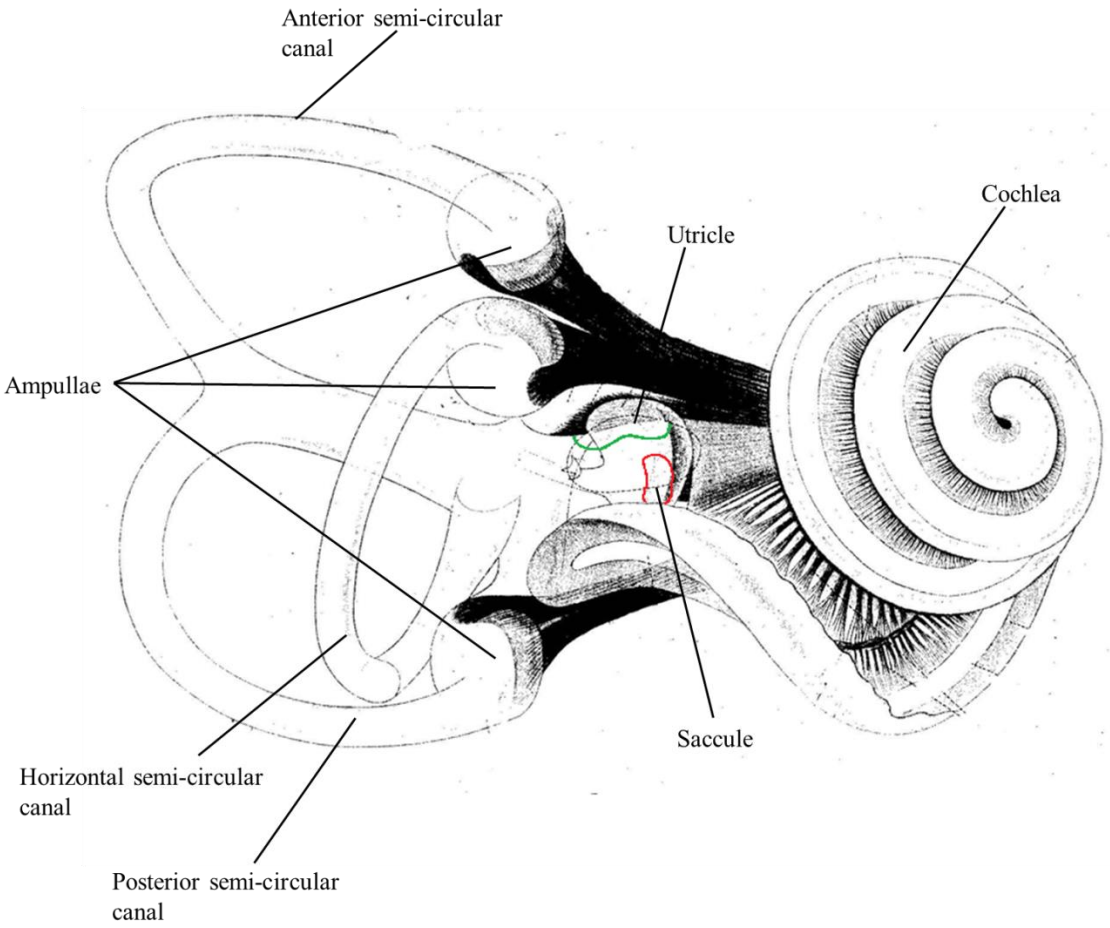

Figure 1-8 Anatomy of the Mammalian Vestibular System

Adapted from (Retzius, 1887). The mammalian vestibular system consists of three semi-circular canals, the region of the vestibular system which detects rotational movement. At the base of each canal is an ampulla, containing a hair cell covered crista. The otolith organs, the utricle and saccule, both feature a sensory epithelium made up of vestibular hair cells and supporting cells, with the utricle being the larger of the two organs. The utricular and saccular maculae are responsible for the detection of linear acceleration and head tilts.

Collectively known as the otolith organs, the utricle and saccule are fluid-filled sacs, each with a specialised sensory macula. Overlying the sensory epithelia of these balance organs is the otolithic membrane, on the surface of which sit the otoconia – calcium carbonate crystals (Kachar et al., 1990). The otolith organs are both involved in the detection of linear acceleration and head tilts; the weight of the otoconia means that their movement due to gravitational effects creates mechanical shearing between the otolithic membrane and the macula beneath, resulting in deflection of vestibular hair bundles.

The model tissue for the work carried out in this thesis was the adult mouse utricular macula. The utricular sensory epithelium is made up of two types of vestibular hair cells known as type I and type II hair cells (shown in figure 1-9). Type I vestibular hair cells are 'bottle-shaped,' and their cell body is completely surrounded by an afferent cup-like neural calyx. Type II hair cells have a more typically epithelial columnar shape and are innervated by bouton synapses at the base of the cell (Wersall, 1956). Surrounding the vestibular hair cells within the sensory epithelium are supporting cells; these cells are in contact with the basement membrane at their base and extend all the way to the apex of the epithelium. The apical surfaces of supporting cells are covered in microvilli.

Vestibular hair cell stereocilia are arranged on the apical surface in rows of ascending height as also seen in auditory hair cells, but they are not organised in a 'W' or 'V' shape, instead appearing as a bundle which covers much of the apical surface of the cell. Vestibular hair bundles also have a kinocilium adjacent to the tallest row of stereocilia. The kinocilium, a special type of primary cilium, exhibits a typical '9+2' arrangement of microtubules within its cytoskeletal core (Erkman et al., 1996). Type I hair bundles are typically taller than their counterparts on type II hair cells; there is also variation between bundles arrangement - there are two formations, one 'tight,' the other 'loose' (Bagger-Sjoback and Takumida, 1988; Lapeyre et al., 1992). The utricular epithelial surface features a crescent-shaped region known as the striola. The striola represents the polarity of the vestibular hair bundles; in the utricle, stereocilia are oriented by way of their kinocilia (Denman-Johnson and Forge, 1999) facing towards the striola (shown in figure 1-10). This means that there is a change in the polarity of utricular hair cells dependent upon their location with respect to the striola – this enables the utricle to detect linear accelerations in different directions since some hair cells will be depolarised and others hyperpolarised according to the type of movement experienced.

Figure 1-9 Two Types of Hair Cell within the Utricular Sensory Epithelium

Adapted from (Beckingham et al., 2005). There are two distinct types of vestibular hair cells within the utricular sensory epithelium. Type I hair cells (labelled 'I') are 'flask' shaped; their cell body is completely surrounded by an afferent neural calyx. In contrast, type II hair cells (labelled 'II') are a more typical columnar shape. The afferent synapses for type II hair cells are bouton synapses at the base of the cell body (Wersall, 1956). This figure indicates regions of the vestibular hair cells where integrin α8 was detected (green) in the late embryonic/early postnatal mouse (Littlewood Evans and Muller, 2000). The regions in red highlight areas of the vestibular epithelium where integrins would be hypothesised to localise e.g. the interface between the supporting cells and the basement membrane, in addition to that between the basement membrane and the mesenchymal tissue beneath the epithelium. EFF = efferent neuron, AFF = Afferent neuron.

Figure 1-10 Hair Cell Polarity and the Striola of Vestibular Otolith Organs

Adapted from (Fitzpatrick and Day, 2004). The striola of the utricle divides the macula into two regions of opposing hair bundle polarity. In the utricle, stereocilia are oriented with their kinocilia (adjacent to the tallest row of stereocilia) facing towards the striola (Denman-Johnson and Forge, 1999). In the other otolith organ, the saccule, hair bundles are instead oriented so that their kinocilia face away from the striola. This figure also illustrates how accelerative motion in one direct results in the movement of the otoconia in the opposite direction, leading to the deflection of the stereocilia towards the kinocilium.

1.2.3 Integrins and the Inner Ear

A search of previously published literature reveals that relatively little is known about integrin expression in the inner ear, particularly with regards to the vestibular sensory epithelium. Much of the work carried out on integrins within the inner ear is related to changes in expression during mouse inner ear development at embryonic and very early postnatal stages, and does not examine integrin expression in the mature adult tissue.

Changes in integrin expression during development are thought to be mediated by changes in cell-cell and cell-ECM adhesions. Previous work has investigated the

alteration in expression of several integrin subunits, namely α6, α3 and β4 (Davies and Holley, 2002). Both α3 and α6 are expressed in the epithelial layers of the developing otocysts in E10.5 mouse tissue. The expression of α6 was shown to be concentrated in an atrioventral region of this epithelial layer, in addition to being expressed in cells which go on to form the cochlear ganglion. By E12.5, the expression pattern of both of these α integrin subunits is altered, with α6 becoming more restricted in distribution to pro-sensory regions of the epithelia and neural processes originating from the cochlear-vestibular ganglion. Integrin α3 is at this stage expressed in regions of the epithelium adjacent to those which are pro-sensory and expressing α6. This expression pattern is then maintained from this stage onwards until birth, whereupon a second spatio-temporal alteration in integrin expression occurs. Between birth and P6, α3 expression is up-regulated, whilst α6 expression is down-regulated in both the auditory and vestibular sensory epithelia. Immunolocalisation of β4, which did not show the same expression pattern changes as α6, being expressed in epithelial-mesenchymal borders throughout murine development, determined that the integrin heterodimer present must be α6β1. In the utricle at P0, β4 was expressed in cells underneath the sensory epithelium at the basement membrane-epithelium border, whereas α6 was also present in the supporting and hair cell layer (Davies et al., 2007). Integrins αV and β1 have been detected in the chinchilla cochlea at regions of supporting cell contact with the basement membrane (Tsuprun and Santi, 1999).

Four integrin subunits, α6, αV, β1 and β3, have been detected by a previous study in OC2 cells (Brunetta et al., 2012), a cell line derived from immortalised inner ear cells from the E13 mouse (Rivolta et al., 1998). In this study, integrin β3 was shown to increase in expression level after OC2 cells were induced to differentiate (when they begin to express several hair cell marker proteins) by increasing the incubation temperature at which they were maintained *in vitro*. Over-expression of integrin β3 in these OC2 cells in their undifferentiated state was able to induce expression of myosin Viia. This result suggests that integrin β3 was able to induce OC2 cells to differentiate and potentially implicates a role for integrins in the cellular cues which underlie the signals required to induce a hair cell progenitor to proceed along a differentiation pathway towards becoming a hair cell. This previous work therefore suggests that there may be several different integrins present in auditory hair cells, and that integrins might be involved in the differentiation of hair cells during development.

One particular integrin heterodimer, namely α8β1, has been implicated as the cause of balance defects in a knock-out mouse model (Littlewood Evans and Muller, 2000). Mice which lack integrin α8 usually die shortly after birth due to kidney defects (Muller et al., 1997), but of those which survive, balance defect phenotypes have been observed. Electron microscopy of tissue from α8 knock-out mice with balance problems showed evidence of vestibular hair cells with cytoplasmic herniations and stereocilia abnormalities. Some normal stereocilia were also present, but often the kinocillium was observed to be fused with the surrounding stereocilia. In this previous study α8β1, FAK (focal adhesion kinase) and fibronectin have been shown to co-localise at the apical surface of hair cells in the utricular sensory epithelium of normal mice. Since a lack of integrin α8 results in stereocilia defects, it has been suggested that α8β1 may be responsible for organisation of the actin cytoskeleton at the hair cell apical surface, in conjunction with ECM components, such as fibronectin, thereby playing a role in the initiation of hair bundle formation (Littlewood Evans and Muller, 2000). This previous work also used *in situ* hybridization to look at the localisation of integrin α8 mRNA and several other subunits within the mouse utricle. Integrin α8 mRNA was observed to be localised at the apical surface of hair cells (immunohistochemistry was used to localise integrin α8 protein and showed similar apical localisation); mRNA for αV, α2 and β1 was distributed throughout the hair cell body. Immunohistochemistry was not carried out in this previous work however, to determine whether the mRNA distribution observed correlates with a similar pattern of integrin protein expression. This thesis aims to investigate the expression of integrins, including those such as α8 which have been previously found in the mammalian utricle, in order to determine the full cohort of integrin subunits expressed in the mature murine vestibular epithelium.

1.2.4 Regeneration & Repair in the Mammalian Utricle

Non-mammalian vertebrate species, such as birds, amphibians, reptiles and fish are capable of fully regenerating sensory hair cells which have been lost due to noise damage or exposure to ototoxic drugs. The sensory epithelia of the inner ear and the lateral lines of fish (Corwin, 1981)and amphibians (Corwin, 1985) are continuously renewed throughout the lifetime of the organism. In avian species, the auditory epithelium, populated with two different types of hair cell surrounded by supporting cells, is known as the basilar papilla. The mature avian auditory epithelium is capable of

regenerating hair cells, but only as a response to hair cell loss induced by acoustic trauma or exposure to ototoxic agents (Corwin and Cotanche, 1988; Oesterle et al., 1993; Ryals and Rubel, 1988). In the avian vestibular system, the utricular macula has been shown to be capable of continuous turnover of hair cells (Jorgensen and Mathiesen, 1988; Roberson et al., 1992), in addition to its ability to regenerate vestibular hair cells where hair cell loss has been induced by noise damage or aminoglycoside ototoxicity (Weisleder and Rubel, 1993). Regeneration in the avian inner ear has been demonstrated to occur in two different ways. New hair cells may be produced through proliferation and mitotic division of the supporting cells and the differentiation of their progeny into sensory hair cells (Stone and Rubel, 2000; Warchol and Corwin, 1996). Alternatively, hair cells may be replaced via a direct phenotypic conversion, known as transdifferentiation i.e. a supporting cell re-differentiates as a hair cell without undergoing cell division (Adler and Raphael, 1996; Roberson et al., 1996).

In contrast to the regenerative abilities demonstrated by the sensory epithelia of other vertebrates, the mature organ of Corti is unable to repair or replace dead or damaged hair cells. Within the mammalian vestibular system, however, the adult utricle has demonstrated that it is capable of a limited degree of hair cell regeneration in response to damage induced by exposure to ototoxic drugs. Studies of the mammalian vestibular epithelium and its regenerative capacity have been carried out in several species including chinchilla (Lopez et al., 1997), guinea pig (Forge et al., 1993), mouse (Kawamoto et al., 2009) and humans (Warchol et al., 1993). *In vivo* studies have shown that following gentamicin treatment, few hair cells remain in the mouse utricular epithelium by 7 days post drug exposure (Kawamoto et al., 2009).

Following exposure to ototoxic aminoglycosides, the vestibular sensory epithelium exhibits a high degree of hair cell loss, with epithelia treated *in vivo* typically showing a more complete loss of hair cells than cultured utricular tissue. Hair cell death in utricles maintained *in vitro* and exposed to aminoglycosides is believed to occur predominantly through apoptosis (Cunningham et al., 2002; Forge and Li, 2000; Lang and Liu, 1997); utricular cultures treated with aminoglycosides in the presence of a caspase inhibitor (caspases are proteases involved in apoptotic cell death) was able to prevent hair cell death by apoptosis (Forge and Li, 2000; Matsui et al., 2002). Supporting cells of the vestibular epithelium have been observed to undergo considerable shape change in damaged tissue – at sites of hair cell loss, neighbouring supporting cells (as many as 5

supporting cells have been shown to participate) extend apical processes which fill the space in the epithelium created by the loss of a hair cell, forming a scar (Meiteles and Raphael, 1994). Fragments of dead hair cells remaining within the hair cell layer of the epithelium may also be 'sealed over' by the spreading behaviour of supporting cells. Hair cells which have been irreparably damaged may also be removed intact from the epithelium by extrusion at the apical surface (Li et al., 1995); tight junctions between the hair cell and the surrounding supporting cells maintain the cell being extruded intact, whilst the neighbouring supporting cell apical extensions close off the space which had been occupied by the hair cell. An additional method of removing dying vestibular hair cells has been observed in the mammalian utricle: supporting cells have demonstrated an ability to act as non-professional phagocytes which engulf apoptotic hair cells (Li et al., 1995).

Regeneration of mammalian utricular tissue is typically detected at around 3 to 4 weeks post-aminoglycoside treatment (Forge et al., 1993; Forge et al., 1998; Kawamoto et al., 2009; Lin et al., 2011), through the appearance of hair bundles which are comparable in morphology to short immature stereocilia observed during development, in addition to detecting increased numbers of cells positive for hair cell markers i.e. myosin Viia.

Although regeneration of sensory hair cells has been shown to occur via two different mechanisms in non-mammalian vertebrates such as birds, it is thought that mammalian utricular hair cells are only regenerated by direct transdifferentiation of supporting cells. Studies aimed at detecting proliferation of supporting cells by mitotic division, as had been observed in the avian inner ear e.g. the incubation of damaged utricular tissue with mitotic trackers such as ^{3}H and BrdU detected only a few labelled nuclei within the supporting cell layer. These results did not explain the numbers of regenerated hair cells which had been observed (Rubel et al., 1995; Warchol et al., 1993).

Transdifferentiation, also known as phenotypic conversion, has been described in the vestibular epithelia of numerous other species including the newt (Taylor and Forge, 2005), bullfrog (Baird et al., 2000), mouse (Lin et al., 2011) and guinea pig (Li and Forge, 1997), indicating that this is an ability of supporting cells which is conserved across a wide variety of vertebrate species. Morphological evidence for supporting cell transdifferentiation was observed at 4 weeks post-aminoglycoside treatment in guinea pig utricular macula which received *in vivo* exposure to gentamicin(Li and Forge,

1997). This previous study observed cells in the sensory epithelium which showed evidence of a small, immature apical hair bundle, but which remained attached to the basement membrane in the manner of a supporting cell. Cells with longer hair bundles which more closely resembled stereocilia were also observed; the attachment of these cells to the basement membrane was via a narrow, 'foot-like' process. This study also detected evidence of cells with hair bundles where the basal process was no longer in contact with the basement membrane.

During the process of converting from a supporting cell to a hair cell, in addition to the development of an apical hair bundle, an important step in this regenerative pathway is the detachment of the cell from the basement membrane. Based upon previous studies of the function of integrins, it would be anticipated that there are integrin heterodimers expressed at the region of cellular contact of the basal region of supporting cells and the basement membrane of the utricle, as illustrated in figure 1-11. During transdifferentiation, it would therefore be necessary for such integrin-mediated adhesive links to the basement membrane to be broken in order for the basal process of the converting cell to retract. This might potentially occur in a manner which is similar to that described in 1.3 by keratinocytes during cutaneous wound healing, where they must sever their adhesive anchorages to the basal lamina and alter the type and localisation of their integrin receptors in order to migrate into a wound site. This thesis aims to investigate the presence of integrins in the normal mature murine utricle, with the hypothesis that these proteins would be expressed in regions such as the interface between the supporting cells and the basement membrane. It would therefore be of interest to investigate the effect of aminoglycoside-induced hair cell loss on the expression and localisation of the integrins due to the likelihood of their involvement in the cellular events which occur during transdifferentiation of supporting cells, the predominant mechanism of hair cell regeneration in the mammalian vestibular epithelium.

Figure 1-11 A Hypothesis for Integrin Involvement in Hair Cell Regeneration of the Mammalian Vestibular Epithelium

Adapted from (Groves, 2010) and (Li and Forge, 1997). Following aminoglycoside -induce d hair cell loss, the mammalian utricle is able to regenerate some vestibular hair cells by transdifferentiation; a supporting cell converts into a hair cell. This thesis aims to investigate the hypothesis that integrins are expressed in the utricle – they would be expected to be localised to supporting cell contacts with the basement membrane. The process of transdifferentiation has been shown to involve the detachment of the supporting cell from the basement membrane, as shown by TEM (see insets) in gentamicin-treated guinea pig utricles at 4 weeks post-treatment (Li and Forge, 1997). It would be anticipated that this detachment from the basement membrane would involve breakdown of integrin-mediated linkages between this membrane and converting supporting cells, potentially resulting in changes in integrin expression and localisation within the vestibular epithelium.

1.3 Scope of the Thesis

The sensory epithelium of the mammalian utricle has been shown experimentally to possess a limited capacity for spontaneous regeneration of hair cells lost due to exposure to ototoxic aminoglycosides. Both *in vivo* and *in vitro* studies have observed the emergence of new vestibular hair cells at 3 to 4 weeks post drug treatment, including the appearance of short stereocilia which resemble the morphology of immature hair bundles seen during development of the vestibular epithelium. Since the mammalian auditory epithelium, the organ of Corti, does not possess this same ability to regenerate lost hair cells, investigation as to which proteins and signalling pathways contribute to the regenerative capabilities of the utricle is of great significance. A comprehensive understanding of the regenerative process in the vestibular epithelium would be beneficial in terms of treating vestibular disorders or dysfunction related to ageing – mammalian vestibular regeneration has been shown experimentally as being by no means completely able to replace hair cells to replicate the numbers present in normal adult tissue. It would also be of interest to establish whether auditory hair cell regeneration could be induced in the organ of Corti via the same mechanisms e.g. gene therapy could be utilised to induce expression of key proteins for regeneration which the auditory epithelium lacks.

Integrins, as cell surface receptors, are involved in a wide range of cellular processes including proliferation, differentiation and migration, in addition to their key role in cellular adhesion to both the extracellular matrix and neighbouring cells. In other organ systems, several integrin heterodimers have been implicated as being critical for tissue repair e.g. in the skin during the re-epithelialisation stage of wound healing. During regeneration of vestibular hair cells, numerous cellular changes occur in which integrins could be expected to be involved, including cellular spreading of supporting cells to seal the epithelium, proliferation of supporting cells and detachment from the basement membrane of supporting cells undergoing phenotypic conversion to become hair cells. The work carried out in this study is therefore based upon the hypothesis that integrins would be expected to be expressed within the tissue of interest, in particular at the region of contact between the supporting cells and the basement membrane, and that the expression and localisation of integrins could be anticipated to alter in response to aminoglycoside-induced hair cell loss based upon knowledge of the cellular processes

of hair cell death and spontaneous regeneration which occur in the vestibular epithelium of mammals.

Prior to this work, the presence of integrins and their distribution within the mammalian utricle was largely unknown. This thesis aims to investigate the presence of the integrin family within the adult mouse utricle, in terms of which of the 18 α and 8 β integrin subunits are present normally in this tissue and their distribution within both the sensory epithelium and the underlying connective tissue. The first results section of this thesis focuses on the use of degenerate PCR (polymerase chain reaction) in order to identify the integrins expressed in normal utricular cDNA. In order to study integrins in a regenerating vestibular epithelium, the next section of this thesis describes *in vitro* culture experiments using utricles dissected from adult mice, and the progression of hair cell loss and subsequent regeneration at several time points following aminoglycoside treatment, establishing a model tissue for the study of integrin expression. The final results sections of this thesis centre around experiments using the organotypic culture model of vestibular hair cell loss and regeneration for immunolabelling of integrin subunits in order to investigate any potential changes in their distribution, and for quantitative PCR analysis to investigate changes in expression level during hair cell death and subsequent regeneration. Short discussion sections are included where appropriate immediately following the relevant results; however, discussion of the majority of the results of this work is within a dedicated discussion section as the last chapter of this thesis.

Chapter 2: Materials and Methods

All experimental work presented in this thesis was carried out by N. Stanley unless otherwise specified in this chapter.

2.1 Animals

Utricular maculae were obtained from adult, at least P21 (postnatal day 21), CBA/Ca mice, purchased from Harlan. Animals were sacrificed by CO_2 inhalation and subsequent cervical dislocation in accordance with Schedule 1 of the United Kingdom Animals (Scientific Procedures) Act of 1986.

2.2 Cryosectioning

2.2.1 Inner Ear Sectioning

Following sacrifice of the animals, auditory bullae were dissected from surrounding tissue. Cochleae and vestibular endo-organs were removed in Hanks Buffered Salt Solution (HBSS), with 10mM Hepes solution added (Sigma). Several perforations were made in the bony areas of each bulla using forceps to allow the fixative to perfuse throughout the entire cochlea and ensure thorough fixation of the inner ear tissues. Inner ears were fixed in 4% paraformaldehyde (PFA) for 1.5 hours and then decalcified in 4.13% ethylenediamine tetraacetic acid disodium (EDTA) in phosphate buffered solution (PBS) for 48 hours at 4^{o}C to allow frozen sectioning through the bony structures of the inner ear. In preparation for cryosectioning, cochleae were incubated overnight in 30% sucrose in PBS, to prevent damage from ice crystal formation. A 1% low-gelling temperature agarose gel containing 18% sucrose in PBS was used to embed the tissue in 35mm petri dishes. These dishes were then sealed with Parafilm® to prevent the samples from drying out and stored at 4°C until required.

For cryostat sectioning, a block of agarose containing a single cochlea was cut out from the petri dish and mounted on a chuck using Tissue-Tek® OCT compound (Sakura). Mounted blocks were rapidly frozen by submerging in liquid nitrogen and were then placed inside the cryostat chamber at -25°C to equilibrate before sectioning. Frozen sections of 14µm were sliced through the entire inner ear using a Leica CM1900 cryostat at -25°C until the utricular maculae was reached, whereupon these cryosections were picked up on poly-L-lysine coated slides (VWR); the coating on these slides enhances cellular adhesion to the glass surface, preventing sectioned tissue from being

lost during solution changes. Slides were then incubated in a 37°C oven for 30 minutes to dry before being stored at -20°C until required for immunohistochemistry.

2.2.2 Sectioning of Organotypic Cultures

Utricles which had been maintained in culture were fixed for 1 hour in 4% PFA. Fixed utricles were then prepared for cryosectioning by overnight incubation in 30% sucrose. The tissue was not removed from the filter paper on which it had been grown *in vitro*; small squares, each containing one utricle, were cut from the filter paper and these were then embedded in agarose. This approach allowed the orientation of the tissue to be more easily determined to obtain the required sections. Blocks of agarose containing each utricle were mounted and sectioned in the same way as previously described in 2.2.1 for whole inner ear cryosectioning.

2.3 Immunohistochemistry

2.3.1 General Immunohistochemistry

All tissue (wholemount and cryostat sections) was fixed for 1hr in 4% PFA as described in 2.2.1 and 2.2.2.

A 72-well plate was used for wholemount utricle immunohistochemistry, with the required solutions placed in separate wells – this allowed the utricles to be transferred from well to well, reducing the likelihood of any tissue being removed with discarded solution. For cryostat sections on glass slides, a 'PAP' pen (Sigma) was used to create a hydrophobic barrier around the sections to contain solutions applied during immunostaining.

Cryostat sections and wholemount utricles were incubated with 0.5% Triton X-100 (TX-100), a non-ionic surfactant detergent used to permeablise cell membranes to facilitate the penetration of antibodies into cell bodies during immunostaining, for 20 minutes. Samples were subsequently blocked for 1 hour with 'block' (consisting of 10% horse serum [in order to reduce the incidence of non-specific primary antibody binding] and 0.1% Triton in PBS). The use of serum as a block for immunohistochemistry experiments is based upon the principle of incubating a sample with a solution which contains a high concentration of large proteins and antigens. These antigens will therefore 'block' the tissue, preventing the primary antibody from binding non-

specifically to the sample being immunolabelled, thus reducing the background signal. Samples were subsequently incubated with primary antibody in Lysine-PBS block (0.182g L-lysine in 10ml PBS) overnight at 4°C, unless otherwise stated for a specific primary antibody. The use of lysine, an amino acid, provides an additional block of non-specific binding sites which could potentially interact with the primary antibody during incubation. Table 2-1 lists all primary antibodies used in this project. Following the removal of the primary antibody solution, specimens were washed for 5 minutes in PBS solution; this washing was repeated 3 times in order to remove any remaining unbound primary antibody. Samples were then incubated with an appropriate fluorescently tagged secondary antibody and/or phalloidin in Lysine-PBS block solution for 2 hours at room temperature. Table 2-2 lists all secondary antibodies and conjugated fluorophores used in this project. The samples were protected from light at this point in order to prevent photobleaching of the immunofluorescence. At the end of this incubation period, the secondary antibody solution was removed and the specimens were washed 3 times (for a period of 5 minutes per wash) with PBS solution to remove any remaining unbound antibody/fluorophore.

Immunolabelled cryostat sections were covered with glass coverslips, after the addition of Vectashield™ mount with 4,6-diamidino 2-phenylindole (DAPI). DAPI is able to bind to A-T rich regions of double stranded DNA and is also capable of penetrating intact cell membranes. These properties mean that DAPI is able to selectively label cell nuclei. Wholemount utricles were removed from the 72-well plate and mounted on slides containing individual wells (C A Hendley) using Vectashield™ with DAPI and a glass coverslip. Coverslips were sealed to slides with nail varnish to prevent drying out and stored at 4°C until required for imaging.

	Protein	Type; Host Species	Concentration	Supplier
Integrins				
	α6	Monoclonal; Rat	1:200	Serotec
	αV	Monoclonal; Mouse	1:200 (with TSA amplification kit)	BD Biosciences
	β1	Monoclonal; Rat	1:1000	BD Biosciences
	β3	Polyclonal; Rabbit	1:200	Novus Biologicals
	β5	Polyclonal; Rabbit	1:100	Millipore
Hair Cell Markers				
	Myosin Viia	Monoclonal; Mouse	1:250	National Hybridoma Bank
	Calretinin	Polyclonal; Rabbit	1:100	Chemicon
ECM Proteins				
	Collagen Type IV	Polyclonal; Rabbit	1:1000	Abcam

Table 2-1 Primary antibodies used for immunohistochemistry

Secondary Antibody/Conjugated Fluorophore	Host	Concentration	Supplier
Anti-Rabbit IgG TRITC	Pig	1:500	Dako
Anti-Rabbit IgG FITC	Pig	1:500	Dako
Anti-Rat IgG FITC	Goat	1:500	Sigma
Anti-Mouse IgG TRITC	Rabbit	1:500	Dako
Anti-Mouse IgG FITC	Rabbit	1:500	Dako
Phalloidin-FITC	N/A	1:1000	

Table 2-2 Secondary antibodies and other conjugated fluorophores used for immunohistochemistry

2.3.2 Antibody Amplification using a Tyramide Signal Amplification Kit

The integrin αV antibody, subsequent to testing at a series of dilutions of both the primary and secondary antibody, required the use of an amplification kit in order to visualise the antibody sufficiently in inner ear tissue. It is possible that there was insufficient integrin αV antigen present in the tissue of interest, resulting in poor detection of this integrin using a standard immunohistochemistry protocol. Integrin αV is the alpha subunit able to form the most functional integrin heterodimers, therefore its presence would be expected in the inner ear. The use of a TSA amplification system can improve sensitivity without increasing the level of background staining observed. In this instance, a TSA amplification kit (TSA kit #4 with HRP, goat anti-mouse Ig and Alexa Fluor® 568 tyramide; Invitrogen, Paisley) was selected, since the integrin αV primary antibody being used was a mouse monoclonal antibody.

In accordance with the product protocol, samples (either wholemount utricles or utricle cryosections) were permeablised with 0.1% Triton X-100 for 10 minutes. After rinsing

with PBS, the samples were then incubated in 1% blocking reagent (as supplied in the kit) for 1 hour at room temperature, before a further 1 hour incubation period with the integrin αV antibody diluted 1:200 in 1% blocking reagent. Following three 5 minute washes with PBS to remove any unbound primary antibody, the samples were incubated with a horseradish peroxidase (HRP) conjugate solution for 30 minutes. The TSA amplification system utilises an enzyme (in this case HRP) which is conjugated to a secondary antibody – in this case an anti-mouse secondary antibody in order to detect the mouse monoclonal integrin αV primary antibody. The HRP conjugate solution was removed from the samples by a further 3 washes with PBS and these were then incubated with an Alexa Fluor® 568 tyramide working solution (covered to protect the fluorophore from photobleaching), with the tyramide dye diluted 1:100 in amplification buffer (containing H_2O_2) for 10 minutes. In the presence of H_2O_2, HRP activates the tyramide coupled dye, resulting in the production of highly reactive, short lived tyramide radicals. These molecules are deposited in regions in direct proximity to the original HRP secondary conjugate bound to the primary antibody; in this way the signal is amplified, but with minimal loss of resolution and minimal background signal production. The samples were again washed 3 times with PBS to remove the excess tyramide solution. Any further immunohistochemistry required on these samples was then carried out as previously specified.

2.3.3 EdU Labelling

In order to investigate proliferation within utricular cultures, a Click-iT™ EdU Alexa Fluor® 488 imaging kit, supplied by Invitrogen was used. This imaging method uses 5-ethynyl-2'-deoxyuridine (EdU), a nucleoside analog of thymidine, which may be incorporated into DNA during the S-phase of cellular proliferation. EdU was used as an alternative to 5-bromo-2'-deoxyuridine (BrdU), since it does not require denaturation of the DNA by treatment with HCl in order to be detected. The HCl treatment required for BrdU labelling is liable to disrupt the tissue of interest, with the potential for the damage and destruction of antigen sites which could adversely affect any further immunohistochemistry experiments required to be carried out on EdU labelled samples. The EdU detection system with which cell proliferation experiments were carried out utilises a 'Click' reaction, a copper catalysed covalent reaction between an azide (the

Alexa Fluor® 488 dye) and an alkyne (the EdU), in order to visualise EdU within cell nuclei, as opposed to BrdU, which requires the use of anti-BrdU antibodies.

In accordance with the protocol provided by the manufacturer, utricles were cultured in the presence of a 10µM concentration of EdU. This was achieved by the addition of 10µl of 10mM EdU stock solution to 10ml of culture medium. EdU was not added to the culture medium until after the cultures had been treated with gentamicin in order to only detect proliferation which occurred subsequent to damage and hair cell loss induced by the ototoxic antibiotic.

Following fixation and/or cryostat sectioning, cultures incubated with EdU were washed with 3% bovine serum albumin (BSA) prior to permeablisation with 0.5% Triton-X-100 in PBS for 20 minutes at room temperature. Whole utricles/utricular sections were then washed twice with 3% BSA to remove the permeabilisation solution and the Click-iT™ reaction cocktail prepared from the reagents supplied by the manufacturer; 215µl 1x Click-iT™ reaction buffer, 10µl $CuSO_4$, 0.6µl Alexa Fluor® 488 azide and 25µl reaction buffer additive. The tissue to be labelled was incubated with the Click-iT™ reaction cocktail for 30 minutes at room temperature, whilst covered to protect the Alexa fluorophore from photobleaching. 3% BSA was used to wash the CIick-iT™ reaction cocktail solution off of the samples; any further immunohistochemistry required was then carried out as previously described.

2.3.4 Confocal Microscopy

Imaging of immunofluorescently labelled samples was carried out using a Zeiss Meta laser scanning confocal microscope using the x20 (dry) and x63 (oil) objectives. Z-series stack images were taken at optimised intervals; maximal pixel intensity projections were created from these series by the LSM Image Browser software. For comparative imaging of integrin antibodies in tissue at different time points post-gentamicin treatment, the same confocal settings were used throughout the imaging process.

2.3.5 Cell Counts

Quantification analysis of hair cell numbers was carried out from x63 magnification z-stack confocal images of cultured utricles immunolabelled for the hair cell marker

myosin Viia. For the purposes of this study, hair cells were defined as those cells which were positive for the marker myosin Viia within their cell body. Each utricle studied was sampled 2-3 times; each sample consisted of a x63 image, with an area of 146.2μm x 146.2μm. Samples were randomly selected within the intact region of each individual utricle. Intact, well preserved regions of the tissue were assessed through examination of the quality of the fluorescent labelling of cellular junctions produced by phalloidin staining. Cell counts were carried out using Image J software. Hair cell counts from the samples of each utricle were averaged; these average counts were then normalised – this data is expressed as the number of hair cells per 1000μm^2. Since the data collected from hair cell counts was taken from more than two groups, an analysis of variance (ANOVA) test was selected for carrying out statistical analysis, as opposed to a T-test. The ANOVA statistical test allows the means of multiple groups (in the case of the experiments carried out in this project, this represents the means hair cell counts at multiple time points following gentamicin treatment and non-treated control groups) to be compared. The null hypothesis of the ANOVA test is that the means of each of the groups are equal, representing random samples of the same population and that the experimental conditions applied to each group have no significant effect on the variable being measured i.e. hair cell numbers.

A one-way ANOVA statistical analysis was used, since there was data from a single independent variable (hair cell number) to be compared across the groups investigated; this statistical test was carried out using GraphPad software. Post-hoc analysis of the ANOVA was then carried out using Tukey's Test. This statistical test was used in conjunction with one-way ANOVA, in order to compare all possible pairs of cell count mean values, in order to determine which experimental conditions showed hair cell counts which were significantly different from one another.

Quantification analysis of EdU labelled cell numbers was carried out in the same manner as described for hair cell counts. Utricular cultures incubated with EdU were stained with DAPI in order to visualise all cell nuclei. A Click-iT™ EdU Alexa Fluor® 488 imaging kit was used to visualise all cell nuclei which had incorporated EdU into their DNA. Total cell counts e.g. all cells with DAPI-positive nuclei, in addition to counts of all nuclei positive for EdU were carried out using Image J software. Cell counts were averaged from the samples of each individual utricle studied and the data

normalised in order to be expressed as the number of nuclei/EdU-positive nuclei per 1000 μm^2.

2.4 Scanning Electron Microscopy

Cultured utricles to be analysed by scanning electron microscopy were removed from culture medium but remained attached to the nitrocellulose filter paper culture surface. Tissue was fixed in 2.5% glutaraldehyde in 0.1M sodium cacodylate buffer pH 7.3 with 3mM $CaCl_2$ for 1.5 hours and then post-fixed with 1% OsO_4 in 0.1M cacodylate. Post-fixed tissue was then processed for SEM by a repeated thiocarbohydrazide-osmium procedure prior to dehydration of the samples through an ethanol series to 100% dry ethanol. Specimens were subsequently critical point dried from liquid CO_2 and mounted on stubs using silver paint (Ted Palla) before being sputter coated with gold. Prepared specimens were viewed and digitally imaged using a JEOL JSM 6700F cold field emission instrument, operating at 5Kv. All digital images were adjusted for optimal contrast and brightness using Photoshop CS4 software. Processing of SEM specimens was carried out by G. Nevill and Prof A. Forge.

2.5 Transmission Electron Microscopy

Cultured utricles to be analysed by transmission electron microscopy were removed from culture medium but remained attached to the nitrocellulose filter paper culture surface. Tissue was fixed in 2.5% glutaraldehyde in 0.1M sodium cacodylate buffer pH 7.3 with 3mM $CaCl_2$ for 1.5 hours and then post-fixed with 1% OsO_4 in 0.1M cacodylate. Post-fixed tissue was then processed for TEM by partial dehydration to 70% ethanol and then *en bloc* stained in saturated uranyl acetate in 70% ethanol overnight. Dehydration was subsequently completed to 100% ethanol (samples require dehydration due to being placed into a vacuum for imaging by electron microscopy – if the samples were to contain water, this would evaporate when the sample was subject to a vacuum, potentially resulting in damage to the structural integrity of the tissue of interest) and specimens embedded in plastic. Initial thick sections (~1µm) were cut and stained with toluidine blue for examination under light microscope. Thin sections (80nm) were then cut and stained with uranyl acetate and lead citrate before being examined by a JEOL 1200EXII fitted with a Gatan digital camera; the microscope was operated at 80 Kv. Processing and imaging of utricle cultures by TEM was carried out by G. Nevill and

Prof. A. Forge. All digital images were adjusted for optimal contrast and brightness using Photoshop CS4 software.

2.6 Culture of Adult Mouse Utricles

Adult mice were killed in accordance with Schedule 1 of the Home Office Animals (Scientific Procedures) Act 1986. Bullae were dissected from the animals by removal of the lower jaw and bisection of the head. Subsequent removal of the brain tissue from the bisected heads allowed access to dissect the entire bullae from the animal; the bullae were then transferred to petri dishes containing a Hanks Balanced Salt Solution containing 1M Hepes (4-[2-hydroxyethyl]-1-piperazineethanesulfonic acid) buffer solution, whereupon the utricular maculae were dissected out from the whole inner ear using heat sterilised forceps. The otolithic membrane which overlies the utricle and the otoconia on the surface of the sensory epithelium were each carefully removed with forceps. Dissected utricles were removed of any extraneous tissue i.e. from attachment to the cristae of the vestibular system; it is often the case that during dissection the utricle will be removed with several cristae attached to it. It was the aim of these dissection methods to ensure that only the utricular sensory epithelium and the mesenchymal tissue directly beneath it were placed into culture. All dissection for organotypic cultures was performed under sterile conditions.

Culture medium was made up under sterile conditions and stored at -20°C until required. 1ml of 1M Hepes buffer solution was added to 100ml of Gibco® GlutaMAX™ minimum essential medium containing Earles Salts (Invitrogen). 10ml of this solution was removed and stored in a 15ml Falcon tube; this media was used to make up laminin solutions. To the remaining 90ml of media, 10ml of sterile horse serum was added and the media aliquoted out into 15ml Falcon tubes, each containing 10ml of media – this media (MEM + GlutaMAX™ + 1% Hepes + 10% Horse Serum) was used to maintain organotypic cultures.

Two different methods for maintaining utricles in culture long-term were investigated in this work; the development of the culture technique is described in detail in 4.1. Initially, MatTek™ dishes (MatTek Corp) were coated with laminin (diluted at 1:75 concentration with serum-free culture medium) by placing 200µl of laminin solution onto the glass bottom of the dish and allowing at least one hour before removing the

surplus solution. Dissected utricles were then placed onto the coated region and sufficient culture medium added to completely cover the tissue.

The culture technique was refined during the initial stages of this project and a different culture surface selected. Round 13mm diameter 0.45µm micropore nitrocellulose membrane filters (Millipore) were placed into the wells of a 24-well plate and dissected utricles placed onto the filter paper in each well, before being covered with 450µl of culture medium. It was observed that within 24-48hrs of incubation, the tissue had adhered to the nitrocellulose surface, facilitating the changing of culture media without disturbing the tissue.

During the culture time period, the tissue was maintained at 37°C in an incubator; culture medium was changed every other day. Where cultures were treated with gentamicin to induce hair cell loss, a solution of 2mM gentamicin diluted in normal culture medium was used over a 48hr incubation period. Tissue was then rinsed with medium to remove residual gentamicin and placed in fresh culture medium for the rest of the incubation period.

2.7 Real-Time PCR (Polymerase Chain Reaction)

2.7.1 Tissue

Normal uncultured utricles were dissected from the whole inner ear using forceps in HBSS + 1M Hepes, in the same way as utricular maculae were dissected for organotypic culture experiments. Utricles were placed immediately into labelled Eppendorf tubes containing RNA Later (Invitrogen) to prevent RNA degradation and stored at -80°C until required. These utricles were used to obtain a cDNA sample to be used as the control (calibrator) sample for relative quantification analysis.

Where PCR (polymerase chain reaction) experiments required RNA to be extracted from cultured tissue, utricles were maintained *in vitro* as described in 2.6 for the culture of adult mouse vestibular epithelium. Once the required culture time point was reached, utricles were removed from the nitrocellulose filter paper upon which they had been maintained, placed immediately into RNA Later and stored at -80°C.

Positive control tissue was obtained from adult mice; this tissue was lung, spleen and kidney. Each tissue was placed in RNA Later directly after dissection from the animal and stored at -80°C.

2.7.2 RNA Extraction

RNA extraction was performed using an RNeasy Mini kit (Qiagen) as detailed in the product protocol handbook. Tissue which had been stored at -80°C in RNA Later was allowed to defrost to room temperature. Each positive control tissue was cut and weighed in order to only use 30mg of tissue as recommended, and placed into 600µl buffer RLT containing β-mercaptoethanol (10µl/ml) to be disrupted and homogenised using a rotor-stator homogeniser. The addition of β-mercaptoethanol (β-ME) to the buffer provides additional protection against RNA degradation; β-ME reduces disulphide bonds and is therefore able to irreversibly denature any RNAses which might be present in the sample. Utricular tissue, due to its small size, was disrupted in 600µl buffer RLT containing β-ME by passing the tissue through a 20G needle attached to a sterile syringe twenty times. Subsequently, the utricular lysate was placed into a Qiashredder (Qiagen) spin column with a 2ml collection tube and centrifuged for 2 minutes at full speed (13,000rpm).

Tissue lysate was centrifuged at full speed for 3 minutes; the supernatant was removed by pipette and transferred to a fresh Eppendorf tube, taking care not to disturb any pellet which had formed during centrifugation. Each sample was subsequently processed by successive centrifugation steps as described in the kit protocol handbook.

To aid in the complete removal of ethanol from the extracted RNA, following the final wash centrifugation, the Qiaspin columns were placed in a heat block at 55°C for 1 minute.For the final elution step, 30µl of RNAse free water was used.

The concentration of RNA obtained from the extraction for each sample was measured using a Nanodrop 1000 spectrophotometer (Thermo Scientific).

2.7.3 Reverse Transcription of cDNA

Reverse transcription of extracted RNA to cDNA was performed using a Sensiscript™ Reverse Transcription Kit (Qiagen) as directed in the protocol supplied with this kit. Additional reagents required for the use of this kit were primers for the reaction, for

which Oligo dT primers (which bind to the poly A tail of mRNA) were used (Invitrogen) and a mouse RNAse inhibitor (NEB) which was diluted to the specified final concentration using a 1x solution of the 10x Buffer RT (diluted in RNAse-free water). The reaction cocktail also contained a dNTP mixture supplied in the Sensiscript™ kit consisting of a 5mM concentration of each dNTP. An appropriate volume of RNA was added to each reaction based on the sample concentration (larger tissues e.g. spleen produced higher concentrations of RNA during the extraction process than utricular tissue; the kit protocol recommends that no more than 50ng of RNA should be used per 20µl reaction volume).

Reverse transcription reactions were carried out by placing Eppendorf tubes containing the reaction mix into a heat block at 37°C for 1 hour. At the end of the reverse transcription reaction, the cDNA concentration of each sample was measured using a Nanodrop 1000 Spectrophotometer. cDNA samples were stored at -20°C until required.

2.7.4 Degenerate PCR Primers

Initial RT-PCR experiments were carried out using several sets of degenerate primers, the design process of which is discussed fully in the relevant results chapter. Design of degenerate primers was carried out in collaboration with Dr. S. Dawson. Degenerate primers (Eurofins MWG Operon) were supplied in a lysophilsed state. Each primer was re-suspended in freshly autoclaved double-distilled H_2O, to produce a 100µM primer stock solution. A working solution of 10µM was diluted from this stock solution for use in PCR reactions.

In order to optimise the reaction conditions for each primer pair, initial PCR experiments were carried out on a temperature gradient to determine the optimal annealing temperature i.e. the temperature at which the primers will bind to the template DNA strand. Further refinements were applied as necessary; several primer pairs required an alteration to the concentration of $MgCl_2$ used. The optimised RT-PCR reaction conditions for each set of degenerate primers is summarised in table 2-3. The thermal cycling process for degenerate PCR experiments was carried out by an Eppendorf Mastercycler Gradient PCR machine, using a 3-step PCR reaction i.e. one with individual denaturation (of the double stranded cDNA), annealing and extension (where the DNA polymerase extends the primers and synthesises a new strand of DNA) temperatures.

2.7.5 Integrin Subunit Specific PCR Primers

A small set of specific PCR primers were designed to amplify each of a group of 5 integrin subunits which were believed likely to be expressed in the tissue of interest, but which had not been successfully detected by degenerate PCR; α6, β1, β3, αV and α8.

The primer sequence for each of these integrin subunits are as follows:

Integrin α6 (Forward: 5'-CCTAACAGAATTGACCTCCGCCAGAAG-3';

Reverse: 5'-ACTGAACTCTCGATGACAACCCTGA-3'),

Integrin αV (Forward: 5'-GCCAGACCCGTTGTCACTGTAAATGC-3';

Reverse: 5'-CGTCGGATGGCTCCCTTCTGCTTGAG-3'),

Integrin α8 (Forward: 5'-CCTTCAAGCAAGCGCCCTCCTCTTCC-3';

Reverse: 5'-GCTTGCTGTGTAAACCTCTTGGGG-3'),

Integrin β1 (Forward: 5'-GGAAACTCTAGTAATGTGATCCAGC-3';

Reverse: 5'-CACTTGGGACTGGCTGGGATGCCATG-3') and

Integrin β3 (Forward: 5'-GGGCTGATGACTGAGAAACTATCCCAG-3';

Reverse: 5'-CACGTACTTCCAGCTCCACTTTAGA-3').

Specific primers of a length of 22-25bp were designed, spanning across an exon-exon junction in order to prevent the amplification of any contaminating genomic DNA during the PCR reaction, for the detection individually of each of the selected integrins. The T_m of each forward and reverse primer was assessed using the OligoCalc online tool to ensure that these temperatures were within the optimum range. This tool was also used to check for potential self-complementarity, which would affect the efficiency of the primers and their ability to bind to the template DNA. The specificity of these primers was confirmed by BLAST analysis (http://blast.ncbi.nlm.nih.gov/Blast.cgi).

Specific integrin subunit primers (Sigma) were re-hydrated with ddH_2O to produce a stock 100μM solution of each primer. Optimisation of reaction conditions was carried out as previously described, by using a temperature gradient to determine the optimum annealing temperature for each primer pair and subsequently altering the concentration

of $MgCl_2$ in the reaction master mix. The optimised PCR conditions for each integrin subunit are summarised in table 3-5.

Forward Primer	Reverse Primer	PCR Conditions
Intaall1F	IntaxmdeR	3-Step RT-PCR
		Annealing Temp = 55°C
		$MgCl_2$ concentration = 2mM
		cDNA = 1µg
Inta2110bF	Intaall1R	3-Step RT-PCR
		Annealing Temp = 55°C
		$MgCl_2$ concentration = 5mM
		cDNA = 2µg
Inta82b5vF	Inta75v82bR	3-Step RT-PCR
		Annealing Temp = 55°C
		$MgCl_2$ concentration = 5mM
		cDNA = 2µg
Inta673F	Inta8673R	3-Step RT-PCR
		Annealing Temp = 55°C
		$MgCl_2$ concentration = 4mM
		cDNA = 2µg
Inta49Fb	Inta49Rb	3-Step RT-PCR
		Annealing Temp = 55°C
		$MgCl_2$ concentration = 2mM
		cDNA = 1µg
Intb28F	Intb28R	3-Step PCR
		Annealing temperature = 55°C
		$MgCl_2$ concentration = 2mM
		cDNA = 1µg
Intb147F	Intb147R	3-Step PCR
		Annealing temperature = 55°C
		$MgCl_2$ concentration = 2mM
		cDNA = 1µg
Intb356Fb	Intb356R	3-Step PCR
		Annealing temperature = 55°C
		$MgCl_2$ concentration = 2mM
		cDNA = 1µg

Table 2-3 Summary of Optimised Reaction Conditions for Degenerate PCR Primers

2.7.6 Agarose Gel Electrophoresis of RT-PCR Products

All RT-PCR products (whether amplified using degenerate or specific primers) were run on an agarose gel to determine whether the PCR had been successful and if the DNA fragments produced were of the size expected based on the amplicon designed to be produced by each primer pair; the use of an agarose gel allows DNA fragments of different sizes to be separated and identified using a DNA ladder as a reference point.

Agarose gels were produced by adding the appropriate weight of agarose to 100ml of 1xTAE buffer (2.0 M Tris, 1 M Glacial acetic acid, 50 mM EDTA, pH 8.0) in a conical flask. This solution was heated until the agarose had completely melted before being allowed to cool. In order to visualise the DNA under ultraviolet light, 2µl ethidium bromide was added to the agarose solution prior to pouring into a gel mould; plastic combs were used to create the required number of wells in the gel and this was left to cool and set for 30 minutes. Several different agarose % gels were used to run PCR products on, depending on the size of the expected DNA fragments, and in the case of latter experiments, whether multiple DNA fragments of different sizes required separation by gel electrophoresis. An appropriate DNA ladder (100bp or 1kb; NEB/Invitrogen) was used in order to estimate the size of the DNA fragments run on the gel.

Gel electrophoresis was run by placing the gel in the apparatus filled with 1x TAE buffer and applying an electrical field of approximately -70mv for 30 minutes. DNA run on agarose gels was visualised by the use of a GelDoc-It 3UVTM Transilluminator Imaging system (Jencons-PLS) using the UV-B setting (302nm) and still images of the illuminated gels captured using Labworks (UVP BioImaging Systems) software.

2.7.7 Extraction of PCR Products from Agarose Gel

Since identification of the DNA fragments amplified by degenerate primers required the utilisation of cloning, PCR products which had been detected by gel electrophoresis required extraction from the agarose gel through which they had been run. Gel extraction was carried out using a QIAquick gel extraction kit (Qiagen).

Each DNA band was cut from the agarose gel using a scalpel blade whilst being visualised on a UV lightbox and placed into a 1.5ml Eppendorf tube. Each gel slice was weighed using a digital balance and 3 volumes of Buffer QG from the kit added for

every 1 volume of agarose gel. For the purposes of this protocol 100mg of gel was equivalent to 100µl of buffer solution.

The gel extraction process was carried out by microcentrifugation as described in the protocol supplied for this kit. In order to facilitate the removal of residual ethanol prior to the elution of the DNA fragments, the spin columns were placed on a heat block at 55°C for 1 minute.

2.7.8 Purification of PCR Products

PCR products which were required for use in ligation reactions were first purified, in order to remove leftover primers and any other impurities which might adversely affect subsequent experiments carried out using these DNA fragments, by the use of a QIAquick PCR purification kit (Qiagen).

The purification process was carried out by microcentrifuge as described in the protocol supplied with this kit. In order to facilitate the removal of residual ethanol prior to the elution of the DNA fragments, the spin columns were placed on a heat block at 55°C for 1 minute. The final elution step was carried out using 30µl of RNAse-free water.

2.8 Cloning of PCR Products Using the pGEM®-T Easy Vector System

2.8.1 Ligation Reactions

In order to clone the PCR products obtained from degenerate RT-PCR experiments, the DNA fragments were ligated into the plasmid vector pGEM®-T Easy (Promega). The use of cloning via a plasmid vector allowed the production of a larger volume of the PCR products generated from the degenerate PCR reactions carried out. This facilitated the analysis of the PCR products in order to determine which integrin subunit amplicons were present in each reaction sample.

The pGEM®-T Easy vector used contains an ampicillin resistance gene, allowing for selection of bacteria which have taken up the vector by growing transformed cells on agar plates containing ampicillin. This plasmid also contains the lac operon, a collection of genes, including the enzyme β-galactosidase, and associated regulatory sequences required by bacteria in order to metabolise lactose. The cloning region of the pGEM®-T Easy vector is located within the lac operon, thus if a plasmid has successfully

incorporated a DNA fragment during the ligation stage of the cloning procedure, the lac operon sequence will be disrupted and non-functional. Successfully cloned bacteria maybe therefore be identified by growing cultures on agar plates which have had X-gal and IPTG added. IPTG (isopropylthio-β-galactoside) acts as an inducer of the lac operon, whilst X-gal (5-bromo-4-chloro-3-indolyl-beta-D-galacto-pyranoside) is an analog of lactose which can be metabolised by β-galactosidase. If no DNA fragment has been ligated into the plasmid, the lac operon will be fully functional, and the bacterial colony containing this vector will be able to produce β-galactosidase and metabolise X-gal; this is detectable since unmetabolised X-gal is colourless, whilst the product of its cleavage by β-galactosidase are blue. Colonies which contain plasmids with a DNA fragment insert will therefore appear white, whilst those bacteria containing an unligated vector will appear blue, since they possess an uninterrupted lac operon.

Each reaction was set up in a 0.5ml Eppendorf tube containing the following; 2.5µl 2x Rapid Ligation Buffer (Promega), 0.5µl pGEM®-T Easy vector, 0.5µl T4 DNA ligase (Promega) and 1.5µl of the purified PCR products. This gave a final reaction volume of 5µl. The ligation reactions were carried out overnight at 4°C.

2.8.2 Preparation of Agar Plates for Bacterial Culture

LB-Agar was made up with 5 g tryptone, 2.5 g yeast extract, 5 g NaCl and 1.5% agar in 500ml distilled water and autoclaved for 45 minutes. LB-Agar was stored at room temperature until required; this medium was melted in a microwave and maintained in a water bath at 55°C prior to pouring. To this molten LB-agar 500µl Ampicillin, 500µl of X-gal and 500µl IPTG were added, swirling the bottle to mix before pouring into petri dishes and allowing to the plates to cool and set. Plates were stored at 4°C until required.

2.8.3 Cloning

For the cloning of PCR products, XL10-Gold Ultracompetent cells (Stratagene) were used, which were stored at -80°C until required.

14ml BD Falcon tubes were pre-chilled, one per ligation reaction, whilst the ultracompetent cells were thawed on ice. Each tube was aliquoted 50µl of cells, and then to each tube 2µl of β-mercaptoethanol (Stratagene) was added, swirling the tubes

gently to mix. The cells were kept on ice for 10 minutes, with swirling repeated every 2 minutes. 1µl of ligation reaction was then added, swirling to mix and the tubes left to incubate on ice for 30 minutes. A 30 second heat-shock was given by placing the tubes into a water bath set at 42°C; following heat-shock the tubes were placed immediately back on ice for a further 2 minutes. To each tube 0.45ml of NZY+ broth which had been preheated to 42°C was added. NZY+ broth was made up as follows; 10g of NZ amine (casein hydrolysate), 5 g of yeast extract, 5g of NaCl and deionised water added up to 1L.The pH was adjusted 7.5 using NaOH and the broth was then autoclaved. Filter-sterilized supplements - 12.5 ml of 1 M $MgCl_2$, 12.5 ml of 1 M $MgSO_4$ and 20 ml of 20% (w/v) glucose were added prior to use of the NZY+ broth. The cloning tubes were then placed in a shaker set at 250rpm/37°C for 1 hour.

Following this incubation, each transformation reaction was plated onto an Amp/X-gal/IPTG agar plate. Plates were incubated at 37°C overnight and then examined for colonies using blue-white screening (white colonies contain an insert into the pGEM®-T easy vector, thus disrupting the Lac operon; blue colonies will not contain an insert). White colonies from each plate were 'picked' using a sterile pipette tip which was then dropped into a sterile bottle containing 5ml LB broth. LB broth was made up with 10g tryptone, 5g yeast extract and 10g NaCl. Distilled water was added to 1L, ensuring that the pH was around 7.0. The solids were dissolved in the water then the broth poured into bottles before autoclaving for 30-45 minutes. For each plate, in order to give a representative sample of the PCR product inserts which might have been cloned, 20 colonies were 'picked.' The 'picked' colonies were grown overnight in a shaker at 250rpm/37°C and the resultant bacterial culture stored at 4°C until required.

In order to extract the plasmid DNA from the bacterial cells a QIAprep Miniprep kit (Qiagen) was used. A 1ml sample of the bacterial culture from each bottle was placed into individual 1.5ml Eppendorf tubes and these samples centrifuged at ≥8000rpm for 3 minutes at room temperature. This produced a 'pellet' of bacterial cells from which the remaining medium (supernatant) could then be removed. The plasmid DNA extraction was carried out as specified by the microcentrifugation protocol described in the handbook for this kit. In order to facilitate the removal of residual ethanol prior to the elution of the plasmid DNA, the spin columns were placed on a heat block at 55°C for 1 minute.

2.8.4 Restriction Digests of Plasmid DNA

In order to establish which of the potential integrin subunits had been detected by each set of degenerate primers, restriction enzymes were selected for use based on restriction mapping, such that they would produce easily identifiable band patterns, when run on an agarose gel. For each of the expected amplicons for the α and β integrin subunits, a restriction map was produced using the Restriction Mapper online tool to identify all of the restriction sites present (http://www.restrictionmapper.org/). These restriction maps were then used to select appropriate restriction enzymes. The restriction digest strategies for identification of integrin subunits are provided in tables 2-5 and 2-6.

Restriction digests were set up in 0.5ml Eppendorf tubes. The reaction mixture contained the following; 8µl autoclaved ddH_2O, 2µl of the appropriate buffer for the enzyme, 2µl restriction enzyme and 8µl plasmid DNA, giving a total reaction volume of 20µl. The reactions were incubated at a temperature appropriate for the enzyme being used for 1 hour. Table 2-4 summarises the restriction enzymes used and the conditions under which each reaction was performed. The products of the restriction digests were run on an agarose gel as previous described, on a gel weight appropriate for the expected fragment sizes required to be separated by electrophoresis. The resultant gels were viewed and imaged as described in 2.7.6.

Enzyme	Buffer	Reaction Temperature
EcoRI	Buffer H	37°C
RSAI	Buffer C	37°C
HaeIII	Buffer C	37°C
HaeII	Buffer B	37°C
SalI	Buffer D	37°C
HindIII	Buffer E	37°C
BglI	Buffer D	37°C
TaqI	Buffer E	65°C
NcoI	Buffer D	37°C
BamHI	Buffer E	37°C
XhoI	Buffer D	37°C
ApaI	Buffer A	37°C
PstI	Buffer H	37°C
SphI	Buffer K	37°C
EcoRV	Buffer D	37°C

Table 2-4 Summary of Restriction Enzymes and Digest Reaction Conditions

Forward Primer	Reverse Primer	Integrin Subunits	Restriction Digest Strategy
Intaall1F	IntaxmdeR	αX, αM, αD & αE	BglI digest = 2 band patterns; αX/αD and αM/αE
Inta2110bF	Intaall1R	α1, α2, α10 & α11	BamHI digest = linearises if α1 amplicon, does not cut other amplicons or the plasmid vector
			XhoI = linearises if α2 amplicon, does not cut other amplicons or the plasmid vector
			Rsa I digest = cuts all amplicons once except α10
			SphI digest = linearises if α11 amplicon, does not cut other amplicons or the plasmid vector
Inta82b5vF	Inta75v82bR	αV, αIIb, α5 & α8	Hae II digest = doesn't cut amplicon of αV or αIIb. Cuts α5/α8 amplicon once. Cuts vector 4 times.
			Apa I digest = linearises if αV, 2 cuts if αIIb
			Pst I digest = linearises if α8, 2 cuts if α5
Inta673F	Inta8673R	α3, α6 & α7	EcoRV = linearises if α7, does not cut α3 or α6
			Taq I digest = different banding patterns for α3 and α6. Taq I cuts vector 4 times.
Inta49Fb	Inta49Rb	α4 & α9	RSA I digest = 2 bands if α4
			RSA I digest = 1 band if α9

Table 2-5 Restriction Digest Strategies for Identifying α Integrins in Degenerate PCR Products

Outline of the restriction digests to be used to identify different α integrin amplicons from degenerate PCR products based on restriction mapping.

Forward Primer	Reverse Primer	Integrin Subunits	Restriction Digest Strategy
Intb28F	Intb28R	β2 & β8	Stu I digest = linearised if β2
			Nco I digest = 2 bands if β8
Intb147F	Intb147R	β1, β4 & β7	RSA I digest = 2 bands if β1
			Eco RI = 3 bands if β4
			HindIII digest = linearised if β7
Intb356Fb	ntb356R	β3, β5 &β6	Kpn I digest = linearised if β3
			Sal I digest = 2 bands if β5

Table 2-6 Restriction Digest Strategies for Identifying β Integrins in Degenerate PCR Products

Outline of the restriction digests to be used to identify different β integrin amplicons from degenerate PCR products based on restriction mapping.

2.8.5 DNA Sequencing

As an additional confirmation of which integrin subunits had been detected by degenerate PCR, samples of the plasmid DNA created in the cloning experiments was sent for DNA sequencing (Source Bioscience); samples were sent for sequencing at a concentration of 100ng/µl.

2.9 Quantitative PCR

2.9.1 Utricular cDNA Samples for qPCR

A sample of normal, uncultured adult mouse utricle cDNA was obtained in the same manner as that used for degenerate RT-PCR experiments. This sample consisted of the cDNA produced from a pool of 10 utricles dissected from 5 individual adult mice. The full process of RNA extraction from this tissue and reverse transcription to cDNA is described in 2.1.

Three time points were selected for investigation of integrin expression levels using the utricular culture model developed in chapter 4; these were 4 days, 14 days and 21 days post-gentamicin. These time points were selected in order to represent the tissue at different stages in the process of hair cell death i.e. early on at 4 days where a large amount of hair cell death and then at 14 and 21 days, where there was believed to be a limited amount of regeneration occurring e.g. appearance of immature stereocilia bundles.

Culture experiments were carried out as described in chapter 4, to produce a pooled sample of 8 – 10 individual utricles for each time point. At the end of the culture incubation period, the tissue was placed immediately into RNAlater. RNA extraction and reverse transcription to obtain cDNA was then carried out using the same methods as for normal utricular tissue samples.

2.9.2 Integrin Screen with Custom TaqMan® Array

Quantitative PCR was carried out using TaqMan® Custom 96 well plates (Applied Biosystems) containing TaqMan® assays for individual integrin subunits, in addition to two different endogenous controls and four hair cell markers; calretinin, myosinViia, Atoh1 and Pou4f3. Four replicates of each assay were present on each individual 96

well plate. A single 96-well plate was used per cDNA sample i.e. 4 separate array plates were run. The full plate layout is shown in figure 5-1.

TaqMan® gene expression assay probes feature a reporter dye at their 5' end, such as a FAM™ dye, and a non-fluorescent quencher at their 3' end. In a qPCR reaction, the TaqMan® probe will bind specifically to a complimentary DNA sequence within the target gene for which the assay was designed. When intact, the fluorescence of the reporter dye is suppressed due to its proximity to the quencher dye, however, due to the activity of DNA polymerase during the extension phase of the PCR reaction, the reporter dye at the 5' undergoes cleavage from the TaqMan® probe. The level of fluorescence within the assay is therefore increased as more reporter dye molecules are cleaved during each qPCR reaction cycle; thus detecting the amplification of the target gene within a given assay.

All qPCR experiments were carried out on a SDS7500 real-time PCR System (Applied Biosystems) as described in the protocol provided for the customised 96-well plates. For each cDNA sample, a 'cocktail' containing 432µl of cDNA, 648µl of ddH_20 and 1080µl of TaqMan® master mix (Applied Biosystems) was made up and mixed by pipetting. To each of the 96-wells of a single custom integrin gene expression plate, 20µl of this 'cocktail' was added. Each plate was then sealed with MicroAmp® optical adhesive film (Applied Biosystems) and centrifuged to ensure the whole reaction volume had been brought to the bottom of the plate wells.

Each plate was run using the following thermal cycling conditions summarised in the table 2-7.

		PCR (50 cycles)	
Hold	**Hold**	**Melt**	**Anneal/Extend**
50°C	95°C	95°C	60°C
2:00	0:20	0:15	1:00

Table 2-7 Thermal Cycling Conditions for qPCR Experiments

2.9.3 Relative Quantification of qPCR Experimental Data

Relative quantification (RQ) analysis of the results of the qPCR experiments carried out during this project was performed using SDS1.2.1 software (Applied Biosystems). Relative quantification of this data used the comparative C_T method to establish whether there was any change in the expression of the integrin genes screened for at several time points following gentamicin treatment.

The comparative C_T method of relative quantification calculates the amount of a given target gene e.g. itgb1, normalised to the expression of an endogenous control gene e.g. 18S RNA, relative to a calibrator sample. In these experiments, the calibrator sample for each gene screened for was the expression level in utricular cDNA from tissue dissected from normal adult mice which had not been maintained *in vitro.* The RQ values obtained by using the comparative C_T method are calculated using the formula $RQ = 2^{-\Delta\Delta C_{T,}}$ where C_T represents the fractional cycle number at which the amount of the target amplified during the PCR reaction reaches a set threshold level.

Following initial analysis, the RQ studies carried out in this project were assessed in order to determine whether the baseline and threshold values generated by the SDS software were appropriate. Baseline values (the initial qPCR cycles where there is very little change in the detected fluorescence levels) for each detector were set such that the amplification curve began after the maximum baseline value. The threshold for each detector was set in the exponential phase of the amplification curve, since RQ analysis is only accurate within this phase.

Gene expression plots were generated by the SDS software using the RQ values calculated, showing the fold-difference in expression of each target gene at a particular time point following gentamicin treatment, relative to the calibrator sample which had not been exposed to the ototoxic drug or maintained *in vitro*. Error bars for these graphs were calculated where there were two or more replicates with an RQ value for a given target; these error bars show the RQ maximum and RQ minimum levels. Confidence levels for the RQ maximum/minimum values for these gene expression plots were set at 95%, therefore the error bars on all gene expression plots presented in this thesis show the upper and lower limits within which the true gene expression level of a given target is likely to occur, with 95% confidence. For a particular target gene, where the RQ values at two time points are different and the error bars indicating the RQ

maximum/minimum values do not overlap, the RQ values may be said to be significantly different from one another, with a significance level of 0.05.

2.9.4 Optimisation of qPCR Reactions

The protocol for the use of the customised integrin TaqMan® gene expression arrays recommends the use of 1-100ng of cDNA per 20µl reaction volume. In order to determine the optimal amount of cDNA required for these qPCR experiments with utricular cDNA, a series of control assays were carried out. Individual assays for myosin VI were initially carried out using 50ng cDNA per well. This qPCR run indicated that myosin VI began to be amplified in the cDNA samples from cultured utricles after between 33 and 39 cycles, as shown in figure 2-1 A.

In order to allow amplification to begin at a lower cycle number, and therefore ensure more reliable results, a second control qCPR experiment was run using the cDNA at a higher concentration of 150ng/µl. Each well had 4µl of cDNA solution added – a total of 600ng of cDNA was therefore used per assay. Figure 2-1 B shows that under these conditions, myosin VI amplification began at around cycle 30 for cDNA from utricles maintained for 4 and 14 days post-gentamicin treatment. The cDNA sample from utricles maintained for 21 days post-gentamicin showed myosin VI amplification began at cycle 33. The use of 600ng of cDNA per assay was therefore selected for use on the customised integrin TaqMan® gene expression array plates.

A

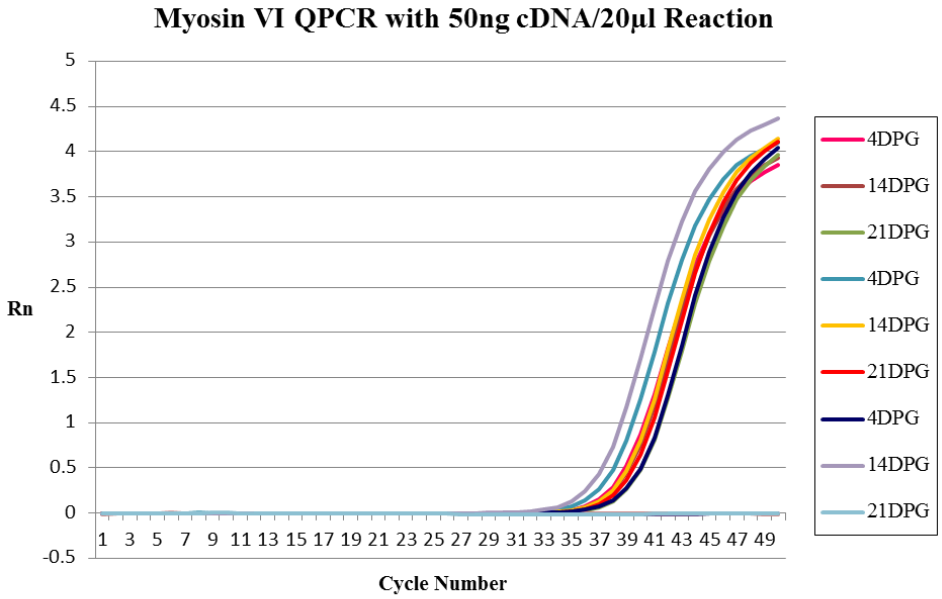

B

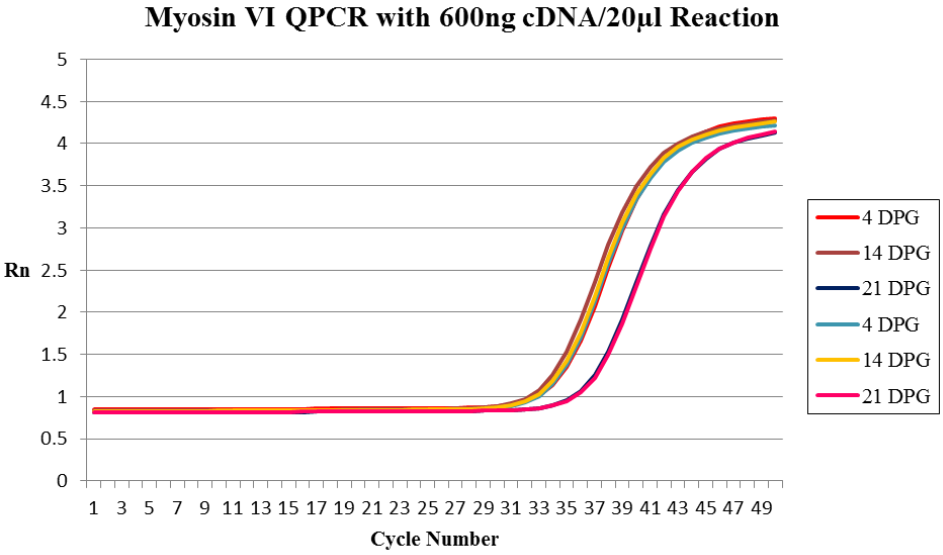

Figure 2-1 Optimisation of the Amount of cDNA Required for qPCR Experiments

(A) Myosin VI assays with each cDNA sample (4, 14 and 21 days post-gentamicin) using 50ng of cDNA per well. Amplification of myosin VI began between cycles 33 and 39. (B) A larger amount of cDNA, 600ng per well, showed that amplification of myosin VI began earlier, at between cycles 30 and 33. Therefore, 600ng of cDNA per assay was selected as the amount to be used per reaction on the customised integrin TaqMan™ gene expression arrays.

2.9.4 Multiplexed Integrin Assays

Individual integrin subunit multiplexed qPCR assays were carried out in 96-well plates (Applied Biosystems). 4µl of each cDNA sample (at a concentration of 150ng/µl) to be analysed was pipetted into individual wells. To each cDNA sample, 6µl of a reaction 'cocktail' was added using a repeat pipettor (Eppendorf); the 'cocktail' consisted of 0.5µl endogenous control (18S RNA) assay, 0.5µl target assay (e.g. an integrin subunit) and 5µl of TaqMan® master mix. All integrin assays and the 18S RNA assay were supplied by Applied Biosystems. The 96-well plates were sealed with MicroAmp® film and centrifuged to bring the reaction mixture to the bottom of each well.

Individual multiplexed assays were run using the same thermal cycling conditions as for the custom gene expression assays as shown in table 2-7. Relative quantification analysis of the results of these qPCR experiments was performed using SDS1.2.1 software as described in 2.9.3.

Chapter 3: Integrin Expression in the Normal Adult Mouse Utricle

3.1 Detection of Integrin Subunits Expressed in the Normal Adult Mouse Utricle by RT-PCR

3.1.1 Objectives

There have been few previous studies regarding the presence of members of the integrin family of proteins in the mammalian inner ear. Of these studies, most only describe the expression of a small number of integrin subunits within the embryonic or very early postnatal mouse (Davies, 2007; Davies and Holley, 2002; Littlewood Evans and Muller, 2000) . The expression of integrins in the normal adult mouse utricle had not been investigated prior to the start of this project.

In order to examine whether there are changes in the expression level or expression pattern of integrins in response to gentamicin-induced hair cell loss and any subsequent regeneration, it was first required to establish which of the 18 α and 8 β integrin subunits are present in the utricle in its normal, undamaged state.

Due to the large number of integrin subunits which exist in mammals, it was determined that the design of degenerate RT-PCR primers would be the most appropriate method for conducting a 'screen' of the normal adult mouse utricle for all of the known murine integrins. Degenerate PCR was intended to be used as a primary screen of the tissue of interest. Using the information gathered by degenerate PCR, further experiments e.g. immunohistochemistry, could then be focused on exploring the expression pattern of those integrins found to be present in the utricle. The use of degenerate primers would be preferable to conducting individual RT-PCR experiments for each of the integrin subunits, since the latter would be more costly, in addition to being more time consuming. The integrin protein family is a large one; consisting of 26 α and β subunits in total. The use of degenerate primers, with the ability to detect multiple integrins within one PCR experiment would therefore be greatly beneficial. The initial aims of this section of the project were to design a set of functional degenerate PCR primers which would detect all of the known murine integrin subunits; one set of primers to detect the α subunits and a second set to screen for the β subunits.

3.1.2 Design of Degenerate Primers

Previous work on the development and use of degenerate primers for detecting the integrins by PCR had been conducted (Pytela et al., 1994) predominantly using the human version of each of the subunits which had been identified at that time. The sequencing of the human genome had not yet been completed when this previous work was undertaken, thus it utilised the amino acid sequences of the known vertebrate integrins, rather than DNA sequences. Since this earlier study took place, a further four integrin subunits have been identified; α10, α11, αE and αD.

The initial method applied to the design of degenerate integrin primers was to use the Clustal W2 program (http://www.ebi.ac.uk/Tools/msa/clustalw2/) to perform sequence alignments of the murine DNA sequences of all 26 known integrin subunits when divided into two groups: the α subunits and the β subunits. The results of this alignment analysis, however, proved to be unsuitable for the production of degenerate PCR primers. There was not a high enough degree of homology between all of the α subunits when aligned as a group, nor between all of the β integrins subunits. Producing degenerate primers from these sequence alignments would have required the incorporation of a large amount of 'wobble,' which would have compromised the ability of the primers to specifically amplify members of the integrin protein family.

3.1.2.1 Division of the Integrins into Subgroups Based on DNA Sequence Homology

Although often described as a "family," the integrins may be further divided into subgroups based on several factors, including the ECM ligands to which they bind (Johnson et al., 2009).The α subunits may be divided into four subgroups as follows; the laminin binding subunits (α3, α7 and α6), the RGD sequence binding subunits (αIIb, αV, α5 and α8), and a small group consisting of α4 and α9. All of the remaining α subunits possess a domain known as the αI domain and thus form a large subgroup, which can be further divided into α subunits which are able to bind collagen (α1, α2, α10 and α11) and those which are expressed in leukocytes (αE, αM, αD, αX, αL).

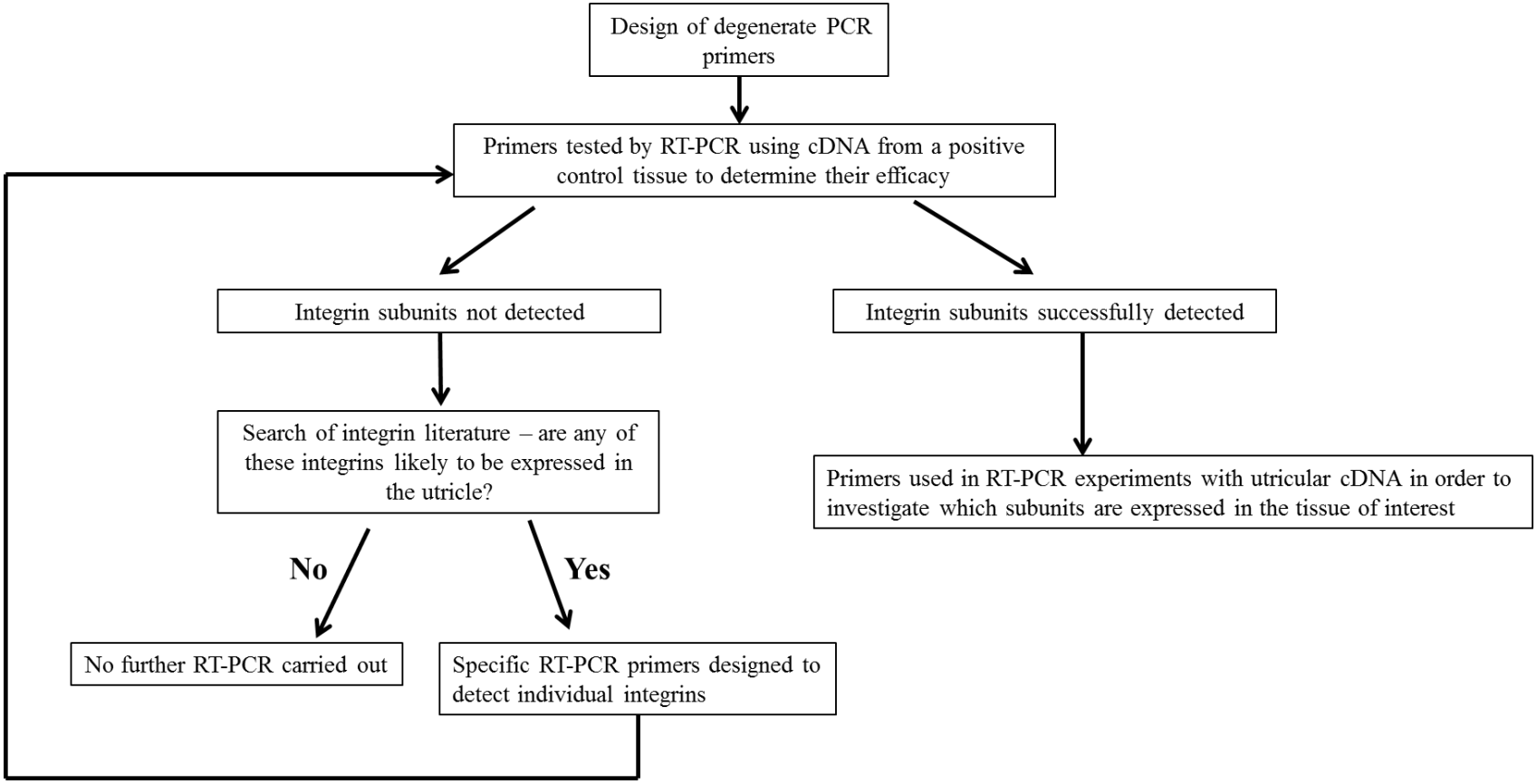

Figure 3-1 A Degenerate PCR-based Approach for Identifying Integrin Subunits Expressed in Normal Adult Mouse Utricular Tissue

This flow chart summarises the strategy used in this project in order to determine which integrin subunits are expressed in the normal adult mouse utricle. Full details of the methods used in these experiments are provided in 2.7.

In order to design degenerate PCR primers, the α and β integrins required division into further subgroups depending on their degree of homology to one another. The ClustalW2 program was used to generate dendrograms in order to illustrate the relationships between the murine α and β subunits in terms of their DNA sequence. These resulting integrin 'family trees' are shown in figure 3-2.

The α subunits (Figure 3-2 A) are divided into five main subgroups based on DNA sequence homology. These groups are similar to those described in terms of the evolution of the integrin family (Johnson et al., 2009). These groups also correspond to the ligand binding properties of the α integrins as described earlier in this chapter. It was possible to align the sequences of the α integrins within each group and obtain a high enough degree of homology in certain regions to be able to design degenerate primers. These regions (shown in figure 3-3) were similar to those consensus regions identified in previous work using the amino acid sequences of vertebrate integrin subunits (Pytela et al., 1994). The β integrin groups identified by the dendrogram produced based upon DNA sequence homology proved more difficult to use to design degenerate primers. The β integrins, although fewer in number, are considered to be more variable in terms of their DNA sequence e.g. integrin β4 has a cytoplasmic tail region which is far longer than any of the other β integrin subunits (Ewan et al., 2005). Further refinement of the β integrin groups was determined by running test alignments of variant combinations; this process resulted in 3 groups of integrin β subunits.

The final groups to be used for degenerate primer design are shown in table 3-1. Integrin αL is not included in these groups; this subunit is shown in the dendrogram in figure 3-2 to be on a branch of its own in terms of DNA sequence homology. Since αL is a highly leucocyte-specific integrin (Berlin et al., 1995), and thus perceived as highly unlikely to be found in the tissue of interest, it was decided to omit this α subunit from the design of integrin degenerate PCR primers.

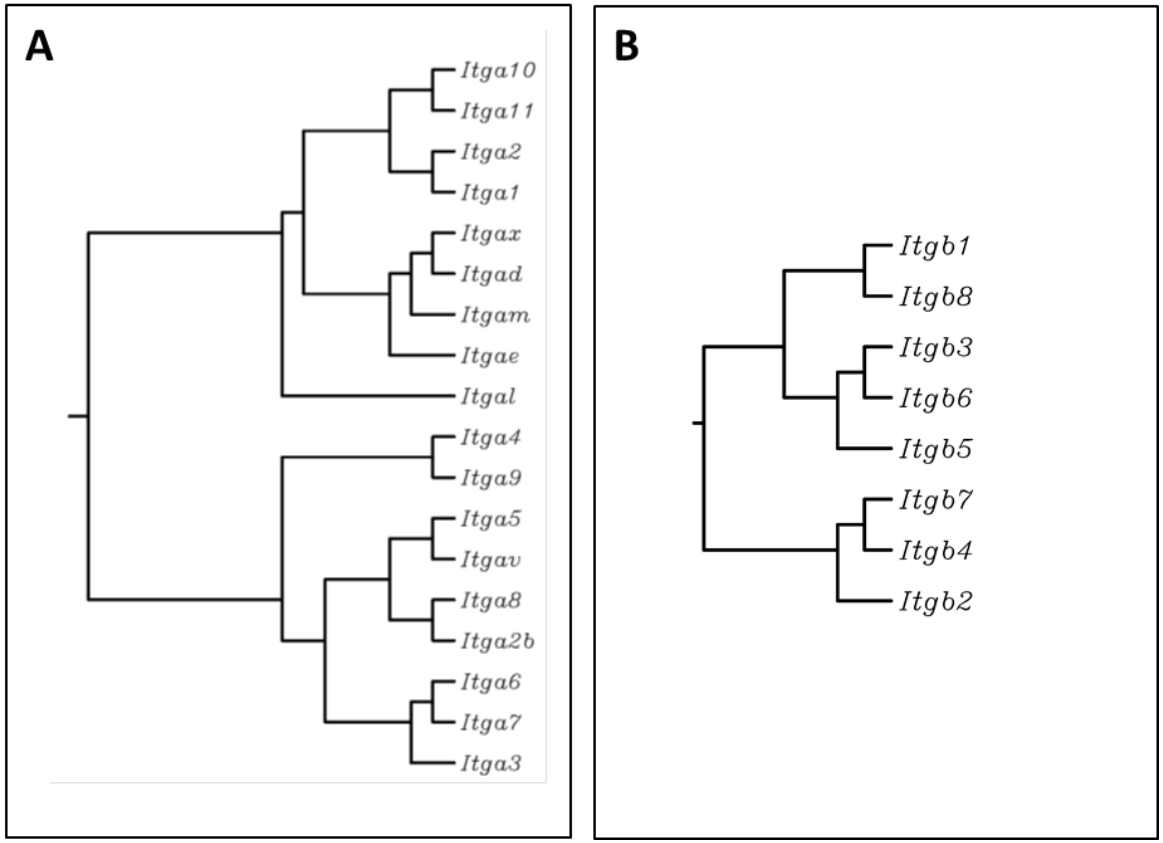

Figure 3-2 Homology of the Murine Integrin Subunit DNA Sequences

Dendrograms produced using the ClustalW2 program based on the murine DNA sequences for all the known (A) α and (B) β integrin subunits. The α integrins are divided into five main groups based on their homology, whilst the β integrins are divided into 3 groups. This data was used to determine how many sets of degenerate primer pairs were required in order to screen normal utricular tissue for all of the known murine integrins.

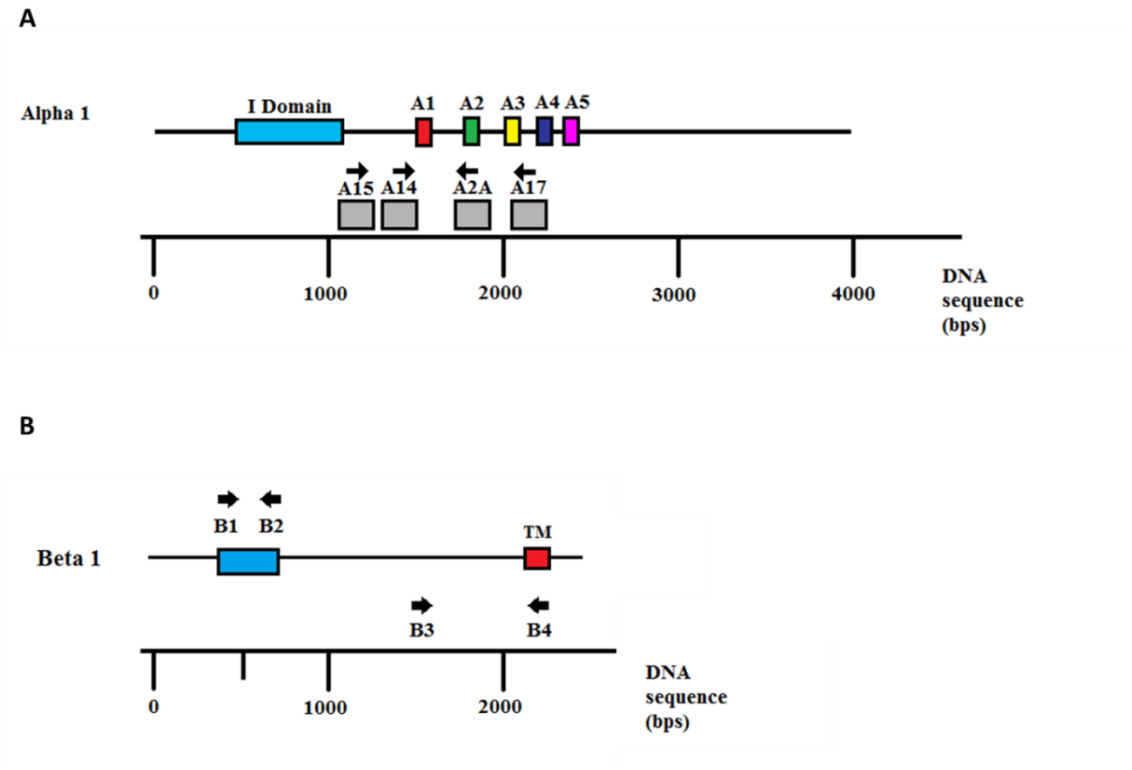

Figure 3-3 Consensus Regions of the α and β Integrin Subunits

(A) DNA sequence of an α integrin, i.e. α1, showing the location of 5 consensus regions (A1 – A5) used to design sets of degenerate PCR primers. The regions represented by grey boxes indicate regions where (Pytela et al., 1994)successfully designed degenerate primers based upon integrin amino acid sequences (direction of the arrows differentiates between forward and reverse primers). I domain = an integrin domain only found in some α integrin subunits. (B) DNA sequence of a β integrin, i.e. β1, indicating the conserved putative ligand-binding domain (blue box). Degenerate primers designed were located within this region (B1 indicates forward primers, B2 reverse primers). Previous work had also used two further regions (B3 & B4) for degenerate primer design. TM = transmembrane domain.

	Group	Integrins
Integrin α Subunits		
	Alpha A	α1, α2, α10, α11
	Alpha B	αX, αE, αM, αD
	Alpha C	α3, α6, α7
	Alpha D	α5, α8, αV, αIIb
	Alpha E	α4, α9
Integrin β Subunits		
	Beta 1	β1, β4, β7
	Beta 2	β2, β8
	Beta 3	β3, β5, β6

Table 3-1 – Integrin α and β Sub-Groups for the Design of Degenerate PCR Primers

This table shows the division of the integrin α and β subunits into groups; 5 for the αs and 3 for the βs. These sub-groups were determined by using the dendrograms shown in figure 3-2 based on DNA sequence homology.

3.1.2.2 Criteria for the Design of Degenerate Primers

For each α and β sub-group, DNA sequence alignments were run using the Clustal W2 program and consensus regions identified. The previous work of (Pytela et al., 1994), demonstrated similar consensus regions to those identified by these alignments. Figure 3-3 highlights the regions of the DNA sequence where degenerate primers designed for this project are located, in relation to those of this previous study. These consensus regions were then used to design a set of degenerate primers, based on a number of criteria. Each forward and reverse primer was required to be at least 23 base pairs (bp) in length. Additionally, an amplicon size of around 200bp was deemed optimal in order to allow for subsequent analysis of the PCR products by restriction digest; smaller amplicons would be more likely to produce small, difficult to detect fragments in such experiments.

Degeneracy scoring was applied in order to select the best possible primers. This allowed the potential number of different primer sequences which could be produced based on the sequence alignments of the integrin subunits of a given group. For example, the INTAallF primer sequence of GGGCCAGATNGGVTCHTAYTTTGG, contains 4 sites at which degeneracy is required. N, Y & H represent sites at which there is 2-fold degeneracy and V a site at which there is 4-fold degeneracy. The degeneracy score for this primer is therefore calculated as 2 x 4 x 2 x 2 = 32. Degeneracy scores were required to be as low as possible, in order to maintain specificity to the integrin family of proteins. During the design process, the Oligo Calc online tool (http://www.basic.northwestern.edu/biotools/OligoCalc.html) was used to analyse potential primer sequences in order to assess their GC content, melting temperature (T_m) and to check for self complimentarity which might affect the efficacy of the primer. Where the T_m of a primer sequence was deemed to be lower than was preferable (which occurred in shorter primer sequences), GGC repeats were added to the 5' end in order to raise the T_m. Figure 3-4 shows a summary of the degenerate primer pairs designed, including the sequences for both forward and reverse primers, the integrin subunits which each pair was designed to detect, the expected amplicon size and the positive control tissue used to test the efficacy of the primers. Each primer pair was also given an abbreviated name e.g. A1, for ease of reference in latter results of PCR experiments.

3.1.3 Testing of Degenerate Primers Using Positive Control Tissue

Degenerate primer efficacy was verified by running PCR experiments using positive control tissue cDNA. Of the 12 degenerate primer pairs designed, 8 pairs produced PCR products of the expected amplicon size when run on an agarose gel. Figures 3-5 and 3-6 show gel images of all successful RT-PCR reactions for the α (Figure 3-5) and β (Figure 3-6) degenerate primers.

Positive control tissue testing i.e. tissue known to express a given integrin subunit, was used to confirm whether each primer pair had the ability to detect each integrin subunit it was designed to, should that subunit be present in a given cDNA sample. Without this confirmation, it would be more difficult to establish in utricular cDNA whether a particular subunit was not present at all, or if it was in fact expressed, but not able to be detected effectively by the degenerate primers.

Appropriate positive control tissues were selected using the NCBI Unigene (http://www.ncbi.nlm.nih.gov/UniGene/ESTProfileViewer.cgi?uglist=Mm.263396) database to view the EST profile of gene expression within a range of tissues for each of the integrin subunits being detected. The control tissue used for each primer pair was selected on the basis that it demonstrated a significant level of expression of each of the integrin subunits which the primer pair was designed to detect. The control tissues used for each set of primers are shown in figure 3-4.

Some primers required optimisation of the PCR reaction conditions in order to function effectively e.g. alteration of the cDNA concentration, annealing temperature or $MgCl_2$ concentration. The optimal RT-PCR reaction conditions for each set of primer pairs are summarised in table 3-2. All of the PCR products from successful degenerate RT-PCR experiments shown in figures 3-5 and 3-6 were cut out of the agarose gel, to be used in cloning experiments to identify which integrin subunits were successfully amplified by each primer pair.

Primer Pair (Oligo Names)	Abbreviated Primer Pair Name	Forward Primer	Reverse Primer	Integrins to be Detected	Control Tissue	Amplicon Size (bp)
INTAall1F + INTAxmdeR	A1	ggcCAGATNGGVTCHTAYTTTGG	GGKGCMCCAATRGCCACATCYG	αX, αM, αD & αE	Spleen	275
INTAxmdeF + INTAxmdeR	A2	ggcCAGATBGGSTCYTAYTTTGGSKC	GGKGCMCCAATRGCCACATCYG	αX, αM, αD & αE	Spleen	275
INTA2110bF + INTA2110R	A3	ggcGTKGGRGCYTWTGACTGGRRBGG	ggcCCAAARTAKGAKCCDATCTGVTC	α1, α2, α10 & α11	Spleen	281 - 290
INTA2110bF + INTAall1R	A4	ggcGTKGGRGCYTWTGACTGGRRBGG	ggcCCAAARTADGABCCNATCTG	α1, α2, α10 & α11	Spleen	281 - 290
INTA673F + INTA8673R	A5	GCHGTBTAYGTSTWCATKAACCAG	AKCCATCYTGGTTVAKRTCMCC	α3, α6 & α7	Spleen & lung	127 - 130
INTA82b5VF + INTA75V82bR	A6	GGWGARCAGATGGCHKCNTAYTT	AKCCRTCYYGGTYSAGGTCHCCCA	α5, α8, αV & αIIb	Spleen & lung	259 - 268
INTA82b5VF + INTA8673R	A7	GGWGARCAGATGGCHKCNTAYTT	AKCCATCYTGGTTVAKRTCMCC	α8	Spleen & lung	262
INTA49Fb + INTA49Rb	A8	CTKGGCGACATTGAYRATGACGG	CCTGAKATRGAYTGYCCAAACATCC	α4 & α9	Spleen	185
INTB28F + INTB28R	B1	ATACCCCRTKGATCTKTAYTAYCT	ATGGCATCMARMCCWCCYTCAGG	β2 & β8	Lung	348
INTB356aF + INTB356R	B2	GAYMTSTAYTACYTSATGGACCTSTC	GYAGCCTGSAKGAYBGCRTCAAA	β3, β5 & β6	Kidney & spleen	350 - 356
INTB356bF + INTB356R	B3	TSTAYTACYTSATGGACCTSTC	GYAGCCTGSAKGAYBGCRTCAAA	β3, β5 & β6	Kidney & spleen	346 - 352
INTB147F + INTB147R	B4	ATACCCCRTKGATCTKTAYTAYCT	CTGCADRATKGCATCAAAGCCVCCTTC	β1, β4 & β7	Lung	333 - 345

Figure 3-4. Degenerate PCR Primers for the Detection of the Integrin α and β Subunits in the Normal Adult Mouse Utricle

Summary table of the degenerate primers pairs used to detect integrins. Wobble was incorporated into the primer sequences as appropriate; Y = C or T, V = A or G or C, M = A or C, R = A or G, H = A or C or T, K = G or T and B = G or C or T. Lower case indicates where GGC repeats were added.

Primer Pair	Band Detected by RT-PCR (Positive Control)	Integrin Subunits Successfully Amplified (Positive Control)	Band Detected by RT-PCR (Normal Utricle)	Integrin Subunits Successfully Amplified (Normal Utricle)
α Integrins				
A1	Yes	* αM &/or αE, *αX &/or αD	No	None
A2	No			
A3	Yes	α1 & α10	Not used	Not used
A4	No			
A5	Yes	α7	Not used	Not used
A6	Yes	**α8 and/or α5, αIIb and/or αV	Not used	Not used
A7	No			
A8	Yes	α4 & α9	Yes	α4 & α9
β Integrins				
B1	Yes	β2 & β8	Yes	β8
B2	Yes	β5 & β6	Yes	β5 & β1
B4	Yes	β7 & β1	Yes	None

Table 3-2 Summary of Integrin Subunits Detected by Degenerate Primers in Positive Control and Normal Utricle cDNA

The results of the RT-PCR experiments using the integrin degenerate primer pairs are summarised to show which primers worked successfully (i.e. a band of the expected amplicon size was detected) and which subunits were identified through restriction digest/DNA sequencing as being present in these PCR products. */** indicates subunits with very similar restriction maps which prevented them from being distinguished from one another. Primers which did not show sufficient capabilities to detect their cohort of subunits are indicated as ‘not used’; these primers were not tested with utricular cDNA.

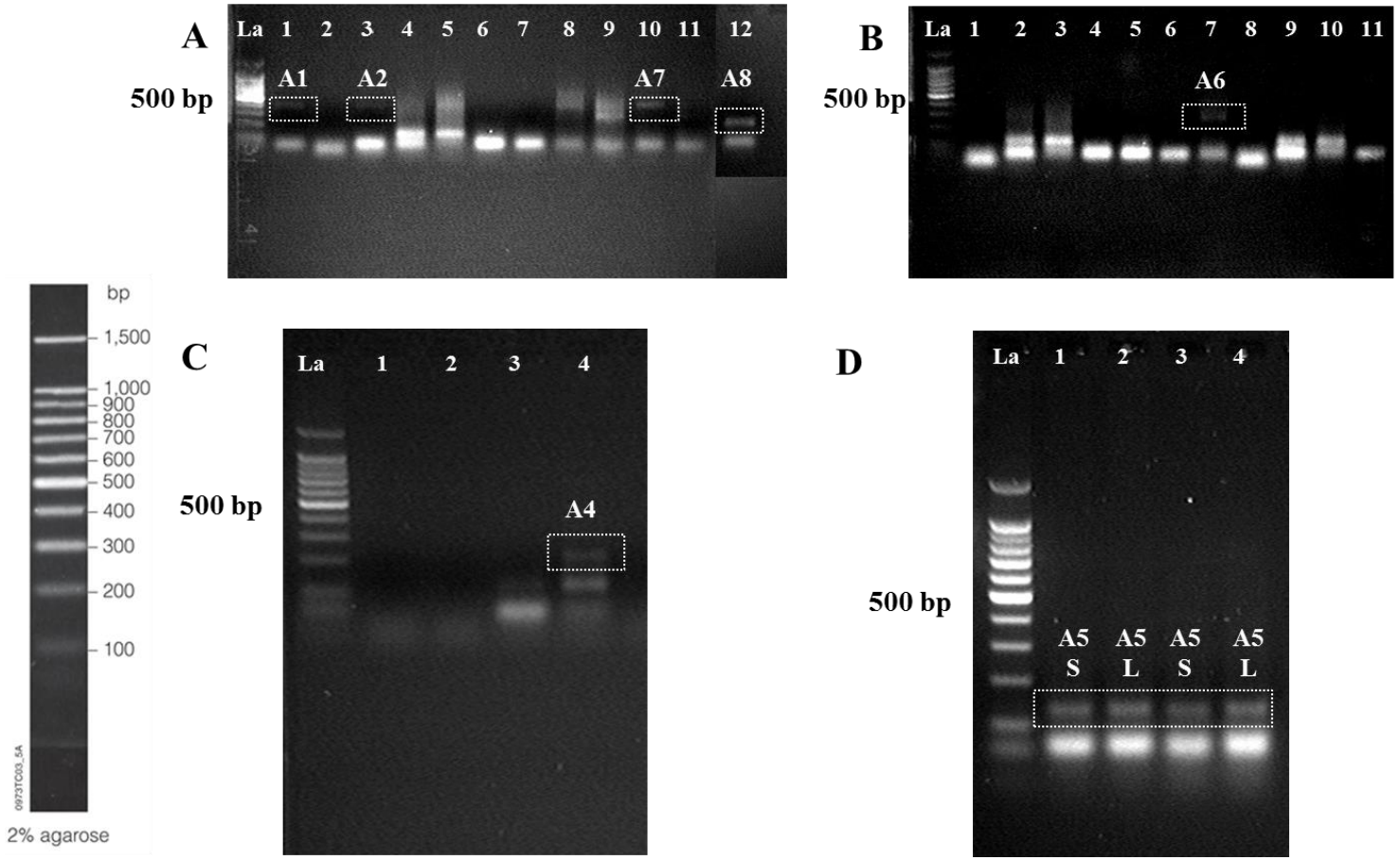

Figure 3-5 Integrin α Subunit Degenerate RT-PCR using Positive Control cDNA

RT-PCR products run on an agarose gel stained with ethidium bromide. Bands consistent with the expected amplicon size were detected for the following primer pairs. (A) Primer pairs A1 (lane 1, 281-290bp), A2 (lane 3, 275bp), A7 (lane 10, 262bp) and A8 (lane 12, 185bp). (B) Primer pair A6 (lane 7, 259-268bp). (C) Primer pair A4 (lane 4, 281-290bp). (D) Primer pair A5, using both spleen (lanes 1 & 3, 127-130bp) and lung (lanes 2 & 4, 127-130bp) control cDNA. La = 100bp DNA ladder (Promega).

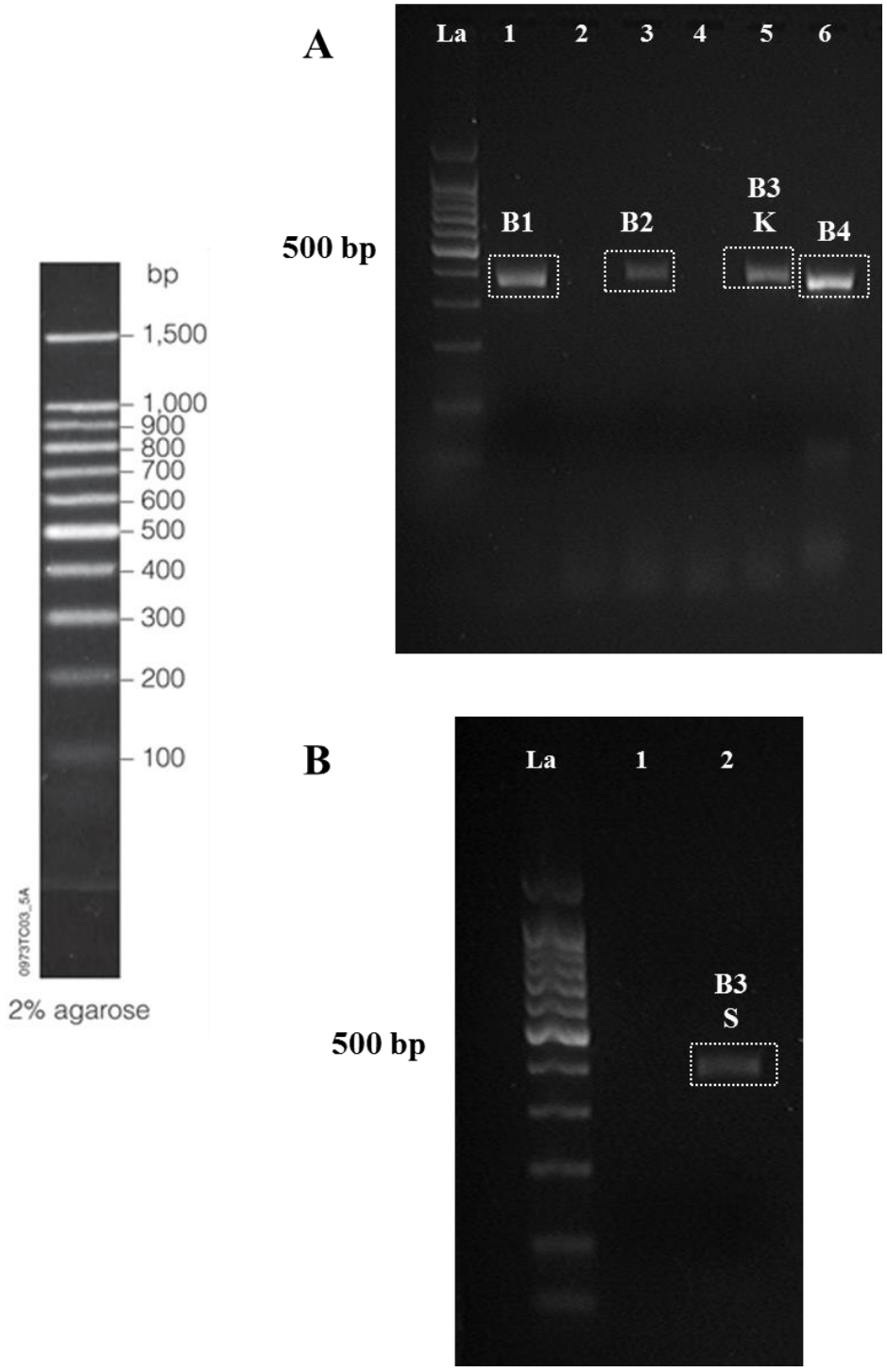

Figure 3-6 Integrin β Subunit Degenerate RT-PCR using Positive Control Tissue cDNA

RT-PCR products run on an agarose gel. Bands consistent with the expected amplicon size were detected with the following primer pairs. (A) Primer pair B1 (lane 1, 348bp), B2 (lane 3, 350-356bp), B3 (lane 5, 346-352bp, with kidney cDNA) and B4 (lane 6, 333-345bp). (B) Primer pair B3 (lane 2, 346-352bp) using spleen control cDNA. La = 100bp DNA ladder (Promega).

3.1.4 Identification of Individual Integrin Subunits Detected in Control Tissue

Individual integrin subunits successfully detected by each primer pair were identified by the cloning of RT-PCR products and restriction digest; full details of this process is given in 2.8. DNA sequencing was also used to confirm the identity of the detected integrins.

A total of at least 15 integrin subunit genes were confirmed as having been detected by degenerate PCR; these were (as shown in table 3-2) *Itga1*, *Itga4*, *Itga7*, *Itga9*, *Itga10*, *Itga8* and/or *Itga5*, *Itga2b* and/or *Itgav*, *Itgam* and/or *Itgae*, *Itgax* and/or *Itgad*, *Itgb1*, *Itgb2*, *Itgb5*, *Itgb6*, *Itgb7* and *Itgb8*.

Figure 3-7 shows an example of a restriction digest which successfully distinguished between two potential integrin gene amplicons within PCR products obtained using the A8 primer pair. An RsaI digest produced different DNA banding patterns depending upon whether the amplicon incorporated into cloned plasmid DNA was from *Itga4* or *Itga9* i.e. *Itga9* would produce two DNA bands of 1898 and 1304 base pairs (bp) in length, whereas incorporation of *Itga4* would result in a single cut of the DNA, linearising the plasmid and visible as a single DNA band when run on an agarose gel. Figure 3-7 shows 5 samples with a single DNA band of 3.1kb, indicating the presence of *Itga4*; the remaining 14 samples produced two DNA bands, thus were determined to contain the *Itga9* amplicon. Restriction digests were utilised in this manner for all degenerate PCR products to identify individual integrins. The restriction digest strategies used are summarised in tables 2-5 and 2-6. Gel photos of these digests are provided in the appendix.

Representative samples believed to have been identified as a given subunit, as well as samples which restriction digest had failed to conclusively identify, were sent for DNA sequencing (Source Bioscience). The DNA sequence data received was run as a BLAST alignment in order to confirm the identity of the integrin subunit detected.

The process of attempting to determine which integrin subunits the degenerate primers designed were successfully able to detect was time consuming, due to the nature of the cloning experiments being carried out to generate sufficient DNA for restriction digest analysis. Colony numbers following transformation of competent cells with plasmids containing PCR product inserts were often very low, which made it difficult to obtain

enough samples so as to have a chance of finding a colony which had taken up each of the different possible amplicons each degenerate primer pair was designed to amplify. Additionally, some of the integrin amplicons displayed such a high homology to one another that their restriction maps were virtually identical, making it impossible to differentiate between some amplicons by restriction digest i.e. the *Itgam* and *Itgae* amplicons. The decision was therefore made to progress on to using the degenerate primers on normal adult utricular tissue despite not having the ability to detect all 26 known murine integrins.

3.2 Degenerate RT-PCR using Normal Adult Mouse Utricular cDNA

Degenerate RT-PCR experiments using cDNA obtained from a sample of normal adult mouse utricles detected the presence of the following integrin genes; *Itga4*, *Itga9*, *Itgb1*, *Itgb5* and *Itgb8*.

The degenerate RT-PCR experiments using utricular cDNA with the following primer pairs, produced bands of the expected amplicon size when PCR products were run on an agarose gel; A8, B1, B3 and B4 (gel images shown in figure 3-8). Positive control reactions were run alongside those using utricular cDNA in order to show that the primers were functioning correctly under the reaction conditions. Primer pair A1 did not produce a DNA band with utricular cDNA; since the positive control reaction did detect PCR products, it was concluded that the utricular cDNA sample did not contain any of the integrins detected by the A1 primers.

PCR products from these experiments were cloned and the resultant plasmid DNA subjected to restriction digest in order to identify individual integrins. Plasmid DNA transformed with PCR products produced using the A8 primer pair were digested with RsaI. This digest, when run on an agarose gel (Figure 3-9) produced one DNA band if the *Itga4* amplicon had been ligated into the vector and two bands if *Itga9*. The results of this digest show that both *Itga9* and *Itga4* were detected in normal utricular cDNA. This result was confirmed by BLAST alignments run using DNA sequence data from samples believed to be *Itga4* (3-10 A) and *Itga9* (3-10 B). The sample identified as containing the *Itga4* amplicon was found to have a homology of 96.79% with the *Itga4* DNA sequence across a length of 156bp (the expected *Itga4* amplicon size was 185bp). The sample identified as containing the *Itga9* amplicon was found to have a homology

of 98.38% with the *Itga9* DNA sequence across the entire length of the amplicon (185bp).

Plasmid DNA samples obtained through cloning of the PCR products produced by the B3 primer pair were digested with EcoRI (Figure 3-8 B) in order to identify which samples contained an amplicon within the vector. There is an EcoRI restriction site on either side of the region where amplicons are ligated into the P-GEM®T Easy vector. Colony numbers in these cloning experiments were low, thus all 8 plasmid DNA samples which proved to have an amplicon insert were sent for DNA sequencing. Using BLAST alignments of the DNA sequencing data, 4 of these samples were identified as *Itgb5*, with a homology of between 94.97 and 98.58% to the *Itgb5* DNA sequence. A further 2 samples were identified as integrin *Itgb1* with a homology of 92.67%. The B3 primer pair was not originally designed to amplify the *Itgb1* gene. The remaining 2 samples did not correspond to any of the known murine integrin genes.

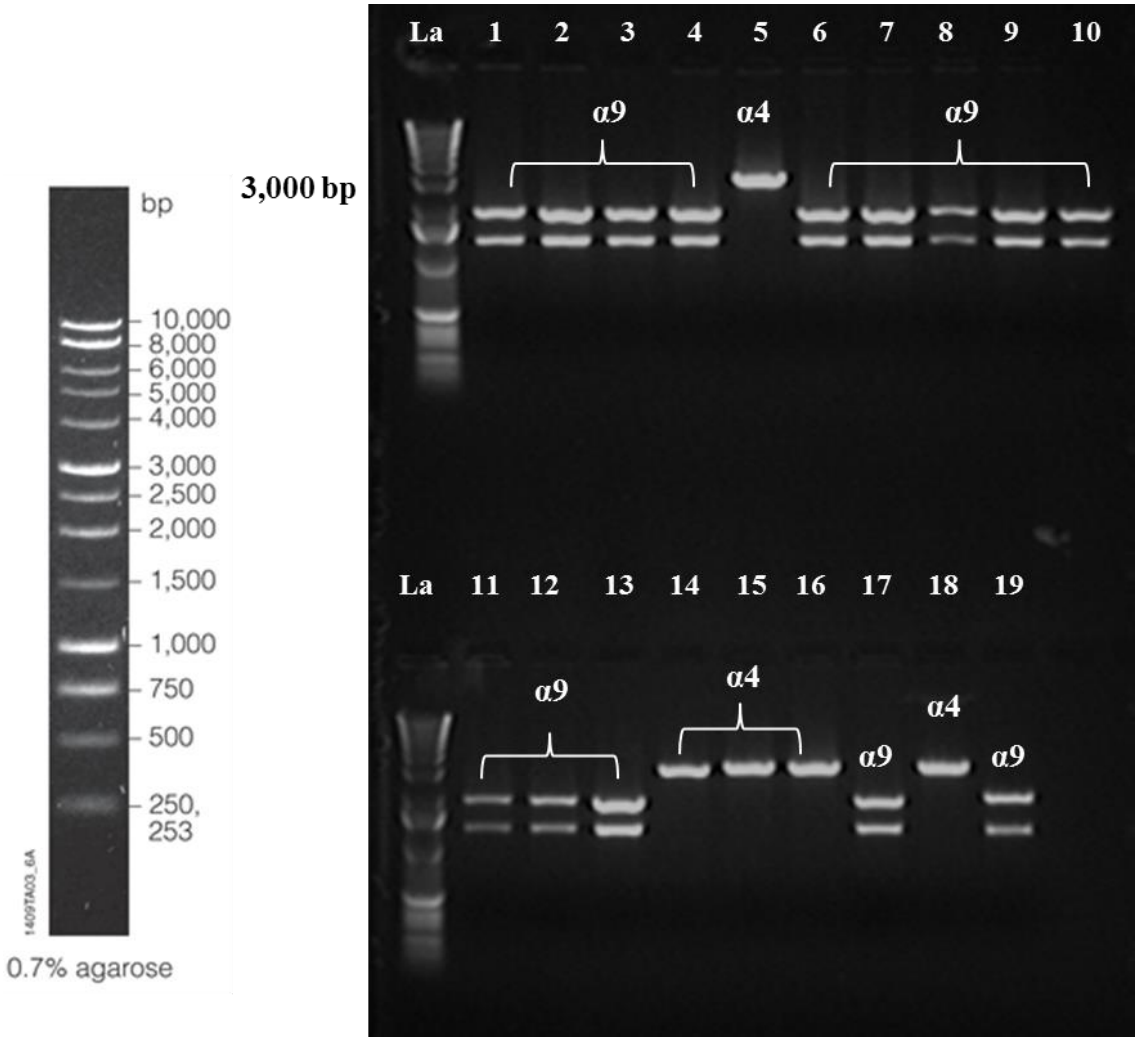

Figure 3-7 Restriction Digest of Cloned PCR Products from RT-PCR with the A8 Degenerate Primer Pair

RsaI digest of A8 cloned PCR products of reactions run using utricular cDNA. Lanes 5, 14, 15, 16 and 18 show clones which contain the *Itga4* amplicon (RsaI linearises the plasmid DNA producing a single 3.1kb band). The remaining lanes show clones which contain the *Itga9* amplicon (RsaI cuts plasmids with this amplicon twice to produce two bands of 1898 and 1304 bp). La = 1kb DNA ladder (Promega)

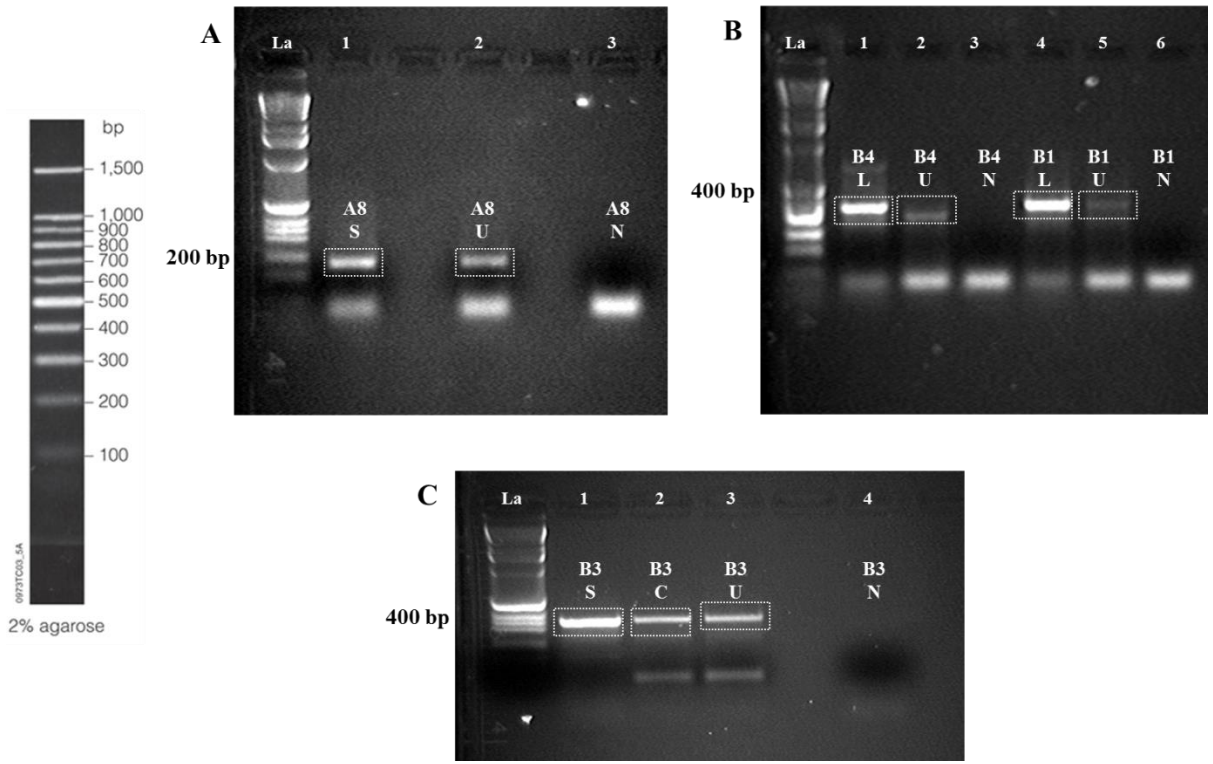

Figure 3-8 Integrin Degenerate RT-PCR using Normal Adult Mouse Utricular cDNA

Gel photos of degenerate PCR reactions using utricular cDNA. Bands of the expected amplicon size were detected using the following primer pairs.

(A) The A8 primer pair (185bp) with positive control (lane 1, spleen) and utricular (lane 2) cDNA. (B) The B4 primer pair (~340bp) for both positive control (lane 1, lung) and utricular (lane 2) cDNA, and the B1 primer pair (348bp) with both positive control (lane 4, lung) and utricular (lane 5) cDNA. (C) The B3 primer pair (~350bp) for both positive control (lane 1, spleen) and utricular (lane 3) cDNA. Cristae cDNA also produced a band with the B3 primers (lane 2). La = 100bp DNA ladder (Promega). S = spleen, U = utricle, C = cristae & N = negative control (no cDNA).

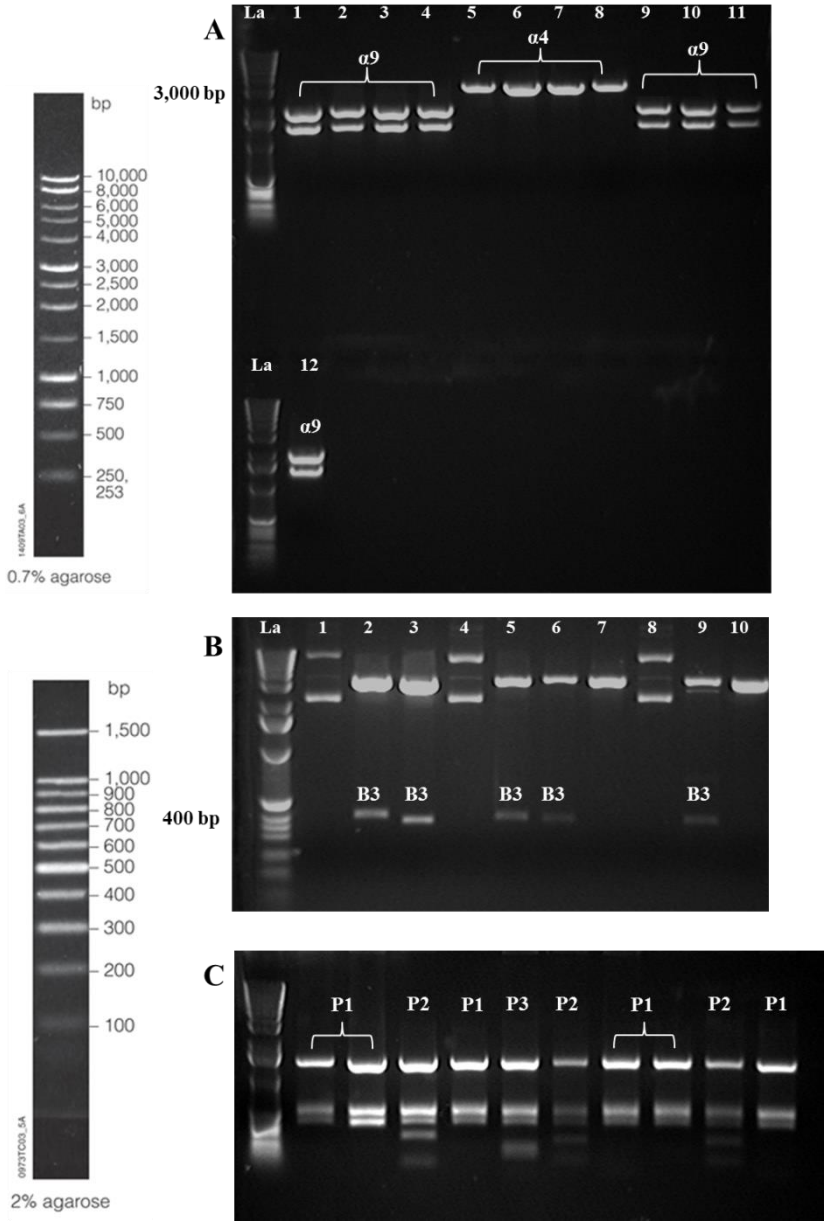

Figure 3-9 Cloned Degenerate PCR Products from Utricular cDNA Analysed by Restriction Digest

(A) Plasmid DNA produced using PCR products of the A8 primers digested with RsaI. Lanes 1 – 4 & 9 – 12 = *Itga9* (two DNA bands of 1898 & 1304 bp). Lanes 5 – 8 = *Itga4* (single 3.1kb DNA band). (B) EcoRI digest of plasmid DNA produced using PCR products of the B3 primers, lanes 2, 3, 5, 6 and 9 show those which have successfully up-taken a plasmid with an amplicon insert; EcoRI 'cuts out' the amplicon from the vector = plasmid DNA band + B3 amplicon (~350bp). (C) TaqI digest of plasmid DNA produced using PCR products of the B3 primers. This digest produced several different banding patterns when run on a gel; lanes 1, 2, 4, 7, 8 & 10 appear similar (P1), as do lanes 3, 6 & 9 (P2). A third banding pattern (P3) was observed in lane 5. Representative samples of each banding pattern were sent for DNA sequencing to conclusively identify individual integrins. La = 1kb DNA ladder and 100bp DNA ladder (Promega).

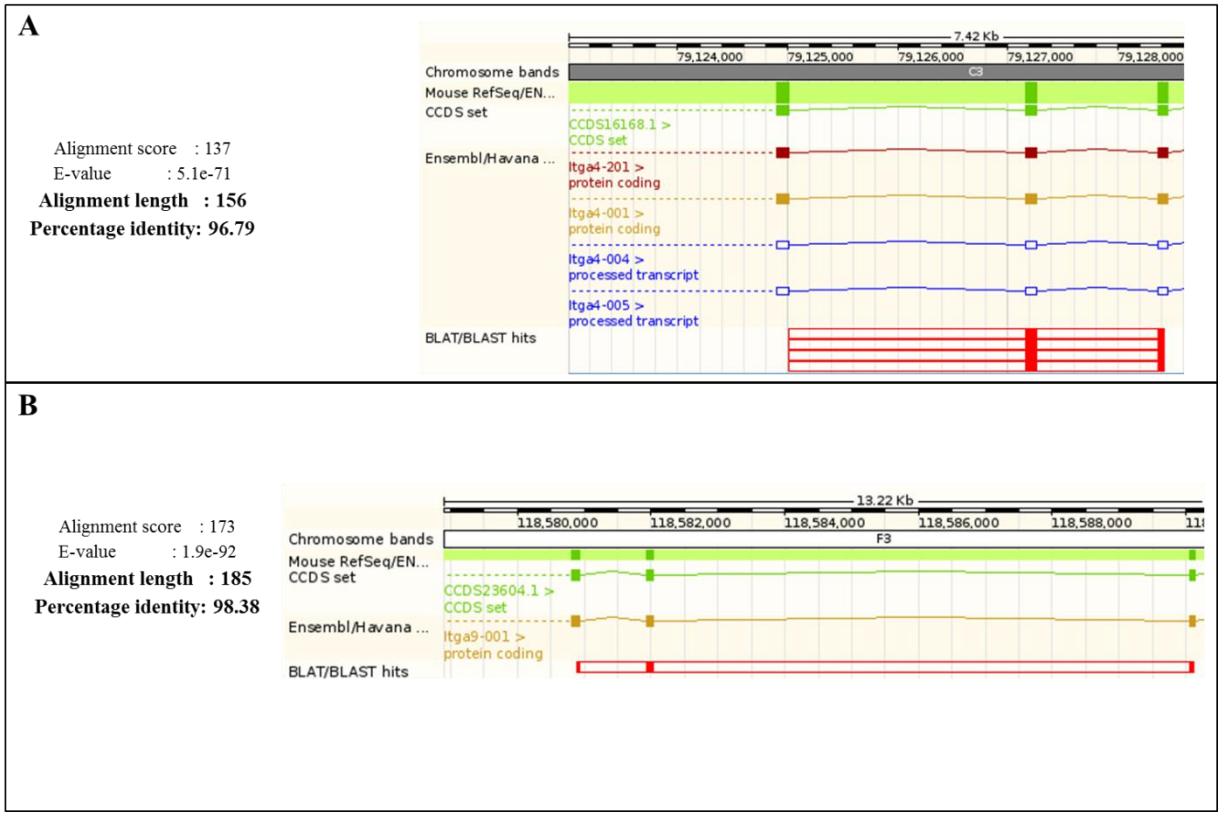

Figure 3-10 DNA Sequencing and BLAST Analysis to Confirm Identification of Subunits Successfully Amplified by Degenerate RT-PCR

Samples from cloning experiments which had undergone restriction digest were sent for DNA sequencing to confirm the identity of the integrin amplicons. Samples believed to be *Itga4* and *Itga9* were sequenced and this data used to perform a Blast alignment. (A) Sample identified as having 96.79% homology with *Itga4* over a length of 156bp. (B) Sample identified as having 98.38% homology with *Itga9* over a length of 185bp. Alignment length and percentage identity are highlighted with bold text. Chromosome diagrams indicate the location of the *Itga9* and *Itga4* genes and the sequence homology found by BLAST (red bar).

Cloning experiments with PCR products of the B4 primer pair produced very few colonies despite repeating the experiment (both the ligation stage and the transformation of competent cells). The only plasmid DNA sample obtained for this primer pair was found not to contain an integrin subunit amplicon when DNA sequence data was subjected to BLAST alignment. B1 primer pair PCR product transformations also demonstrated low colony numbers. Four plasmid DNA samples were obtained for this primer pair; these were all identified as *Itgb8* by BLAST alignment of the DNA sequence. A homology of between 95.11 and 99.71% was recorded for these samples.

3.3 RT-PCR with Specific Integrin Primers

3.3.1 Positive Control cDNA

Integrin subunits which had not been detected by degenerate PCR primers in control tissue were evaluated as indicated in figure 3-1. Through consultation of published literature, a group of 5 integrin subunits which were believed likely to be expressed in utricular cDNA was identified. This group was comprised of several highly abundant subunits, as well as integrins which had been detected in inner ear tissue in previous studies; αV, α8, β1, β3 and α6. Individual specific PCR primers were therefore designed to detect each of these integrins; this design process is described in 2.7.5. Primer sequence data for these specific integrin subunit RT-PCR primers is provided in table 3-3.

As with the degenerate primers, specific integrin subunit primers were tested for efficacy using cDNA from an appropriate positive control tissue; spleen for integrins αV, α8 and β3, and lung for α6 and β1. Bands of the expected size were detected using control tissue with the primers for integrin α6, β1, β3 and αV. The results of these RT-PCR experiments are shown in figure 3-11 where PCR products were run on an agarose gel. The integrin α8 primer pair was not observed to produce any PCR products, despite several different reaction conditions being tested. Table 3-4 summarises the optimised reaction conditions at which each of the specific primer pairs functioned most effectively.

Integrin Subunit	Forward Primer	T_m (Salt adjusted)	Reverse Primer	T_m (Salt adjusted)	Amplicon Size
α6	ATCACAGTGACTCCTAACAGAATTG	63°C	ACTGAACTCTCGATGACAACCCTGA	66°C	143bp
β1	CTCTCTTTCTTCAGAAGTCATT	56°C	ATTTATTAGCAGTTATGCTAATTTC	56°C	134bp
β3	TGCAGTGACTGAAAATGTCGTCAGC	66°C	CACGTACTTCCAGCTCCACTTTAGA	66°C	108bp
α8	GGACAGGTCTACTTGTACCTTCAAG	66°C	CATTGTAAATGAGGACTTTACCTCG	63°C	149bp
αV	CTGGCCTTGAAGTGTACCCTAGCAT	67°C	TGCTTGAGTTTATCCAGTAGAAGCT	63°C	128bp

Table 3-3 Integrin Subunit Specific RT-PCR Primers

A summary of the 5 integrin subunits selected for the design of specific RT-PCR primers. The forward and reverse primer sequences are provided, as well as their T_m, as determined by the OligoCalc online tool. These integrin subunits were selected based upon their abundance in functional heterodimers (integrin αV and β1 are the two most 'promiscuous' integrin subunits) and have been previously identified in inner ear tissue in previous work.

3.3.2 Utricular cDNA

All four integrin genes for which the specific integrin primer pairs were functional (*Itga6*, *Itgav*, *Itgb1* and *Itgb3*) detected a band of the expected size when used in RT-PCR reactions with utricular cDNA. *Itga6* and *Itgb3* were also detected in cDNA from a sample of cristae. The results of these RT-PCR experiments are shown in figure 3-12 where PCR products were run on an agarose gel.

The same RT-PCR reaction conditions determined by using positive control tissue were applied to experiments using utricular cDNA. Some primer pairs required further optimisation by alteration of the $MgCl_2$ concentration to detect integrins in utricular cDNA effectively. Table 3-4 summarises the reaction conditions required for RT-PCR using utricular cDNA in comparison to those required for positive controls.

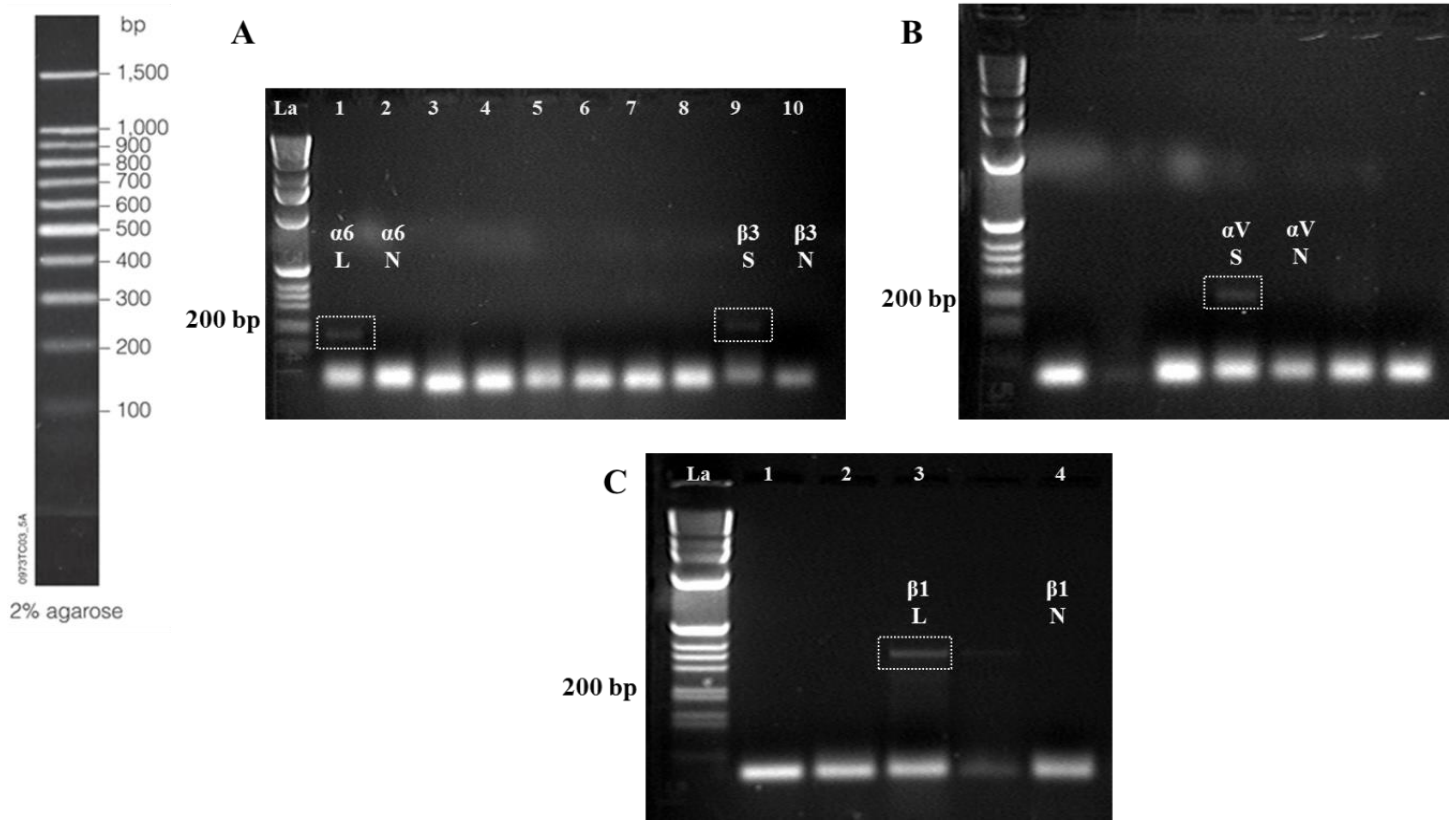

Figure 3-11 Testing of Specific Integrin Subunit RT-PCR Primers using Positive Control cDNA

PCR products from specific integrin subunit primers and positive control tissue run on an agarose gel. (A) 2mM $MgCl_2$ and an annealing temperature of 55°C produced bands of the expected size for *Itga6* (lane 1 = lung cDNA) and *Itgb3* (lane 9 = spleen cDNA). (B) 2mM $MgCl_2$ and an annealing temperature of 60°C produced a band of the expected size with the *Itgav* primer pair (lane 3 = spleen cDNA). (C) 3mM $MgCl_2$ and an annealing temperature of 62°C produced a band of the expected size with the *Itgb1* primer pair (lane 3 = lung cDNA). The *Itga8* primer pair did not function successfully under these conditions (lane 2). La = 100bp DNA ladder (Promega). L = lung, S = spleen & N = negative control (no cDNA).

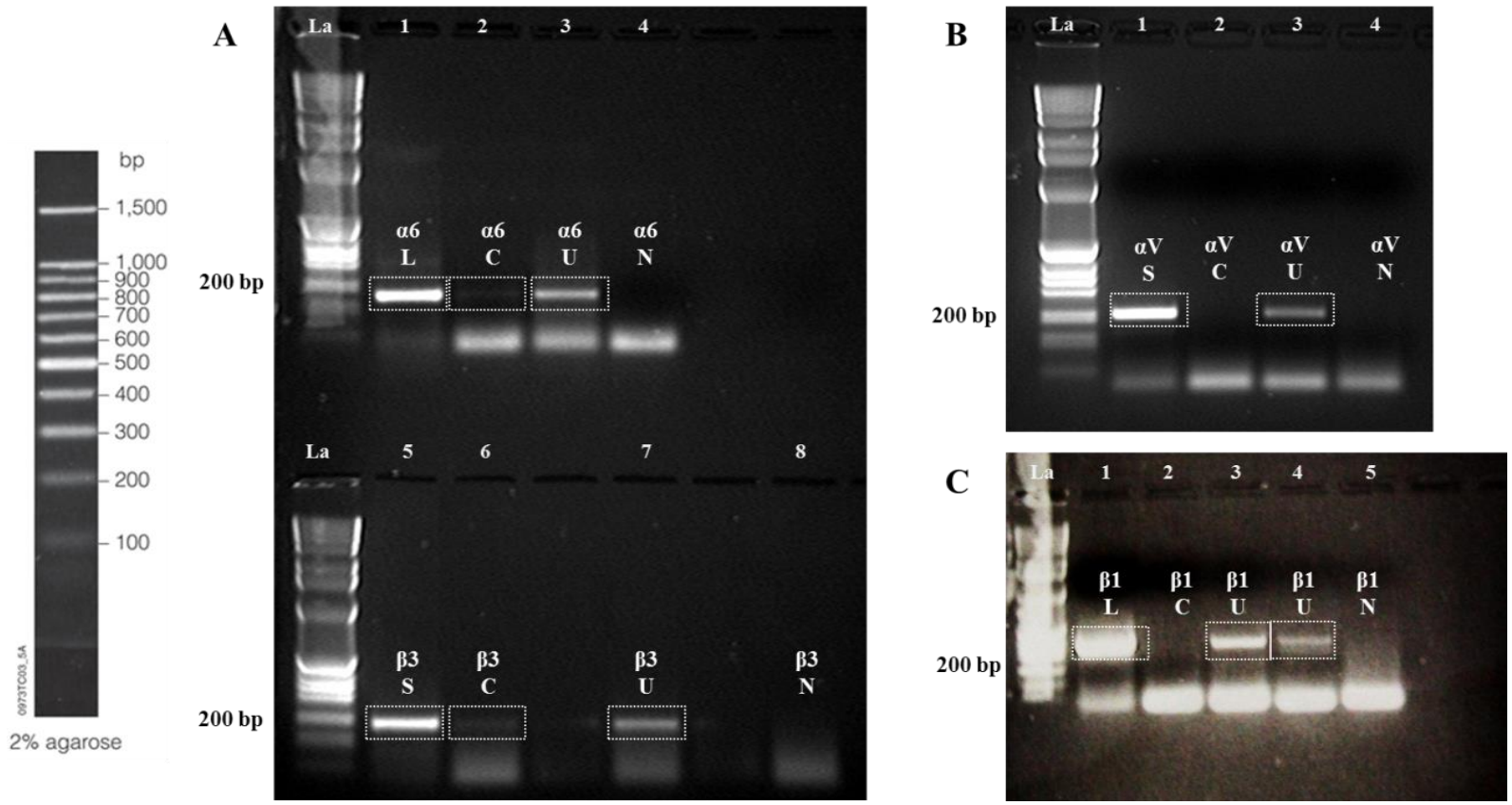

Figure 3-12 Specific Integrin RT-PCR using cDNA from Normal Adult Mouse Utricles

Specific RT-PCR primers detected *Itga6* (A - lane 3), *Itgb3* (A – lane 7), *Itgav* (B – lane 3) and Itgb1 (C – lanes 3 & 4) in utricular cDNA. *Itga6* (A – lane 2) and *Itgb3* (A – lane 6) were also detected in a cristae cDNA sample. *Itgav* (B – lane 2) and *Itgb1* (C – lane 2) were not detected in cristae cDNA. Positive controls (using cDNA from an appropriate tissue) and negative controls (no cDNA) were run alongside inner ear cDNA RT-PCR reactions for each set of primers. S = spleen, L = lung, U = utricle, C = cristae & N = negative control. La = 100 bp DNA ladder (Promega).

Specific RT-PCR Primers	PCR Reaction Conditions (Positive Control cDNA)	PCR Reaction Conditions (Utricular cDNA)
α6	Lung cDNA = 2µg	Utricle cDNA = 2µg
	Annealing temperature = 55°C	Annealing temperature = 55°C
	$MgCl_2$ concentration = 2mM	$MgCl_2$ concentration = 2mM
αV	Spleen cDNA = 2µG	Utricle cDNA = 2µg
	Annealing temperature = 60°C	Annealing temperature = 60°C
	$MgCl_2$ Concentration = 2mM	$MgCl_2$ concentration = 1mM
α8	Not successful	N/A
β1	Lung cDNA = 2µg	Utricle cDNA = 2µg
	Annealing temperature = 65°C	Annealing temperature = 65°C
	$MgCl_2$ concentration = 4mM	$MgCl_2$ concentration = 4mM
β3	Spleen cDNA = 2µg	Utricle cDNA = 2µg
	Annealing temperature = 55°C	Annealing temperature = 55°C
	$MgCl_2$ concentration = 2mM	$MgCl_2$ concentration = 1mM

Table 3-4 Summary of Optimised Reaction Conditions for RT-PCR Experiments with Specific Integrin Subunit Primers

Optimised RT-PCR reaction conditions for the specific integrin subunit primer pairs are shown for both positive control tissue and utricular cDNA. In some instances, conditions which worked for positive control cDNA did not function as efficiently with utricle cDNA. The α8 primer pair was tested with multiple reaction conditions using control cDNA (up to 5mM $MgCl_2$ & an annealing temperature of 68°C) but no PCR products were detected. These primers were therefore not used with utricular cDNA.

3.4 Discussion

3.4.1 The Homology of the Integrin Family of Proteins and Its Implications for Degenerate PCR

In order to design a set of degenerate PCR primers which would be able to detect all of the known murine integrin subunits, an approach based on the homology of DNA sequences for these proteins was adopted. An initial attempt to design two sets of degenerate primers (one for detection of the α integrins and one for the βs) proved unsuccessful due to the lack of homology within these groups. Consensus regions sufficient for the design of an effective set of degenerate primers were not present amongst the α or the β integrin subunits.

The dendrograms shown in figure 3-2, created using the murine DNA sequence information for the integrin subunits, represent the relationships between the α and β integrins in terms of their DNA sequence homology. The α subunits are divided into 5 groups, which may be compared to previous studies on the evolution of the integrin subunits. Phylogenetic studies involving the comparison of integrin α subunits from numerous species including humans, mice and invertebrates such as *Drosophila melanogaster*, place these subunits into groups which correspond to those shown in figure 3-2 A (Hughes, 2001; Huhtala et al., 2005; Johnson et al., 2009). Each of these studies indicates that those α integrins which possess an I-domain form two separate groups; the collagen receptor integrins (α1, α2, α10 and α11), and the leucocyte integrins (αL, αM, αD, αE and αX). These previous studies describe a further two groups, known as the PSI and PSII integrin 'families' which feature Drosophila homologues. The PSI α integrins are α3, α6 and α7, as well as the Drosophila αPSI. These integrins (including the invertebrate homolog) are known laminin receptors (Belkin and Stepp, 2000). The PSII α integrins are α5, αV, αIIb and α8, plus αPSII from Drosophila. This group once again is linked by their ligand binding attributes; PSII α integrins are those capable of recognising and binding a particular RGD amino acid sequence in the ligands with which they interact. The mammalian integrins α4 and α9 form the final α subgroup. Previous studies, however, also described an additional group – the PSIII integrins, of which there are no mammalian members, only invertebrate proteins (Johnson et al., 2009). It has been suggested that at some point in their evolutionary history, vertebrates lost this family of α integrins, whilst diversification

occurred within the other families in order to produce the numerous α subunits known today (Hughes, 2001). The α integrin groups defined in this work for the purpose of creating degenerate PCR primers are therefore supported by previous studies and investigation of the evolutionary origins of the integrins.

During this project, the β integrins were divided into three groups based on a dendrogram of their DNA sequence homology (figure 3-2 B) which was refined by running test alignments and investigating these for appropriate consensus regions. Previous work (Hughes, 2001; Huhtala et al., 2005) divides the β integrins into two main subgroups; the β1 group – containing β1, β2 and β7 and the β3 group – containing β3, β5 and β6. The two remaining β integrins (β4 and β8) are described as each being a 'group' of their own (Holmes and Rout, 2011), although integrin β8 is also described as being more closely related to the β3 group integrins (Hughes, 2001). Integrin β4, a considerably larger protein than the other β subunits, has been recently postulated as being the original 'primordial' β integrin (Holmes and Rout, 2011). Studies involving the integrins of organisms such as the invertebrate *Ciona intestinalis*, have shown that this proteostome possesses an integrin which is an orthologue of vertebrate β4 (Ewan et al., 2005), supporting the theory that the β4 integrin subunit had evolved prior to the divergence of vertebrate and ascidian species such as *C. intestinalis*.

The dendrogram produced in this work using the mouse DNA sequences of the 8 mammalian β integrins, differs somewhat from previous studies. Although figure 3-2 B, groups the 'β3' integrins together as in previous work, it places β1 and β8 together as a group, with the remaining subunits (β2, β4 and β7) forming a third group; this third group is most similar to the previously described 'β1' group, with β1 having been replaced by β4. Following initial examination by DNA sequence alignment, these groups were revised and whilst the 'β3' group remained unchanged, the two other groups were altered so that one consisted of β2 and β8, the other β1, β4 and β7.

That the grouping of β integrin subunits does not completely agree with previous phylogenetic studies may be attributed to their high level of divergence in terms of DNA sequence which has been previously described. It has been observed that there is a far greater degree of homology between the sequences of one β subunit when compared across its homologs in other species, than there is amongst all of the β integrins from a single species (Pytela et al., 1994). The result observed in this project for the β integrins

is therefore likely to represent the way in which the DNA sequences of the 8 β subunits diverge which is specific to the mouse version of each gene.

3.4.2 Integrin Subunits Detected in the Normal Adult Mouse Utricle by RT-PCR

The results of the degenerate RT-PCR experiments on utricular cDNA carried out in this project indicate the presence of five integrin genes; *Itga4*, *Itga9*, *Itgb1*, *Itgb5* and *Itgb8*. The use of specific integrin PCR primers on the same cDNA sample detected the presence of a further three subunits, namely *Itga6*, *Itgav* and *Itgb3*, and supported the finding that *Itgb1* had been detected in the tissue of interest by the degenerate PCR primers. Of these eight integrin subunits detected in the normal mouse utricle using this type of PCR, there are several potential heterodimers. All four of the α subunits detected can form a heterodimer with integrin β1, the most 'promiscuous' of the β subunits (it is present in a total of 12 known mammalian integrin heterodimers). Integrins α4 and α6 can also associate with β7 and β4 respectively, although these integrins were not detected in the cDNA sample by RT-PCR. Integrin αV, the most 'promiscuous' α integrin, could also potentially associate with the β3, β5 and β8 subunits which were positively identified in these experiments.

The degenerate PCR primers designed during this project were not proven to be able to detect all of the integrin subunits for which each primer pair was intended. This may potentially be attributed to certain integrin subunits not being expressed at a high enough level in the control tissue they were tested on. Where a primer pair was potentially able to detect any of four different subunits, it may have been possible that the control tissue selected contained some subunits at a higher expression level than others, making their detection more likely than those expressed in much lower quantities. Cloning experiments used to identify which subunits were present in the RT-PCR product samples often produced low bacterial colony yields. Therefore, even if as many as 20 clones were examined, if a given subunit had been present in the cDNA at higher levels than others, this subunit would be more likely to be present in the cloned plasmid DNA. Based upon the results obtained during this project, degenerate PCR would not be considered the most effective method for conducting a screen of utricular cDNA for a protein family as diverse as the integrins. Had the full extent of the lack of homology amongst the α and β subunits been known, an alternative experimental approach for integrin screening would have been selected e.g. the use of a DNA

microarray, which could have been utilised to provide information on expression levels of integrins, in addition to their presence or absence from the murine utricle. It would also have been possible to begin this study with a selected cohort of integrin subunits most likely to be expressed in the tissue of interest based upon a search of the literature, as was carried out after the capabilities of the degenerate PCR primers had been exhausted.

The integrins represent a group of proteins which are described as a 'family,' but which lack the degree of DNA sequence homology which might be expected of such a family of molecules. In the current era of genomics, with entire genomes for an ever-growing number of organisms being sequenced, it would seem unlikely, based upon the findings of this project, that by analysis of DNA sequence data alone, the 26 integrin subunits described in mammals would be considered homologous enough to warrant the term 'family.' It might be conceivable that some of the integrin subgroups identified in this thesis show the degree of homology that might now be expected of a protein family i.e. those α integrins which possess an I domain. Whilst they do not exhibit such largely conserved DNA sequences as shown by other protein families, the integrins do share a great deal in terms of their protein structure and cellular functions. All integrins are comprised of an α and β subunit to form a heterodimer, creating an adhesion molecule which provides a link between the surroundings of a cell (be it the extracellular matrix or the surface of a neighbouring cell) and its intracellular environment. The integrin cell surface receptors, which might be considered unlikely to be identified as a protein family were their individual members discovered today with the weight of genomic data available, remain linked as a highly divergent family group through their shared functional role as adhesion molecules.

In order to provide a more conclusive 'screen' of the normal adult mouse utricle and further establish which of the integrin α and β subunits are expressed in this tissue, a quantitative PCR based approach was deemed most appropriate. Using specific gene expression assays for each integrin subunit would remove the potential bias shown by the degenerate RT- PCR and cloning based strategies towards subunits expressed at a higher level in a given cDNA sample. Further discussion of the individual integrins detected in utricular cDNA in these degenerate and specific primer RT-PCR experiments is given in chapter 7, in order to provide a comparison with the results of subsequent qPCR analysis.

Chapter 4: Organotypic Culture of Mouse Utricles

4.1 Development of Organotypic Adult Mouse Utricle Culture Techniques

4.1.1 Objectives

The adult mouse utricle was selected as the tissue culture model for the work to be undertaken during this project. There have been numerous studies carried out using mature mammalian vestibular sensory epithelium, maintaining this inner ear tissue *in vitro* for considerable time periods. Previous work has shown how mammalian utricular tissue maintained in culture can be damaged and hair cell loss induced by treatment with aminoglycoside antibiotics (Warchol et al., 1993). This tissue, both *in vivo* and *in vitro*, has also been shown to partially recover, with the observation of immature stereocilia bundles appearing on the apical surface which gradually develop a more mature morphology(Bermingham et al., 1999; Forge et al., 1993; Lin et al., 2011).

Through the use of an *in vitro* culture system, it would be possible to alter the culture conditions of the tissue in order to successfully induce hair cell loss. The addition of an ototoxic drug i.e. gentamicin, to the culture medium would provide an easy method of manipulating the tissue as opposed to the systemic administration of antibiotic required for an *in vivo* approach.

In order to establish a sustainable model, experiments were initially carried out using methods previously practised by the research group for the culture of mammalian vestibular tissue (Forge and Li, 2000; Li et al., 1995). With these techniques as a starting point, experiments were carried out to investigate how adult mouse utricular tissue responded when cultured in this way, leading to the refinement and adaption of the methods and culture conditions as was required to produce a degree of hair cell loss sufficient for use in later experiments and to maintain the tissue for a substantial length of time whilst retaining manipulative capacity.

4.1.2 Use of MatTek™ Dishes Coated With Laminin

Initially, organotypic cultures were grown on MatTek™ dishes. These dishes have a glass bottom surface, allowing high resolution images to be taken directly. To this glass, a coating of the extracellular matrix protein laminin (Sigma) was added. A laminin solution at concentration of 1µg/75µl in serum-free culture medium and a thin layer of this solution was spread over the glass. The solution was air dried for one hour and the

remaining excess liquid removed by pipetting to leave a thin coating of laminin on the bottom of the dish.

Following dissection of the utricular tissue from the animal, a small volume of culture medium was added to the glass well of the MatTek™ dish on top of the laminin coating, and the tissue introduced with forceps, gently manipulating it in such a way that the utricles laid flat on the glass bottom, with the sensory epithelium uppermost. Culture medium was changed every other day, by removing and replacing half the total volume (200µl) of medium in order not to remove any essential secreted growth factors or other molecules.

When attempting to maintain organotypic cultures in this manner for longer time periods, the tissue became noticeably thinner and flatter, with cells 'growing out' from the utricle. On reaching 21 days in culture and beyond, the tissue had become extremely thin. This change in morphology made subsequent manipulation of the cultured tissue i.e. immunohistochemistry of wholemounts, difficult and it would have proved to be an even greater challenge to use these utricles for cryosectioning.

Initial experiments involved treatment of cultures with 2mM gentamicin for 24 hours only. This treatment failed to induce a significant degree of hair cell loss, when the tissue was labelled with hair cell markers (data not shown) to check for the presence of hair cells. Subsequently, all cultures were treated with 2mM gentamicin for a period of 48 hours. This aminoglycoside treatment was administered 24 hours after the initial tissue dissection and the start of the culture time period in order to allow the dissected tissue time to stabilise in the *in vitro* environment.

Although this approach successfully induced a sufficient degree of hair cell loss to be considered suitable for the study of the potential effects of hair cell loss on the integrin family, culturing on glass coated with laminin was not believed to be the optimal method of growing these cultures. The level of outgrowth seen and the difficultly this introduced into the use of the cultured tissue in subsequent experiments meant that an alternative surface on which to maintain the utricles was required. Laminin is an extracellular matrix protein and is therefore a potential ligand with which some integrin subunits are able to bind and interact; there were therefore concerns that using a laminin substrate could in itself have an effect on the expression and distribution of integrins during the culture process.

4.1.3 Use of Nitrocellulose Filter Papers

As an alternative surface on which to maintain organotypic utricle cultures, the use of 13mm diameter 0.45µm micropore nitrocellulose membrane filters (Millipore) was investigated. A single filter was added per individual well within a sterile 24-well plate (BD Falcon). Dissected utricles were carefully transferred onto the surface of these membrane filters with the sensory epithelium uppermost and covered with culture medium (400µl). Allowing a 24 hour period after dissection for the cultures to 'settle' prior to any gentamicin treatment, it was observed that the tissue appeared to settle quicker upon this surface and was therefore less inclined to be dislodged during subsequent changes of media.

In comparison to observations of utricles grown on laminin-coated glass, utricles maintained on nitrocellulose filters exhibited less outgrowth and did not become as thin and flattened when kept for longer time periods as had previously occurred. This allowed easier removal of the utricles from the membrane filter surface for use in subsequent immunohistochemistry experiments than had previously been possible. Additionally, the membrane filters were used to an advantage when cultures required cryosectioning. By keeping the tissue *in situ* on the membrane filter and cutting out a small square of the filter around each utricle, the filter could be used as a guide when embedding the tissue in agarose to achieve the required orientation for sectioning and to ensure that the tissue remained flat. Since the filter paper could clearly be seen within the agarose block when mounted on a cryostat chuck, and also within cut sections, the filter paper could be used to accurately judge when sectioning the tissue that the required point in the agarose block had been reached. This enabled the maximum amount of cryosections from each utricle to be acquired. If culture explants grown on laminin had been used for this purpose, they would have been extremely difficult to visualise and there would have been a far greater risk of missing the tissue entirely whilst using the cryostat.

4.2 Gentamicin Treatment Induces Hair Cell Loss In Adult Mouse Utricular Cultures

4.2.1 Organotypic Utricle Culture Morphology Under Transmission Electron Microscope

To examine the ultrastructure of utricular culture tissue, control tissue which had been maintained *in vitro* for a total of 7 days and had not undergone gentamicin treatment was fixed and prepared as described in 2.5 for viewing by transmission electron microscopy.

TEM sections of control utricles at this time point exhibit similar morphology to that expected within normal vestibular tissue. The sensory epithelium was well populated with hair cells which appeared to be viable, surrounded by supporting cells. The cytoplasm of hair cells has a lower electron density than that of supporting cells allowing these two cell types to be easily distinguished. Bundles of stereocilia are present on the apical surface of hair cells (Figure 4-1) whilst supporting cells have numerous microvilli apparent at their apices (Figure 4-2). A clearly defined basement membrane can be seen, dividing the distinct and separate regions of the organotypic culture tissue; the sensory epithelium (containing vestibular hair cells and supporting cells) and the underlying mesenchymal tissue (Figure 4-2).

Many of the vestibular hair cells in these TEM sections appear in good condition; several different types of organelle can be discerned at high magnification within the hair cell bodies. Mitochondria of a healthy size and shape (shown in Figure 4-1) are one indicator which supports the data obtained from the immunohistochemistry experiments carried out in this project; a large number of vestibular hair cells continue to populate the sensory epithelium of the utricle when cultured for 7 days without the addition of gentamicin. Additional features of sensory hair cells visible in higher magnification images of these cell bodies include the golgi apparatus or golgi body (Figure 4-3) and a lamellar body towards the base of the cell. Lamellar bodies consist of sheets of lamellae which resemble rough endoplasmic reticulum in appearance - their presence has been previously documented in sensory hair cells (Saito, 1983) .

In supporting cells, the cell cytoplasm is richly populated by vesicles (Figure 4-3) that appear to be full of an electron dense material, suggesting that they may be transport

vesicles in the process of conveying synthesised protein to the cell surface. This observation is supported by the results of subsequent imaging of utricular cultures under the scanning electron microscope (data presented in 4.2.4). It is possible that the vesicles observed by TEM could contain material synthesised within the supporting cell and that they are in the process of transporting this material to the apex of the cell to be secreted. This would also be an indicator of the health and survival of utricular tissue in culture using the techniques developed during this work.

Although the vestibular sensory epithelium appears generally healthy, there is some evidence of a limited amount of hair cell death occurring in tissue which has not been exposed to the ototoxic antibiotic. Cellular debris (figure 4-2) is visible outside of the epithelium above the apical surface of the cells. From the observed size and shape of this debris, it would appear to have originated from a hair cell which has undergone cell death and been extruded from the epithelium. It would be expected that despite the best efforts during dissection and the culture period, some cell death might be inevitable due to the removal of the tissue from its natural environment. The immunohistochemistry studies carried out earlier in this project, however, would support the belief that hair cells survive well using the culture techniques developed and that the majority of the hair cell damage and loss observed in gentamicin treated utricles is as a direct result of the ototoxic drug and not a product of the culture process itself.

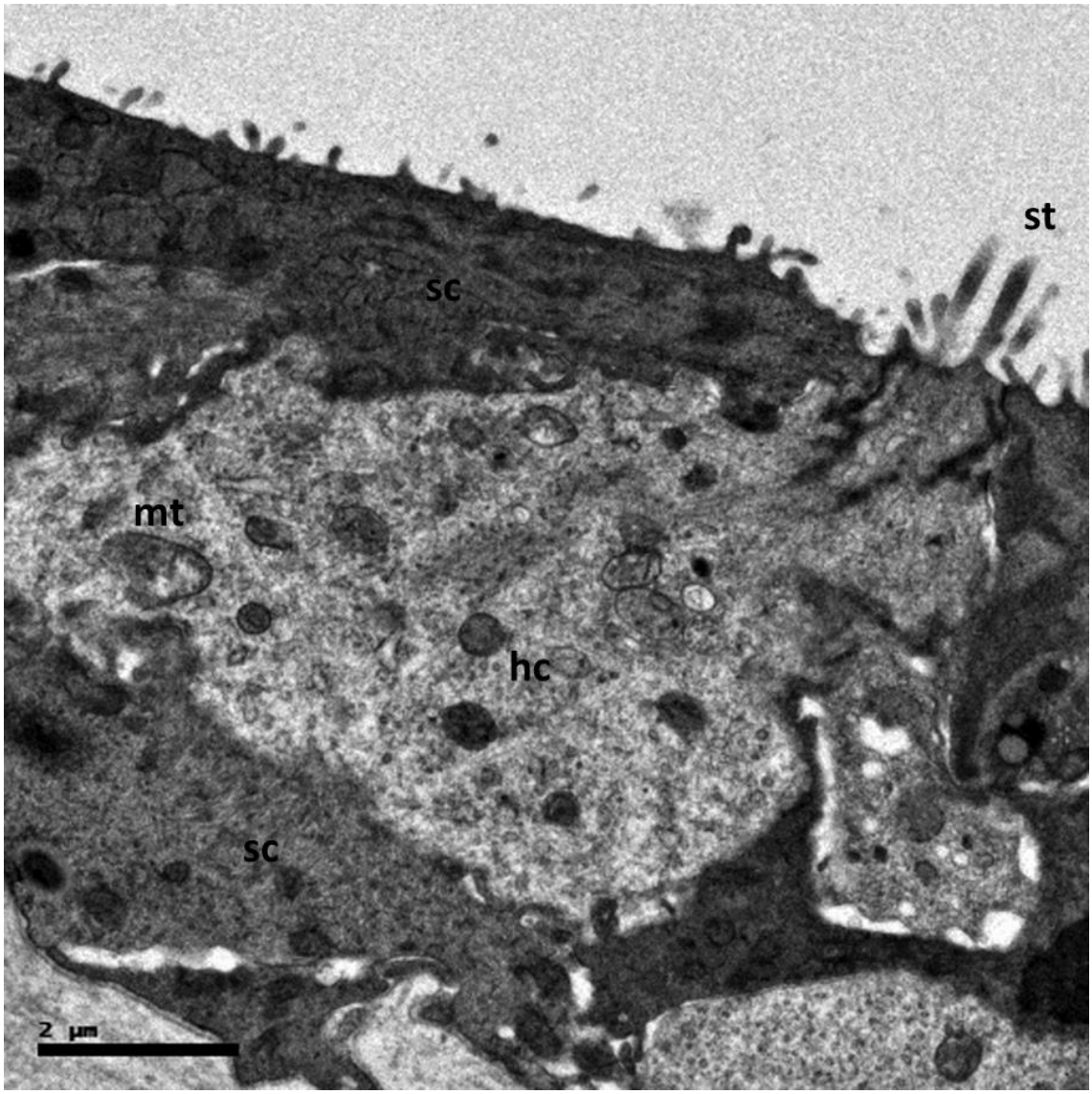

Figure 4-1 TEM of the Utricular Macula at 7 Days *In Vitro*

TEM section of a control utricle maintained for 7 days in culture without gentamicin treatment. 'Hc' indicates a vestibular hair cell, whilst 'sc' denotes the surrounding supporting cells, which have cell bodies that are considerably more electron dense than those of hair cells. Mitochondria (mt) and an apical stereocilia bundle (st) are also shown in this section of the epithelial layer of the tissue. Bar = 2µm.

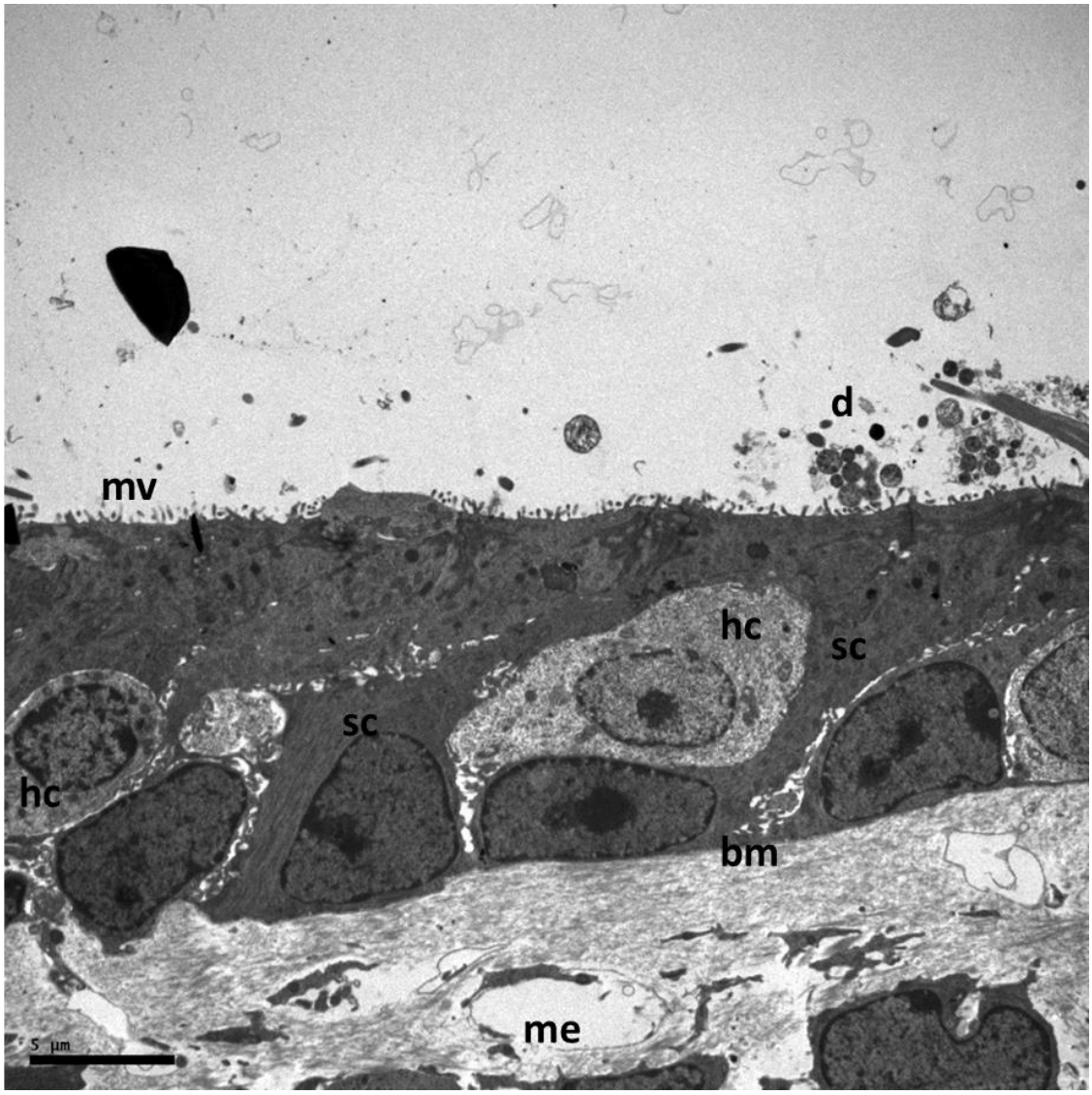

Figure 4-2 TEM of Utricular Sensory Epithelium and Underlying Mesenchyme at 7 Days *in vitro*

Utricular culture tissue maintained *in vitro* for 7 days without treatment with gentamicin viewed under TEM. The two main layers of the utricle; the sensory epithelium populated with hair cells 'hc' and supporting cells 'sc' and the underlying mesenchyme ('me') are separated by the clear border of the basement membrane 'bm.' Supporting cells have numerous microvilli (mv) projecting from their apical surface. Cellular debris ('d') is also visible outside of the epithelium in this section of tissue. Bar = 5µm.

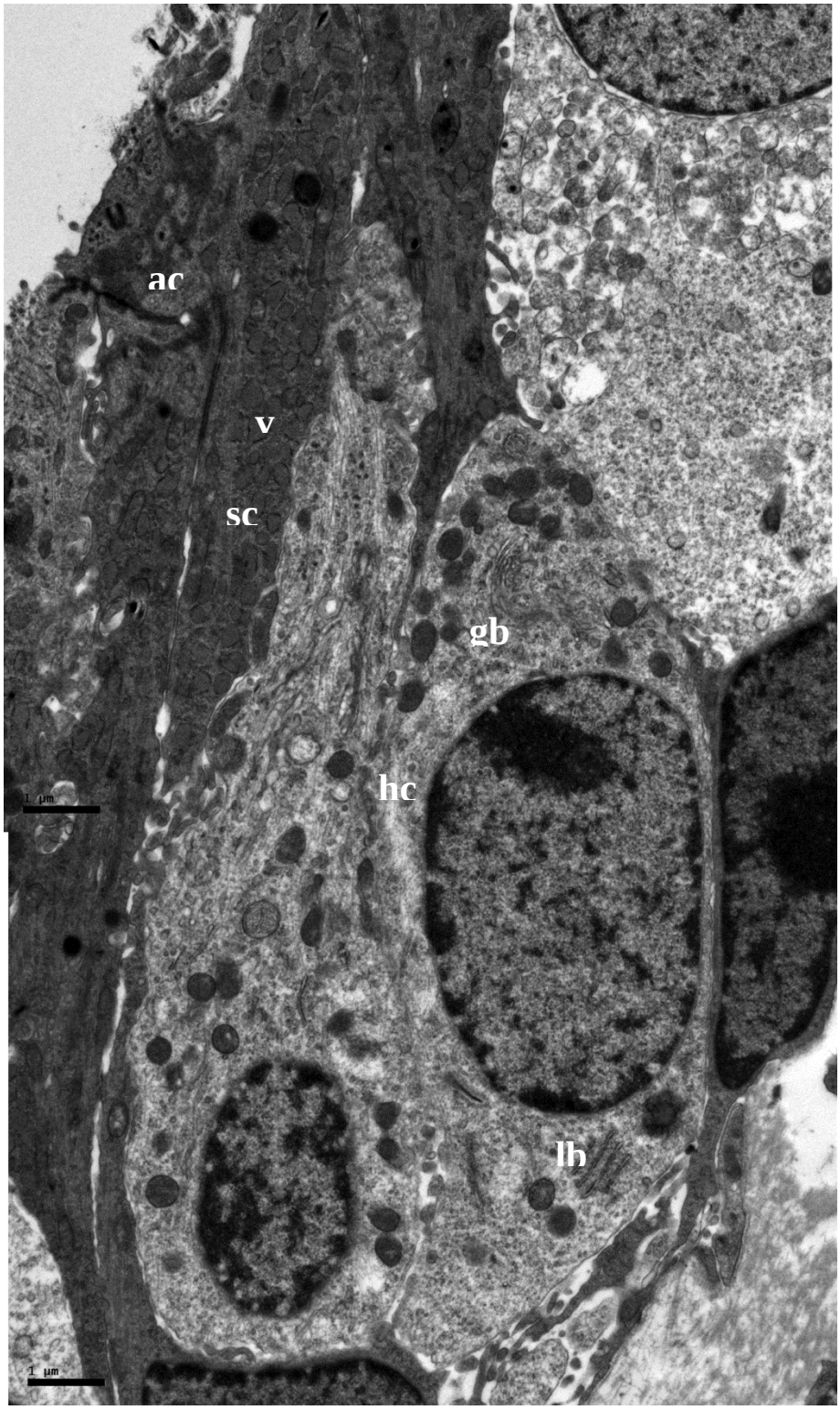

Figure 4-3 TEM of Hair Cells and Supporting Cells in Utricular Tissue at 7 Days *in vitro*

Utricular tissue cultured for 7 days in normal medium viewed by TEM. Supporting cell (sc) bodies are filled with vesicles (v) which appear to be filled with an electron dense material. An electron dense region at the apex of this supporting cell indicates an area of actin filaments (ac). Within the hair cell (hc) body, the golgi body (gb) and a lamellar body (lb) are both apparent within the cytoplasm. Bar = 1µm.

4.2.2 Immunohistochemistry of Adult Utricles Treated With Gentamicin

Utricular Cultures at 4 Days Post-Gentamicin Treatment

Organotypic utricle cultures which had been subjected to 48 hours incubation with 2mM gentamicin and had been fixed as described in 2.2.2, were labelled with fluorophore tagged phalloidin, in this case FITC-tagged (Fluorescein isothiocyanate). Phalloidin binds to f-actin and is used to visualise the actin cytoskeleton. In this tissue, Phalloidin-FITC labelled stereocilia bundles on the apices of vestibular hair cells and cell junctions. Utricles were also labelled with a hair cell marker; antibodies against either myosin Viia (which specifically labels the cytoplasm and hair bundles of sensory hair cells (Hasson et al., 1995)) or calretinin (a calcium binding protein which has also previously been used to label post-mitotic hair cells (Erkman et al., 1996)) were used to visualise vestibular hair cells. Calretinin is known to label only type I vestibular hair cells which are innervated by afferents which form calyces (Holmes and Rout, 2011). Utricular tissue maintained in culture for a total of 5 days, incubated in culture medium only, showed extensive coverage of the sensory epithelium with vestibular hair cells labelled with an antibody for myosin Viia (Figure 4-4 A). Hair cells also showed evidence of stereocilia still present on their apical surface following a 5 day period in culture, when labelled for actin filaments with a phalloidin-FITC fluorophore (Figure 4-4 Aii)

In comparison, utricles which had undergone 48 hours exposure to gentamicin show a considerable decrease in the number of cells positively labelled for the hair cell marker antibody to myosin Viia (Figure 4-4 Bi & Ci). Hair cell counts of gentamicin treated utricles at 2 days post-gentamicin showed a 42% decrease in hair cell numbers in comparison to control counterparts maintained *in vitro* for the same length of time (Figure 4-8), indicating that the decrease in hair cell numbers is attributable to aminoglycoside exposure and not purely a side-effect of the culture conditions. One-way ANOVA analysis of hair cell count data calculated a P value of 0.0012, indicating that the variation of the mean hair cell counts of the groups (in this case the groups consisted of 2, 14 and 28 days post-gentamicin utricles, with control counterpart groups at 2 and 28 days), is significantly higher than would be expected to occur by chance through random sampling. However, the use of the post-hoc Tukey's test (shown in table 4-1) to compare the mean hair cell numbers at 2 days post-gentamicin and in

control counterparts cultured for the same time period calculated a P value > 0.05, and therefore could not be considered statistically significant. Myosin Viia positive hair cells in such cultures were also seen to lack stereocilia (Figure 4-4 Dii), whilst their control counterparts cultured for the same length of time overall maintained their apical bundles, suggesting that this observed difference was also a result of the gentamicin treatment. Gentamicin treated utricles at 4 days post-gentamicin also showed evidence of cellular debris within the sensory epithelium; (Figure 4-4 Di, arrows) irregular plaques of myosin Viia positive labelling can be seen at the same level as vestibular hair cells which have survived the drug exposure. There is also evidence of scar formation, where supporting cells have spread in order to close the breach in the epithelium caused by loss of hair cells, indicated by the labelling of cell junctions by Phalloidin-FITC (Figure 4-4 Dii, arrow).

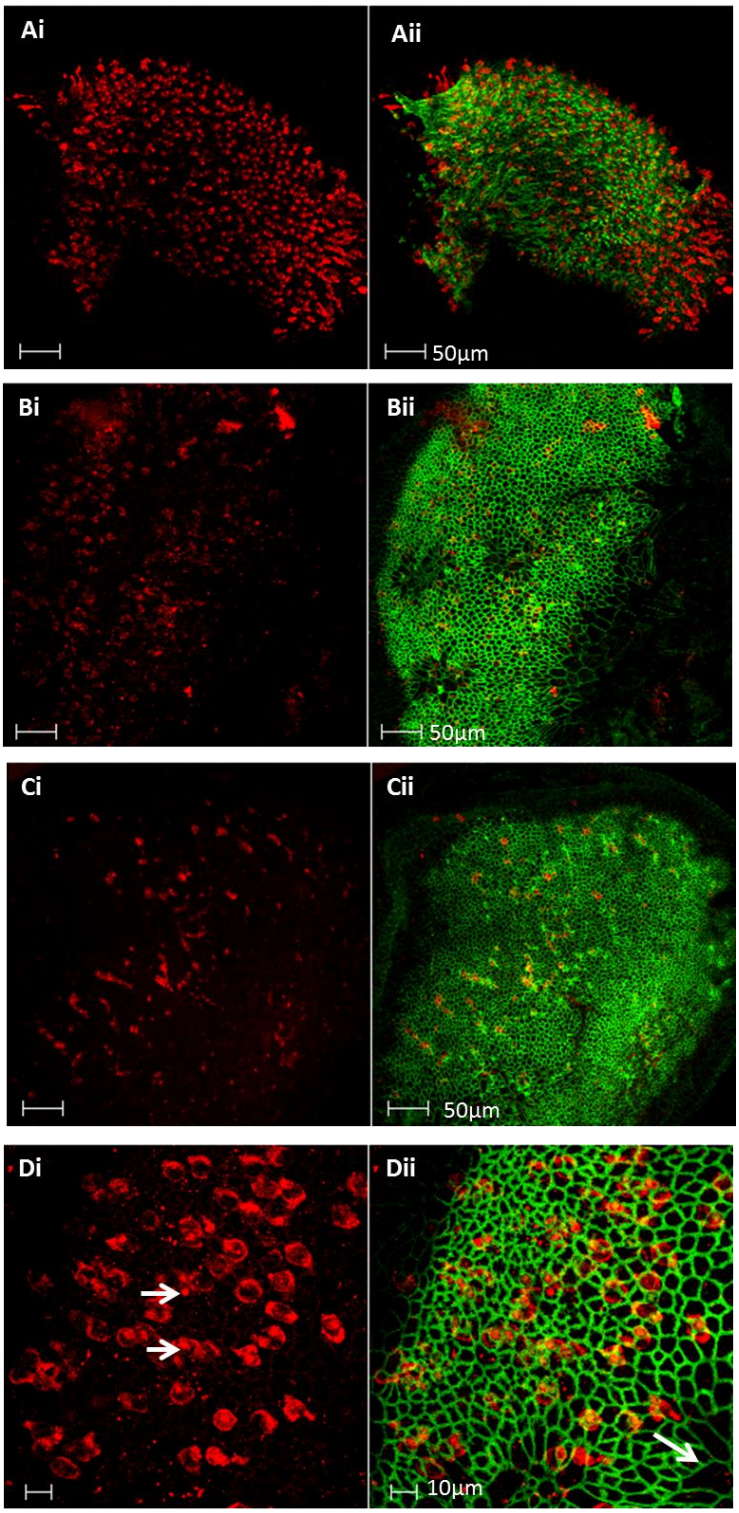

Figure 4-4 Utricular Cultures at 4 Days Post Gentamicin Treatment

Wholemount utricular cultures labelled with phalloidin-FITC (green) and antibody to myosin Viia as a marker for hair cells (red). (A) Control tissue cultured for 5 days without gentamicin treatment. (B & C) Utricles after 4 days recovery following gentamicin treatment. (D) Utricle from (B) imaged at x63. (Di) Arrows = myosin Viia positive plaques within the epithelium. (Dii) Arrow = scar formation.

Utricular Cultures at 10 and 14 Days Post-Gentamicin Treatment

Control utricles maintained *in vitro* for 13 days (in parallel with gentamicin treated tissue which was fixed and labelled 10 days after the cessation of gentamicin incubation) continued to survive after this length of time in culture. Hair cells positive for myosin Viia were abundant (Figure 4-5 Ai) across the sensory epithelium. These hair cells also continued to maintain an apical bundle of stereocilia as shown by labelling with phalloidin-FITC (Figure 4-5 Aii).

Gentamicin treated utricles cultured for the same time period, showed markedly fewer hair cells positive for myosin Viia (Figure 4-5 Bi). It is also possible to observe atypical irregular plaques of myosin Viia positive immunolabelling which appear to be the 'debris' from hair cells which have been disrupted by the aminoglycoside treatment, as was observed at 4 days post-gentamicin. This debris is visible within the sensory epithelium itself. Of those hair cells which have survived, Phalloidin-FITC indicates that the majority do not have intact stereocilia at their apices (Figure 4-5 Bii).

Immunofluorescent labelling of control cultures grown for 17 days, in parallel with utricles which were gentamicin treated and maintained for a further 14 days afterwards, demonstrates the ability of adult utricular tissue to survive well using the culture technique which has been developed during this work. Control tissue at this time point is highly populated with vestibular hair cells with a large number of cells labelled positively for the hair cell marker calretinin (red) (Figure 4-3 Ai). Hair cell counts (sampled from utricles labelled with myosin Viia as the hair cell marker) reveal that there is a further 65% decrease in hair cell numbers between utricles cultured for 2 days post-gentamicin in comparison to those maintained for 14 days post treatment (Figure 4-8). Comparison of the mean hair cell counts at 2 and 14 days post-gentamicin using Tukey's test did not calculate the difference in hair cell numbers between these experimental conditions as being statistically significant ($P > 0.05$).

Gentamicin treated utricles at 14 days post drug exposure, appear very similar to those fixed at 10 days post-gentamicin treatment. The sensory epithelium shows a distinct reduction in hair cells positively labelled with myosin Viia (Figure 4-6 Bi); hair cell counts show an 80% decrease in hair cells which are myosin Viia positive (Figure 4-8) compared to hair cell numbers in control utricles cultured for 5 days. When the mean hair cell count at 14 days post-gentamicin was compared to that of the 2 day-post

gentamicin control counterpart group, Tukey's test calculated a P value of <.0.01; the difference in the mean hair cell numbers of these two groups can therefore be considered statistically significant. Phalloidin labelling also shows the presence of scars formed on the epithelial surface (Figure 4-6 Bii, arrow).

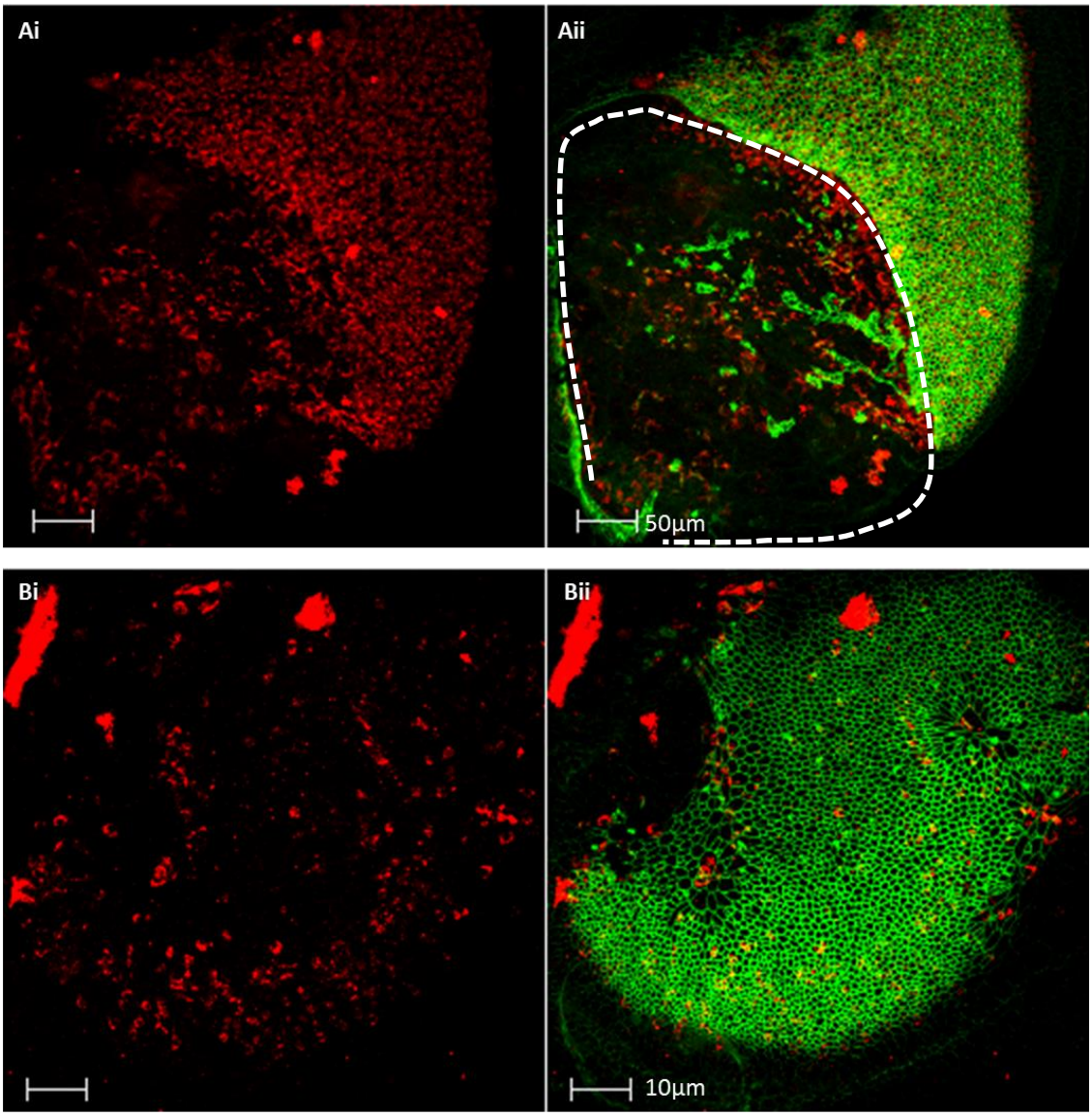

Figure 4-5 Utricular Cultures at 10 Days Post Gentamicin Treatment

Wholemount organotypic utricular cultures labelled with phalloidin-FITC (green) and for the hair cell marker myosin Viia (red). (A) A control utricle maintained for a total of 13 days *in vitro* without being subject to gentamicin treatment. The outlined region is believed to be an area in which the epithelial surface of the tissue was damaged during the dissection process. (B) Gentamicin treated utricular tissue fixed following a 10 day recovery period. 'D' indicates irregular plaques of myosin Viia positive labelling believed to be cellular debris.

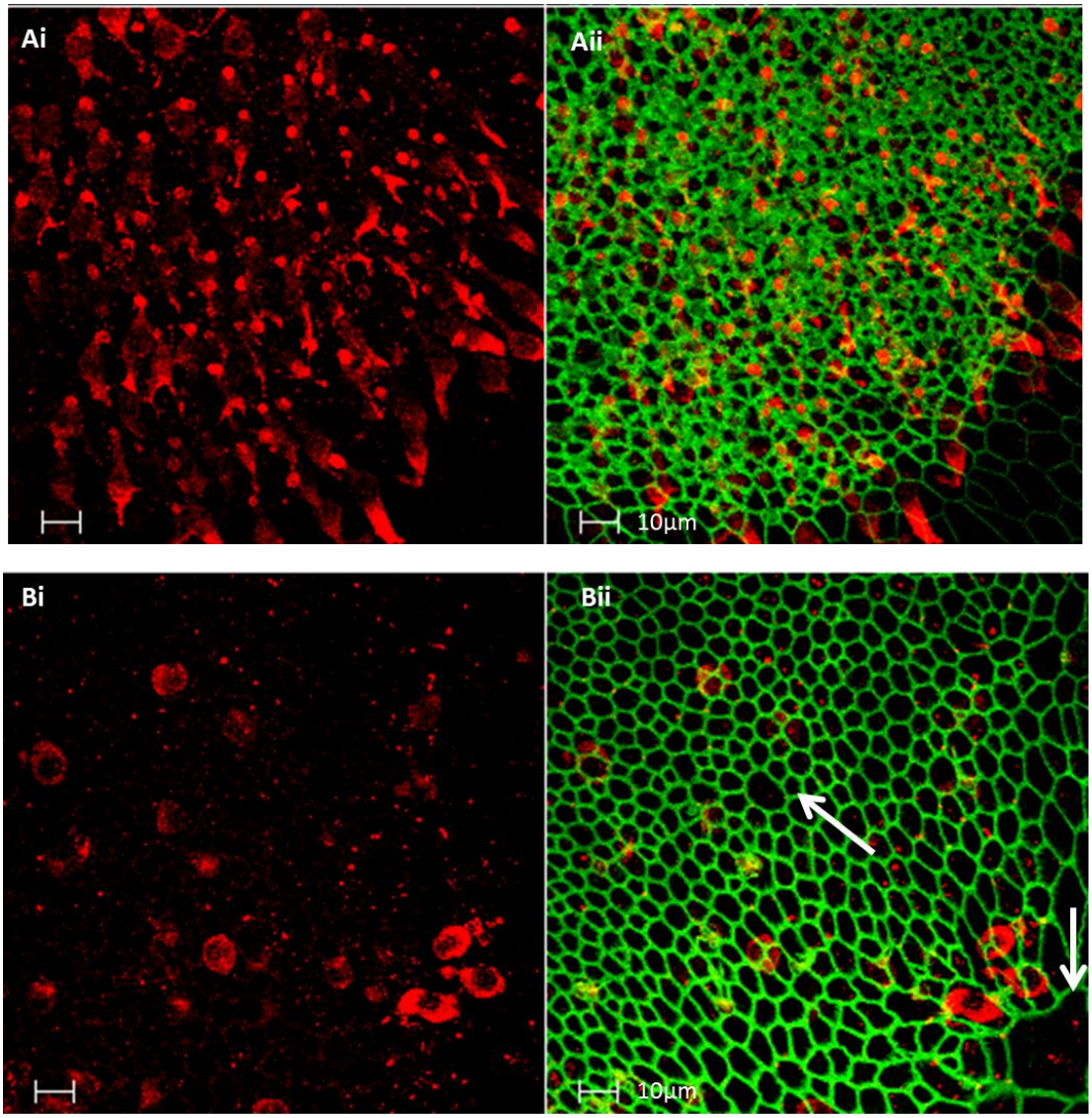

Figure 4-6 Utricular Cultures at 14 Days Post Gentamicin Treatment

Wholemount organotypic utricular cultures labelled with phalloidin-FITC (green) and for the hair cell marker myosin Viia (red). (A) Control tissue cultured for a total of 17 days labelled with the hair cell marker calretinin (red). DAPI (blue) labels cell nuclei. (B) Gentamicin treated utricular tissue fixed after a 14 day recovery period labelled with the hair cell marker myosin Viia (red). Arrowheads indicate scarring on the epithelial surface where Phalloidin-FITC labelled actin filaments are present at cellular junctions.

Utricular Cultures at 28 Days Post-Gentamicin Treatment

The longest time period for which adult mouse utricles were maintained *in vitro* during these studies was 31 days. Control tissue cultured for this time period continued to survive well under these experimental conditions; the sensory epithelium of these utricles exhibits dense population with myosin Viia positive vestibular hair cells (Figure 4-7 Ai). Bundles of stereocilia, visualised by Phalloidin-FITC staining, are both apparent and abundant (Figure 4-7 Aii), although not present on every myosin Viia positive hair cell.

Gentamicin treated utricles which were maintained for the same total length of time i.e. grown for 28 days post-gentamicin treatment, show a marked reduction in hair cell numbers when immunofluorescently labelled with a hair cell marker (Figure 4-7 Bi) When compared to gentamicin treated utricles fixed at 14 days post antibiotic exposure, there is not a large visible difference in the degree of hair cell loss. Hair cell counts show an 82% decrease in hair cell number in utricular tissue at 28 days post-gentamicin when compared to hair cell numbers in control counterparts maintained *in vitro* for the same time period (Figure 4-8). Tukey's test calculated a P value of < 0.01 when comparing the mean hair cells counts of these two groups, therefore the difference observed between control and gentamicin-treated utricles at this time point can be considered statistically significant. This data also demonstrates that control utricles cultured for a total of 31 days show an 18% decrease in hair cell numbers in comparison to control utricles cultured for 5 days. However, Tukey's test calculated a P value $>$ 0.05 when comparing the mean hair cell numbers of control utricles maintained *in vitro* for 5 and 31 days, showing that the difference between these two groups is not statistically significant. This finding supports the observations of immunolabelling on long term control cultured utricular tissue, that vestibular hair cells survive well under these experimental conditions, and that the observed hair cell loss in gentamicin treated tissue is not purely a side effect of the culture technique used.

When viewed at higher magnification (x63 objective) what appear to be small immature hair bundles (Figure 4-7 Cii & Dii, insets indicated with arrows) can be seen in these utricular cultures, which are positively labelled with Phalloidin-FITC. As previously described in birds during regeneration (Cotanche, 1987) and mammals – e.g. in regenerating guinea pig utricles (Forge et al., 1998) and in mouse utricles during

development (Denman-Johnson and Forge, 1999), cells bearing these short hair bundles also appear to have a smaller surface area than would be expected of a mature hair cell, suggesting that they may potentially be regenerated cells. A sampling of 4 utricles calculated these immature bundles to be present at an average of 0.42 bundles/1000μm^2 (to 2 d.p.). This suggests there is some limited degree of regeneration occurring within the vestibular sensory epithelium after 4weeks *in vitro* following gentamicin-induced hair cell loss.

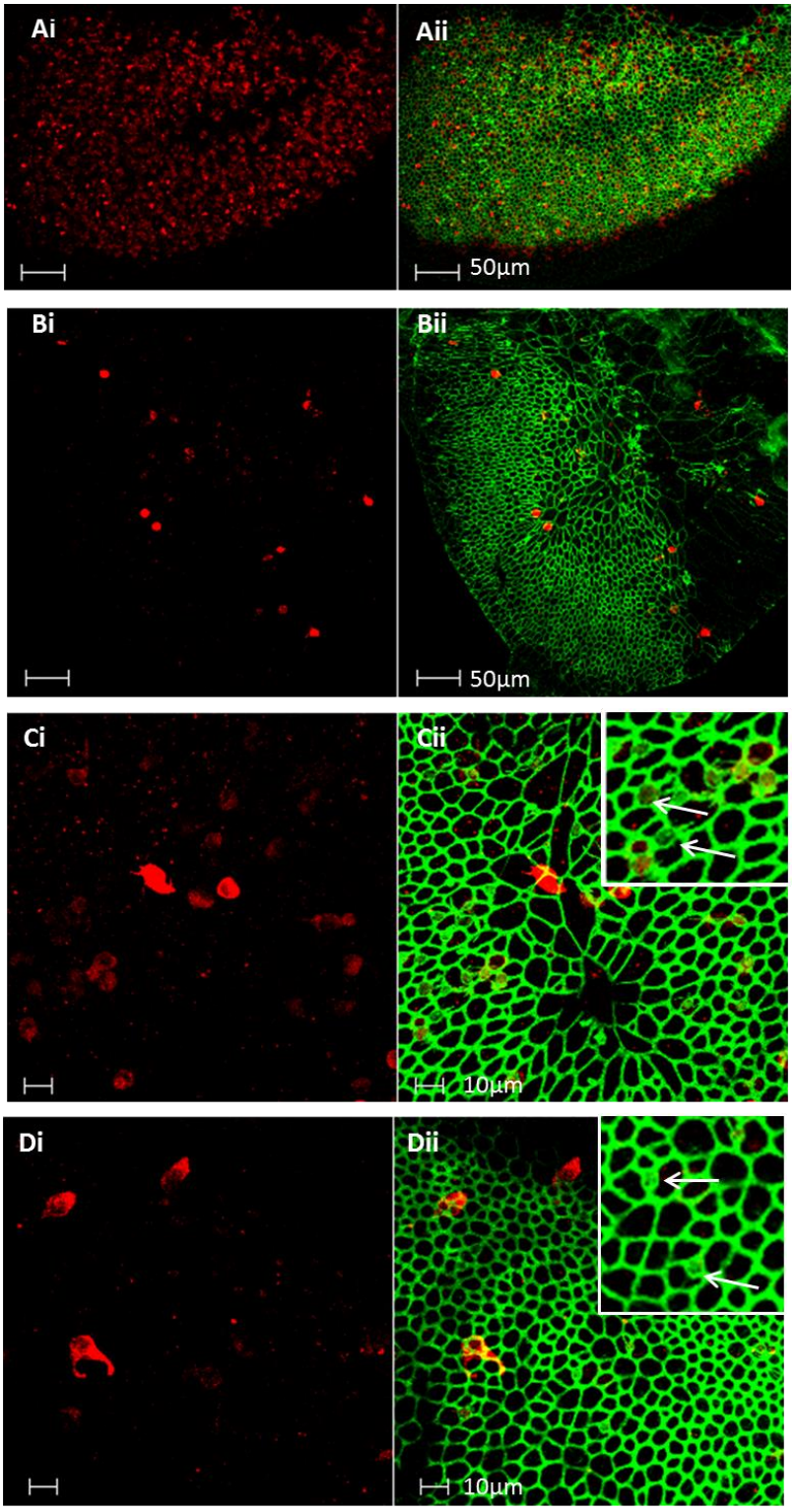

Figure 4-7 Utricular Cultures at 28 Days Post Gentamicin Treatment

Wholemount organotypic utricular cultures labelled with phalloidin-FITC (green) and for the hair cell marker myosin Viia (red). (A) Control tissue maintained for a total of 31 days *in vitro* without receiving gentamicin treatment. (B) Gentamicin treated cultured utricular tissue fixed after a 28 day recovery period. (C & D) Gentamicin treated utricles viewed with the x63 objective. (Cii & Dii insets) Arrows indicate the presence of small immature stereocilia bundles on the apical surface of some cells.

A

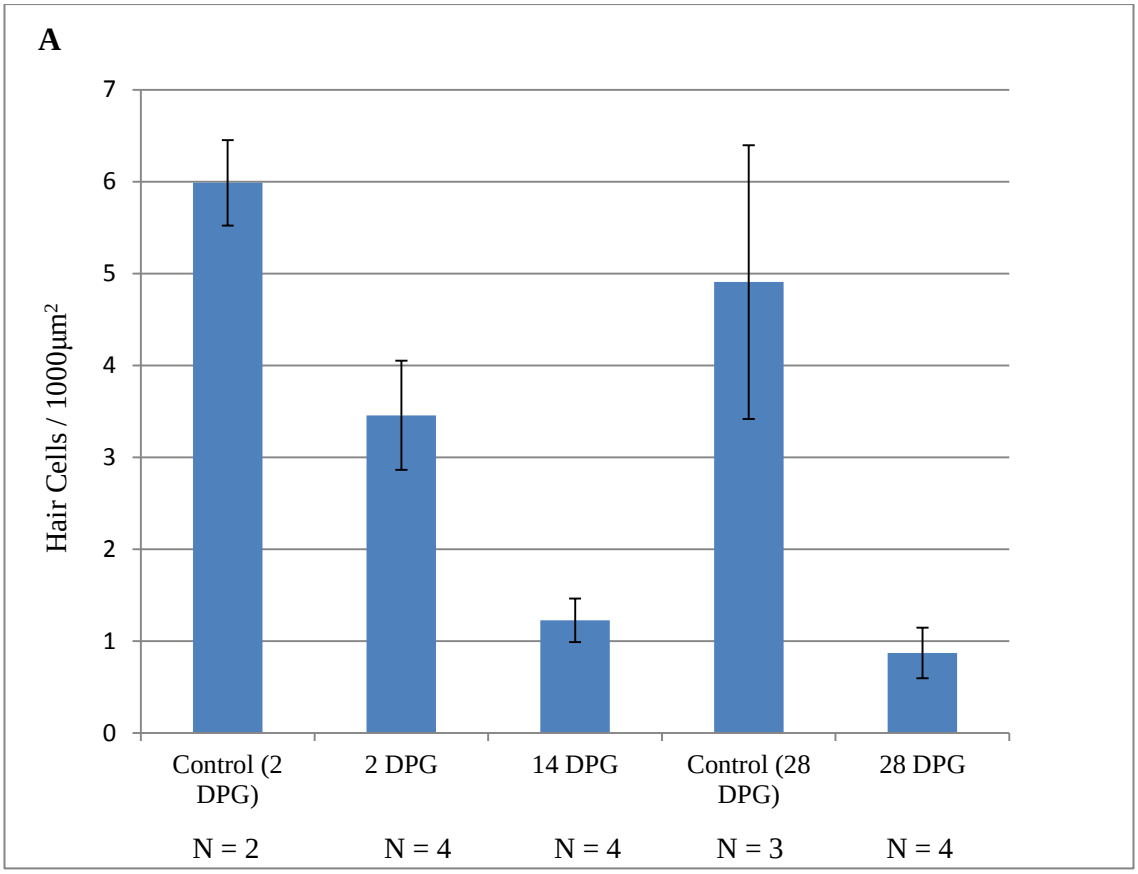

B

	HC/1000µm² (to 2 d.p.)	N (No of utricles)	SD (to 2 d.p.)	SEM (to 2 d.p.)
Control (2 DPG)	5.99	2	0.66	0.46
2 DPG	3.46	4	1.19	0.59
14 DPG	1.23	4	0.47	0.24
Control (28 DPG)	4.91	3	2.58	1.49
28 DPG	0.87	4	0.55	0.28

Figure 4-8 Hair Cell Loss in Gentamicin Treated Cultured Utricles

Hair cell counts (i.e. cells positive for myosin Viia) from utricles cultured for several incubation periods following gentamicin treatment (and untreated controls). HC numbers were counted from x63 magnification confocal images using Image J software. Controls were maintained for the same length of time as their gentamicin treated counterparts, but were cultured in normal medium only. Each utricle was sampled 2-3 times and HC counts averaged, before being normalised to give hair cell numbers as a value of HCs/1000µm^2. (A) Comparison of HC numbers at different time points in culture. Error bars show standard error. Percentage decrease of hair cell numbers given in chapter 4 were calculated using the HC/1000µm^2 values shown in table (B).

Comparison	Mean Difference	q	P Value
Control (2 D) vs Gent (2 DPG)	2.53	3.239	ns P>0.05
Control (2 D) vs Gent (14 DPG)	4.761	6.095	** P<0.01
Control (2 D) vs Control (28 D)	1.08	1.312	ns P>0.05
Control (2 D) vs Gent (28 DPG)	5.116	6.55	** P<0.01
Gent (2 DPG) vs Gent (14 DPG)	2.231	3.498	ns P>0.05
Gent (2 DPG) vs Control (28 D)	-1.449	2.104	ns P>0.05
Gent (2 DPG) vs Gent (28 DPG)	2.586	4.055	ns P>0.05
Gent (14 DPG) vs Control (28 D)	-3.681	5.343	* P<0.05
Gent (14 DPG) vs Gent (28 DPG)	0.3551	0.5568	ns P>0.05
Control (28 D) vs Gent (28 DPG)	4.036	5.858	** P<0.01

Table 4-1 One-way ANOVA Statistical Analysis; Post-Hoc Analysis by Tukey's Test

This table shows the results of the Tukey's test carried out on the hair cell count data collected from utricles maintained for multiple time periods following gentamicin treatment and control counterparts. Each pairwise comparison of mean hair cell count values analysed by the Tukey's test is shown, in addition to the resulting P value; this statistical analysis indicates whether the differences in the mean values for each pair of experimental conditions are significantly different from one another. The following abbreviations are used by the GraphPad software to denote significance; ns = not significant, * = significant (P = 0.01 – 0.05), ** = very significant (P = 0.001 – 0.01).

4.2.3 EdU Labelling of Organotypic Utricular Cultures to Measure Cell Proliferation

In order to investigate the level of cell proliferation taking place in the utricular culture model system, 5-ethynyl-2´-deoxyuridine (EdU) labelling was utilised to allow the visualisation of all cells which had undergone mitosis during the culture period. EdU, an alternative to 5-bromo-2'-deoxyuridine (BrdU), is a nucleoside analog of thymidine, which can become incorporated instead of a natural nucleoside during the DNA synthesis process; DNA synthesis is a required phase for any cell which is undergoing mitotic division (Hynes, 2004). EdU is good alternative to BrdU, since it does not require the same treatment with hydrochloric acid (HCL) that BrdU necessitates in order to detect labelled cells, and thus the potential for damage to the tissue and other antigens which may be required for antibody labelling is reduced. Utricular tissue was cultured in the presence of 10µM EdU in normal culture medium solution. EdU-containing medium was only used for culture experiments after the 48 hour gentamicin treatment had been completed; thus limiting the cells detected to those which had undergone mitotic events occurring after ototoxic drug exposure. This would focus results on the behaviour of the tissue during its period of hair cell loss and potential recovery. A 'Click-IT'™ kit (Invitrogen) was used to visualise any EdU labelled nuclei after fixation of the culture tissue. As described in the kit protocol, the detection of EdU is based on a click reaction, a copper catalysed covalent reaction between an azide (the Alexa Fluor® 488 dye) and an alkyne (the EdU).

EdU Labelling in Cultured Utricles at 3 Weeks Post-Gentamicin Treatment

Cultured tissue maintained *in vitro* for 3 weeks post-gentamicin treatment (i.e. a total of 24 days), was labelled with a hair cell marker and for EdU to visualise any cells which had incorporated the EdU supplied to them whilst in culture into their genetic material during DNA synthesis. Using the LSM image browser software, it was possible to analyse z-stack confocal images of wholemount utricles by orthogonal sections, which visualised the location of EdU positive cells within different layers of the utricular tissue.

A control utricle (Figure 4-9) maintained *in vitro* for the same time period, but which was not exposed to the ototoxic drug, showed that cell proliferation occurs in these organotypic cultures irrespective of drug induced hair cell death. There are a high

number of hair cells present on the sensory epithelium of this utricle (Figure 4-9 B) which are positively labelled with the hair cell marker calretinin, as seen in previous immunohistochemistry experiments examining the culture model system development. Orthogonal sectioning of this image (Figure 4-9 A) shows that EdU positive cells (labelled in green) are localised to the mesenchymal tissue underlying the sensory epithelium (Figure 4-9 A, far right). There are no cells visible which show co-localisation of the hair cell marker and EdU. There are also no supporting cell nuclei which are EdU positive, indicating that none of the cells of the sensory epithelium have undergone mitotic division. It would appear that the cell proliferation observed by this EdU labelling is mostly confined to the area of the cultured tissue which is involved in the outgrowth of the original tissue on the nitrocellulose filter surface upon which the cultures are maintained.

Organotypic cultures which received 48hrs gentamicin treatment and were then allowed a further 3 week recovery period *in vitro* (Figure 4-10) showed evidence of cell proliferation when labelled for EdU. Cell counts of DAPI positive nuclei and EdU positive nuclei (data presented in figure 4-11) from the entire utricle, indicate that approximately 27% of cell nuclei were positive for the mitotic marker, although, as with control utricles, there was no evidence of cells positive for EdU (labelled in red) also being positive for the hair cell marker calretinin. This would suggest that any regenerated hair cells present at this time point are not the product of supporting cells re-entering the cell cycle and dividing mitotically. The use of orthogonal sections to assess z-stack images of gentamicin treated cultures at this point allows visualisation of the level at which EdU positive nuclei are present and how this corresponds to the level where hair cell bodies are located.

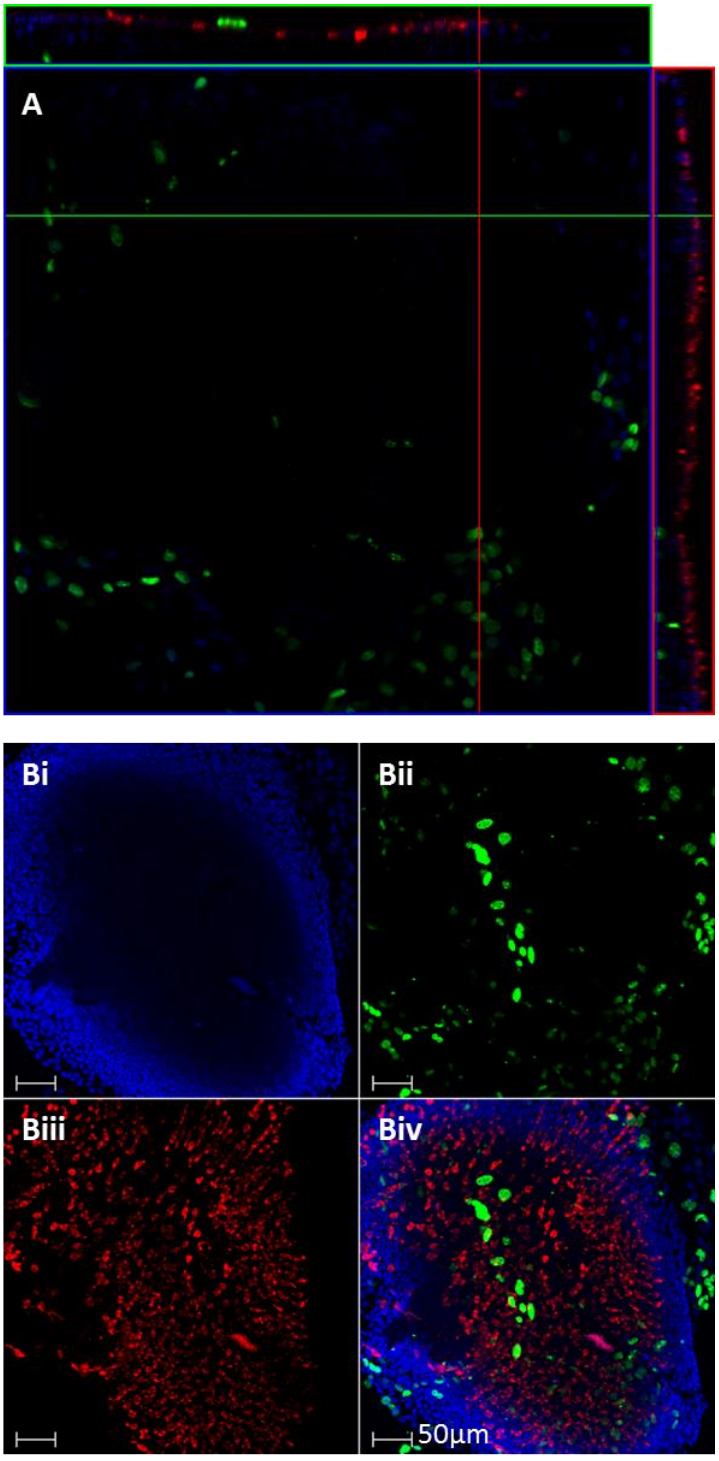

Figure 4-9 Proliferation in Cultured Utricle Tissue at 24 Days *In Vitro* Without Gentamicin Treatment

Organotypic utricular cultures immunolabelled as wholemount tissue using DAPI (blue) to label cell nuclei, calretinin (red) to label vestibular hair cells and the Click-IT™ reaction system with Alexa Fluor® 488 to label EdU positive nuclei. (A) Z-stack image of control tissue maintained *in vitro* for 24 days without gentamicin treatment, viewed by orthogonal sectioning. The location of EdU positive nuclei within the cell layers of the utricle is visualised in this way. (B) Maximal projection of the same z-stack used for orthogonal sectioning in (A).

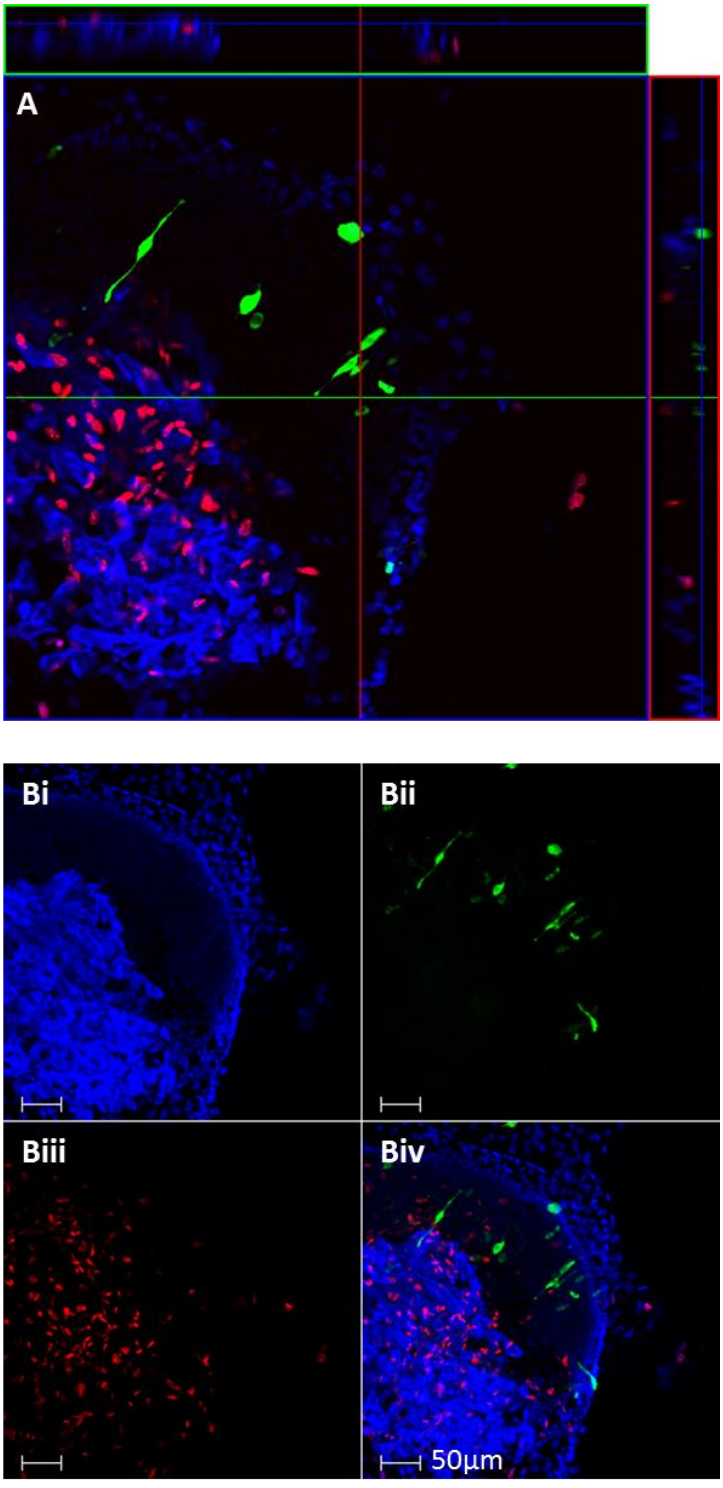

Figure 4-10 EdU labelling of Cultured Utricles at 21 Days Post Gentamicin Treatment

Organotypic utricular cultures immunolabelled as wholemount tissue using DAPI (blue) to label cell nuclei, calretinin (green) to label vestibular hair cells and the Click-IT™ reaction system with Alexa Fluor® 488 to label EdU positive nuclei (red). (A) Z-stack confocal image of a utricle cultured for 21 days post gentamicin treatment, viewed by orthogonal sectioning to show the relative location of hair cells and EdU positive nuclei within the cultured tissue. (B) Maximal projection of the z-stack image used for analysis by orthogonal sectioning in (A).

A

	Nuclei/1000µm^2 (to 2 d.p.)	N (No of utricles)	SD (to 2 d.p.)	SEM (to 2 d.p.)
Total Nuclei (DAPI +ve)	8.26	8	3.03	1.07
EdU +ve Nuclei	2.25	8	1.07	0.38

B

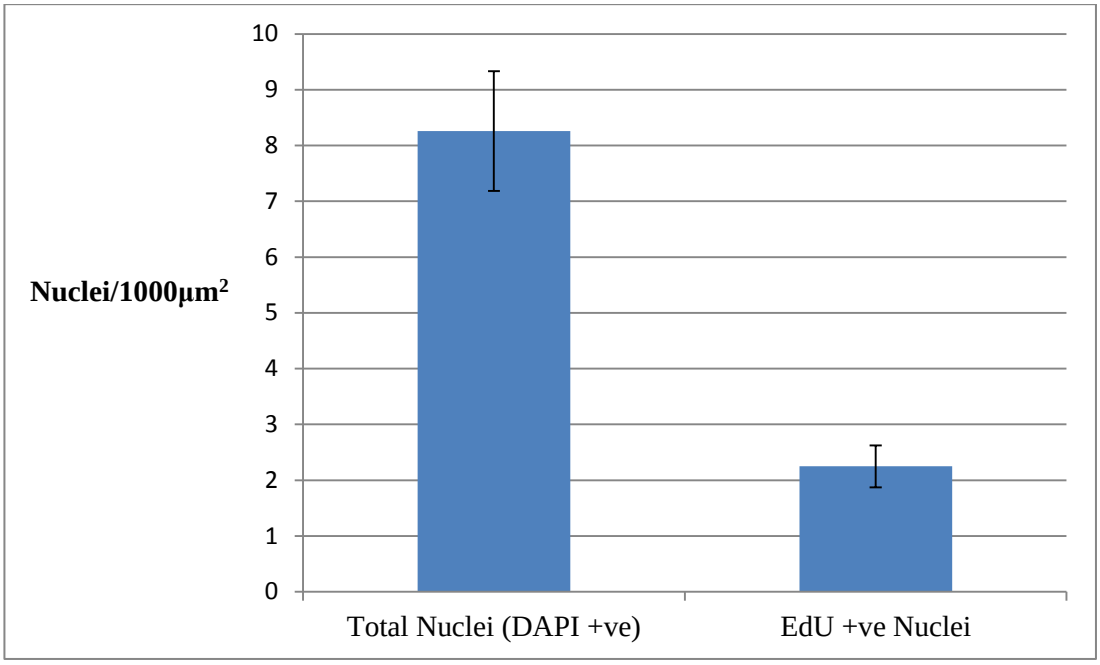

Figure 4-11 Proliferation in the Adult Mouse Utricle at 21 Days Post-Gentamicin

Cell counts were carried out on z-stack confocal images of utricles cultured for 21 days post-gentamicin in the presence of the mitotic marker, EdU. Total nuclei (those positive for DAPI) and EdU positive nuclei were counted using Image J on random samples of a total of 8 utricles; each utricle was sampled 2-3 times. SD = Standard deviation. SEM = Standard error. (A) Cell count data was used to calculate the percentage of nuclei that were EdU positive. (B) Graph compares the numbers of DAPI positive nuclei to those also positive for EdU. Error bars show standard error.

4.2.4 Organotypic Utricle Culture Morphology Examined Under the Scanning Electron Microscope

Utricular Tissue Cultured for 5 Days Post-Gentamicin and Control Counterparts

Scanning electron microscopy was utilised to provide further morphological evidence as to how the appearance of the vestibular sensory epithelium alters in response to ototoxic drug treatment.

Control utricles, cultured for a total of 8 days, appear healthy and demonstrate an intact, regular, sensory epithelial surface which is widely populated with hair cells and supporting cells (Figure 4-12 A). When viewed at a higher magnification, there is widespread persistence and maintenance of stereocilia bundles on the apical surface of vestibular hair cells (Figure 4-12 B) as seen previously by labelling cultured utricles with phalloidin. These stereocilia appear normal in their morphology and organisation.

In addition to the cells of the epithelium, the presence of a fibrilar substance which extends across much of the surface of the epithelium is visible. From the structural appearance of this material, it is believed to be otolithic membrane which has been produced by the supporting cells, acting as a potential indicator that the supporting cells survive well in the tissue under these culture conditions. That this membrane is still in the process of being actively synthesized by these cells is supported by evidence of vesicles which appear to be full of material, being present in the supporting cell cytoplasm when viewed by TEM.

In comparison, tissue maintained for the same total number of days, but which was subjected to a 48 hour gentamicin treatment, shows a marked decrease in the number of hair cells visible on the surface of the epithelium (Figure 4-13 A) and there are large areas of the tissue where supporting cell scars have formed to maintain an unbroken epithelial layer. Despite the large decrease in the number of vestibular hair cells in this tissue, some have retained stereocilia (Figure 4-13 B). Many of these hair cells are located towards the periphery of the tissue, suggesting that perhaps hair cells in this region are less sensitive to the ototoxic drug. There are hair cells present which maintain apical hair bundles with a more normal morphology (Figure 4-14 B), whilst stereocilia in varying stages of disarray and disorder are also visible; including those which have become fused (Figure 4-13 B and Figure 4-15 A). Additional observation shows what

appears to be an immature bundle with a kinocilium (Figure 4-13). From these SEM images, it is not possible to determine whether this stereocilia structure has been created by regeneration of the tissue in response to gentamicin-induced hair cell loss, or whether this was a hair cell that was not fully mature at the time the tissue was dissected from the animal.

In addition to hair cells with fused, disorganised stereocilia, which are likely to be in the process of dying, there is evidence of vestibular hair cells which are further ahead in the cell death process. Numerous incidences across the damaged epithelial surface (Figure 4-16 B) of dying hair cells being extruded from the tissue at the apical region may be seen, as supporting cells expand and seek to remove the dead hair cell and close any consequent breakage in the epithelial layer.

In gentamicin-treated utricles at this time point the epithelial surface is covered with material that resembles otolithic membrane (Figure 4-15 A). This membrane has a distinctive ‘honeycomb’ like appearance and its continued presence indicates that the supporting cells have not been affected by the ototoxic drug exposure. It is possible to see healthy looking microvilli protruding from the apical surfaces of the supporting cells underneath the otolithic membrane structure.

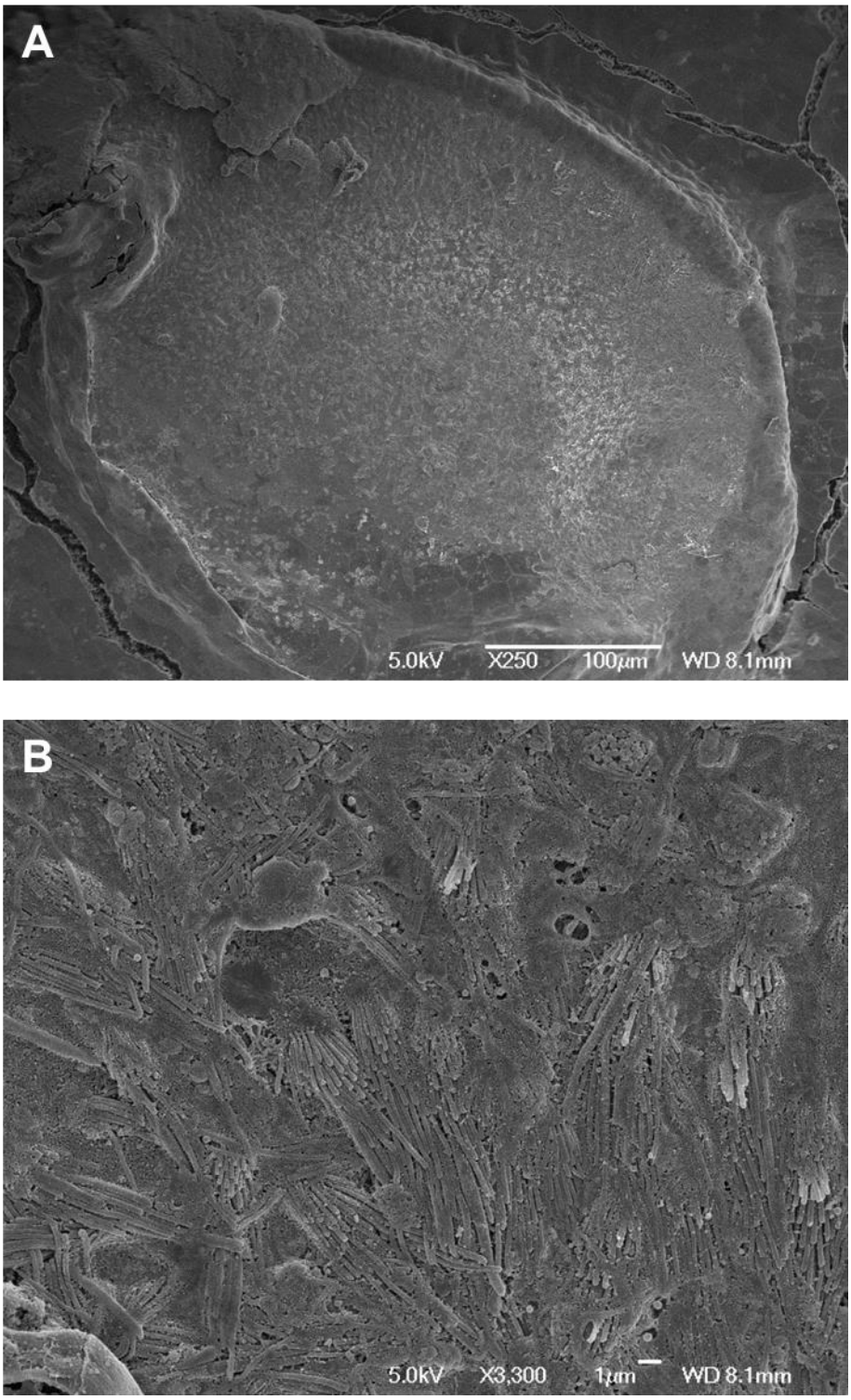

Figure 4-12 Control Utricular Tissue Maintained in Culture for 8 Days Viewed by Scanning Electron Microscopy

The surface of the sensory epithelium from utricle cultures maintained *in vitro* for 8 days with no gentamicin treatment. (A) An overview of the surface of the entire utricle. Bar = 100µm. (B) Stereocilia of the vestibular hair cells. There is a fibrilar, membranous material which has covered much of the epithelium; this is obscuring the apices of the supporting cells. Bar = 1µm.

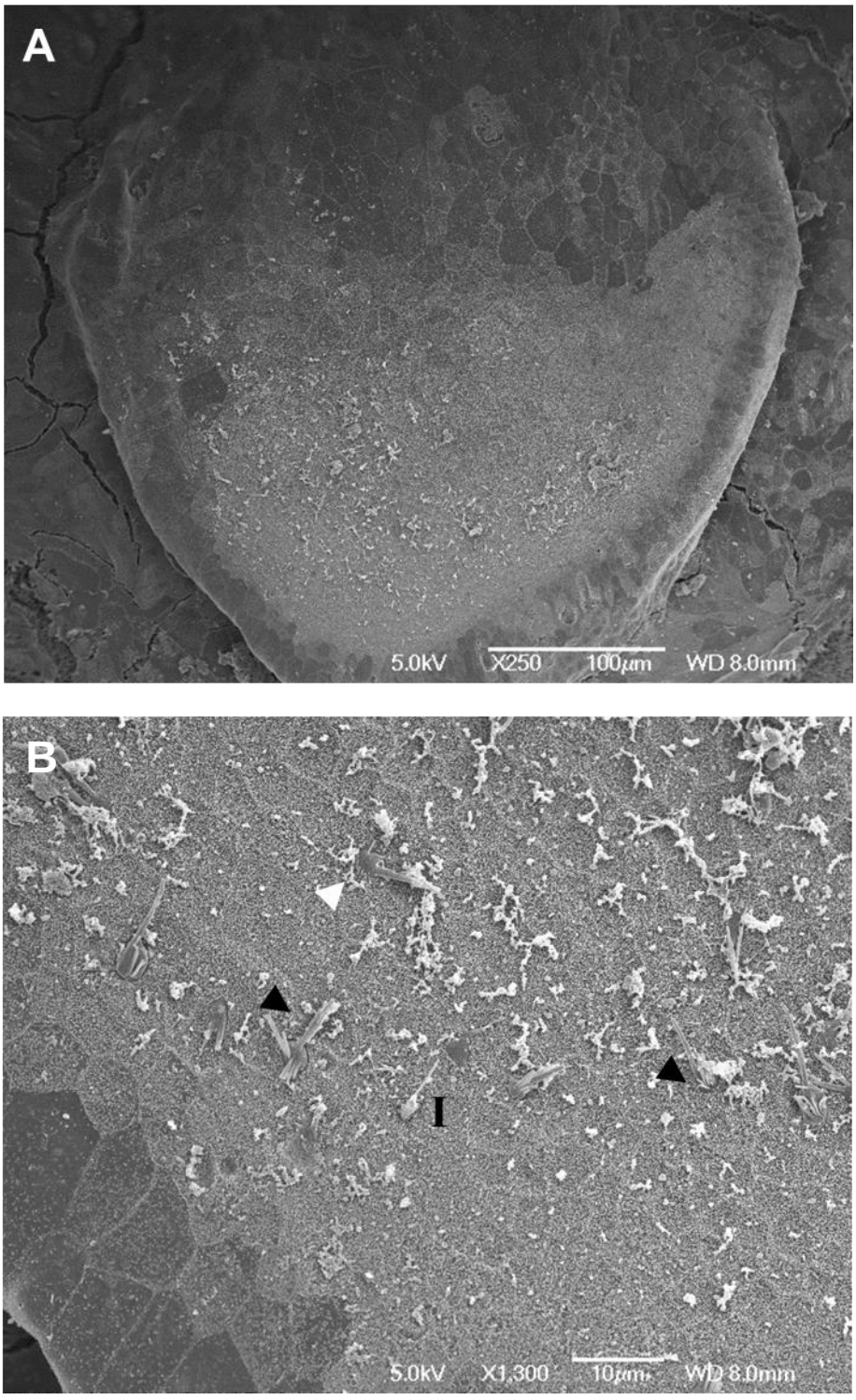

Figure 4-13 Utricular Cultures at 5 Days Post Gentamicin Viewed by Scanning Electron Microscope

The surface of the sensory epithelium from utricle cultures maintained *in vitro* at 5 days post gentamicin treatment. (A) An overview of the entire utricle surface shows the decrease in hair cell numbers in comparison to control cultures. Bar = 100µm. (B) Some stereocilia are still present on the apical surface (black arrowheads), however, others are in disarray or have become fused (white arrowhead). What appears to be an immature bundle 'I' is visible on the surface of one hair cell. Bar = 10µm.

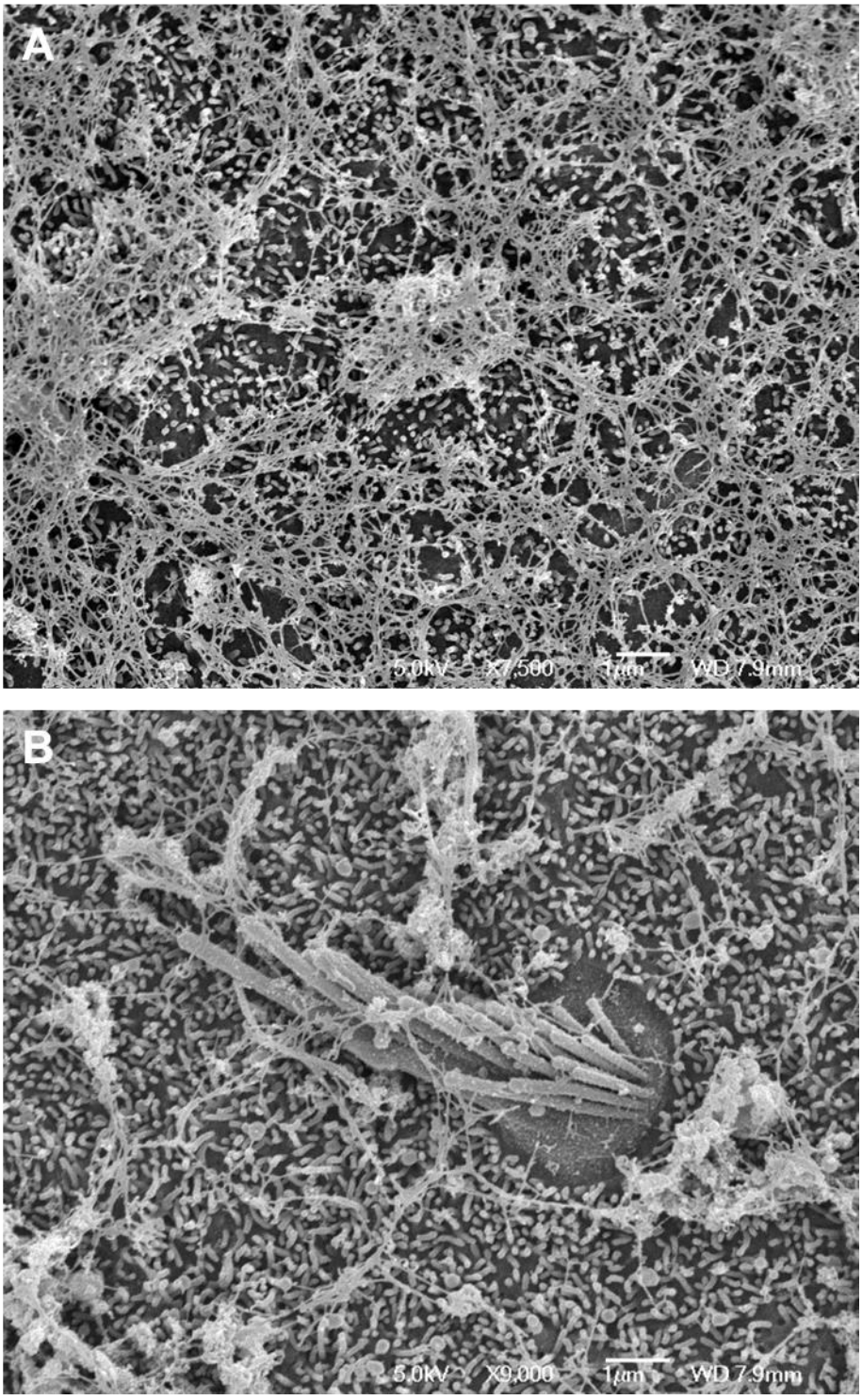

Figure 4-14 Vestibular Hair Cells of Utricular Tissue at 5 Days Post Gentamicin Viewed by SEM

The surface of the sensory epithelium from utricle cultures maintained *in vitro* at 5 days post gentamicin treatment. (A) The 'honeycomb-like' structure of the fibrilar material present on the surface of the sensory epithelium. (B) A surviving vestibular hair cell with a normal stereocilia bundle; the supporting cells surrounding it have apices covered in microvilli. Bar = 1μm.

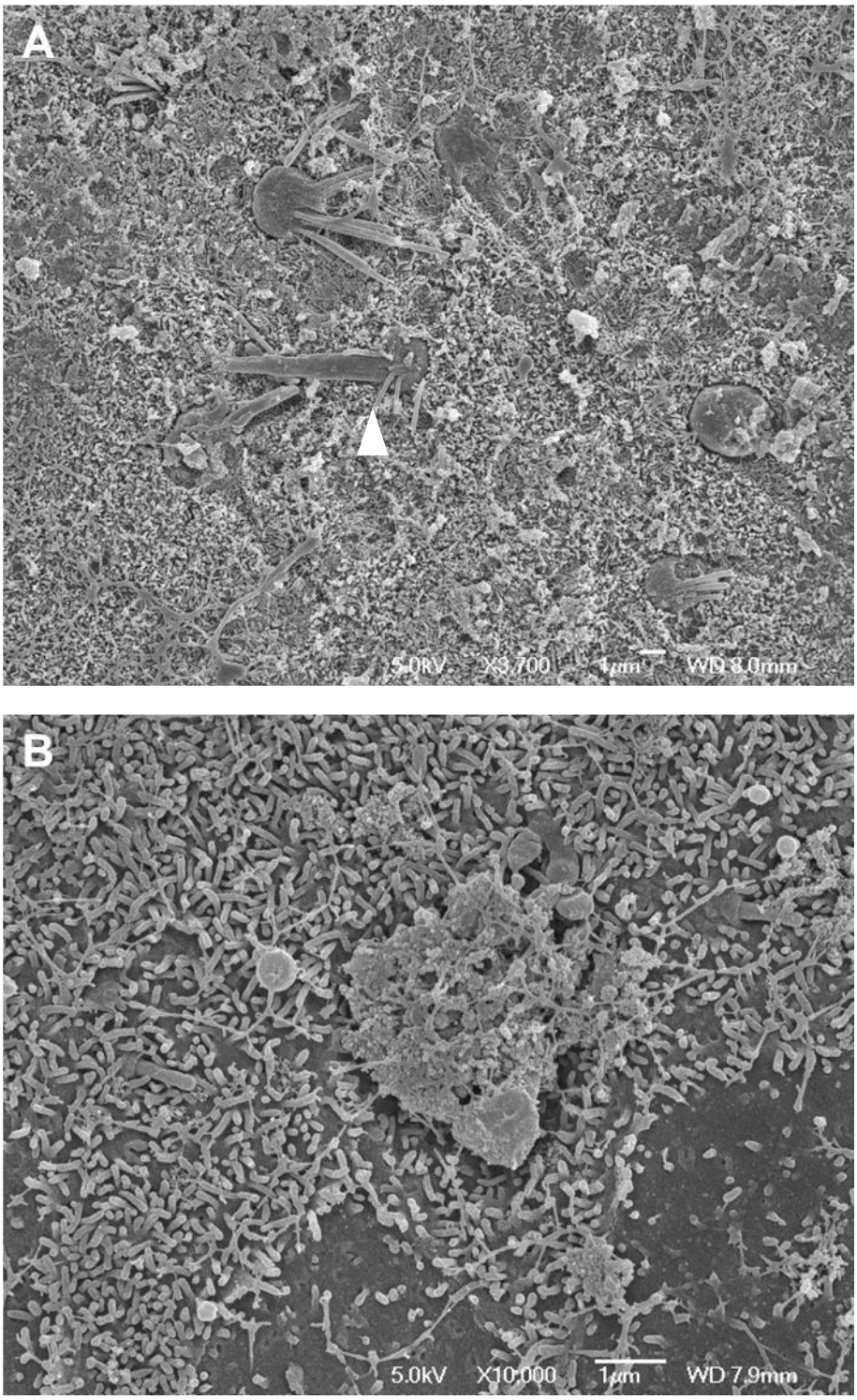

Figure 4-15 Hair Cell Death in Utricular Cultures at 5 Days Post Gentamicin Viewed by SEM

The surface of vestibular hair cells and supporting cells in utricle cultures maintained for 5 days post gentamicin treatment. (A) Remaining stereocilia often appear fused (white arrowhead) and disorganised. Bar = 1μm. (B) Remnants of a vestibular hair cell (centre) are extruded from the epithelium after undergoing cell death. Bar = 1μm.

Utricular Tissue Cultured for 14 Days Post-Gentamicin Treatment Viewed by Scanning Electron Microscope

Following a two week period of recovery after 48 hours gentamicin exposure, utricles viewed by SEM appear, similar to those studied at 5 days post-gentamicin treatment, to have fewer vestibular hair cells (Figure 4-16 A). The process of vestibular hair cell loss is ongoing, with stereocilia present in various disorganised formations as the cell death cycle progresses (Figure 4-16 B), and very long kinocilia also visible. These hair cells are often found towards the periphery of the utricle, as seen in the tissue at 5 days post-gentamicin treatment. This would appear to support the idea that the vestibular hair cells at the periphery of the sensory epithelium are those which are most resilient, but not completely resistant, to ototoxic drug induced hair cell loss. Dead hair cells also continue to be extruded from the utricle at this time point (Figure 4-17 A).

Evidence of cellular proliferation occurring in the underlying mesenchyme of cultured utricles was observed by EdU labelling of these tissues, as described in 4. Further evidence of this proliferation and remodelling of the utricular connective tissue is also visible under SEM. Figure 4-17B shows the surface morphology of tissue which has ‘grown out’ from the original utricle after being maintained in culture. This outgrowth across the surface of the nitrocellulose filter paper appears ‘stretched’ and sheet-like, with an apical surface populated by numerous microvilli. From their surface appearance it might be expected that the cells of these ‘outgrowths’ are of a fibroblast-like nature.

Despite the continuation of the response of the tissue to gentamicin treatment in terms of hair cell loss, at 14 days post-gentamicin potential evidence of regeneration occurring begins to appear. The emergence of short, but highly organised bundles (Figure 4-18, inset) which resemble the morphology of an emerging, immature stereocilia bundle on the apex of a hair cell can be observed. It is not possible to determine with scanning electron microscopy as to whether a complete regenerative event has occurred i.e. that this immature bundle is developing from a hair cell which itself is entirely new and regenerated, rather than from a hair cell which lost its original stereocilia formation due to the gentamicin treatment and has been subsequently stimulated to produce a new bundle.

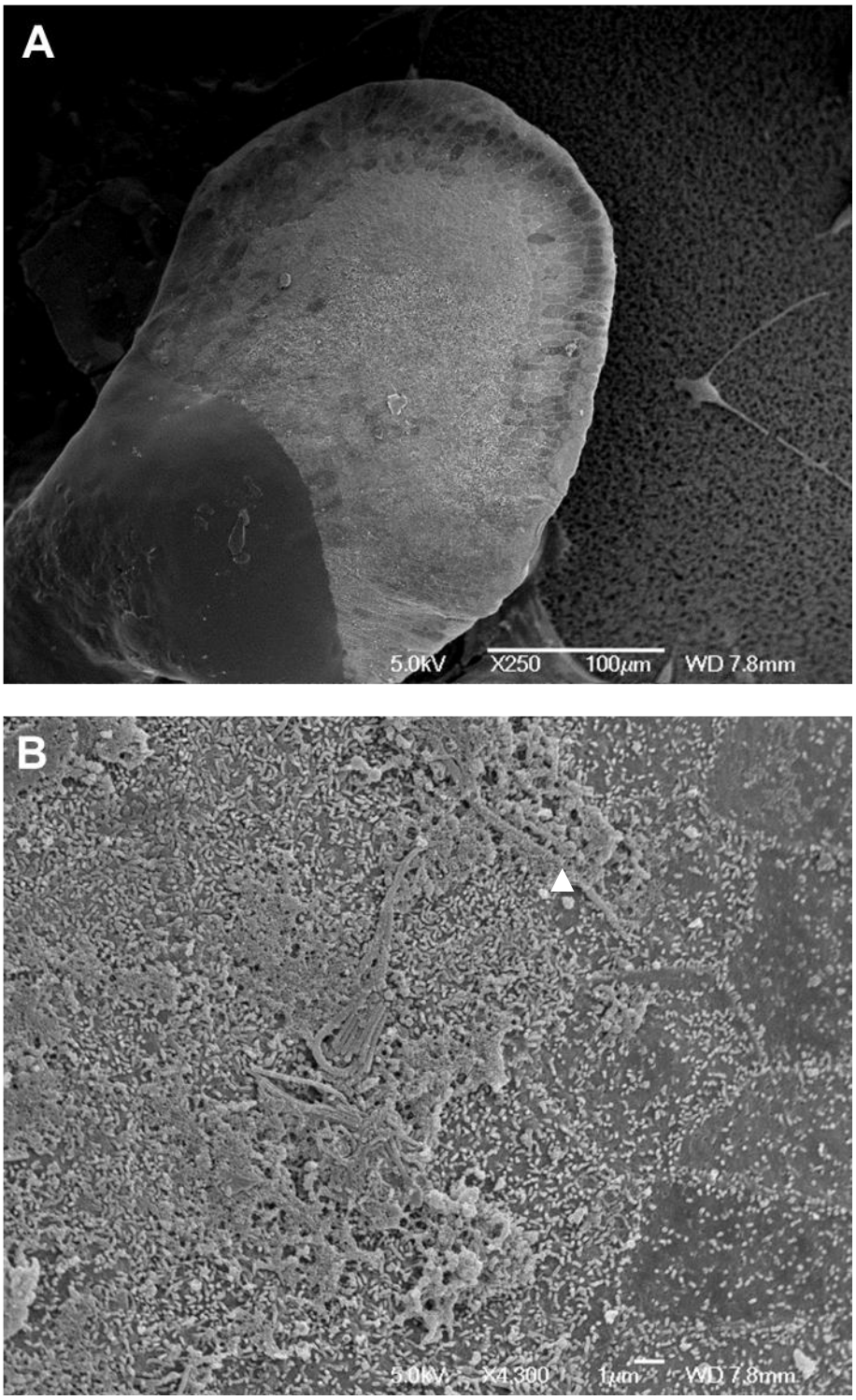

Figure 4-16 SEM of Utricular Tissue at 14 Days Post Gentamicin Treatment

The epithelial surface of utricles maintained *in vitro* for 14 days post gentamicin treatment. (A) An overview of the entire surface of a single utricle demonstrates the decrease in hair cell numbers seen at this stage. Bar = 100µm. (B) Disorganised stereocilia and long kinocilia (arrowhead) on the surface of the tissue which shows a marked decrease in vestibular hair cell numbers at this time point. Bar = 1µm.

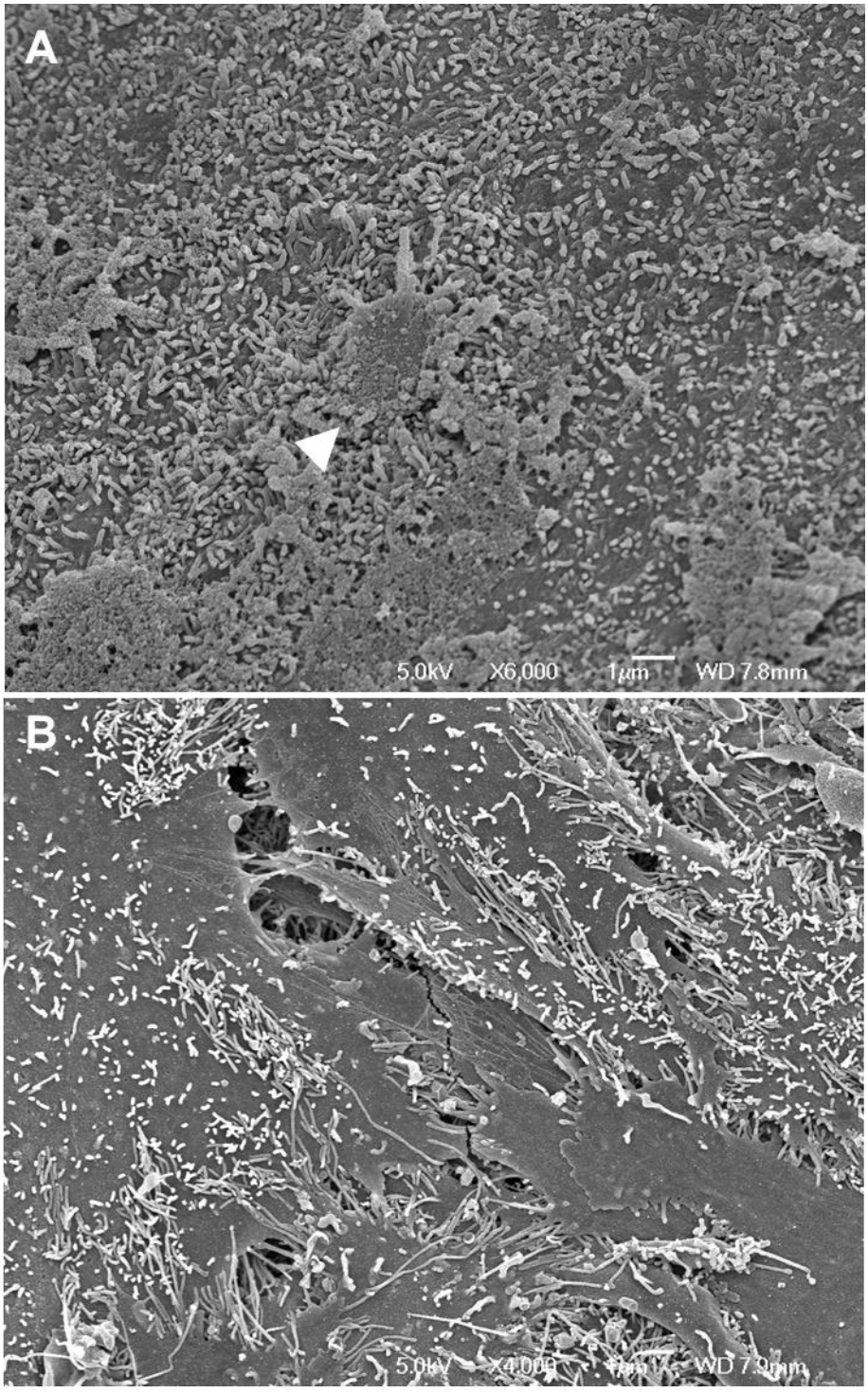

Figure 4-17 SEM of Hair Cell Death at 14 Days Post Gentamicin and Explant Outgrowth

The surface of utricles cultured for 14 days post gentamicin treatment viewed by scanning electron microscopy. (A) A vestibular hair cell (arrowhead) is extruded from the sensory epithelium. Bar = 1μm. (B) The morphology of the 'outgrowth' of cells from the original utricular tissue. Bar = 1μm.

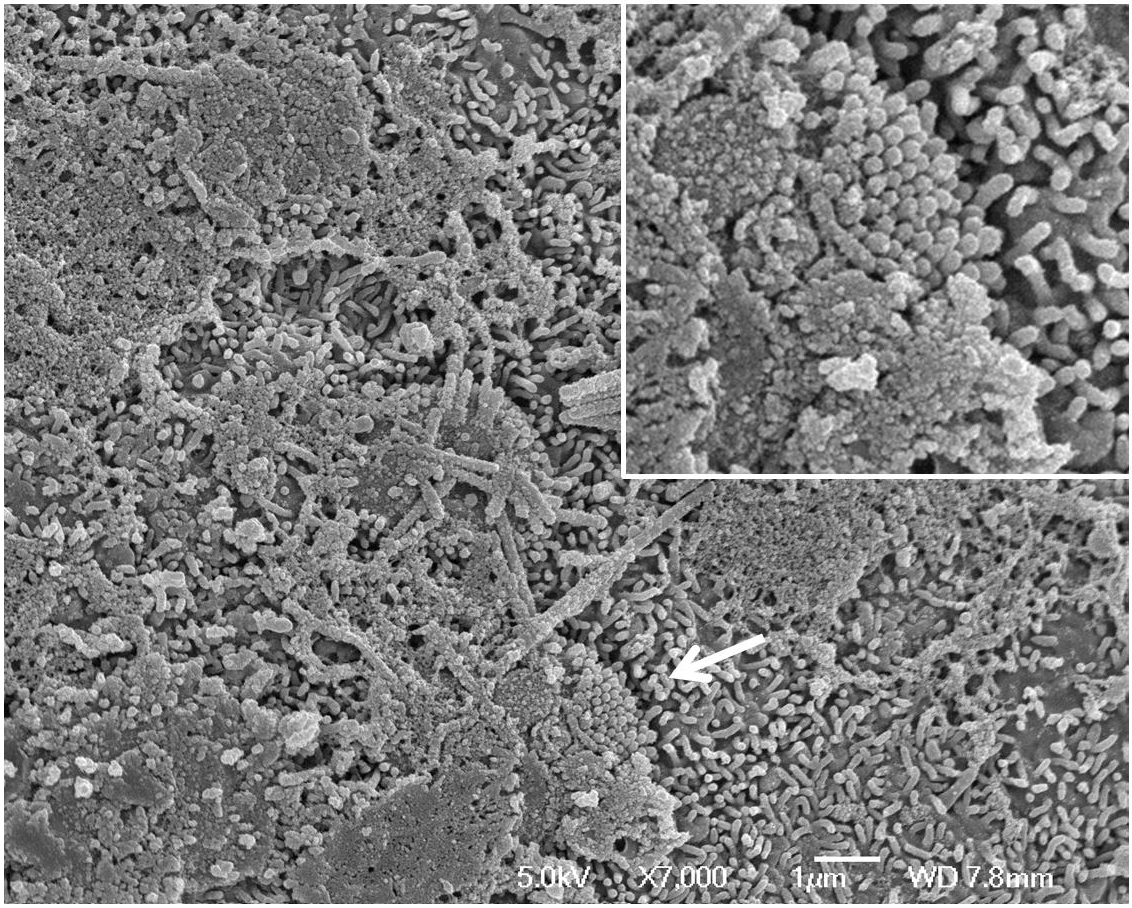

Figure 4-18 SEM of the Potentially Regenerating Vestibular Epithelium at 14 Days Post Gentamicin

The surface of a utricle cultured for 14 days post gentamicin viewed under the scanning electron microscope. At this time point, structures which resemble an immature stereocilia bundle (arrowhead, inset) are seen on the apical surface of the sensory epithelium. Bar = 1μm.

Chapter 5: Integrin Expression in Response to Hair Cell Loss in the Adult Mouse Utricle

5.1 Quantitative PCR for the Investigation of Integrin Expression During Hair Cell Loss and Regeneration

5.1.1 Objectives

Through the use of RT-PCR with both degenerate and specific PCR primers, 8 individual integrin subunits were identified as being expressed in the normal adult mouse utricle. The degenerate PCR primers designed for this project were not proven to be able to detect all of the known murine integrin subunits. It was therefore not possible to screen utricular cDNA for all of the α and β subunits using this method.

In order to both conduct a full screen of normal adult mouse utricular cDNA for members of the integrin family, and to investigate the relative expression levels of particular integrin genes in response to hair cell loss, a set of quantitative PCR experiments was carried out. The abbreviated gene names of all known mammalian integrin subunits are summarised in table 1-1 and 1-2.

5.1.2 Design of Custom TaqMan™ qPCR Gene Expression Array Plates

Commercially available gene expression arrays for integrin subunits used the human version of the gene and thus could not be guaranteed to detect the genes for each of the murine integrins in mouse utricular cDNA samples. It was therefore decided to create a custom array, using the 96-well plate TaqMan® array system from Applied Biosystems. Figure 5-1 shows the layout of the selected assays within a single 96-well plate - each gene assay was replicated four times per plate. Gene expression assays for a total of 18 integrin α and β subunits were used in customised array. *Rn18s* and *Gapdh* assays were included in order to provide two endogenous controls. Gene assays for four hair cell markers were also included on the plate; *Myo7a* (myosin Viia), *Pou4f3*, C*alb2* (calretinin) and *Atoh1*. Each gene assay was repeated four times per array plate. It was anticipated that utricular cDNA samples from organotypic utricle cultures harvested at several time points following treatment with gentamicin would demonstrate changes in the expression level of these markers. Significant hair cell loss had been observed in these cultured utricles by immunohistochemistry; myosin Viia-positive hair cell numbers were observed to decrease in the utricle following gentamicin treatment and it would therefore be expected that the expression of *Myo7a* would be lower in utricular cDNA obtained from such cultures, in comparison to untreated controls.

Through a search of previously published literature, several integrins were identified as being unlikely candidates for expression in the utricle, due to their known cell type specificity e.g. *Itga2b* is specifically expressed by platelets as a key adhesion molecule in the platelet aggregation events which occur during the process of forming blood clots (Ruegg et al., 1992). The following integrin subunits were therefore omitted from the customised qPCR gene expression array; αIIb, αX, αM, αE, αD, αL, α10 and β2.

5.2 Relative Quantification of Custom Integrin TaqMan™ Gene Expression Array qPCR Data

A successful qPCR run of the integrin gene expression array was achieved with each of the four utricular cDNA samples. The four samples tested were cDNA from normal utricular tissue which had not been maintained *in vitro* (0 DC) and cDNA from utricular cultures harvested at the following time points post-gentamicin treatment; 4 days (4 DPG), 14 days (14 DPG) and 21 days (21 DPG). A gene was determined as being 'detected' in a given cDNA sample if it had been successfully amplified by at least 3 of the 4 replicate assays for that gene. Of the 18 integrin genes screened for, 11 α and β subunits were detected in normal utricular cDNA; *Itga3*, *Itga6*, *Itga8*, *Itgav*, *Itgb1*, *Itgb3*, *Itgb4*, *Itgb5*, *Itgb6*, *Itgb7* and *Itgb8*. The remaining integrins (*Itga1*, *Itga4*, *Itga5*, *Itga7*, *Itga9* and *Itga11*) were not detected in normal utricular cDNA. These subunits were also not found in any of the gentamicin-treated utricular cDNA samples analysed.

Relative quantification (RQ) analysis of the data from these experiments was carried out using SDS software (Applied Biosystems) as described in 2.9.3. Gene expression plots showing the RQ values for the α integrins are shown in figure 5-4 and those for the β integrins in figure 5-5.The array plate run using cDNA from normal adult mouse utricles which had not been cultured (0 DC) was used as the calibrator for this RQ study, in order to investigate the gene expression levels of integrins and hair cell markers in gentamicin treated tissue, relative to their expression in the normal, undamaged utricle. Error bars (figures 5-4 and 5-5) indicate the minimum and maximum RQ values based on the four replicate assays for each individual gene per array plate. Where error bars do not overlap i.e. when comparing the expression of a gene in normal tissue, to utricular tissue at 4 days post-gentamicin, the difference in expression level observed may be described as being significant with 95% confidence.

	1	2	3	4	5	6	7	8	9	10	11	12
A	*Rn18s*	*Rn18s*	*Rn18s*	*Rn18s*	*Gapdh*	*Gapdh*	*Gapdh*	*Gapdh*	*Itga1*	*Itga1*	*Itga1*	*Itga1*
B	*Itga2*	*Itga2*	*Itga2*	*Itga2*	*Itga3*	*Itga3*	*Itga3*	*Itga3*	*Itga4*	*Itga4*	*Itga4*	*Itga4*
C	*Itga5*	*Itga5*	*Itga5*	*Itga5*	*Itga6*	*Itga6*	*Itga6*	*Itga6*	*Itga7*	*Itga7*	*Itga7*	*Itga7*
D	*Itga8*	*Itga8*	*Itga8*	*Itga8*	*Itga9*	*Itga9*	*Itga9*	*Itga9*	*Itga11*	*Itga11*	*Itga11*	*Itga11*
E	*Itgav*	*Itgav*	*Itgav*	*Itgav*	*Itgb1*	*Itgb1*	*Itgb1*	*Itgb1*	*Itgb3*	*Itgb3*	*Itgb3*	*Itgb3*
F	*Itgb4*	*Itgb4*	*Itgb4*	*Itgb4*	*Itgb5*	*Itgb5*	*Itgb5*	*Itgb5*	*Itgb6*	*Itgb6*	*Itgb6*	*Itgb6*
G	*Itgb7*	*Itgb7*	*Itgb7*	*Itgb7*	*Itgb8*	*Itgb8*	*Itgb8*	*Itgb8*	*Myo7a*	*Myo7a*	*Myo7a*	*Myo7a*
H	*Calb2*	*Calb2*	*Calb2*	*Calb2*	*Atoh1*	*Atoh1*	*Atoh1*	*Atoh1*	*Pou4f3*	*Pou4f3*	*Pou4f3*	*Pou4f3*

Figure 5-1 Layout of Custom TaqMan™ Gene Array for Integrin qPCR Experiments

This figure shows the design of a single 96-well plate gene expression array for 18 individual integrin subunits. Each gene assay was replicated four times on a single plate. *Rn18s* and *Gapdh* were selected as endogenous control assays. Four hair cell marker gene assays were also included; *Myo7a*, *Calb2*, *Atoh1* and *Pou4f3*. qPCR experiments were run on these customised arrays using one 96-well plate per cDNA sample.

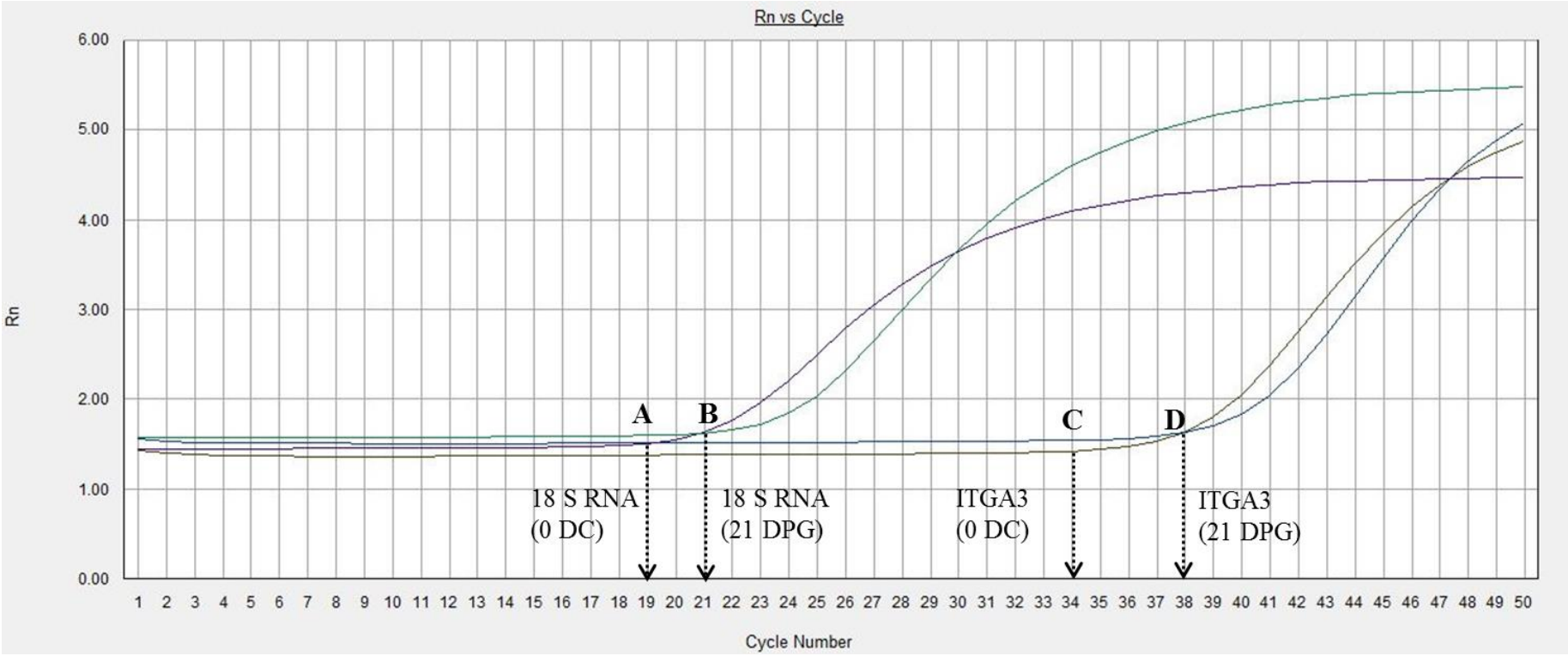

Figure 5-2 Omission of 21 DPG qPCR Data from RQ Analysis

The qPCR data from the array plate run using 21days post-gentamicin cDNA was omitted from the RQ study; it was observed that the 21 DPG sample contained less cDNA than those of the other time points investigated. (A) With 0 day control (0 DC) cDNA, the *Rn18s* endogenous control began to be amplified at around 18 cycles, whilst *Itga3* (C) began to be amplified at around 34 cycles. Using 21 DPG cDNA, *Rn18s* amplification (B) started at around 20 cycles; *Itga3* (D) did not begin to be detected until as late as 38 cycles.

5.2.1 Expression Changes in Hair Cell Markers

Changes in the expression level of each of the four hair cell markers which were included in the custom array plate were observed (shown in Figure 5-3). *Atoh1*, *Calb2*, *Myo7a* and P*ou4f3* were all detected in normal utricular cDNA (0 DC).

Hair Cell Associated Proteins

Myo7a and *Calb2* showed a significant decrease in gene expression at 4 DPG in comparison to the level detected in the 0 day control sample; *Myo7a* expression had decreased to an extent that it was undetectable at 4 days post-gentamicin. At 14 DPG, *Calb2* expression continued to be significantly lower than that observed in normal tissue, but did not differ significantly from the level of expression detected at 4 DPG. *Myo7a* was detected at 14 days post-gentamicin, at a level of gene expression which was still significantly lower than had been detected in the 0 day control cDNA sample.

Hair Cell Transcription Factors

Atoh1 and *Pou4f3*, both transcription factors which are involved in hair cell differentiation, each show a significant increase in gene expression at 4 DPG in comparison to the level seen in normal utricular cDNA. *Pou4f3* in particular, demonstrates a large (approximately 5-fold) increase in expression at 4 DPG; the expression level of this transcription factor decreases significantly by 14 DPG, to a level which is significantly lower than that observed in normal tissue. *Atoh1* levels also show a significant decrease at 14 DPG, compared to the elevated gene expression seen at 4 DPG, however, at 14 DPG, *Atoh1* gene expression had returned to a level which was not significantly different to that observed in the normal utricle.

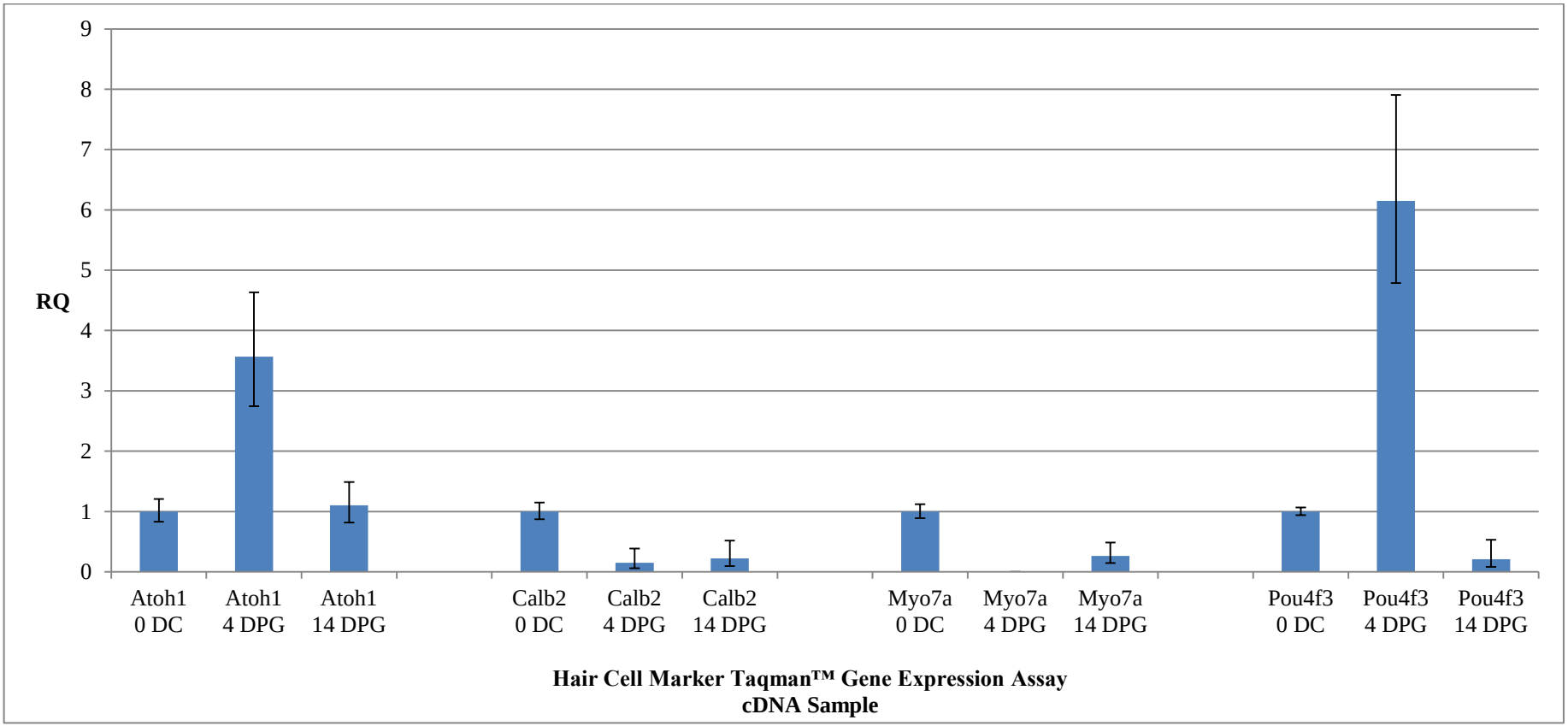

Figure 5-3 Changes in Hair Cell Marker Gene Expression Levels in Response to Gentamicin-Induced Hair Cell Loss

Relative quantification (RQ) analysis of the gene expression of four hair cell markers; *Atoh1*, *Myo7a*, *Pou4f3* and *Calb2*. Data from the array plate run using cDNA from normal adult mouse utricles which had not been maintained *in vitro* (0 DC) was used as a calibrator in order to investigate gene expression levels at 4 (4 DPG) and 14 days post-gentamicin treatment (14 DPG) in comparison to expression in normal tissue. Error bars indicate 95% confidence intervals for RQ values.

5.2.2 Increased Expression of Integrins in Utricular cDNA Post-Gentamicin Treatment

Five integrin subunits demonstrated an increase in gene expression level in utricular cDNA at 4 and 14 days post-gentamicin; *Itga3*, *Itgav*, *Itgb1*, *Itgb5* and *Itgb8*. Each of these integrins was detected in normal utricular cDNA.

Itga3 and *Itgb5* gene expression shows an increase at 4 DPG compared to normal tissue, however, this increase was only calculated as being significant for *Itga3*. At 14 DPG, the expression of these two integrins was higher than that observed at 4 days, although neither increase was found to be significant.

Itgav, *Itgb1* and *Itgb8* also exhibited increased gene expression at 4 DPG; this increase was significant for *Itgav* (an approximately 7-fold increase) and *Itgb1* (an approximately 10-fold increase), but not for *Itgb8*. All three subunits show a subsequent decrease in gene expression at 14 DPG compared to the level observed at 4 DPG. This decrease was only found to be significant for *Itgb1*; this subunit was also the only subunit in this group to show a level of expression at 14 DPG which was significantly higher than that detected in normal utricular cDNA.

5.2.3 Integrins Only Expressed in Normal Utricular cDNA

Of the 18 integrins screened for, two subunits, namely *Itgb7* and *Itga8* were only detected in the normal utricular cDNA sample (0 DC). It is possible that these genes were either not present at all in cDNA from gentamicin treated utricles, or that they were expressed at such a low level as to be undetectable by qPCR.

5.2.4 Integrins Not Detectable at 4 Days Post-Gentamicin

Integrins *Itgb6* and *Itga6* were detected in both normal utricular cDNA and at 14 DPG, but were undetectable in the 4 DPG cDNA sample. The gene expression of *Itga6* was higher at 14 DPG in comparison to the level observed in normal tissue, however, this difference was not calculated as significant. Integrin *Itgb6* expression showed a significant, but small decrease at 14 DPG in relation to expression level of this gene in normal utricular cDNA

5.2.5 Integrins Not Detectable at 14 Days Post-Gentamicin

Integrins *Itgb3* and *Itgb4* were found to be present in normal utricular cDNA; each of these subunits also demonstrated a significant increase in gene expression at 4 DPG in comparison to that observed in normal tissue. These expression level increases were relatively large in comparison to other changes observed in integrin expression – *Itgb3* showed an approximately 11-fold increase in gene expression, and *Itgb4* expression was approximately 12-fold higher than that of normal utricular cDNA. Neither integrin was detected in the 14 DPG cDNA sample – therefore *Itgb3* and *Itgb4* could be considered as being expressed at such a low level as to be undetectable by qPCR at this time point, or to be absent from this cDNA sample altogether.

5.2.6 Integrins Not Detectable in Normal Utricular cDNA but Present in Gentamicin-Treated Tissue

Of the 18 subunits screened for, only integrin *Itga2* was undetectable in the normal utricular cDNA (0 DC) sample, but was then found to be expressed at both 4 and 14 DPG. Expression of *Itga2* was observed to be lower at 14 DPG than at 4 DPG, although this difference was not found to be significant.

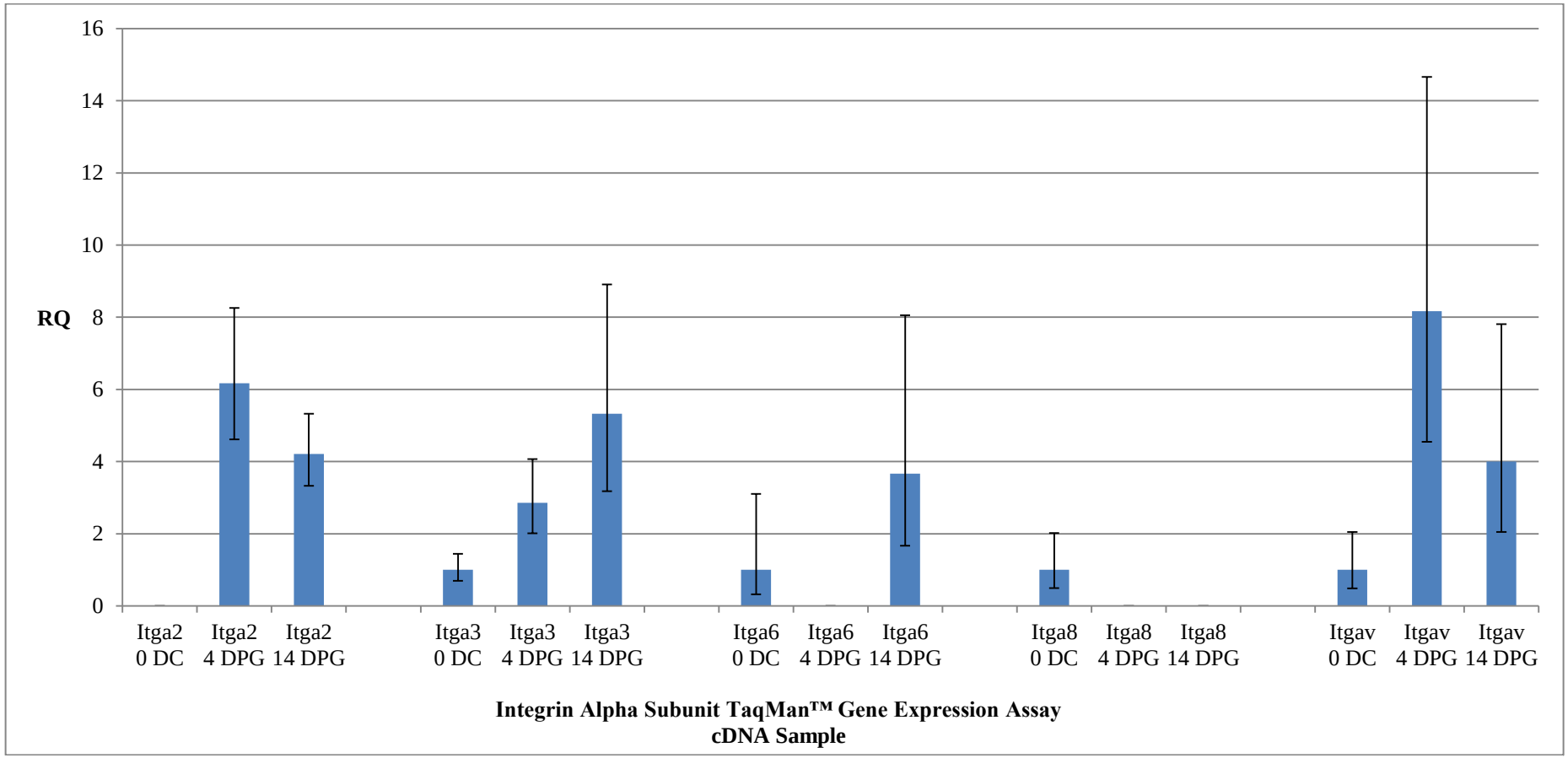

Figure 5-4 Changes Integrin α Subunit Gene Expression in Response to Gentamicin-Induced Hair Cell Loss

Relative quantification (RQ) of integrin α subunit qPCR data from gene expression array plates run using cDNA from normal adult mouse utricles which had not been cultured (0 DC) and utricular cultures harvested at 4 (4 DPG) and 14 days post-gentamicin treatment (14 DPG). Error bars indicate the 95% confidence intervals for each RQ value.

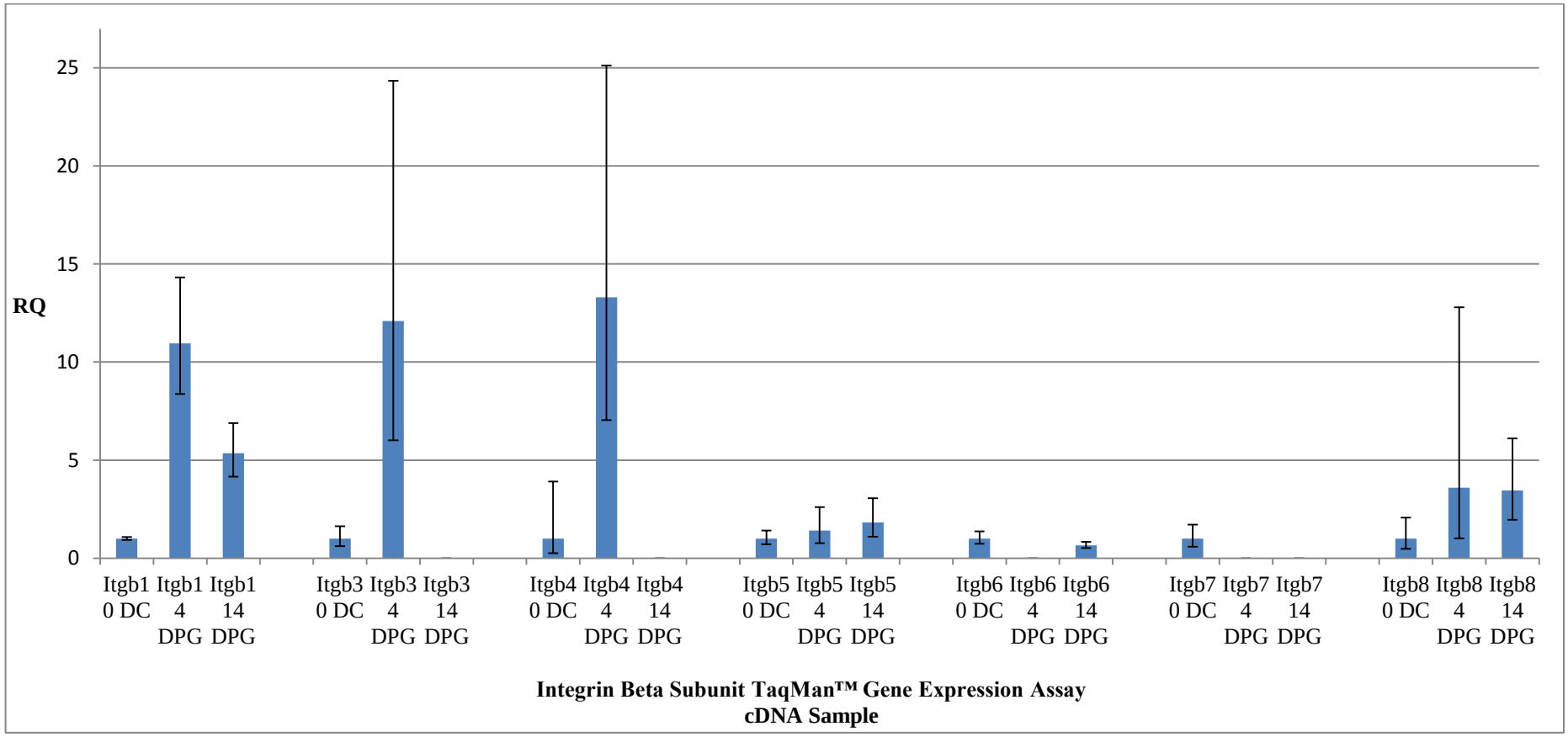

Figure 5-5 Changes in Integrin β Subunit Gene Expression in Response to Gentamicin-Induced Hair Cell Loss

Relative quantification (RQ) of integrin β subunit qPCR data from gene expression array plates run using cDNA from normal adult mouse utricles which had not been cultured (0 DC) and utricular cultures harvested at 4 (4 DPG) and 14 days post-gentamicin treatment (14 DPG). Error bars indicate the 95% confidence intervals for each RQ value.

5.3 Multiplexed Individual Integrin Subunit qPCR Assays

Following the RQ study of qPCR data obtained from the customised TaqMan™ integrin gene expression arrays, several subunits were selected for further investigation using multiplexed assays in order to confirm the results of the initial screen. Subunits to be included in these individual assays were selected on a basis of those which demonstrated larger changes in integrin expression level that were calculated as being significant. The five integrin subunits which were chosen for multiplexed qPCR assays were integrin α2, αV, β1, β3 and β4. The results of the RQ analysis of these assays are shown in figure 5-6. The same cDNA samples run on the array plates were also used for these individual assays.

5.3.1 Relative Quantification

All five integrin genes investigated using multiplexed assays were found to be expressed in normal utricular cDNA. These subunits had all been detected in normal utricular tissue by the initial qPCR screen, except for integrin *Itga2*.

5.3.2 Increased Expression of Integrins in Utricular cDNA Post-Gentamicin Treatment

Integrins *Itgav*, *Itgb1* and *Itgb3* all show a trend towards their gene expression being increased at 4 DPG, although differences between the levels detected at 4 days and in normal control tissue were not significant. These three subunits had all previously shown an increase in gene expression at 4DPG compared to normal utricular cDNA in the initial integrin qPCR screen. Integrin *Itgav* shows a subsequent decrease in expression at 14 DPG which was not calculated as being significant, but was higher than the level observed for this integrin in normal tissue. The changes in gene expression exhibited by *Itgav* follow the same trend as those observed for this subunit in the initial qPCR screen.

Integrin *Itgb3* also maintained a level of gene expression at 14 DPG which was higher than that detected in normal tissue, although this difference was not significant; integrin *Itgb3* was not detected in the 14 DPG cDNA sample in the initial qPCR screen, but had shown increased expression at 4 DPG. This integrin exhibited a higher level of gene expression at 14 DPG than was detected at 4 DPG by multiplexed assay.

Integrin *Itgb1*, following an increase in gene expression at 4 DPG, shows a subsequent decrease in its expression level at 14 DPG. The expression of the *Itgb1* gene appeared to show a small decrease from that observed in normal utricular cDNA, however, its expression at 14 DPG was not calculated as being significantly different from that detected in the 0 DC sample. Examination of the raw data from these multiplexed ssays indicates that integrin *Itgb1* is likely to be present at a higher level than the other 4 subunits investigated by these multiplexed assays; integrin *Itgb1* expression begins to be detected after approximately 30 PCR reaction cycles in normal utricular cDNA, earlier than any of the other integrins in this sample.

5.3.3 Integrin Multiplexed Assays Not Consistent with the Initial qPCR Screen

Multiplexed assays for integrins *Itga2* and *Itgb4* detected these subunits in all 3 cDNA samples tested; *Itga2* had not been detected in the 0 DC sample in the initial qPCR screen and *Itgb4* had previously been undetectable at 14 DPG. Based upon the raw data from these assays, these two integrins are likely to be expressed in lower quantities in normal utricular cDNA compared to the other integrins for which multiplexed assays were carried out; *Itgb4* does not begin to be detected until 35PCR reaction cycles and the start of *Itga2* amplification occurs even later at around 37 cycles.

Integrin *Itgb4* shows a trend towards a decrease in gene expression at 4 DPG compared to its expression in normal utricular cDNA. This is the opposite of the trend observed in the initial qPCR screen, where *Itgb4* was shown to increase significantly between the 0 DC and 4 DPG samples. *Itga2* gene expression displays a trend towards an increase at 4DPG when compared to the 0 DC sample, and towards a further increase at 14 DPG. The significance of these RQ values cannot be calculated from the data obtained in these experiments; expression of these subunits being detected by only one of the three replicate assays carried out for each cDNA sample (with the exception of *Itga2* in the 0 DC sample). It was therefore not possible to calculate RQ maximum and minimum values for these assays, thus the RQ analysis for these subunits lacks 95% confidence intervals.

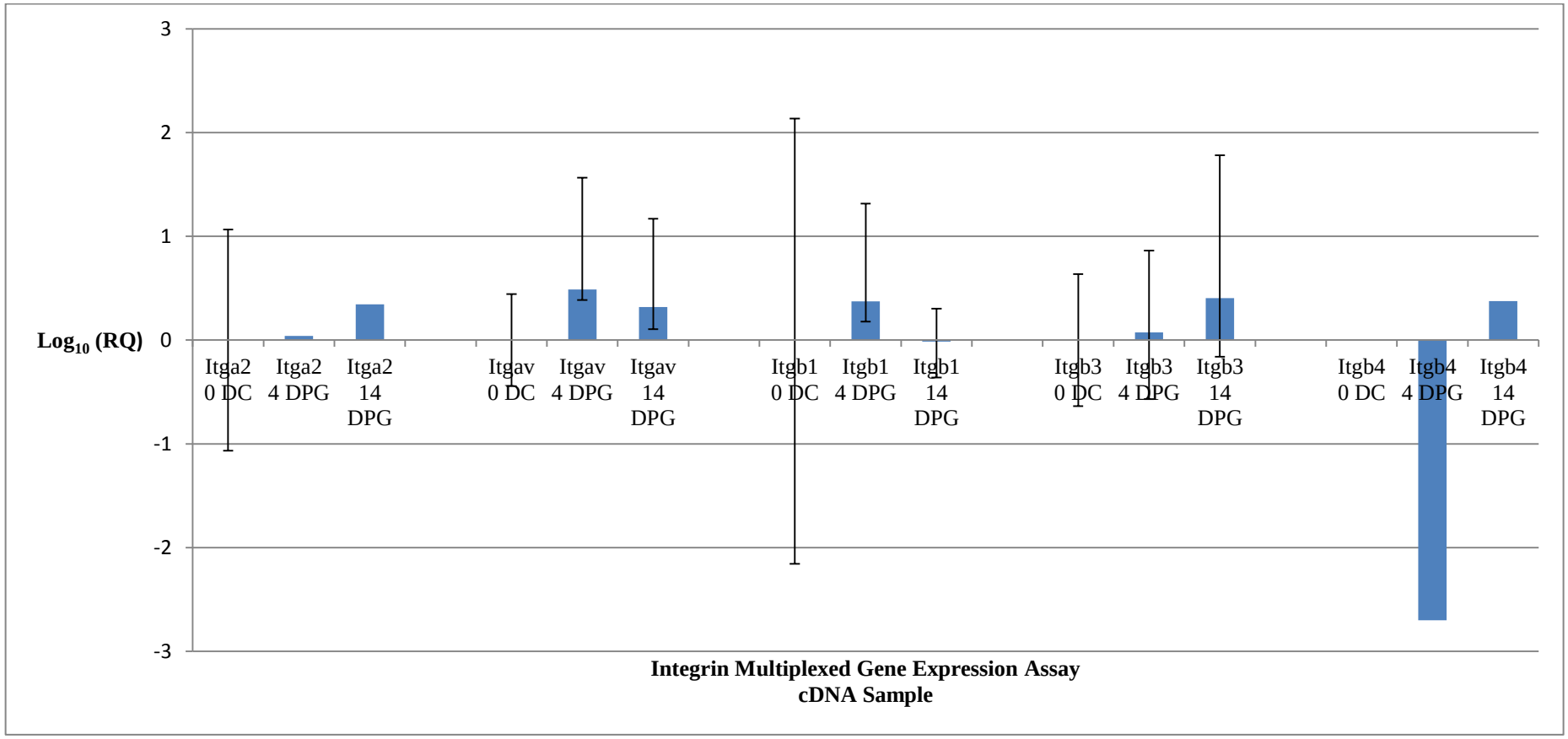

Figure 5-6 Multiplexed Individual Integrin Gene Expression Assays

RQ analysis of individual multiplexed gene expression assays for five integrin subunits; *Itga2*, *Itgav*, *Itgb1*, *Itgb3* and *Itgb4*. *Rn18s* was used as the endogenous control. Data from assays run using the 0 DC (normal, uncultured utricle) cDNA sample were used to calibrate the expression of each integrin at 4 and 14 DPG relative to its expression in normal tissue. Error bars indicate 95% confidence intervals. Where no error bars are shown, RQ values were obtained from only one assay.

5.3 Discussion

The custom integrin TaqMan ™ gene expression arrays carried out during this project detected the gene expression of 11 integrin subunits in normal adult mouse utricular cDNA. These arrays were also able to identify a group of 10 subunits which showed changes in their gene expression level in cDNA from utricles cultured for 4 and 14 days post-gentamicin treatment i.e. utricular tissue undergoing hair cell loss. Additionally, a subset of the integrins screened for in these qPCR experiments were identified as being undetectable in either normal or gentamicin utricular tissue. The changes exhibited by the gene assay carried out in this project, both integrins and hair cell markers, are summarised in table 5-1.

A full discussion of those integrins determined as showing significant changes in gene expression in gentamicin treated utricles is given in chapter 7, in order to analyse these results in conjunction with the those obtained by degenerate RT-PCR (chapter 4) and subsequent immunohistochemistry experiments (chapter 6) and explore the implications of the presence of these integrins in the mammalian utricle.

5.3.1 Limiting Factors for Integrin qPCR Experiments Using Utricular cDNA

The cDNA samples utilised for both the custom integrin gene expression array plates as well as the individual multiplexed integrin assays represent the gene expression of a single ‘pool’ of utricular tissue; the cDNA from between 8 to 10 utricles from 4 to 5 individual animals. Due to the size of the tissue of interest, pooling of tissue was necessary in order to obtain sufficient cDNA to run the number of assays carried out. However, this also introduces a greater variability of the genetic makeup of the cDNA within the sample, further complicating the investigation of changes in gene expression level by qPCR. In order to investigate this further, it would be necessary to carry out integrin gene expression assays with multiple ‘pools’ of cDNA, to assess whether the how replicable the results of the initial qPCR array plate screen are e.g. to reduce the potential for a single a-typical utricle within a given pool distorting the outcome of the results.

The individual integrin subunit multiplexed assays carried out were limited by the amount of cDNA which was available after the initial screen had been carried out. Integrins selected for further investigation by multiplexed assay were chosen based

Genes Not Expressed in Normal or Gentamicin-Treated Utricles	Genes Only Expressed In Normal Utricle	Genes Showing Increased Expression in Gentamicin-Treated Utricles	Genes Showing Decreased Expression in Gentamicin Treated Utricles
Itga1	*Itga8*	*Itga2*	*Myo7a*
Itga4	*Itgb7*	*Itga3*	*Calb2*
Itga5		*Itga6*	
Itga7		*Itgav*	
Itga9		*Itgb1*	
Itga11		*Itgb3*	
		Itgb4	
		Itgb5	
		Itgb8	
		Pou4f3	
		Atoh1	

Table 5-1 Summary of Gene Expression Changes Detected by qPCR in the Utricle Following Gentamicin Treatment

This table summarises the findings of the qPCR gene expression arrays carried out using cDNA from both normal and gentamicin treated utricle.

upon which subunits had shown a significant change in gene expression in the initial qPCR screen. Repeating the investigation of integrin gene expression in normal and gentamicin-treated tissue through the use of these multiplexed assays was carried out with the aim of establishing how replicable (and therefore how reliable) the results of the initial qPCR arrays were. Multiplexing of a target assay with an endogenous control limits the error that was potentially introduced into the array plate results - the assays on the customised integrin TaqMan™ gene expression arrays were not multiplexed. By having the endogenous control assay in the same well as each integrin target assay, their relative expression levels would be more directly comparable due to being subject to the same reaction conditions i.e. reagent and cDNA quantities and well position within the plate (wells which are nearer the edges of the 96-well plate are more susceptible to evaporation during the qPCR thermocycling process). It is possible that due to the samples used being the very last of the cDNA samples for each time point, that this may have caused pipetting errors and differences in the PCR reaction mixtures, which resulted in only one of the three replicate assays detecting the presence of integrins *Itga2* and *Itgb4* in the majority of the cDNA samples examined. It may also have contributed to the size of the error bars seen in figure 5-6 and explain why the results of the multiplexed assays show gene expression changes which generally follow the same trend as was observed in the initial screen, but which were not calculated as being significant. If qPCR experiments carried out in this project were to be attempted again, it would be important to obtain utricular tissue in greater quantities, both from normal control tissue and from gentamicin-treated utricle cultures, in order to ensure that the amount of cDNA being used was not a limiting factor. Since the cDNA samples used in this study were from pools of 8 – 10 individual utricles, it would be preferential to harvest at least double this amount of tissue for each time point being investigated.

Quantitative PCR is a sensitive molecular technique, which results in studies such as this work which uses cDNA from a pool of tissue, being subject to subtle variations of individual utricles and therefore ultimately making significant expression level changes more difficult to establish. It is also possible that any changes in integrin expression which occur after gentamicin exposure are inherently small and more difficult to detect. RQ analysis in this project was only carried out comparing two time points (utricular cultures at 4 and 14 days post-gentamicin treatment) to normal utricular cDNA. cDNA

from utricles at 21 days post-gentamicin was also run on an TaqMan™ gene expression array, however there was insufficient cDNA in this sample for the data collected to be reliable and it was therefore omitted from the relative quantification study. It may therefore be the case that more significant changes in integrin expression occur in between the time points studied and up-regulation or down-regulation events at their most significant levels have been missed.

5.3.2 Changes in the Expression of Hair Cell Markers in Gentamicin-Treated Utricular Tissue

Pou4f3, a transcription factor expressed in sensory hair cells (also known as brn3c/brn-3.1) exhibited a significant increase in gene expression at 4 days post-gentamicin in comparison to its expression in normal utricular cDNA. Pou4f3 has been previously identified as being involved in hair cell maturation and survival in the inner ear (Xiang et al., 1998) in both auditory and vestibular hair cells. Mutation of this transcription factor causes deafness and vestibular deficiency in *Pou4f3*-deficient mice; animals lacking the *Pou4f3* gene do not develop hair cells within their sensory epithelia (Erkman et al., 1996; Xiang et al., 1997). *Pou4f3* mutation has also been linked to a type of progressive hearing loss in humans (Vahava et al., 1998). Research into understanding the downstream targets of Pou4f3 and the hair cell survival pathways in which they are involved is on-going. The observation of an increase in *Pou4f3* gene expression in utricular cDNA at 4 days post-gentamicin would lend support to the current understanding that this transcription factor is important for hair cell survival as part of the damage responses triggered within sensory hair cells by aminoglycoside ototoxicity (Towers et al., 2011).

Atoh1 is another hair cell associated transcription factor, which is known to be critical for the development and differentiation of sensory hair cells (Bermingham et al., 1999). The qPCR data from this project shows that *Atoh1* (also known as math1) is present in the normal adult utricle and exhibits an increase in gene expression at 4 days-post-gentamicin. This result is consistent with the findings of previous studies (Wang et al., 2010) where *Atoh1* mRNA was shown by qRT-PCR to be increased in the mouse utricle following aminoglycoside-induced hair cell loss. It would be anticipated, since Atoh1 is involved in the differentiation of hair cells, that the organotypic utricle culture model

used during this project i.e. a tissue known to exhibit a limited regenerative capability, would require up-regulation of the *Atoh1* gene in order to induce the transdifferentiation of supporting cells into new hair cells. Adenoviral transfection with the *Atoh1* gene has been shown to induce hair cell regeneration, above the level of spontaneous regeneration, in the aminoglycoside-damaged murine vestibular system (Schlecker et al., 2011).

Immunohistochemistry using antibodies against the hair cell markers myosin Viia and calretinin in this project demonstrated that hair cells positive for each of these proteins are depleted in gentamicin-treated utricular tissue by 4 days post-gentamicin. The decrease in gene expression shown by *Calb2* and *Myo7a* in this study by qPCR in cDNA from cultured utricles harvested at 4 days post-gentamicin follows the same trend as would be expected. That the expression of these hair cell markers subsequently begins to recover by 14 days post-gentamicin would support the known ability of the utricular epithelium to regenerate vestibular hair cells. A full discussion of the process of regeneration in the mammalian vestibular system is included in chapter 7.

5.3.3 Summary

The integrin qPCR gene expression assays carried out in this project served as an initial screen of utricular tissue for integrin subunits present in normal tissue and for changes in integrin gene expression within organotypic utricular cultures undergoing aminoglycoside-induced hair cell loss. The results of this qPCR study of integrin expression in the adult mouse utricle highlighted a group of integrin subunits which will be the subject of further analysis into a potential role for these cell surface receptors in hair cell loss and spontaneous regeneration in the vestibular sensory epithelium.

Chapter 6: The Expression Pattern of Integrins in Response to Gentamicin-Induced Hair Cell Loss

The development of an *in vitro* mouse utricle culture model provided a method of studying the effect of gentamicin-induced hair cell loss (and any subsequent regeneration) upon the expression of the integrin family of proteins. Immunofluorescent labelling of individual integrin α and β subunits was used to investigate both their presence in the murine vestibular sensory epithelium and their expression pattern.

Primary antibodies against individual integrins subunits were initially used to label cryostat sections of adult mouse utricles which had not been maintained in culture, to investigate the 'normal' expression of each subunit in control tissue. Where necessary, the dilutions required for the use of the primary antibodies were determined by the use of an appropriate positive control tissue.

A series of *in vitro* culture experiments were carried out to provide the tissue required for time series immunolabelling for several integrin subunits. Three time points at which to observe the tissue of interest were selected; 4, 14 and 21 days post-gentamicin treatment. These time points were chosen based on the findings of previous work (Berggren et al., 2003; Forge et al., 1998; Kawamoto et al., 2009). An early time point of 4 days post-gentamicin treatment was selected to show the tissue in a damaged state with surface scarring and substantial hair cell loss. The latter time points of 14 and 21 days post-gentamicin were selected due to these previous studies indicating that regenerative events began to be observed at 14 days and were more evident at 21 days after ototoxic drug damage.

A 'group' of utricles (a group was defined as the dissection of 5 animals i.e. 10 individual utricles) were dissected from adult mice and placed into culture on the same day, with one control utricle and two gentamicin-exposed utricles being maintained for each of the three time points, This process was then repeated in triplicate. The use of such an experimental approach provided three groups of tissue, with each time point represented by both control and gentamicin treated utricles. This tissue underwent cryostat frozen sectioning. Immunolabelling was carried out on a section of tissue from each group at each time point, for both control and gentamicin-treated utricles. Immunofluorescent labelling was therefore repeated in triplicate with control and gentamicin-treated cultured tissue, in order to allow for any potential variation occurring within the *in vitro* culture set up and subsequent incubation period.

All cryostat sections in these immunohistochemistry experiments were labelled with primary antibodies against an integrin subunit and a hair cell marker (either a mouse monoclonal myosin Viia antibody [dilution of 1:250] or a polyclonal rabbit calretinin antibody [dilution of 1:100]). A full description of the methods used for immunohistochemistry is provided in 2.3; tables 2-1 and 2-2 give full details of the primary and secondary antibodies used during this project.

6.1 The Expression of Integrin β1 in the Adult Mouse Utricle

6.1.1 Expression of Integrin β1 in the Normal Adult Mouse Utricle

Cryostat sections of normal, uncultured adult mouse utricular tissue, fixed immediately after dissection from the animal, were immunofluorescently labelled for integrin β1 (green) using an integrin β1 (CD29) goat anti-rat primary antibody (BD Biosciences) at a dilution of 1:1000. The hair cell marker calretinin (red) was also used to label these sections in order to visualise vestibular hair cells within the sensory epithelium.

In the normal adult utricle, integrin β1 appears to be expressed at the border between the vestibular sensory epithelium and the basement membrane (Figure 6-1 Ai & Bi). There is no co-localisation of integrin β1 and calretinin, indicating that this integrin is not present in mature vestibular hair cells. Calretinin is also a neuronal marker, and labels the nerve fibres which innervate the utricle (Figure 6-1 Bii, arrow). There is no integrin β1 labelling in this region. In addition to its localisation at the basement membrane, the other main region of significant integrin β1 positive labelling is located within the mesenchymal tissue underlying the epithelium. In particular, blood capillaries found in the mesenchyme demonstrate punctate integrin β1 expression along their length (Figure 6-1 Ci, arrow).

6.1.2 Co-labelling of Normal Adult Utricular Tissue with Integrin β1 and Collagen Type IV

To confirm that integrin β1 expression occurs at the basement membrane border in the normal adult mouse utricle, cryostat sections were co-labelled for integrinβ1 (green) and collagen type IV (red). Collagen type IV is the main constituent protein found in basal lamina (Kefalides, 1973) and it was selected for use as a basement membrane marker.

The collagen type IV anti-rabbit primary antibody (Abcam) was used at a dilution of 1:1000.

As expected, collagen type IV (red) positively labels the basement membrane upon which the sensory epithelium of the utricle lies (Figure 6-2 Aii). This marker also labels capillaries within the mesenchyme (Figure 6-2 Bii), since the endothelia of these blood vessels also possess a basement membrane (Kramer et al., 1985). Integrin β1 co-localises with collagen type IV both within the blood capillaries (Figure 6-2 Biii, arrow) and at the epithelial-basement membrane border (Figure 6-2 D). At higher magnification, integrin β1 labelling is punctate in appearance across the length of this border. Integrin β1 expression in the capillaries of the mesenchyme appears to be in closer proximity to the luminal surface of the vessels, in comparison to that of collagen type IV, which appears to label the outer region of these structures.

6.1.3 Integrin β1 Expression in Gentamicin Treated Utricles

Cryostat sections of utricular tissue cultured for 4, 14 and 21 days post-gentamicin were labelled for integrin β1 (green) in conjunction with a hair cell marker myosin Viia (red). Control tissue was grown *in vitro* for the same total time period (i.e. 7 days in the case of control counterparts of 4 day post-gentamicin utricles) without receiving 48 hours antibiotic treatment.

In control tissue, the expression pattern of integrin β1 is similar to that seen in normal, uncultured adult mouse tissue. Integrin β1 expression occurs at the epithelial-basement membrane border (Figure 6-3 Ai). There also appears to be integrin β1 positive labelling, similar to that observed in non-cultured tissue, in blood capillaries of the mesenchyme (Figure 6-3 Bi, arrowhead). This labelling is not as clearly defined as previously seen, appearing as irregular β1-positive plaques as opposed to the finer punctae observed in normal tissue. This could be attributed to the likelihood that these blood vessels die away following tissue dissection. The hair cell marker myosin Viia indicates that vestibular hair cells are abundant in control tissue at this time point *in vitro* (Figure 6-3 Aii). This pattern of β1 labelling was observed in all control utricles at each of the 3 time points examined (Figure 6-4A & 6-5A). A general observation of cultured utricles which have been maintained for this length of time *in vitro* is their tendency to show a greatly flattened appearance, which is especially evident when

examining sections through this tissue as opposed to wholemounts. The mesenchyme underlying the epithelium is demonstrably thinner than that of uncultured tissue.

At 4 days post-gentamicin, β1 expression is very similar to that observed in the normal utricle. Despite the loss of vestibular hair cells indicated by the decreased number of cells labelled positive for myosin Viia (Figure 6-3 Bii) integrin β1 expression remains most evident at the epithelial-basement membrane border (Figure 6-3 Ci). As observed in control tissue which spent the same length of time under culture conditions, integrin β1 labelling of the blood vessels within the mesenchyme is sporadic and not as clearly defined as that seen in normal tissue (Figure 6-3 Ci); the capillaries are expected to have degenerated *in vitro* and thus the labelling seen is likely to be residual debris from these structures.

At 14 (Figure 6-4) and 21 (Figure 6-5) days post-gentamicin, few vestibular hair cells positive for myosin Viia (Figure 6-4 Bii & 6-5Bii) are visible. Integrin β1 expression at these two latter time points does not appear to differ greatly from that observed at 4 days post-gentamicin treatment. Integrin β1 is expressed at the basement membrane throughout the process of hair cell loss and any subsequent tissue recovery for the entire time period investigated (Figure 6-4 Ci & Figure 6-5 Ci). Irregular integrin β1 positive plaques also continue to be observed in gentamicin treated tissue within the underlying mesenchyme at all three time points.

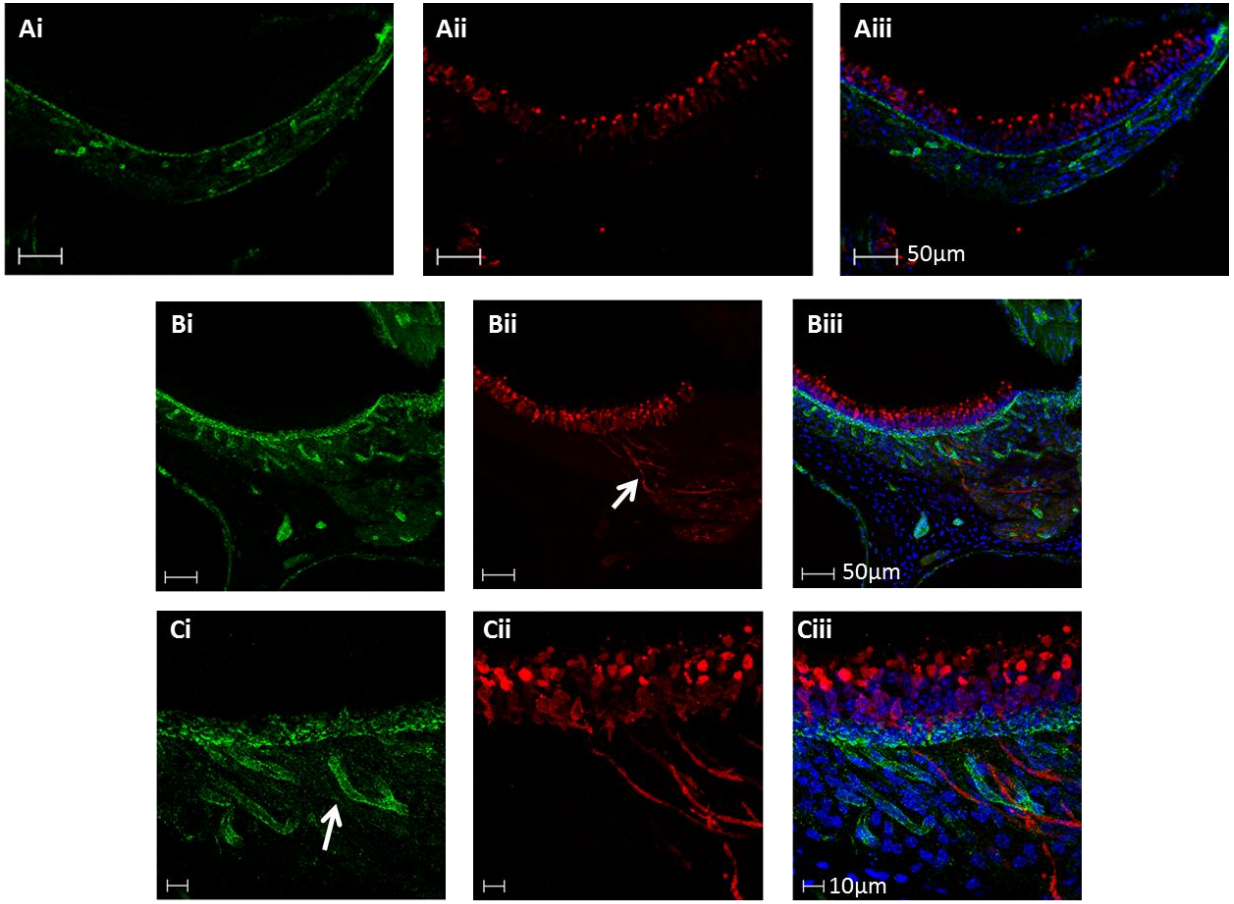

Figure 6-1 Integrin β1 Expression in the Normal, Uncultured Mouse Utricle

Cryosections of normal mouse utricle which had not been cultured immunolabelled for integrin β1 (green) and calretinin (red). DAPI labels cell nuclei blue. (A & B) Vestibular hair cells are positive for calretinin (red) which also labels the neurons which innervate this tissue (Bii, arrow). (C) The same section as in B at higher magnification in a region where there are both neurons and blood capillaries visible (Ci, arrow).

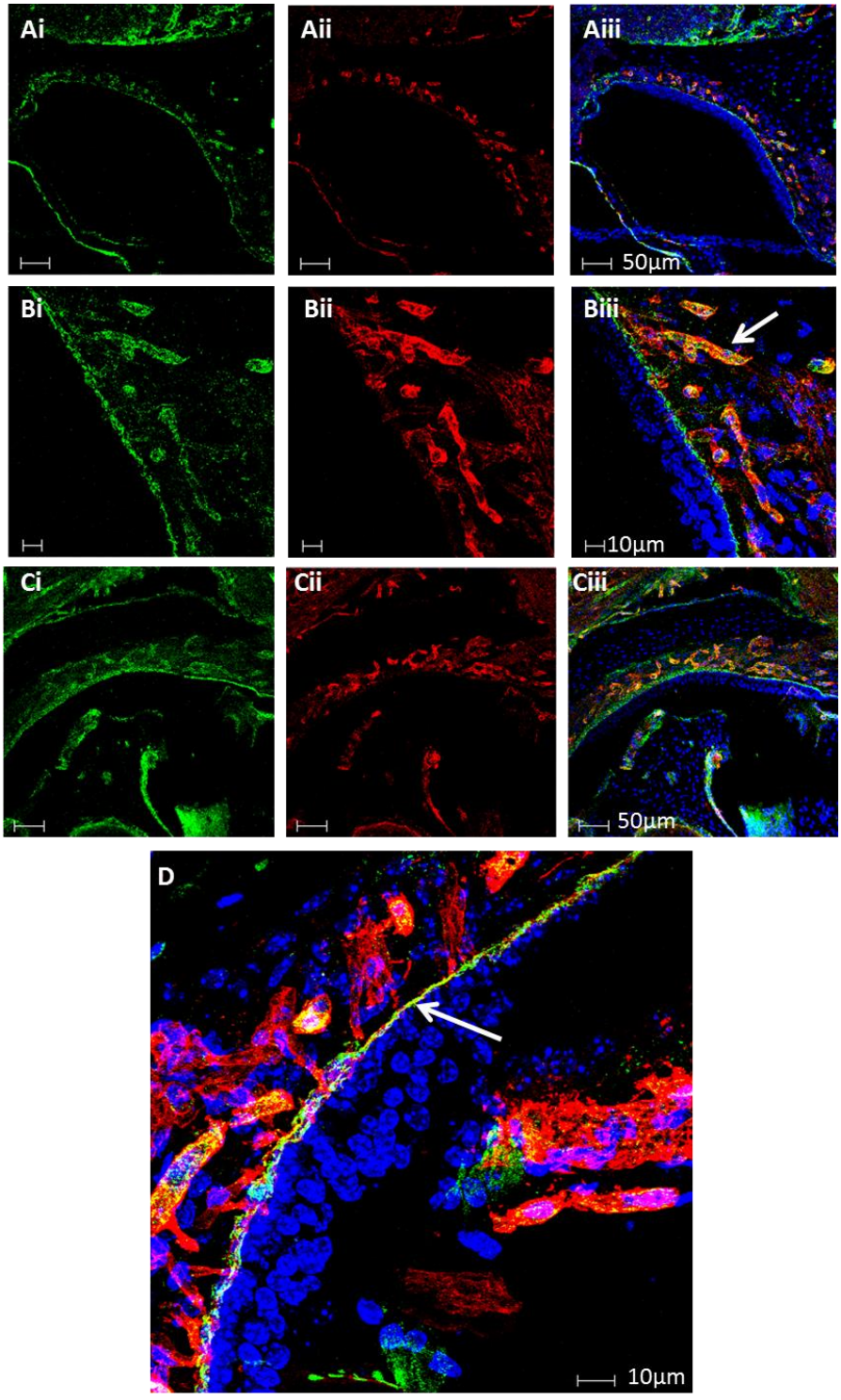

Figure 6-2 Co-labelling of Normal Adult Utricles for Integrin β1 and Collagen Type IV

Cryosections of a normal uncultured adult mouse utricle labelled for integrin β1 (green) and collagen type IV (red). DAPI labels cell nuclei blue. (A & C) Overview of the entire utricle. (B) The same section as in A is viewed under higher magnification, focussing on a region containing several blood vessels (Biii, arrow). (D) Co-labelling of integrin β1 and collagen type IV, both in the underlying mesenchyme and at the epithelial-basement membrane border (arrow).

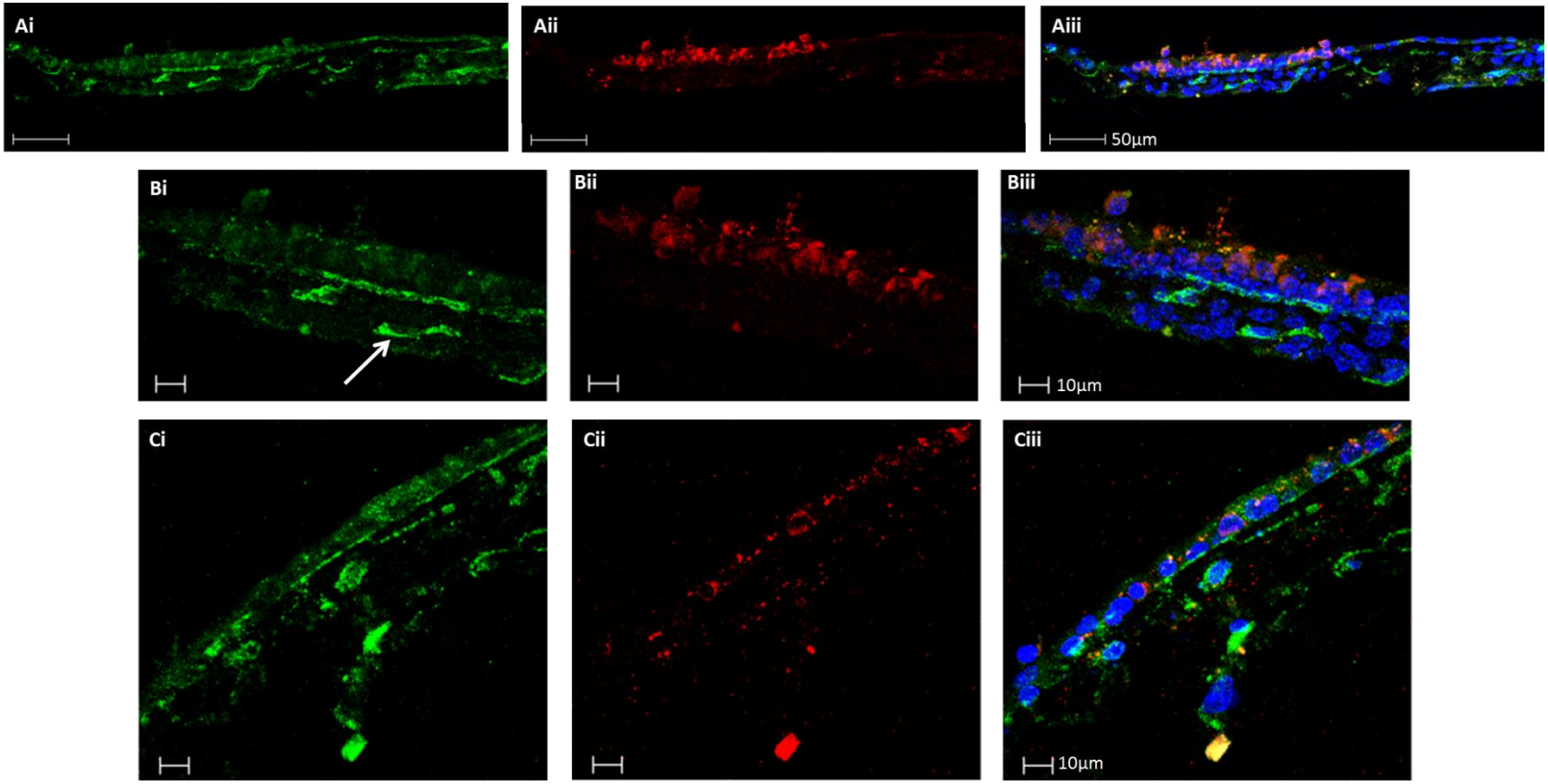

Figure 6-3 Integrin β1 Expression in Control and Gentamicin Treated Tissue at 4 Days Post-Gentamicin Exposure

Cryostat sections of utricular tissue cultured for 4 days post-gentamicin labelled for integrin β1 (green) and myosin Viia (red). DAPI labels cell nuclei blue. (A & B) Control tissue cultured for a total of 7 days, without receiving 48 hours antibiotic treatment. Irregular integrin β1 positive plaques (arrow) are thought to be due to degradation of the blood vessels *in vitro*. (C) Aminoglycoside treated tissue at 4 days post gentamicin treatment.

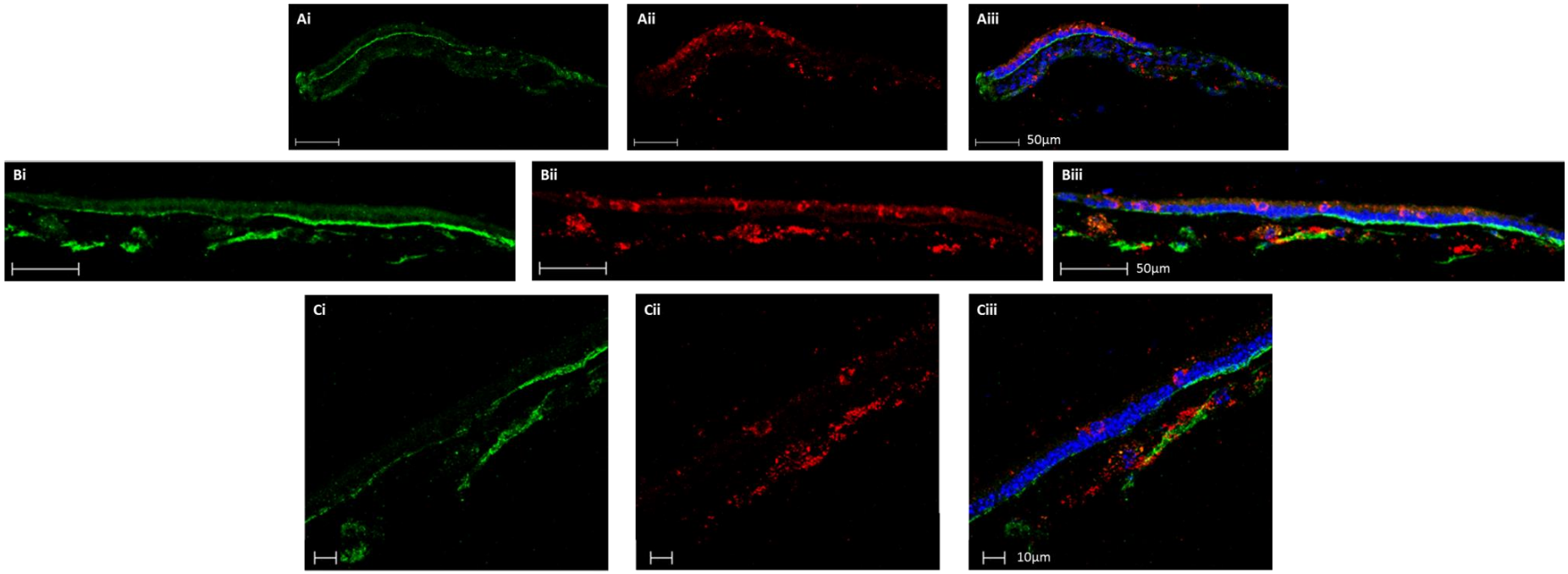

Figure 6-4 Integrin β1 Expression in Control and Gentamicin Treated Utricular Tissue at 14 Days Post-Gentamicin

Cryostat sections of utricles cultured for 14 days post gentamicin treatment labelled for integrin β1 (green) and myosin Viia (red). DAPI labels cell nuclei blue. (A) Control tissue maintained *in vitro* for a total of 17 days without receiving gentamicin treatment. (B & C) Gentamicin treated utricular sections at 14 days post gentamicin treatment. There is little remaining mesenchyme tissue at this time point. Plaques positive for integrin β1 (Ciii, arrowhead) correlated to the region where the blood capillaries of the tissue would have been located.

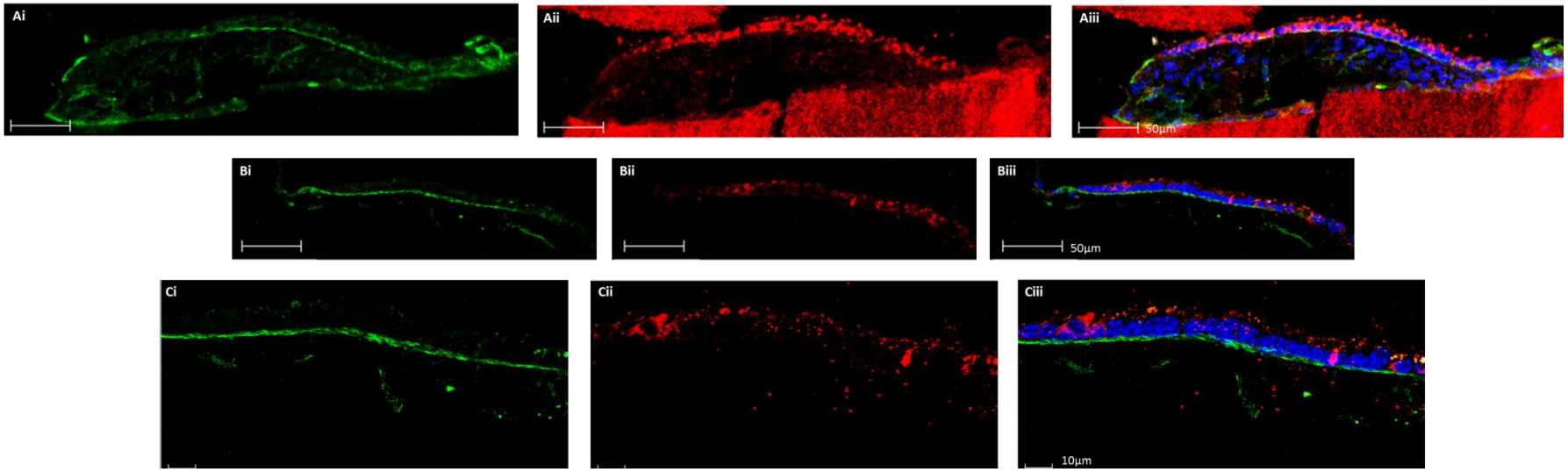

Figure 6-5 Integrin β1 Expression in Control and Gentamicin Treated Utricular Tissue at 21 Days Post-Gentamicin

Cryostat sections of utricles cultured for 21 days post gentamicin treatment labelled for integrin β1 (green) and myosin Viia (red). DAPI labels cell nuclei blue. (A) Control tissue maintained *in vitro* for a total of 24 days without being treated with gentamicin. In this section the tissue is still sitting on the filter paper on which it was cultured. (B & C) Gentamicin treated utricular sections at 21 days post gentamicin exposure. Mesenchymal tissue is greatly reduced in these sections after 24 days in culture.

6.2 The Expression of Integrin αV in the Murine Vestibular Epithelium

6.2.1 Integrin αV Expression in the Normal Adult Mouse Utricle

Cryostat sections of mouse skin were used as a positive control tissue in order to determine an appropriate concentration at which to use the integrin αV primary antibody (BD Biosciences). Phalloidin-FITC (red), used at a 1:1000 dilution, labels muscle fibres within the skin (Figure 6-6 Aii) with the distinctive striated appearance of actin filaments evident in muscle fibres present within this tissue. Integrin αV (green) used at a dilution of 1:200, labelled only at the periphery of these muscle fibres (Figure 6-6 Ai).

The dilution established from positive control experiments was used to label cryostat sections of normal adult mouse utricles which had not been maintained *in vitro*. The results of these experiments proved to be far less well defined in terms of reliable, specific labelling with the integrin αV antibody. Figure 6-6 B represents the clearest example of immunohistochemistry in the normal utricle under these conditions; this result was not consistently replicable. Integrin αV (green) exhibits widespread labelling in the mesenchymal tissue beneath the vestibular hair cells and supporting cells, with regions of greater signal intensity at the edge of the mesenchyme closest to the epithelium and also in a pattern which would correspond to blood vessels. Although there is a small amount of background staining of αV within the epithelium, calretinin (red) labelling of the vestibular hair cells indicates that there is no co-localisation of the two proteins within these cells. The calretinin antibody has also labelled the neurons of the utricle in this section (Figure 6-6 Bii).

It was thought that the poor labelling for integrin αV might be improved in utricular tissue by using a tyramide signal amplification kit to enhance the signal from integrin αV above that of the abundant background level within the mesenchymal tissue. This signal amplification system utilises a horse radish peroxidase (HRP) conjugate to activate a fluorescently tagged tyramide derivative. This process (which requires hydrogen peroxide) creates tyramide radicals which will then localise in the vicinity of the site at which the HRP conjugate interacts with the primary antibody being used.

In normal uncultured adult mouse tissue immunolabelled for integrin αV (Figure 6-7) with the use of the TSA amplification kit, a region of intense labelling (green) is detected at the top of the mesenchyme i.e. the area directly beneath the basement membrane (Figure 6-7 Aii). This is similar to the pattern seen without the use of tyramide amplification, but this region appears brighter and more pronounced over and above the background labelling visible across the majority of the mesenchyme. Co-labelling of cryosectioned normal utricular tissue with integrin αV and the basement membrane marker collagen type IV (Figure 6-9), shows that integrin αV appears to be expressed only in the underlying mesenchyme, in particular at the region of the connective tissue which lies directly beneath the basement membrane ((Figure 6-9 Biii). Integrin αV positive-staining does not extend above this membrane into the sensory epithelium, indicating that this integrin is not expressed normally in either vestibular hair cells or the surrounding supporting cells. Phalloidin-FITC (red) labels the stereociliary bundles at the apex of cells within the sensory epithelial layer (Figure 6-7 Ai). Tissue which would correspond with the vascular network of the utricle within the mesenchyme also appears to be positively labelled for integrin αV (Figure 6-7 Bii). In wholemount tissue, integrin αV positive undulating lineate structures (Figure 6-8 Aii) are visible beneath the layer of the tissue which contains calretinin-positive (red) vestibular hair cells. The morphology of these structures would correlate with blood capillaries present in the utricle.

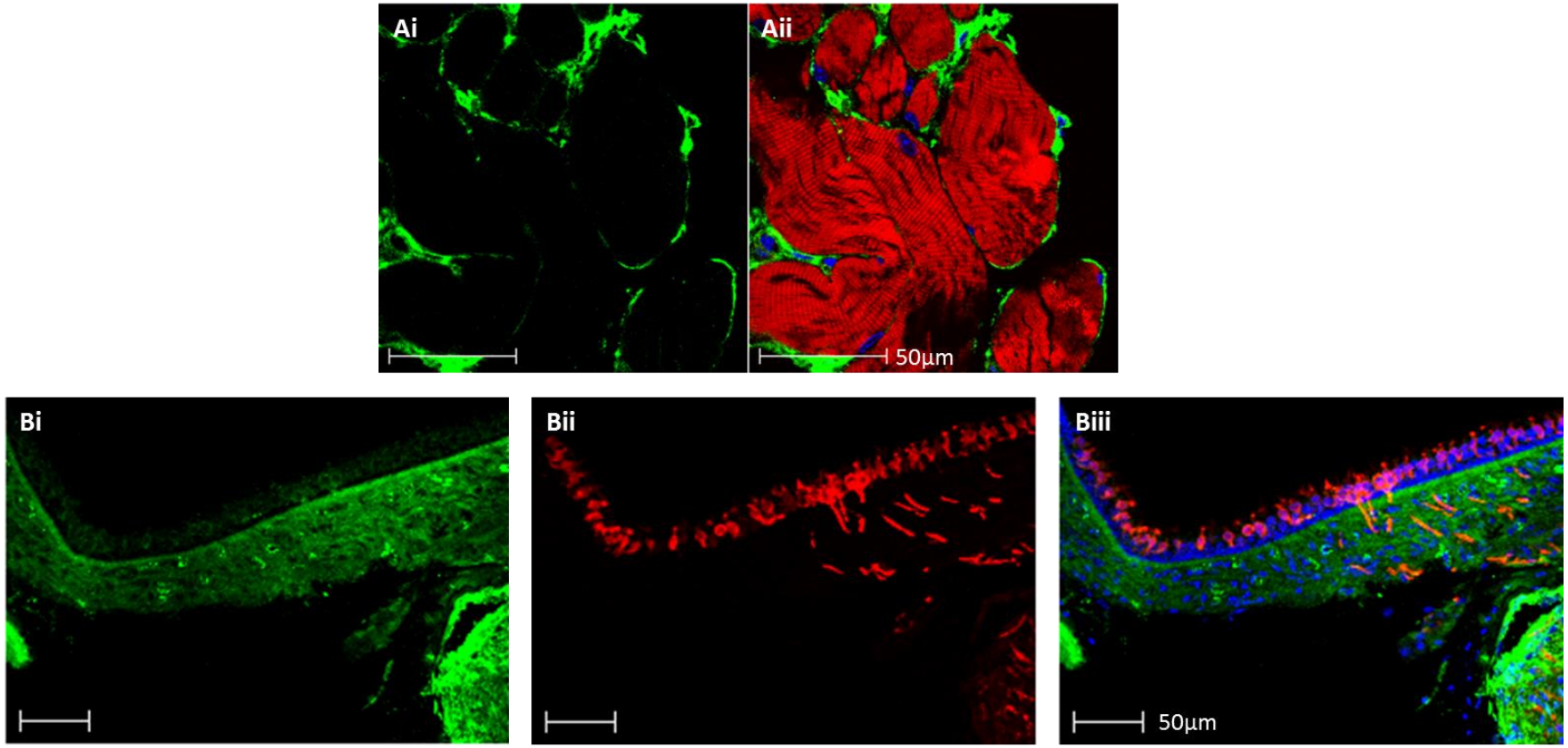

Figure 6-6 Integrin αV Labelling of Mouse Skin and the Normal Uncultured Mouse Utricle

(A) Cryosection of mouse skin tissue (as a positive control) immunolabelled with Phalloidin-FITC (red) and integrin αV at a dilution of 1:200 (green). DAPI labels cell nuclei blue. (B) Cryosection of normal uncultured adult mouse utricle immunolabelled with integrin αV (green), calretinin (red) as a hair cell marker. DAPI labels cell nuclei blue.

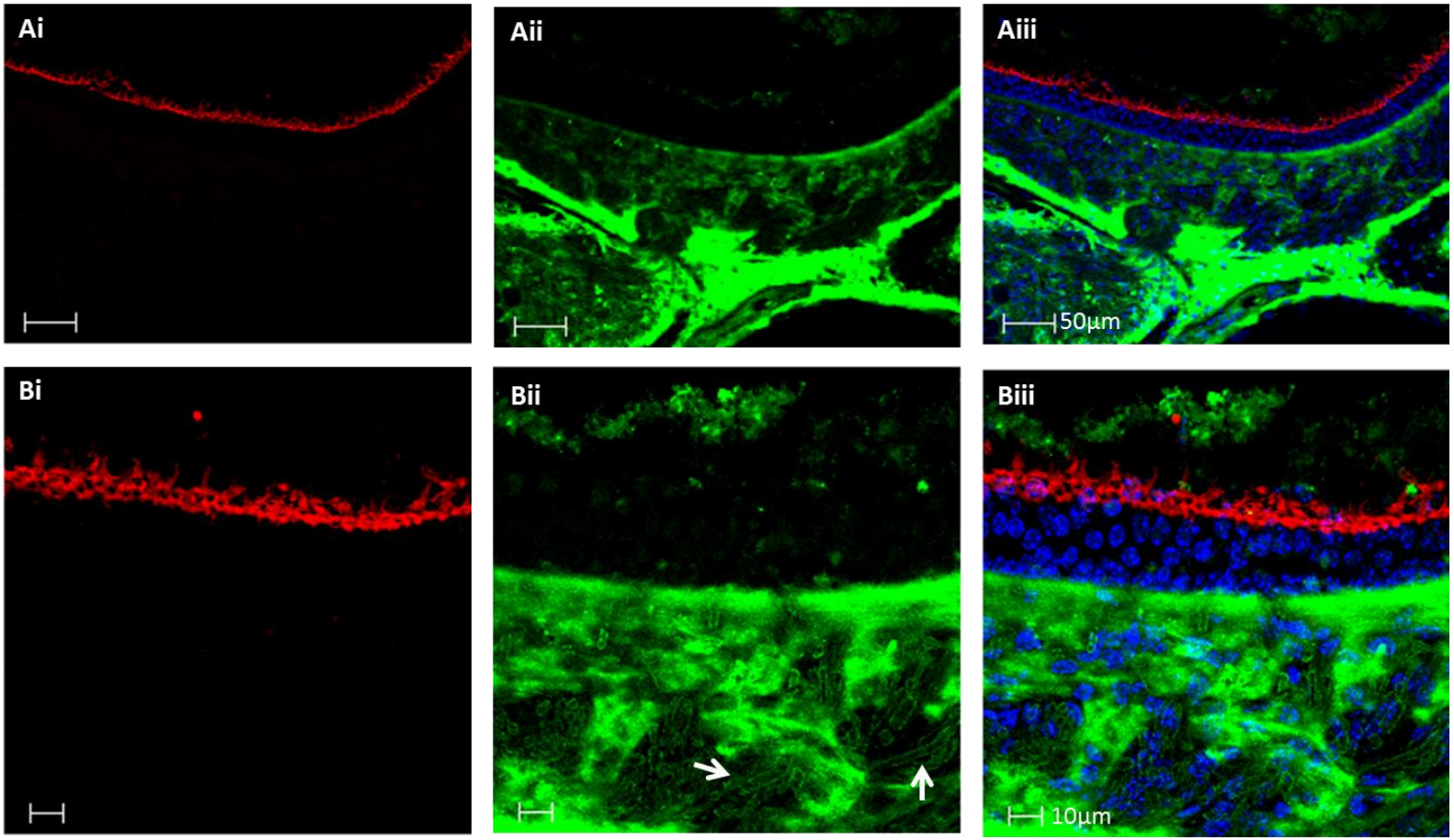

Figure 6-7 Integrin αV Expression in the Normal Adult Mouse Utricle Amplified using a TSA Kit

Cryosections of normal uncultured adult mouse utricle labelled for integrin αV using a TSA amplification kit to provide better definition of the true signal above background labelling. (A) Phalloidin-FITC labels stereocilia (red). Integrin αV (green) is detected predominantly in the mesenchyme. DAPI labels cell nuclei blue. (B) Arrows indicate blood capillaries within the mesenchymal tissue which are also positive for integrin αV.

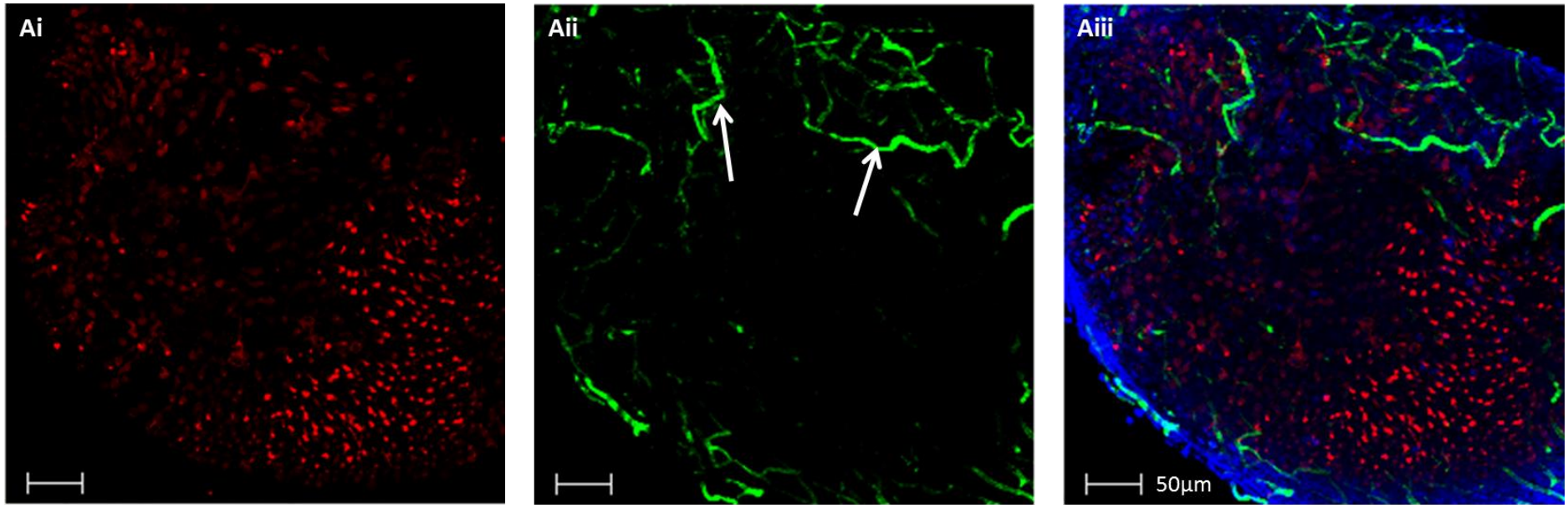

Figure 6-8 Integrin αV Expression in Normal Wholemount Utricular Tissue

Normal uncultured adult mouse utricular tissue immunolabelled as a wholemount with calretinin (red) as a hair cell marker, integrin αV (green) and DAPI (blue) indicating cell nuclei. (A) Integrin αV (signal amplified using TSA kit) positively labels the vascular network (arrows) of the utricle within the underlying mesenchyme.

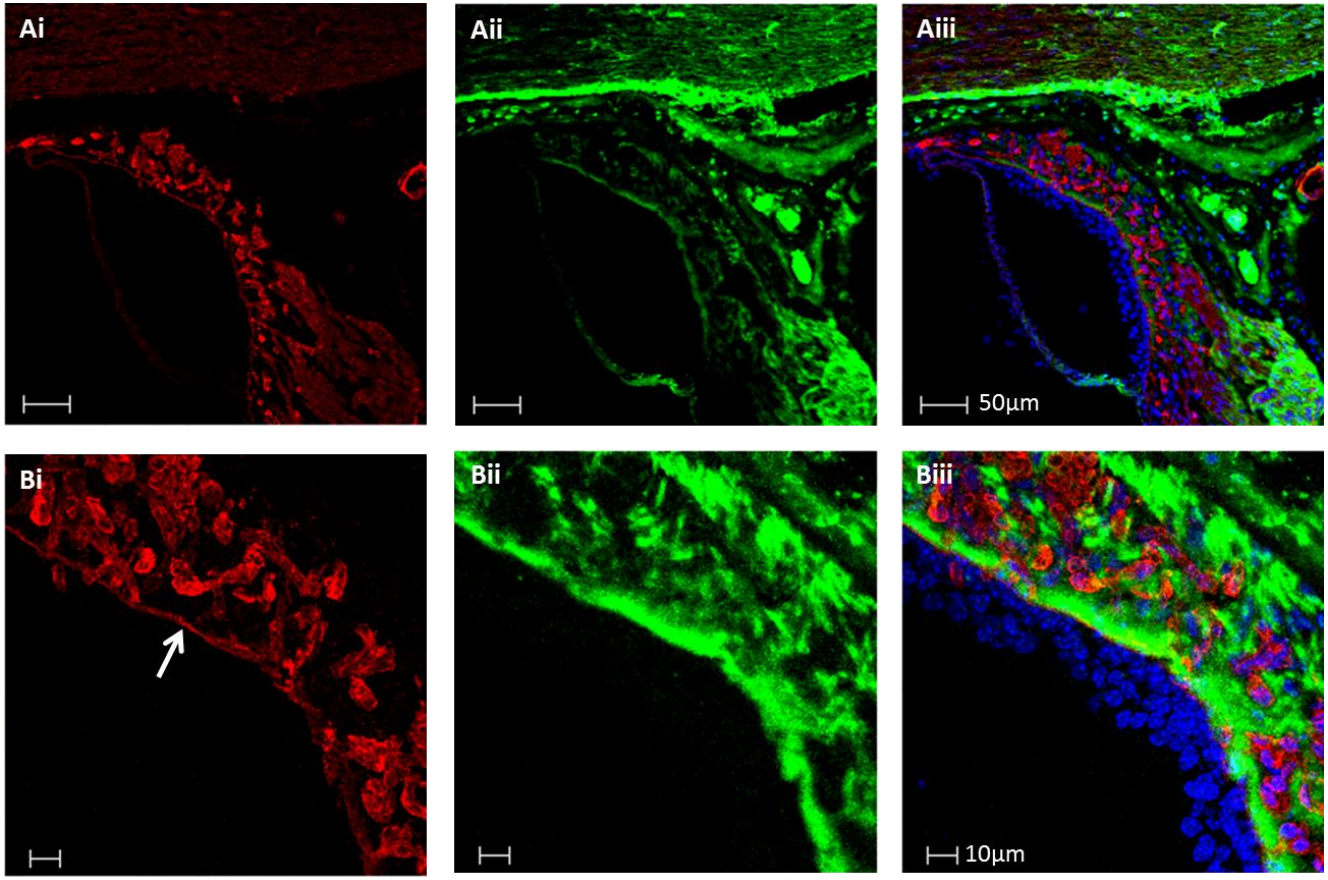

Figure 6-9 Integrin αV and Collagen Type IV Co-Expression in the Normal Utricle

Cryostat sections of normal adult utricular tissue co-labelled for integrin αV (green) and collagen type IV (red). DAPI labels cell nuclei blue. (A) Co-localisation of integrin αV and collagen type IV occurs predominately at the basement membrane. (B) There is no integrin αV expression above the basement membrane (Arrow indicates basement membrane at the epithelial-mesenchymal border); integrin αV is not expressed in the sensory epithelium.

6.2.2 Integrin αV Expression in Gentamicin Treated Utricles

Cryosections of cultured utricular tissue were labelled for integrin αV (green, with the use of a TSA amplification kit) in conjunction with the hair cell marker calretinin (red). Control tissue was grown *in vitro* for the same total time period (i.e. 7 days in the case of control counterparts of 4 day post-gentamicin utricles) without receiving aminoglycoside treatment.

In control sections across all three time points studied (Figure 6-10, 6-12 A & 6-13 A) integrin αV positive labelling appears similar to that observed in normal uncultured utricular tissue, with labelling most evident in the mesenchyme directly beneath the basement membrane (Figure 6-10 Aii & Bii). There is no co-localisation of calretinin and integrin αV visible (Figure 6-10 Aiii & Biii). As was observed in time series immunohistochemistry experiments with integrin β1, which also showed a tendency to label the vasculature of the utricle, staining of these structures is less evident in cultured tissue both in control and gentamicin treated utricles, since these features of the underlying mesenchyme tend to disappear after being maintained *in vitro*. The sensory epithelium remains populated with calretinin-positive vestibular hair cells in these cultures (Figure 6-13 Bi).

At 4 days post-gentamicin, utricles have undergone considerable hair cell loss (Figure 6-11 Ai) and exhibit the same pattern of integrin αV expression (Figure 6-11 Aii & Bii) as seen in their control counterparts. The remaining mesenchyme, as in control tissue at this time point, lacks the clearly defined labelling of blood capillaries with integrin αV that is seen in normal uncultured utricles. By 14 days post-gentamicin (Figure 6-12 C) there remains no significant difference in terms of integrin αV expression in comparison to either control tissue maintained *in vitro* for the same length of time, or utricular tissue at 4 days post-gentamicin treatment.

Following a 21 day recovery period, the expression pattern of αV appears little different to that observed in control counterparts and in gentamicin treated utricles at earlier time points. Despite the sensory epithelium being largely depleted in terms of hair cell numbers (Figure 6-13 Ci), the band of mesenchymal tissue immediately beneath the epithelial layer remains the focal point of integrin αV positive labelling in these cultures (Figure 6-13 Cii).

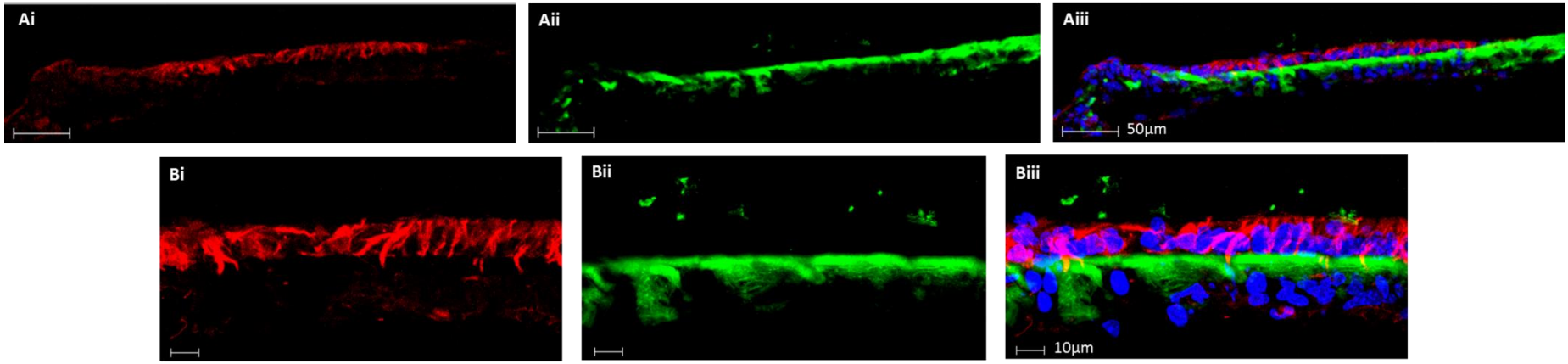

Figure 6-10 Integrin αV Expression in Control Utricular Tissue Cultured for 7 Days

Cryostat sections of utricular tissue maintained in culture for a total of 7 days without gentamicin treatment, immunolabelled for calretinin (red) and integrin αV (green). DAPI labels cell nuclei blue. (A) Control tissue is well populated with vestibular hair cells. (B) x63 objective view of the same utricle section.

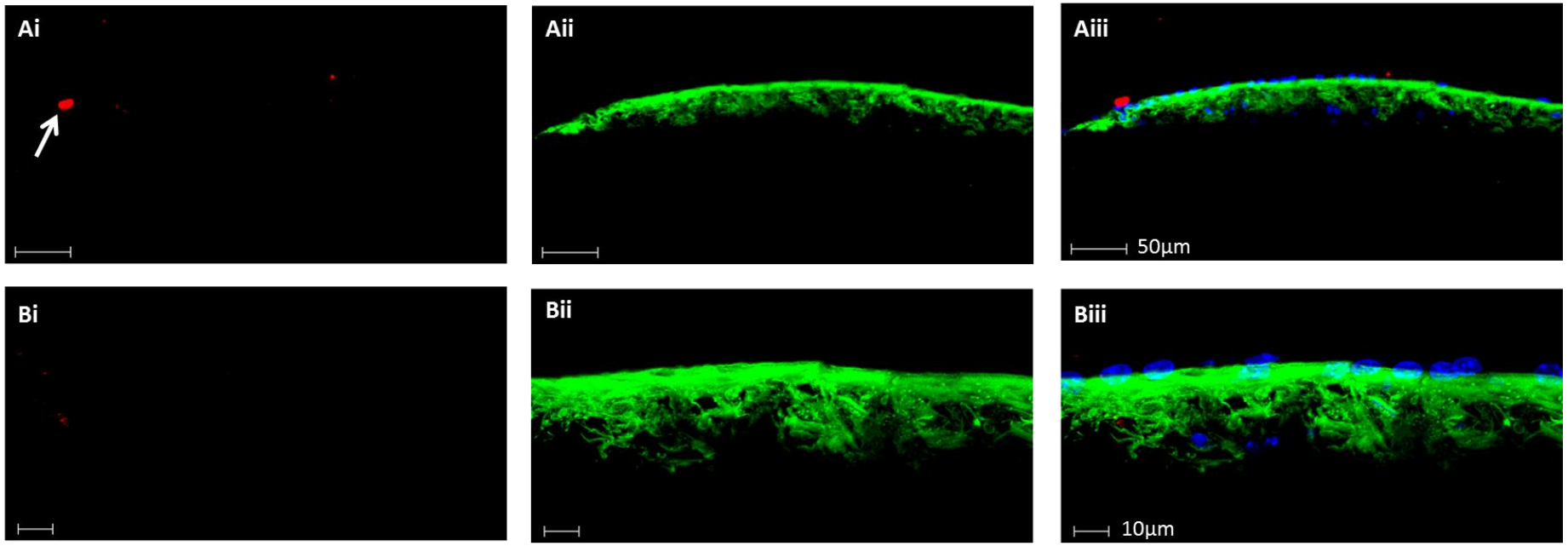

Figure 6-11 Integrin αV Expression in Utricular Tissue at 4 Days Post-Gentamicin Treatment

Cryostat sections of cultured utricular tissue at 4 days post-gentamicin exposure were immunolabelled for calretinin (red) and integrin αV (green). DAPI labels cell nuclei blue. (A) Calretinin positive cellular 'debris' of hair cells which have undergone cell death (arrowhead). (B) A x63 objective view of the same section as in A.

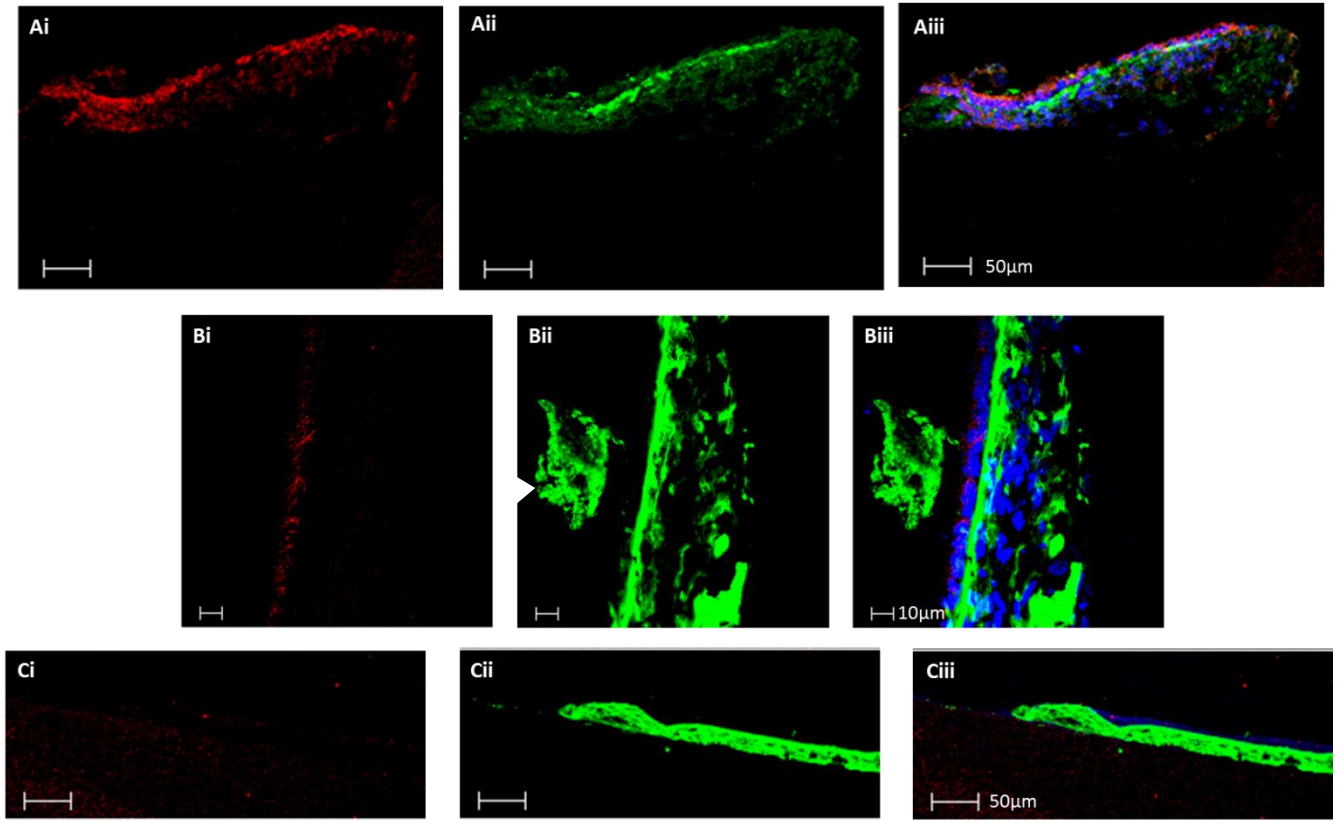

Figure 6-12 Integrin αV Expression in Utricular Tissue at 14 Days Post-Gentamicin Treatment

Cryostat sections of cultured control utricles grown for 17 days with any gentamicin exposure immunolabelled with calretinin (red) as a hair cell marker and integrin αV (green), using the TSA amplification kit. DAPI labels cell nuclei blue. (A & B) Control tissue cultured for 17 days *in vitro*. (C) Tissue treated with gentamicin after a 14 day recovery period.

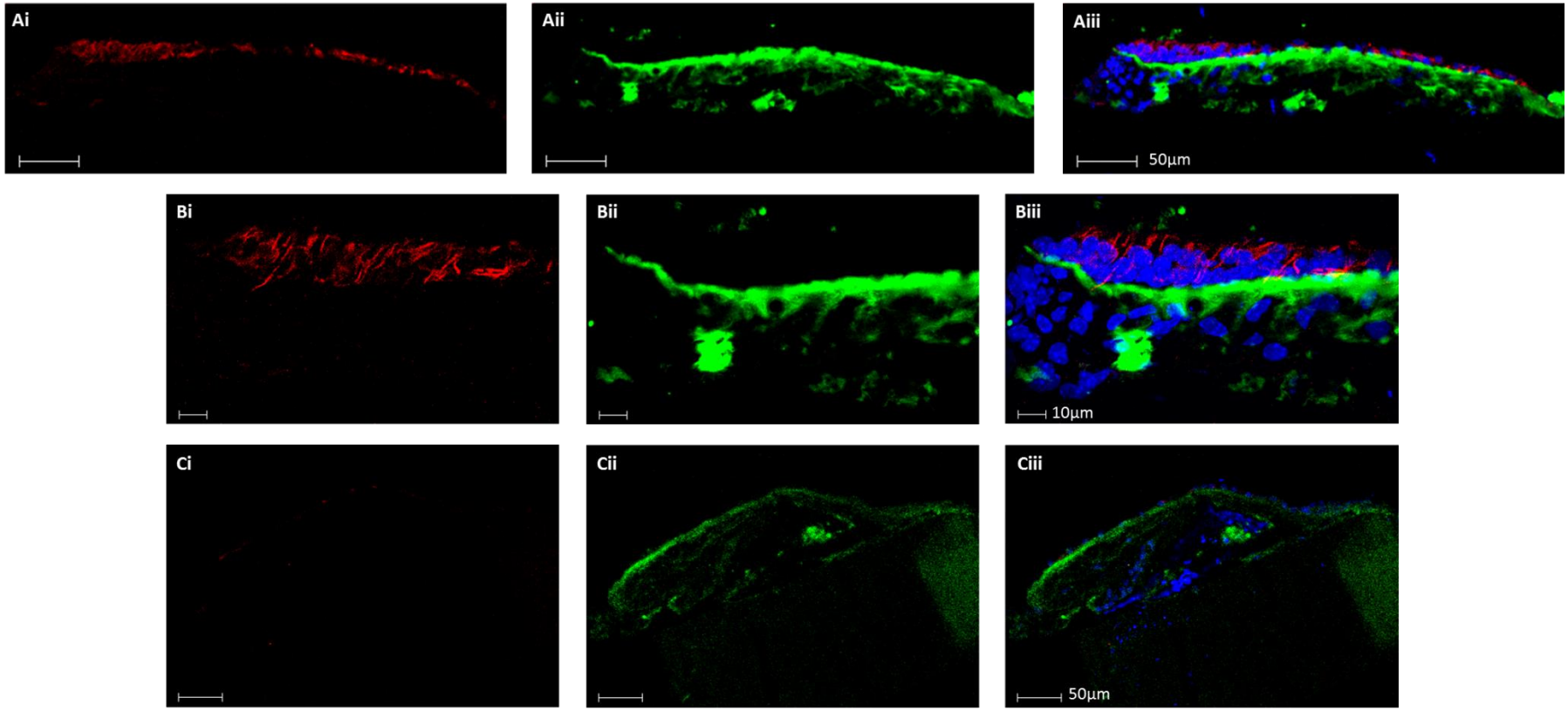

Figure 6-13 Integrin αV Expression in Cultured Utricular Tissue at 21 Days Post-Gentamicin Treatment

Cryostat sections of utricular tissue grown in culture for 21 days post gentamicin, immunolabelled for calretinin (red) and integrin αV (green). DAPI labels cell nuclei blue. (A & B) Control tissue demonstrates a well-populated sensory epithelium of calretinin-positive hair cells. (C) Gentamicin treated tissue at 21 days post aminoglycoside exposure.

6.3 The Expression of Integrin β5 in the Adult Mouse Utricle

6.3.1 Integrin β5 Expression in the Normal Uncultured Adult Mouse Utricle

Cryosections of adult mouse small intestine (Figure 6-14 A) were used as a positive control in order to establish an appropriate concentration at which to use the integrin β5 primary antibody (Millipore). Phalloidin-FITC (red) positively labels the muscular outer wall of the intestinal tissue which is rich in filamentous actin (Figure 6-14 Aii). Integrin β5 (green) at a dilution of 1:100 positively labels cells located within the tissue at the centre of the numerous villi present at the luminal surface (Figure 6-14 Ai). Additional integrin β5 positive cell bodies are seen at the base of crypts and villi in close proximity to the outer wall.

In cryosections of normal adult mouse utricular tissue which had not been maintained *in vitro*, labelled with integrin β5 (green) and myosin Viia (red) as a hair cell marker, there appeared to be relatively widespread β5 expression within both the mesenchyme and sensory epithelial layers of the tissue (Figure 6-14 Bi). This subunit does not appear to be associated with the basement membrane as was observed for integrin β1 and αV. Integrin β5 appears to be associated with vestibular hair cells (Figure 6-14 C), in particular, towards the base of type I hair cells where they associate with neural calyces. There is a clear 'gap' in the tissue between the underlying mesenchyme and the myosin Viia-positive hair cell layer which shows no integrin β5 expression, corresponding to the supporting cell layer of the epithelium.

6.3.2 Integrin β5 Expression in Gentamicin Treated Utricles

Control tissue shows greater numbers of myosin Viia positive hair cells than seen in sections of gentamicin treated utricles; this occurs at each of the time points examined in this study (Figure 6-15 A, 6-16 A & B). At 4 days post-gentamicin (Figure 6-15), both control counterparts and gentamicin treated utricles appear to have lost integrin β5 positive labelling within hair cell bodies in the region of the nerve calyces, where it had been observed in normal tissue. Irregular plaques positive for integrin β5 appear at the apical region of the sensory epithelium.

At 14 days post-gentamicin (Figure 6-16), there appears to be a re-distribution of integrin β5 expression. Punctate β5-positive labelling is visible at the basement membrane, a region of the tissue where it had not been detected in normal, uncultured utricles. This change is observed both in gentamicin treated utricles and their control counterparts. The lack of integrin β5 expression within the hair cells in the region of afferent calyces seen at 4 days persists at 14 days post-gentamicin treatment (Figure 6-16 C & D). The irregular integrin β5 positive plaques seen at 4 days are also still visible after a 14 day recovery period; both in control and drug exposed utricles.

By 21 days post-gentamicin (Figure 6-17), it was possible to see evidence that integrin β5 expression had begun to return to its original distribution. Myosin Viia positive hair cells showing integrin β5 labelling within the hair cell body towards the basal region which associates with the neural calyces may be seen in the sensory epithelium. However, there remain hair cells which are positive for myosin Viia, which are not integrin β5 positive, suggesting that this redistribution may only be partial.

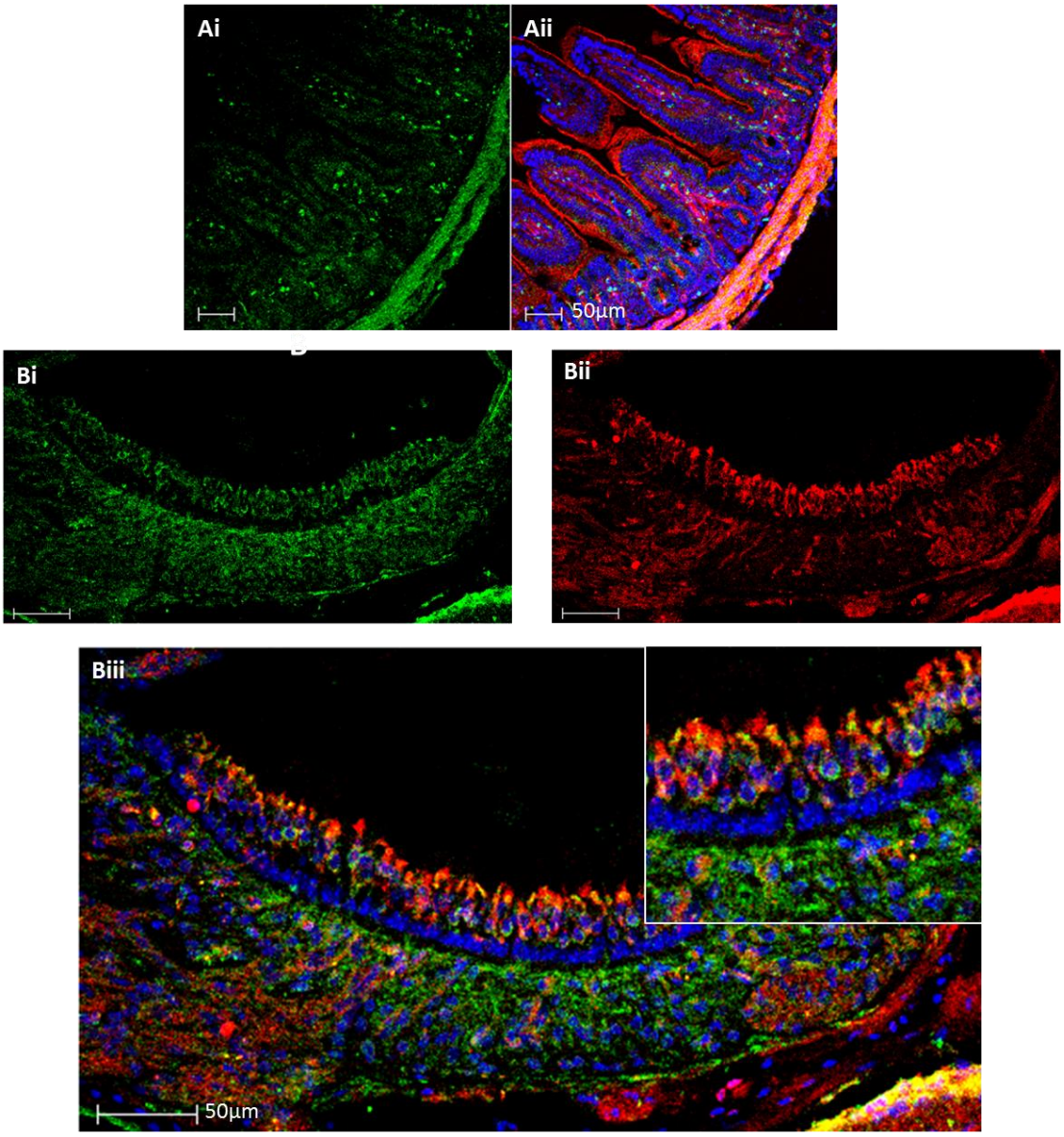

Figure 6-14 Expression of Integrin β5 in Small Intestine and the Normal Mouse Utricle

Cryostat sections of (A) mouse small intestine and (B) normal, uncultured adult mouse utricle. (A) Small intestine was used a positive control to determine an appropriate primary antibody concentration. Phalloidin-FITC (red) labels the muscular outer wall of the intestine. Integrin β5 (green) diluted 1:100. DAPI labels nuclei blue. (B) The normal mouse utricle labelled for integrin β5 (green) and the hair cell marker myosin Viia (red).

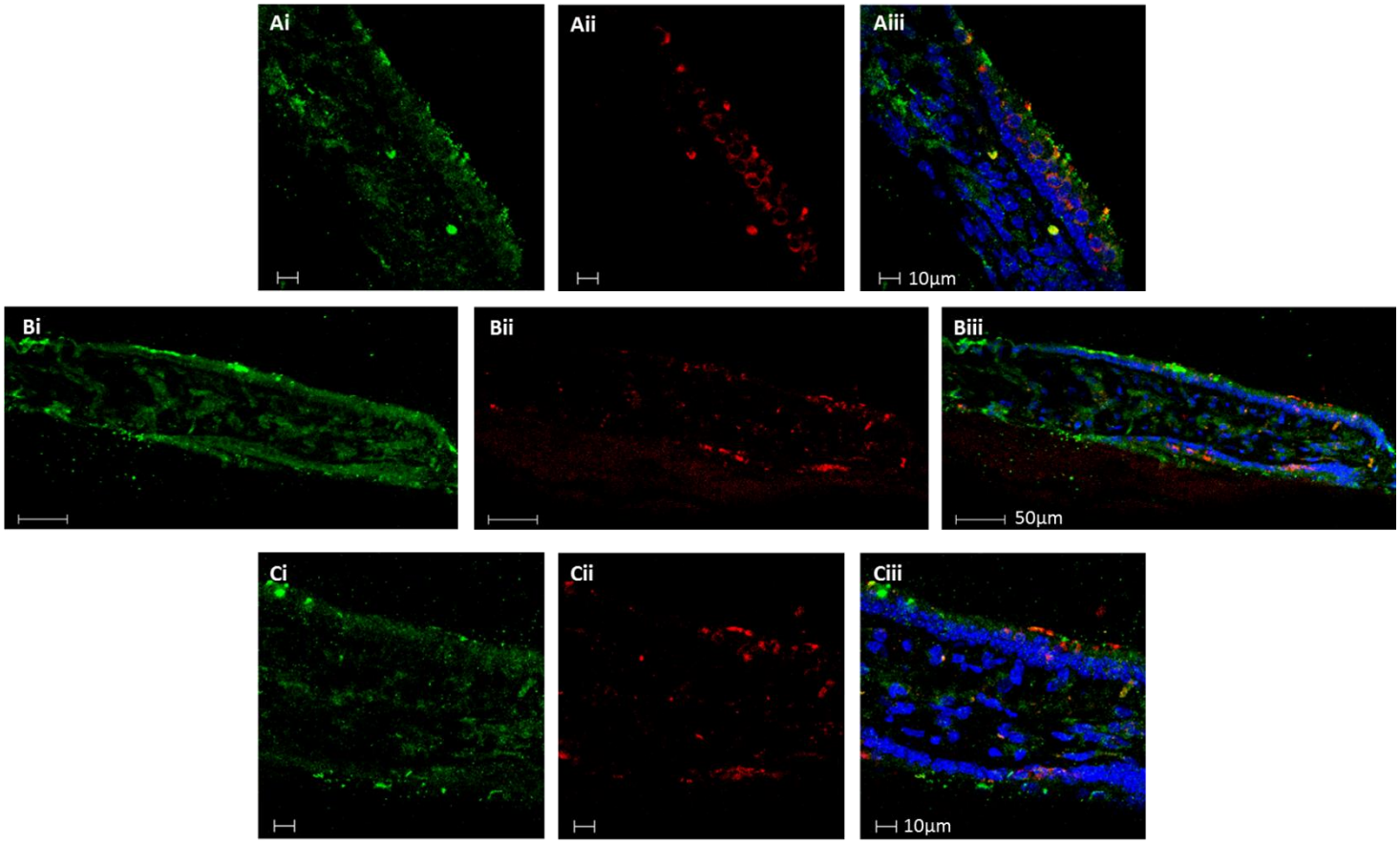

Figure 6-15 Expression of Integrin β5 in Cultured Utricular Tissue at 4 Days Post-Gentamicin Treatment

Cryostat sections of cultured utricle grown for 4 days after gentamicin treatment immunolabelled for integrin β5 (green) and myosin Viia (red). DAPI labels cell nuclei blue. (A) Control tissue cultured for a total of 7 days without receiving gentamicin treatment. (B & C) Gentamicin treated tissue after a 4 day recovery period.

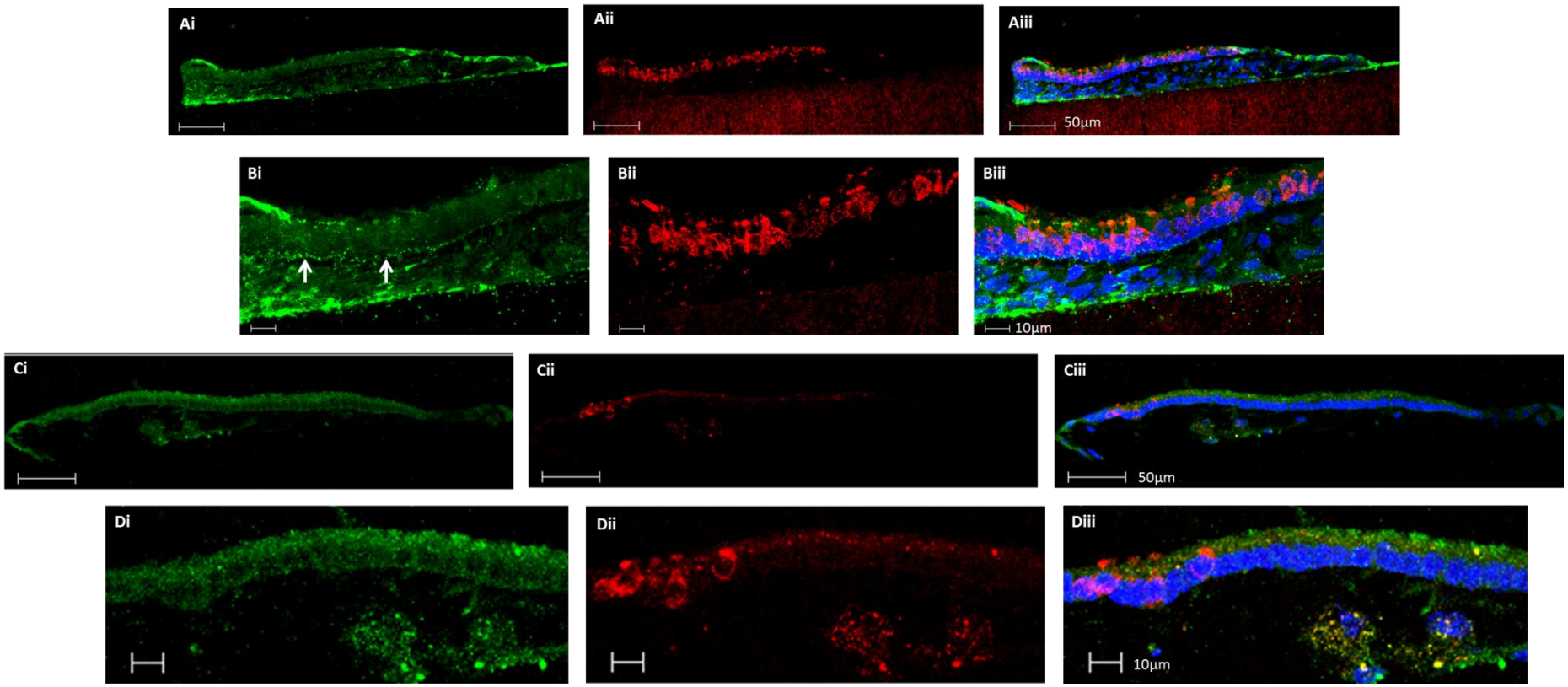

Figure 6-16 Expression of Integrin β5 in Utricular Tissue Cultured for 14 Days Post-Gentamicin Treatment

Cryostat sections of utricular tissue maintained *in vitro* for 14 days post gentamicin treatment immunolabelled for integrin β5 (green) and myosin Viia (red). DAPI labels cell nuclei blue. (A & B) Control tissue cultured for a total of 17 days without gentamicin exposure. (Bi) Arrows indicate β5-positive punctae at the basement membrane. (C & D) Gentamicin treated tissue following a 14 day recovery period.

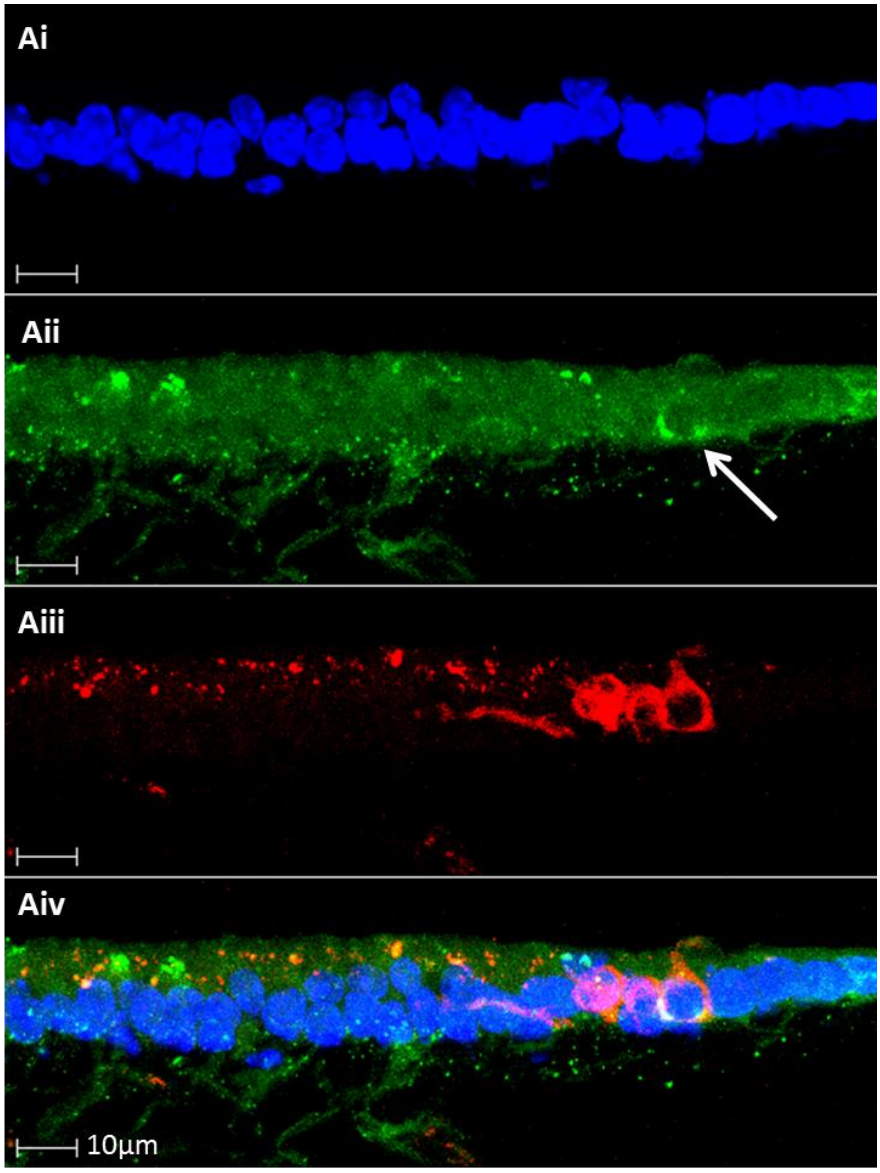

Figure 6-17 Integrin β5 Expression in Utricular Tissue Cultured for 21 Days Post - Gentamicin Treatment

Cultured utricular tissue at 21 days post gentamicin treatment, immunolabelled for integrin β5 (green) and myosin Viia (red). DAPI labels cell nuclei blue. (Aii) Arrow indicates integrin β5 positive labelling similar to that observed in normal tissue.

6.4 The Expression of Integrin α6 in the Adult Mouse Utricle

6.4.1 Integrin α6 in the Normal Uncultured Adult Mouse Utricle

Cryosections of adult mouse lung tissue were used as a positive control in order to determine an appropriate concentration at which to use the integrin α6 (Serotec) primary antibody. Previous work on integrins in the inner ear using this α6 antibody used a 1:200 dilution (Davies and Holley, 2002). Integrin α6 (green) shows widespread background labelling in mouse lung tissue (Figure 6-18 Aii), with lineate expression in regions that would correlate with the basement membranes of alveolar capillaries.

Cryosections of normal adult mouse utricular tissue which had not been maintained *in vitro* were immunolabelled for integrin α6 (green) and myosin Viia (red) as a hair cell marker. Integrin α6 positive punctae are visible along the length of the epithelial-basement membrane (Figure 6-18 Bi & Ci) similar to the pattern exhibited by integrin β1 in the same tissue. Integrin α6 also appears to label the vascular bed of the underlying mesenchyme and shows more widespread staining within the mesenchymal tissue at the lower regions of the utricle. There is no co-localisation of the hair cell marker and integrin α6 within the sensory epithelium.

6.4.2 Integrin α6 Expression in Gentamicin Treated Utricles

In control counterparts of utricles cultured for 4 days post-gentamicin, the sensory epithelium is populated with vestibular hair cells positive for myosin Viia (Figure 6-19 Aii); the section shown does however exhibit a breakage point at the centre, likely to be the result of damage during the initial tissue dissection. Integrin α6 positive labelling is, as in normal uncultured utricular tissue, present at the border between the epithelial and mesenchymal layers of the utricle (Figure 19 Ai). As observed with other integrin subunits in this work which label the blood capillaries of the mesenchyme, the integrin α6 labelling of these structures is less defined and more irregular than in tissue which had not been maintained *in vitro*. This is attributed to the fact that the mesenchymal tissue undergoes considerable remodelling and outgrowth under culture conditions. Control tissue continues to show this pattern of integrin α6 expression in the non-treated counterparts of 14 and 21 days post-gentamicin utricles (Figure 6-20 A and Figure 6-21 A).

At 4 days post-gentamicin (Figure 6-19), the integrin α6 expression pattern remains relatively unaltered from that seen in control tissue, in response to hair cell loss. Plaques of myosin Viia positive labelling believed to be cellular debris as the result of dying hair cells being extruded from the epithelial layer are visible in the tissue at this time point (Figure 6-19 Bii). Despite the loss of hair cells, integrin α6 expression persists at the epithelial-mesenchyme border in the region of the basement membrane (Figure 6-19 Bi & Ci). There are also large plaques positive for integrin α6 which are likely to correspond to the mesenchymal tissue and vascular network in which integrin α6 expression was observed in uncultured tissue. The same tendency is seen in control counterparts, indicating that this occurrence is more likely to be as a result of remodelling of tissue in the mesenchyme caused by the culture process, than it is to be triggered through gentamicin treatment.

Integrin α6 expression at the basement membrane is maintained in gentamicin treated tissue at both 14 (Figure 6-20 B) and 21 days (Figure 6-21 B) post drug exposure. The appearance of irregular integrin α6 positive plaques in the underlying mesenchyme also continues to be evident across each of the time points examined. Outgrowth and tissue remodelling continues in these organotypic cultures throughout the recovery period studied, and therefore these plaques would appear to be the result of the neural and vascular elements of the mesenchyme having been lost over time spent *in vitro*.

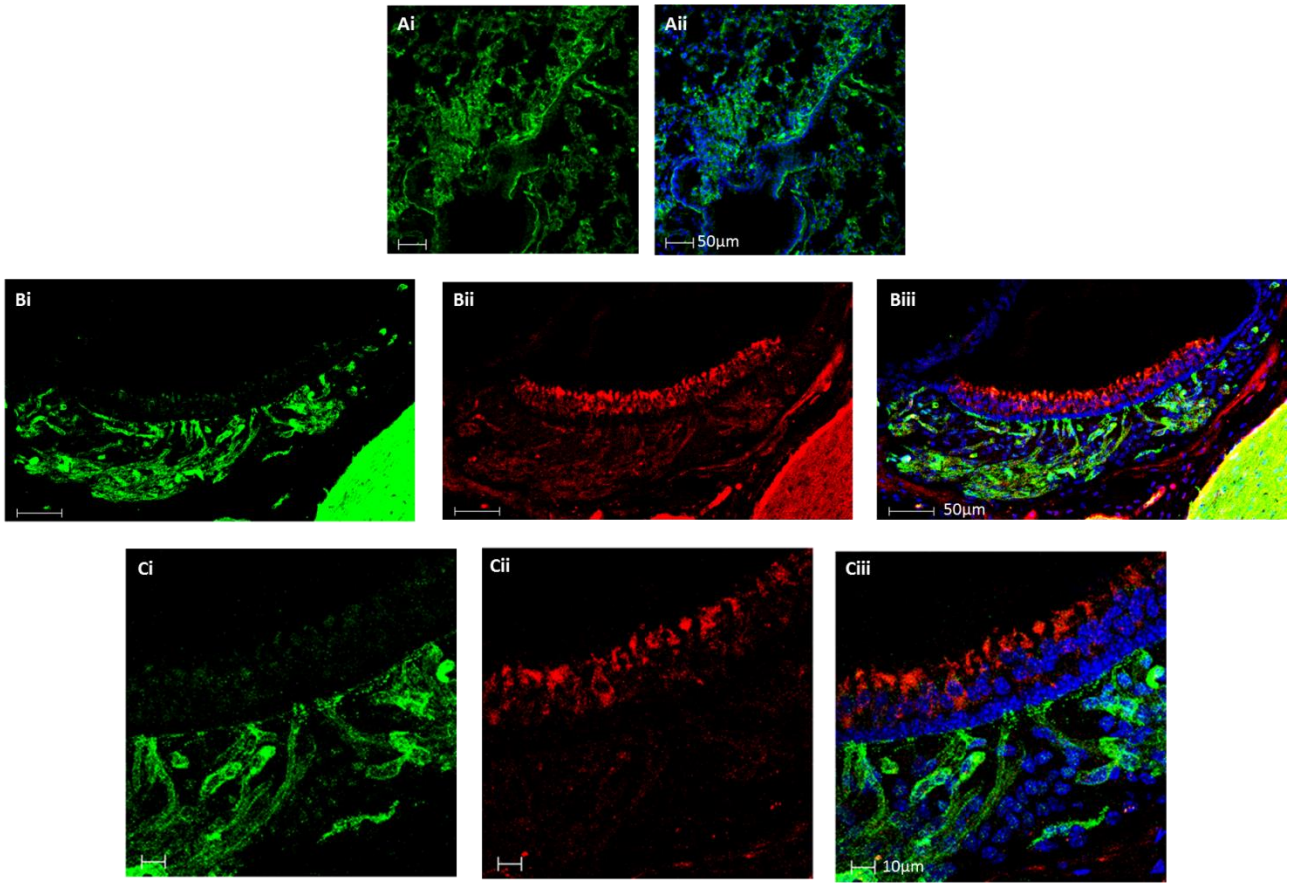

Figure 6-18 Integrin α6 Expression in Lung Positive Control Tissue and the Normal Adult Mouse Utricle

(A) Cryosection of adult mouse lung tissue as a positive control to determine an appropriate concentration for the integrin α6 (green) primary antibody. DAPI labels cell nuclei blue. (B & C) Cryosections of normal, uncultured adult mouse utricle immunolabelled for integrin α6 (green) and myosin Viia (red). DAPI labels cell nuclei blue.

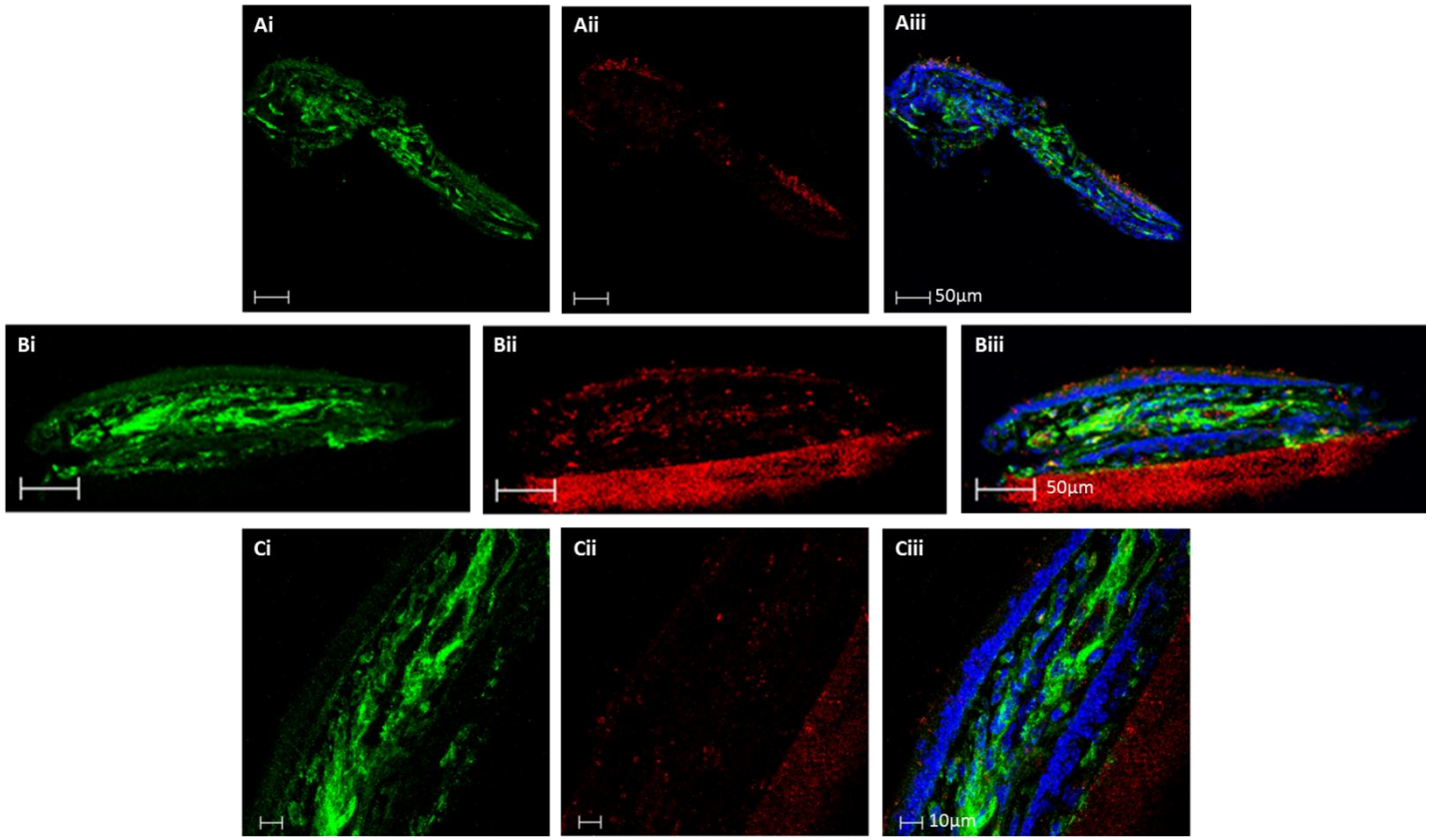

Figure 6-19 Integrin α6 Expression in Utricular Tissue Cultured for 4 Days Post-Gentamicin Treatment

Cryosections of cultured utricular tissue at 4 days post gentamicin treatment immunolabelled for integrin α6 (green) and myosin Viia (red). DAPI labels cell nuclei blue. (A) Control tissue maintained *in vitro* for a total of 7 days without receiving gentamicin treatment. (B & C) Gentamicin treated utricular tissue after a 4 day recovery period. (B) This section remains sitting on top of the nitrocellulose filter upon which it was cultured; the filter tends to take up the TRITC secondary antibody thus appearing red.

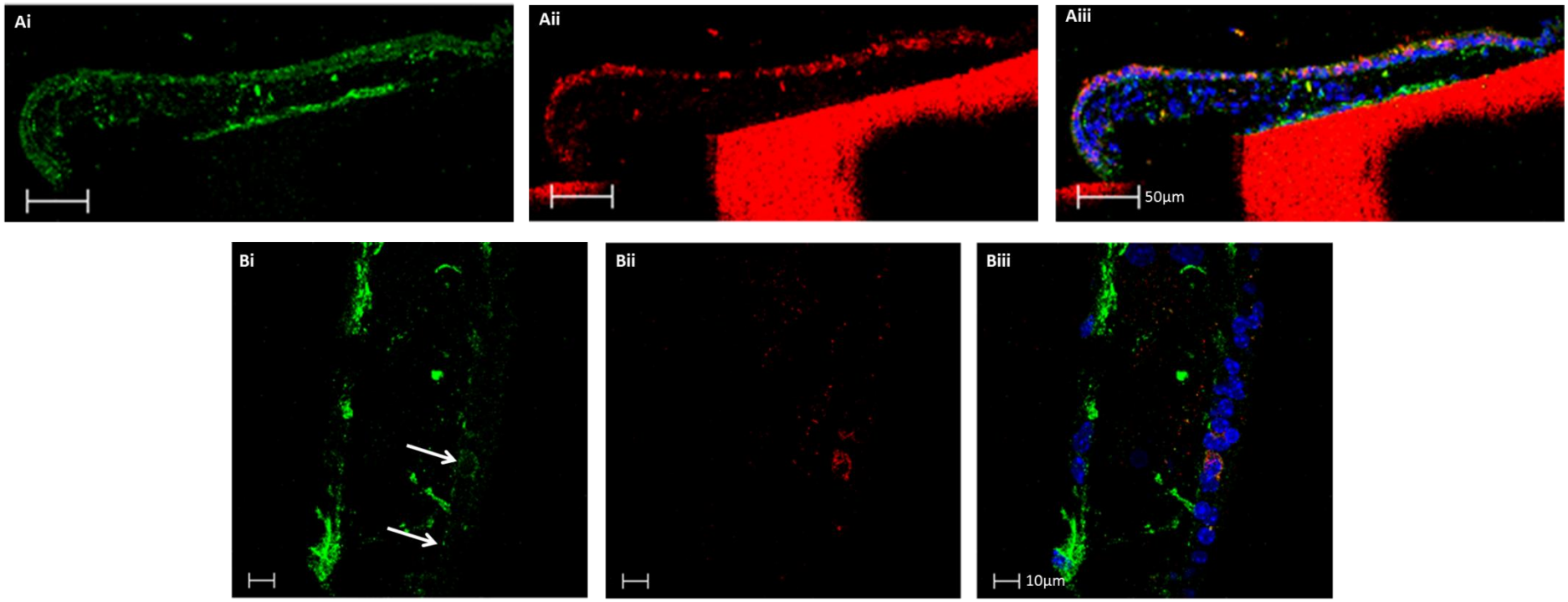

Figure 6-20 Integrin α6 Expression in Utricular Tissue Cultured for 14 Days Post-Gentamicin Treatment

Cryosections of cultured utricular tissue immunolabelled for integrin α6 (green) and myosin Viia (red). DAPI labels cell nuclei blue. (A) Control tissue maintained *in vitro* for 17 days without being treated with aminoglycoside antibiotic. (B) Gentamicin treated tissue following a 14 day recovery period.

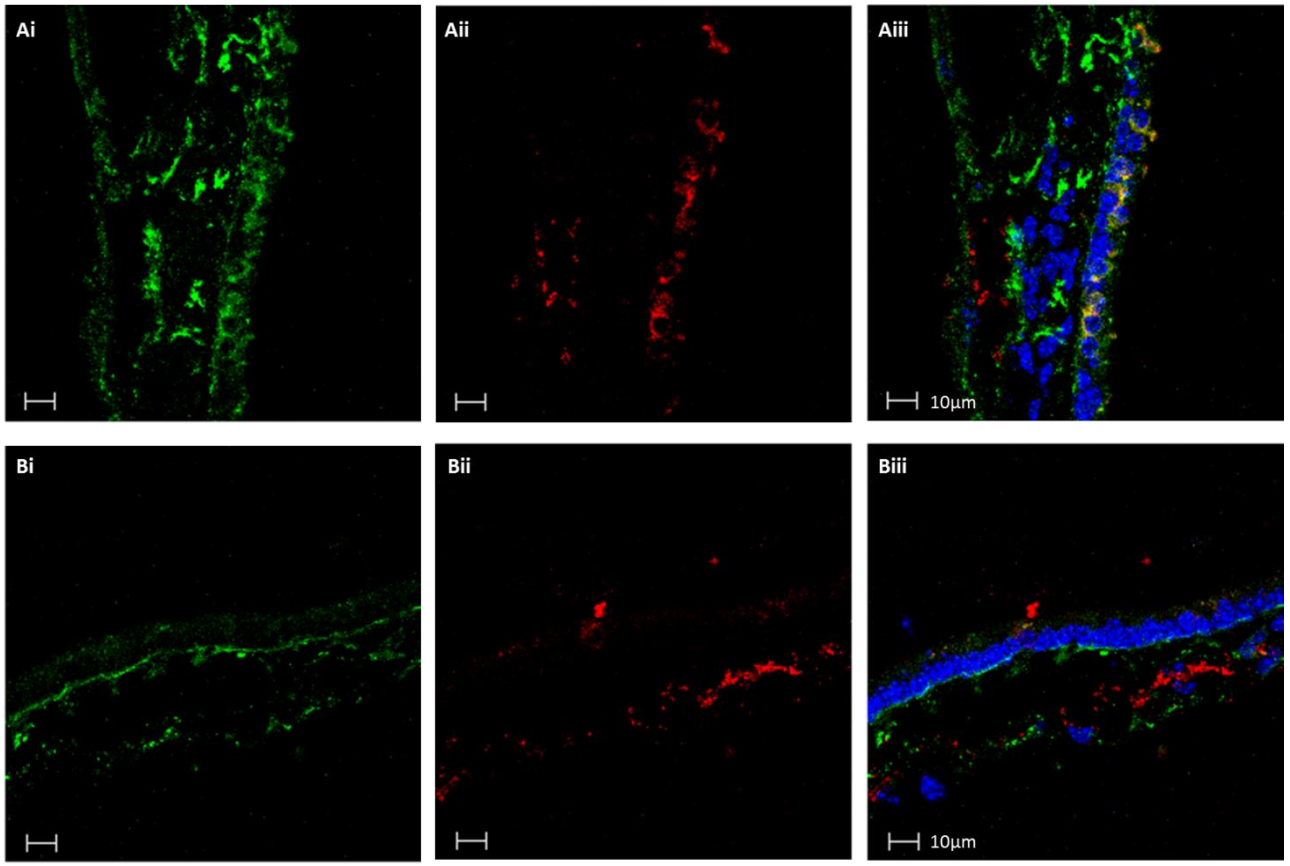

Figure 6-21 Integrin α6 Expression at 21 Days Post-Gentamicin Treatment

Cryosections of cultured utricular tissue immunolabelled for integrin α6 (green) and myosin Viia (red). DAPI labels cell nuclei blue. (A) Control tissue grown *in vitro* for a total of 24 days without receiving 48 hours gentamicin exposure.(B) Gentamicin treated tissue after a 21 day recovery period in culture.

6.5 The Expression of Integrin β3 in the Adult Mouse Utricle

6.5.1 Integrin β3 Expression in the Normal Adult Mouse Utricle

Cryostat sections of mouse skin were used as a positive control tissue in order to determine an appropriate concentration for the use of the integrin β3 primary antibody (BD Biosciences). Phalloidin-FITC (red), used at a 1:1000 dilution, labels muscle fibres within the skin (Figure 6-22 Aii) with the distinctive striated appearance of actin filaments evident in muscle fibres present within this tissue. As was seen with integrin αV, the β3 antibody (green), at a dilution of 1:200, labelled only at the periphery of the muscle cells (Figure 6-22 Ai).

When this primary antibody was used on cryosections of normal mouse utricle, it was generally very difficult to distinguish true β3 (green) positive labelling from widespread background staining (shown in Figure 6-22 B). There does appear (Figure 6-22 C represents the clearest labelling achieved with this antibody, although this result did not prove replicable) to be higher intensity β3 positive labelling in the region of neurons which are positive for calretinin (red). Further attempts to optimise the dilution at which the antibody was used did not prove successful in improving the quality of immunolabelling produced. An alternative β3 primary antibody (Novus Biochemicals) was tested on cryosectioned mouse small intestine to determine an appropriate dilution (Figure 6-23 A). When used to label cryosections of normal mouse utricle, there appeared to be widespread labelling within both the mesenchyme and the sensory epithelium (Figure 6-23 Bi). It was however, possible to observe regions of higher intensity β3 positive labelling within vestibular hair cells (believed to be type I hair cells base upon their shape) in the region of their neural calyces, similar to the labelling shown by integrin β5 (Figure 6-23 Ci).

6.5.2 Integrin β3 Expression in Gentamicin Treated Utricles

Control counterparts of utricles cultured for 4 days post-gentamicin show a similar pattern of integrin β3 labelling as that observed in normal, uncultured utricular tissue (Figure 6-24 Ai). The sensory epithelium is populated with myosin Viia-positive hair cells (Figure 6-24 Aii); integrin β3 is present in the hair cell layer in regions which correspond to the interface between type I hair cells and their neural calyces (Figure 6-

24 Ai). There is also integrin β3 expression within the underlying mesenchyme. Control counterparts of 14 and 21 days post-gentamicin treatment utricles were not able to be carried out with the integrin β3 antibody due to a lack of tissue sections; immunohistochemistry experiments with this antibody were the last in the series of integrins investigated to be carried out.

At 4 days post-gentamicin treatment (Figure 6-24 Bii), myosin Viia-positive hair cell numbers are substantially decreased – there are no hair cells visible in the section shown in this figure, only myosin Viia-positive debris. Integrin β3 labelling in this tissue, in the absence of hair cells, appears to have been redistributed, with integrin β3 expression associated with the supporting cells, suggesting that this integrin may be present at the interface between supporting cells and neurons. As seen with other integrins which localised to the mesenchyme, β3 labelling is present in the underlying connective tissue at 4 days post-gentamicin, but this expression appears more punctate and plaque-like due to the extensive remodelling which occurs in the mesenchyme *in vitro*.

At 14 days post-gentamicin integrin β3 expression appears similar to that observed at 4 days (Figure 8-25 i). The section shown in figure 8-25 lacks myosin-Viia positive hair cells. As seen at 4 days post-gentamicin, in the absence of vestibular hair cells, integrin β3 localises to regions which would correspond with the interface between a neuron and a supporting cell.

By 21 days post-gentamicin, there is evidence which might suggest that integrin β3 is redistributed to the region of neural calyces at type I vestibular hair cells. It is not possible to determine from these immunohistochemistry experiments as to whether the myosin Viia-positive cells visible in figure 8-26 are hair cells which have been regenerated, or are instead hair cells which were able to survive the aminoglycoside treatment. The hair cells labelled with myosin Viia in this utricular section, however, demonstrate integrin β3 labelling which is similar to that observed in normal utricular tissue.

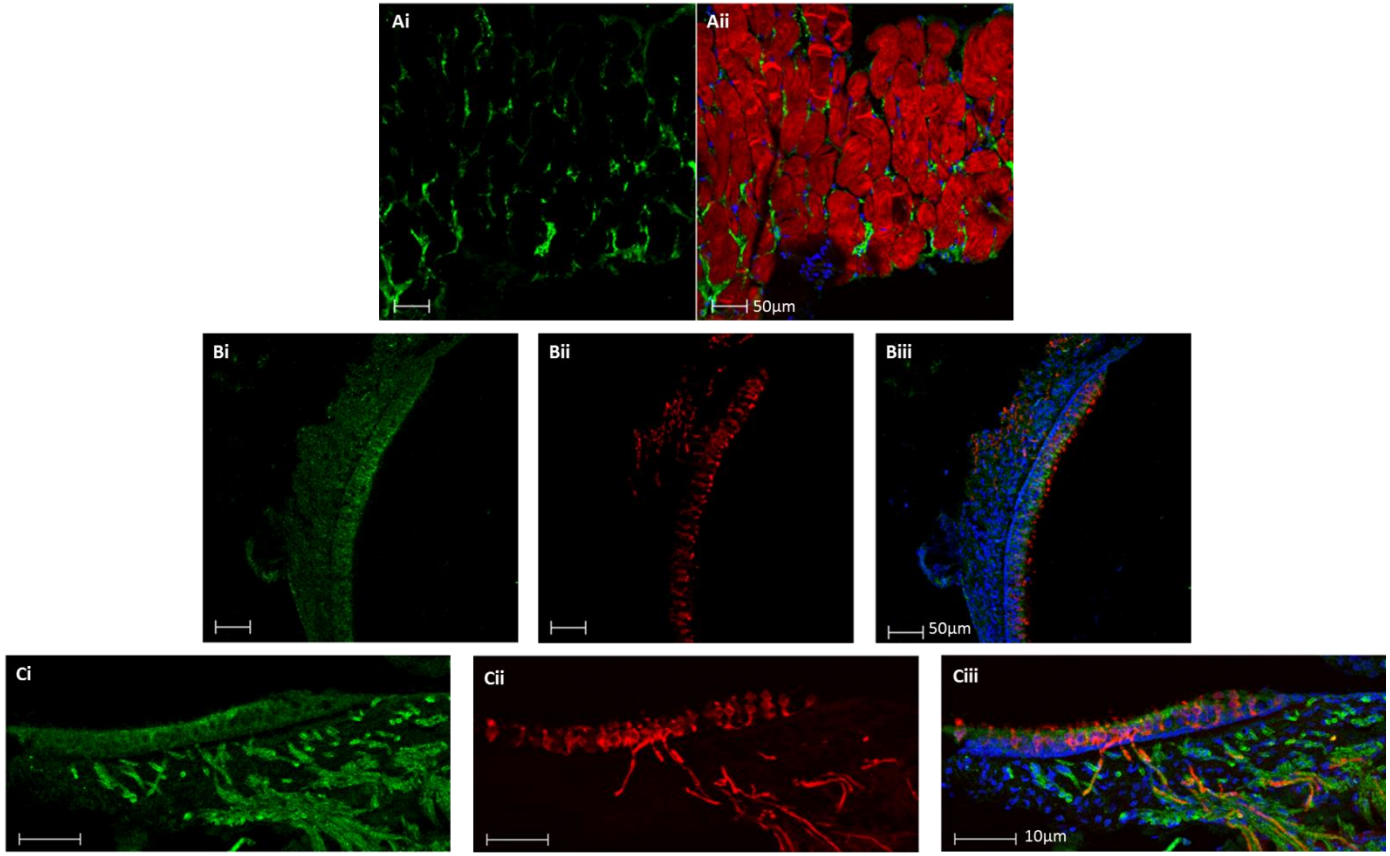

Figure 6-22 Integrin β3 Expression in Skin as a Positive Control Tissue and In the Normal Adult Mouse Utricle

Cryostat sections of mouse tissue immunolabelled with an integrin β3 primary antibody (BD Biosciences). DAPI labels cell nuclei blue.(A) Adult mouse skin was used as a positive control to determine an appropriate concentration for the use of the integrin β3 (green) antibody. Phalloidin-FITC (red) labels actin filaments. (B & C) Normal uncultured adult mouse utricle cryosections labelled for integrin β3 (green) and calretinin (red).

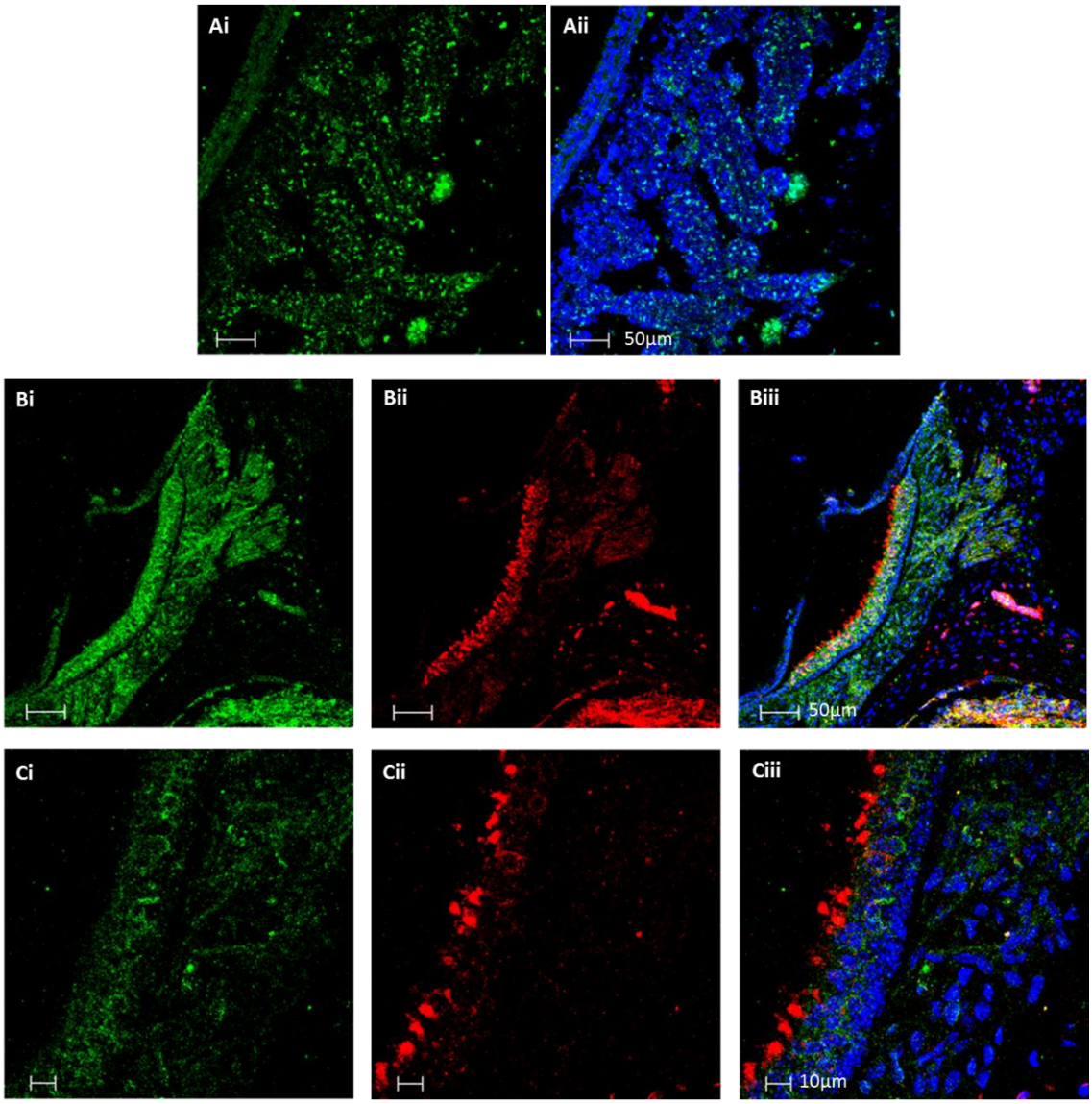

Figure 6-23 Integrin β3 Expression in Positive Control Tissue and the Normal Adult Mouse Utricle

Cryosections of adult mouse tissue were immunolabelled for integrin β3 with an alternative primary antibody (Novus Biochemicals). DAPI labels cell nuclei blue. (A) Mouse small intestine was used as a positive control tissue in order to determine an appropriate concentration at which to use the integrin β3 (green) primary antibody. (B & C) Cryosections of normal, uncultured adult mouse utricle immunolabelled for integrin β3 (green) and myosin Viia (red).

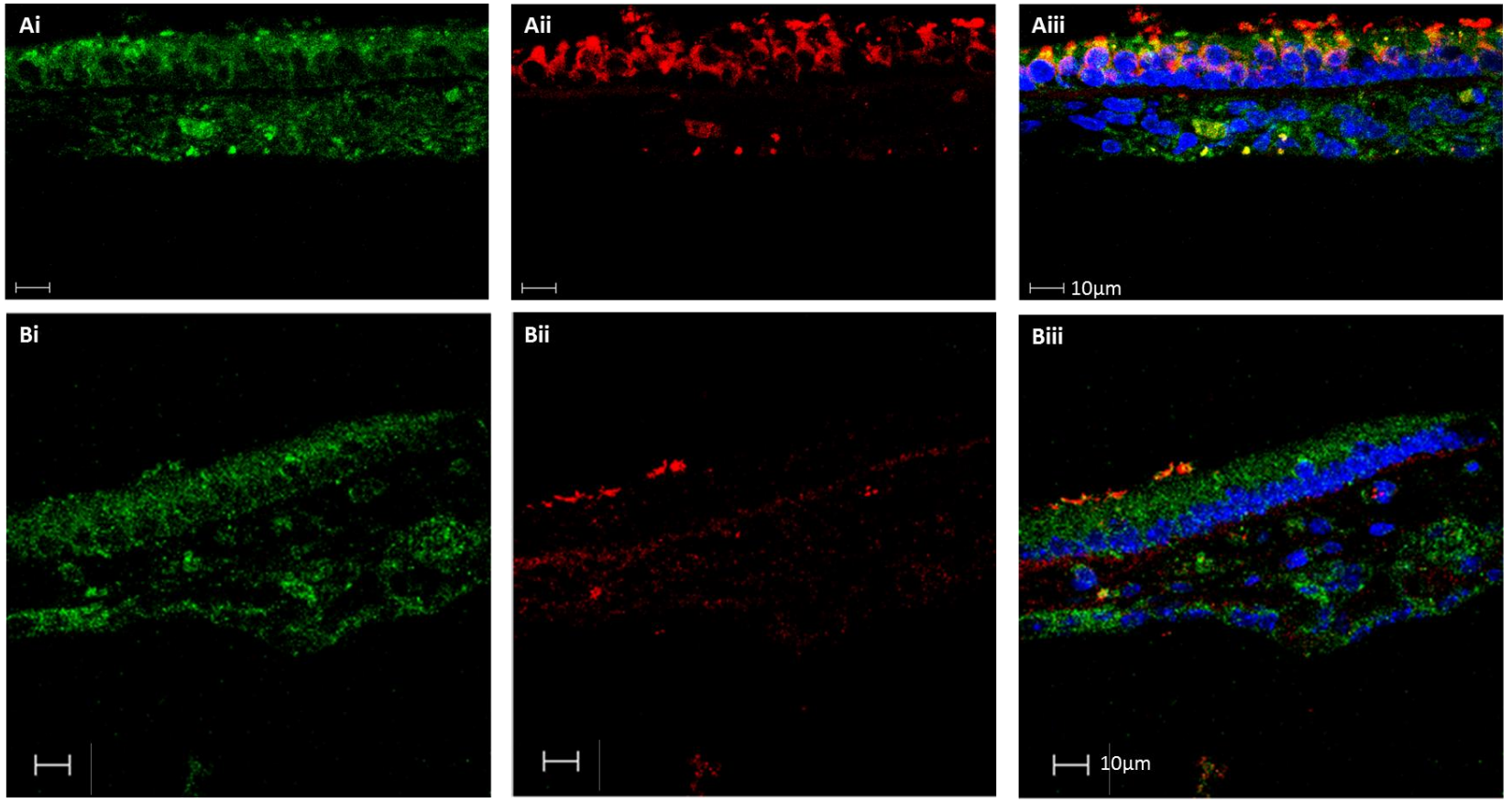

Figure 6-24 Integrin β3 Expression at 4 Days Post-Gentamicin Treatment

Cryosections of cultured utricular tissue immunolabelled for integrin β3 (green) and myosin Viia (red). DAPI labels cell nuclei blue. (A) Control tissue cultured for a total of 7 days without exposure to gentamicin. (B) Gentamicin treated tissue following a 4 day recovery period.

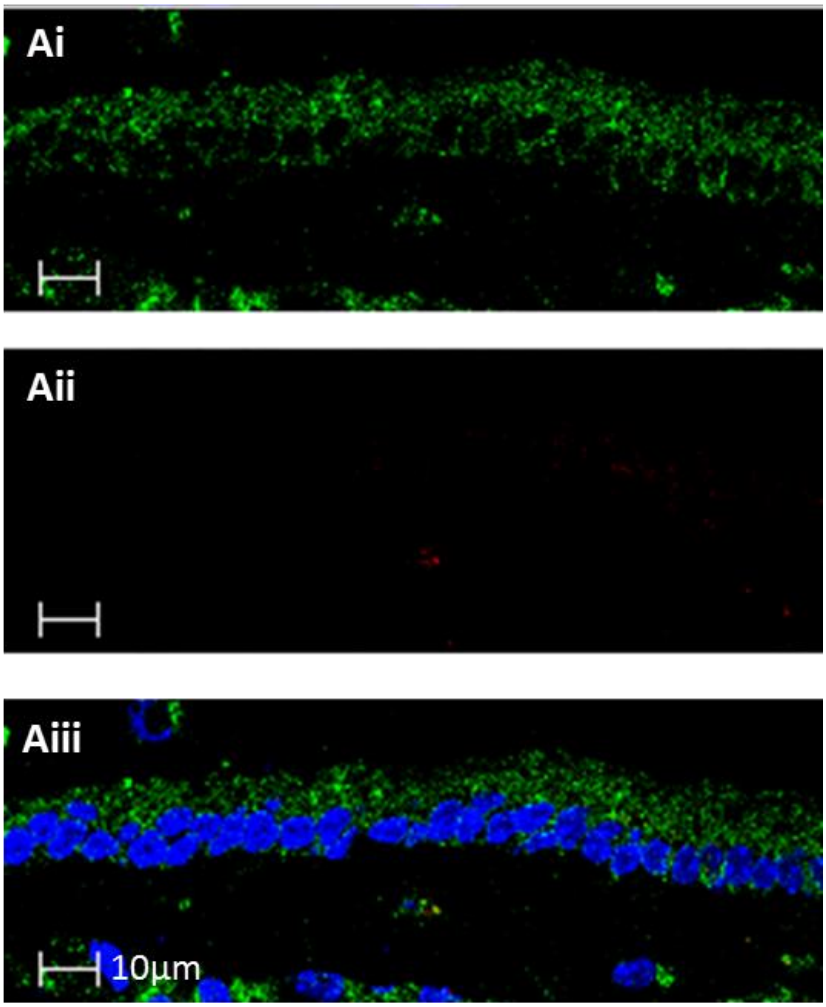

Figure 6-25 Integrin β3 Expression at 14 Days Post-Gentamicin Treatment

Cryosection of utricular tissue immunolabelled for integrin β3 (green) and myosin Viia (red) at 14 days post gentamicin. DAPI labels cell nuclei blue.

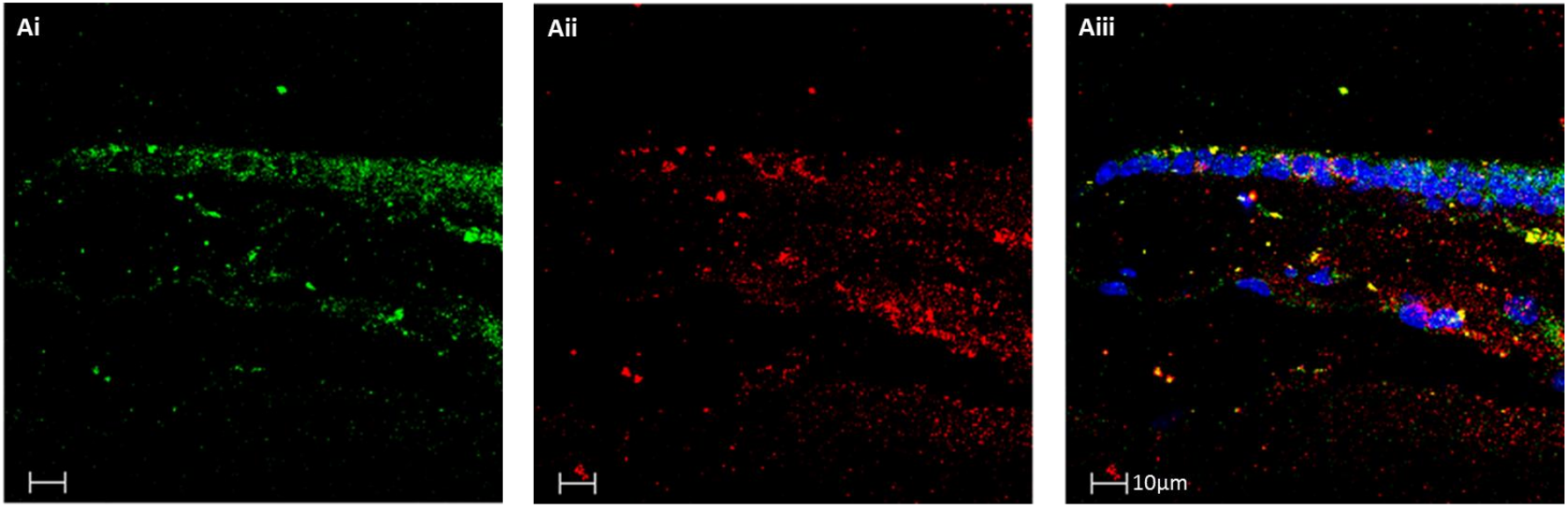

Figure 6-26 Integrin β3 Expression at 21 Days Post-Gentamicin Treatment

Cryosection of utricular tissue at 21 days post gentamicin immunolabelled for integrin β3 (green) and myosin Viia (red). DAPI labels cell nuclei blue.

Chapter 7: Discussion

The experiments carried out during this project represent the first investigation into the expression of members of the integrin family of cell surface adhesion molecules within the adult mouse vestibular system. The data obtained also demonstrates a novel bioinformatics based assessment of the relationships between the alpha and beta integrin subunits in terms of their DNA sequence, which is specific to the mouse model species used.

The mammalian utricle was chosen as the model tissue for this project since it has been established through previous work of this research group as being a sensory epithelium which is capable of some spontaneous regeneration. The structure of this tissue is such that the supporting cells of the sensory epithelium are in contact with the basement membrane which lies between the epithelium and the underlying mesenchymal tissue. Integrins are known to bind several extracellular matrix proteins which are major constituents of basement membranes, forming cellular adhesions between the membrane and cells such as epithelial cells which are in direct contact with it. Vestibular hair cells in the normal mature utricle do not have any contact with the basement membrane since they are surrounded by the supporting cells. However, during spontaneous regeneration following loss of hair cells, where supporting cells have been shown to undergo a phenotypic conversion (Li and Forge, 1997), it is thought necessary for these cells which are to become new hair cells to break their contacts with the basement membrane. This would allow regenerated cells to relocate to the apical layer of the sensory epithelium; previous work has shown cells believed to be undergoing transdifferentiation at several stages in this process of detachment, observing cells with apical bundles which appear immature, in addition to being in contact with the basement membrane by a 'foot-like' process (Li and Forge, 1997). The cellular processes which underlie these events during transdifferentiation would therefore be anticipated to involve integrin cell surface receptors. Additional events that could be suggested as requiring members of the integrin family are the cellular shape changes which occur as supporting cells fill the gaps in the epithelium created by the death of hair cells in order to seal the lesion and maintain the endocochlear potential. Supporting cells nearest utricular lesions have been shown to spread and become more squamous in their morphology (Meyers and Corwin, 2007). Integrins are known to be involved in cell spreading through their interaction with their surroundings via focal adhesion

complexes, in addition to playing a role in the re-organisation of the actin cytoskeleton (Cavalcanti-Adam et al., 2007). This work therefore presents the mouse utricle as a viable inner ear tissue for the study of integrin involvement in the repair and regeneration of the vestibular sensory epithelium.

7.1 *In Vitro* Culture of Adult Mouse Utricular Tissue is a Viable Model System for the Induction of Hair Cell Loss

7.1.1 *In Vitro* Vs *In Vivo*; Limitations of the Adult Mouse Utricular Culture Model

The experimental data presented in chapter 4 illustrates the morphological changes which occur in organotypic adult mouse utricle cultures in response to exposure to the ototoxic aminoglycoside antibiotic gentamicin.

Initial culture experiments were carried out on glass-bottomed Mattek™ dishes coated with laminin. Although utricles survived well on this culture surface, it was deemed unsatisfactory for continued use in the work carried out during this project. Utricles maintained *in vitro* on laminin coated glass showed a tendency to spread and 'grow out' from the original explant with the laminin acting as a substrate. Utricles maintained for longer time periods i.e. 14 days and longer, would prove to be very difficult to remove from the dish at the end of the experiment; in some instances the utricular tissue would appear virtually indistinguishable from the laminin coated glass. Laminin, an extracellular matrix protein is a known ligand for several integrin heterodimers including α3β1, α6β1 and αVβ5 (Belkin and Stepp, 2000). If utricular tissue maintained on a laminin substrate had been used for integrin immunofluorescent labelling, it would be possible that focal adhesion complexes containing one or more of the known laminin-binding integrin heterodimers might form at the base of the connective tissue i.e. the region of the explant in direct contact with the culture substrate. This could potentially have resulted in integrin positive immunofluorescent labelling being visible which is not usually present in the normal tissue. Other previous studies which have carried out utricular culturing have allowed the dissected maculae to be maintained free floating in 24 well plate dishes containing culture medium (Cunningham, 2006). It could be suggested that this method of incubation might be less likely to induce artificial changes in the integrins of the utricular tissue, in particular the mesenchyme, if

the cultured utricles are not adhering to a culture substrate. However, tissue maintained in this manner has a tendency towards the utricle 'curling inwards' on itself at its peripheral regions. This would have implications for the manipulability of the tissue for use in further experiments i.e. cryostat section for immunohistochemistry – tissue which is not flat would be extremely difficult to cut straight, even transverse sections through to provide optimal sections for immunolabelling . With the experimental requirements of the work to be carried out using the utricle culture model system in mind, it was deemed that the use of nitrocellulose filters as a surface on which to maintain explants was best suited to obtaining accurate results whilst preserving the ability to manipulate the tissue after the cessation of growth *in vitro*. It should be taken into consideration that the dissection methods utilised in order to prepare the tissue of interest for *in vitro* incubation are also altering the utricle in a manner that is not encountered *in vivo*. The utricular maculae cultured during this project had the overlying otolithic membrane and otoconia removed during the dissection process; these alterations to the utricle would not occur in an *in vivo* model, and represent an additional deviation of the culture system from the tissue in its natural state which might have the potential to influence the results observed in any studies of utricles maintained *in vitro*.

The results of the immunolabelling experiments on cultured utricular tissue carried out during this study indicate that the tissue of interest, in particular the underlying mesenchyme, undergoes a considerable degree of remodelling and proliferation in response to the *in vitro* experimental conditions. The initial laminin culture substrate used was substituted for nitrocellulose filter paper due to the extent of cellular spreading observed and since laminin is a known ligand for multiple integrin heterodimers; in doing this it was hoped that a potential source of artificial changes to integrin localisation and expression had been removed from the model system. Despite this alteration to the culture technique, it is clear that the mesenchyme which underlies the vestibular epithelium continues to undergo cellular changes which are not representative of or comparable to the tissue *in vivo*. It is therefore possible that the remodelling which occurs in the mesenchymal tissue, particularly that which lies in closest proximity to the basement membrane (a key location within the tissue of interest where integrin expression would be expected), might artificially alter integrin expression levels or localisation patterns in a manner which does not occur naturally *in vivo*.

The immunohistochemistry experiments carried out in this project to investigate potential changes in the localisation pattern of several integrin alpha and beta subunits at several time points following gentamicin exposure were carried out only using the *in vitro* model. Control counterparts for each post-gentamicin time point were also immunolabelled for the integrin subunits investigated, in order to provide a comparison between untreated utricular tissue after a period of time grown in culture, and utricular tissue maintained *in vitro* for the same total length of time, but subjected to 48 hours gentamicin-treatment. However, based on the observation of these experiments, it is not possible rule out whether the results have been influenced by the culture conditions and show localisation patterns which would not be present *in vivo*. The immunohistochemistry experiments presented in this thesis could be repeated *in vivo* to verify the results obtained *in vitro*; this would involve treating adult mice with gentamicin (either systemically or directly into the inner ear.

7.1.2 *In Vitro* Vs *In Vivo* Studies of the Effects of Aminoglycosides on Mammalian Utricular Sensory Hair Cells

7.1.2.1 Gentamicin-Induced Hair Cell Loss

The use of mammalian vestibular sensory epithelia to study changes which occur after hair cell loss induced by aminoglycoside antibiotics has been carried out in numerous previous studies. The work of members of this research group has developed and utilised organotypic utricular cultures as a method for investigating hair cell loss and spontaneous regeneration in the vestibular system, using tissue from several different species including the newt (Taylor and Forge, 2005), and guinea pigs (Forge and Li, 2000). The use of an *in vitro* system in this project in order to study the expression of integrins in a tissue undergoing hair cell loss and spontaneous regeneration therefore represents an original progression of the work established by other members of this research group.

The selection of an *in vitro* model for gentamicin-induced hair cell loss in order to study the effects of this damage and any subsequent spontaneous regeneration on integrin expression was based upon consideration of the benefits and limitations of *in vitro* methods compared to an *in vivo* approach. A key benefit of using an *in vitro* system is

the ability to easily manipulate the environment in which the sensory epithelium is being maintained. During this project, the culture medium in which the tissue of interest was grown was utilised to treat the sensory epithelium with gentamicin at a specific concentration for a given time period and additionally to expose the tissue to EdU in order to investigate cellular proliferation. Manipulation of the external environment to which the sensory epithelium is exposed is far easier with an *in vitro* system, with the culture medium being removed and replaced as required, and drug treatments added at the appropriate dilutions and removed from the culture dish after a specific incubation period has elapsed. This ease of manipulation would also be advantageous for potential future experiments i.e. for administering integrin chemical blockers or blocking antibodies in order to study the effects of integrin inactivation on gentamicin-induced hair cell loss and the regeneration.

An *in vivo* model of gentamicin-induced hair cell loss requires that the aminoglycoside be administered to the animal directly. This may be carried out systemically via subcutaneous injection; requiring repeated injections over an extended time period in order to elicit a damage response – treatment carried out in this manner is not able to induce complete hair cell loss and it is not possible to carry out the drug treatment in a single dose, since this results in systemic toxicity to the animal, particularly in the mouse (Wu et al., 2001). Alternatively, aminoglycosides may be administered *in vivo* via several different surgical methods, including cochlear perfusion and direct application of a gentamicin-soaked pledget via the semi-circular canal or round window. The requirement of an *in vivo* model for repeated injection of an animal or surgery to manipulate experimental conditions is more complex and time consuming than *in vitro* methods; surgery on an animal carries risks that the subject might die as a result of the procedure before the end point of the experiment; additionally, the injection of an animal with a drug treatment results in the 'end point' of drug treatment being less clearly distinguished, due to the potential for the antibiotic to remain present systemically even after cessation of treatment. Additionally, in an *in vivo model*, the damaged sensory epithelium will still be able to receive, and therefore respond to, stimuli and signalling molecules which originate outside of the epithelial and mesenchymal tissue. *In vitro*, the death and degeneration of the neurons which innervate the utricle is observed as the mesenchyme beneath the hair cell and supporting cell

layers undergoes considerable remodelling. Spontaneous regeneration *in vitro* is therefore reliant upon molecular signalling which originates from the remaining mesenchymal tissue and the supporting cells of the sensory epithelium. The cellular spreading and mesenchymal remodelling observed *in vitro* would not occur *in vivo*, and it could be that the changes taking place within this region as a result of being maintained in culture have an effect on the response of the sensory epithelium to aminoglycoside treatment.

A key factor in the considered in the selection of an *in vitro* model over an *in vivo* system is that the underlying cellular mechanisms and pathways by which sensory hair cells die in response to aminoglycoside exposure appear to be the same. Despite variability of the number of hair cells lost from the vestibular epithelia of mammals depending upon the method of aminoglycoside administration and duration of exposure to the ototoxic drug, previous studies have shown that the mechanism of hair cell death is preserved both *in vitro* and *in vivo*.

The entry of ototoxic aminoglycoside antibiotics, has been shown through previous work to involve the mechanotransduction (MET) channels located within hair cell stereocilia. The styryl dye FM1-43 had demonstrated the ability to selectively label sensory hair cells in several different species (Gale et al., 2000; Nishikawa and Sasaki, 1996; Seiler and Nicolson, 1999). Having been shown to enter hair cells via MET channels, FM1-43 uptake by sensory hair cells resulted in these channels being permanently blocked. Pre-treatment of hair cells with FM1-43 prior to exposure to aminoglycosides resulted in a reduction of the damage and hair cell death observed. This finding suggests that aminoglycosides share the same route of entry into hair cells as FM1-43 (Gale et al., 2001; Marcotti et al., 2005).

Exposure of the inner ear to aminoglycosides results in loss of the sensory hair cells in both the auditory and vestibular sensory epithelia. Previous studies have shown that this cell death is apoptotic in nature; occurring both *in vitro* and *in vivo*. Apoptosis, a type of programmed cell death, has distinctive morphological characteristics which include condensation of chromatin within the nucleus, cell shrinkage, ‘blebbing’ of the cell membrane and the formation of apoptotic bodies which may then be removed from the tissue by phagocytosis. Apoptotic hair cell death has been identified through visual

identification of these morphological changes in tissue obtained via an *in vivo* model (Li et al., 1995) , and also using terminal deoxynucleotidyl transferase dUTP nick end labelling (TUNEL) assay to detect apoptotic changes in the DNA of dying hair cells (Lang and Liu, 1997) in the vestibular epithelia of guinea pigs.

Further *in vivo* evidence of apoptotic hair cell death centres on the use of inhibitors of key apoptotic proteins and signalling pathways. Caspases are specialised proteases which when activated are able to cleave proteins linked to cell survival e.g. Bcl-2, as well as contributing to the disassembly of cellular structures and the cytoskeleton (Thornberry and Lazebnik, 1998). Observations made *in vivo* in mammalian (Nakagawa et al., 2003) and avian (Matsui et al., 2003) species, indicate that the effects of aminoglycoside treatment are reduced by administration of the drug simultaneously with a caspase inhibitor; these animals exhibited increased hair cell survival and a reduction in the amount of apoptotic cells detected in both auditory and vestibular sensory epithelia. Similar studies conducted *in vitro* using mouse (Cunningham et al., 2002) and guinea pig (Forge and Li, 2000) vestibular epithelia also showed that aminoglycoside treatment resulted in the activation of multiple caspases, including the upstream caspase-9 and downstream caspase-3, and that incubation of cultures with a caspase inhibitor protected the vestibular epithelium from aminoglycoside-induced hair cell death. It would therefore appear that *in vitro* and *in vivo* models of mammalian hair cell loss induced by aminoglycosides share a common mechanism of cell death via apoptotic pathways. Some evidence suggests there may be other mechanisms involved in *in vivo* responses to ototoxicity; one *in vivo* mouse model of hair cell loss induced by kanamycin, demonstrated a lack of classic apoptosis markers and instead other molecules such as calpains, were detected – these proteases are involved in both apoptotic and necrotic cell death (Jiang et al., 2006). It is clear that whilst there are similarities in the response of inner ear sensory epithelia to ototoxic drugs and the way in which hair cells die *in vitro* in comparison to *in vivo*, there may also be differences that have consequences for results obtained using *in vitro* model systems.

7.1.2.2 Similarities of the Adult Mouse Utricle *In Vitro* Model to Previous Studies

The response of adult mouse utricles to gentamicin treatment over an *in vitro* recovery period of 21 days described in this work is similar temporally and spatially to previous

studies of regeneration of the mammalian vestibular epithelium in mouse (Lin et al., 2011) and guinea pig (Forge et al., 1993; Warchol et al., 1993). Relatively few previous studies have maintained murine utricular tissue *in vitro* long term; utricular tissue was cultured for 21 to 28 days used utricles from early postnatal rats (Berggren et al., 2003; Werner et al., 2012). The culture experiments in this work present the adult mouse utricle as a tissue which is able to be maintained for up to 28 days *in vitro* whilst supporting the survival of sensory hair cells; mean hair cell counts of control utricles after 5 and 31 days *in vitro* showed no statistically significant difference. Hair cell loss in these utricular cultures (Figure 4-4) occurs soon after gentamicin exposure. By 4 days post-treatment, hair cell numbers in the sensory epithelium are reduced in comparison to control counterparts cultured in parallel. Aminoglycoside treatment *in vitro* does not induce a complete loss of hair cells (Figure 4-6 and 4-7); the decrease in hair cell numbers compared to control utricles maintained in vitro for 5 days was not found to be statistically significant at 2 days post-gentamicin, but was significant both at 14 and 28 days.

FITC-phalloidin labelling of also reveals that some cells which remain positive for a hair cell marker (calretinin or myosin Viia) do not possess an apical stereociliary bundle. This occurs in tissue treated with ototoxic drugs and in control counterparts. Utricular cultures examined by transmission electron microscopy (Figure 4-2) also display evidence of hair cell bodies within the sensory epithelial layer which lack an apical hair bundle. Previous studies using the Organ of Corti (Sobkowicz et al., 1996) report the presence of auditory hair cells which remained following physical injury *in vitro*. In this instance, hair cells which did not die, yet which did not exhibit a stereociliary bundle, were often found to have been ‘covered over’ by the expansion of supporting cells to seal the breach in the epithelium following damage. This observation of supporting cell spreading is again, the kind of cellular shape change process in which it might be expected cell adhesion molecules like the integrin family to be involved. Scanning electron microscopy also shows evidence of stereocilia degeneration. At 5 days post-gentamicin (Figure 4-13) examples of disorganised apical hair bundles can be seen on the epithelial surface. There are also stereociliary bundles present which have become fused; some of these bundles appear to have aggregated all of the filamentous actin from their stereocilia into one large projection. Disorganised stereocilia are also

observed in these utricular cultures at 14 days post-gentamicin treatment (Figure 4-16). Previous studies of the effect of aminoglycoside antibiotics on the mammalian vestibular epithelia (Forge and Li, 2000) have also observed these features of apical hair bundles under such experimental conditions.

Scar formation as previously reported at the sites of hair cell loss (Meiteles and Raphael, 1994) in the mammalian utricle, is present in gentamicin treated utricular tissue at each of the time points investigated, from 4 to 28 days post-gentamicin exposure. Supporting cells have also been previously shown to engulf and phagocytose dying hair cells (Bird et al., 2010) in chick utricles when treated with aminoglycosides. Integrins have been documented as being mediators of phagocytosis via both inside-out and outside-in signalling cascades which are able to trigger re-modelling of the actin cytoskeleton (Dupuy and Caron, 2008). Integrins αVβ5 and αVβ3 (all three constituent subunits of which have been detected during this project in normal mouse utricular tissue) have been described as being involved in the phagocytosis of apoptotic cells; αVβ5 has been shown to be involved in phagocytosis carried out by non-professional phagocytes such as retinal pigmented epithelial cells (Finnemann et al., 1997). It is therefore possible that integrins might play a role in facilitating the phagocytosis of apoptotic hair cells in the vestibular epithelium.

The reduction in hair cell numbers, stereociliary degeneration and scar formation observed in this study as a response to aminoglycoside treatment supports the idea that this *in vitro* model system responds in a manner which resembles hair cell loss *in vivo* in the vestibular epithelium. These findings support the use of an organotypic culture model in order to study the role of integrins in the mammalian vestibular system. If hair cells are dying and the supporting cells are undergoing morphological changes in order to maintain the integrity of the epithelial barrier, then there may be changes occurring in terms of the expression and localisation of members of the integrin family of proteins.

7.1.3 Regenerative Capacity Following Gentamicin-Induced Hair Cell Loss

Several non-mammalian vertebrate species have been shown to possess the ability to regenerate lost auditory and vestibular hair cells, including amphibians (Baird et al., 1993; Taylor and Forge, 2005) and birds (Corwin and Cotanche, 1988; Cotanche, 1987) following both acoustic trauma and insult by ototoxic drug exposure. It has also been

established that in the avian vestibular epithelium, there is a continual turnover of vestibular hair cells, with on-going regeneration in response to the losses which occur naturally over time (Jorgensen and Mathiesen, 1988). The mammalian vestibular system possesses a limited ability to regenerate hair cells following aminoglycoside treatment or the physical creation of a lesion in the tissue. Previous work on the mouse utricle has documented the appearance of apparently regenerated vestibular hair cells with immature, embryonic-like apical bundles (Kawamoto et al., 2009; Lin et al., 2011). The appearance of these immature hair cell-like cells began to occur at between 14 to 21 days after treatment with an aminoglycoside. The bundles then continued to elongate and acquire more mature morphological features e.g. tip-links between stereocilia. In this work, immature bundles did not become evident until 21 days post-gentamicin treatment; in order to determine an exact time point at which these structures start to emerge it would be necessary to examine organotypic cultures at time points between 14 and 21 days post-gentamicin.

Previous work on the utricular maculae of adult guinea pigs (Forge et al., 1993) observed the appearance of immature embryonic-like bundles by scanning electron microscopy which appear very similar in morphology to that observed on adult mouse utricles maintained *in vitro* for 14 days after ototoxic drug treatment (Figure 4-18). The immature bundles observed consist of short stereocilia which are all of an approximately similar length. The stereocilia are grouped very closely together and although they are not overtly dissimilar in length to the microvilli which cover the apices of the supporting cells surrounding them, they are easily distinguishable by their 'organised' appearance. What appear to be new stereocilia are also visible in utricles at 28 days post-gentamicin labelled with FITC-phalloidin (Figure 4-7). It may be possible to observe similar new bundles on utricles cultured for 14 days post-gentamicin (Figure 4-6), however they are fewer in number and the bundle shorter and therefore less apparent than those seen at 28 days post-gentamicin.

The use of mitotic trackers such as bromodeoxyuridine (BrdU) and tritiated thymidine in both *in vitro* and *in vivo* models of aminoglycoside-induced hair cell death in the mammalian vestibular system has been carried out in order to investigate whether cellular proliferation is responsible for the partial repopulation and regeneration of the utricle seen in this tissue. This project utilised EdU (a nucleoside analog which is an

alternative to BrdU) in order to investigate the proliferative events occurring in the *in vitro* culture model developed. Examination of cultured utricles incubated with EdU at 21 days post-gentamicin did not detect the presence of any cells co-labelled for both myosin Viia and EdU, which is reminiscent of the findings of previous studies that regenerated hair cells were produced by phenotypic conversion of supporting cells and not mitotically; EdU-positive cells were visible predominantly at the level of the underlying utricular mesenchyme.

The results presented in this thesis suggest that the *in vitro* adult mouse utricle model studied does possess some capacity to regenerate vestibular hair cells following gentamicin-induced hair cell loss.

7.3 Integrin Expression in the Adult Mouse Utricle: A Potential Role for Integrins in the Mammalian Vestibular System

The presence of the integrin family of cell surface glycoproteins within the inner ear has only been explored in a few previous studies (Davies, 2007; Davies and Holley, 2002; Littlewood Evans and Muller, 2000). This work presents evidence of the presence of multiple integrin α and β subunits in the adult murine utricle using a combination of RT and quantitative PCR. This cohort of integrins represents the subunits expressed by a number of different cell types, since the tissue from which cDNA was extracted contained mesenchyme, endothelium and other cell types in addition to the cells of the sensory epithelium. Relative quantification analysis of an initial qPCR-based screen of the tissue of interest suggests that some integrin subunits appear to be undergoing a change in their level of expression in response to damage and hair cell loss induced in by treatment with gentamicin *in vitro*. Immunofluorescent labelling of both normal and gentamicin treated utricular tissue has allowed the localisation of some of the integrins identified as being present in the tissue of interest to be investigated and for any changes in integrin distribution to be detected.

Since this work has identified as many as 11 integrins as being present in the adult murine utricle in its normal state, in this discussion, integrins which have been previously identified in the inner ear as well as those which have been described in earlier studies as being involved in tissue repair in other model systems, are focussed on, in addition to those identified as showing significant expression level changes.

7.3.1 Integrin Immunohistochemistry

During this project, primary antibodies raised against 5 different murine integrin subunits were used to label utricular sections, initially using tissue processed directly after dissection from normal adult mice, in order to visualise their expression pattern in the utricle in its normal state. These experiments observed the localisation of integrins at the basement membrane, to structures such as blood capillaries within the underlying mesenchyme, and in some cases the hair cells of the vestibular sensory epithelium. The localisation of each of the five integrin subunits examined is summarised in figure 7-1.

Utricular sections of organotypic cultures maintained for 4, 14 and 21 days post-gentamicin were also immunolabelled for α6, αV, β1, β3 and β5 in order to establish

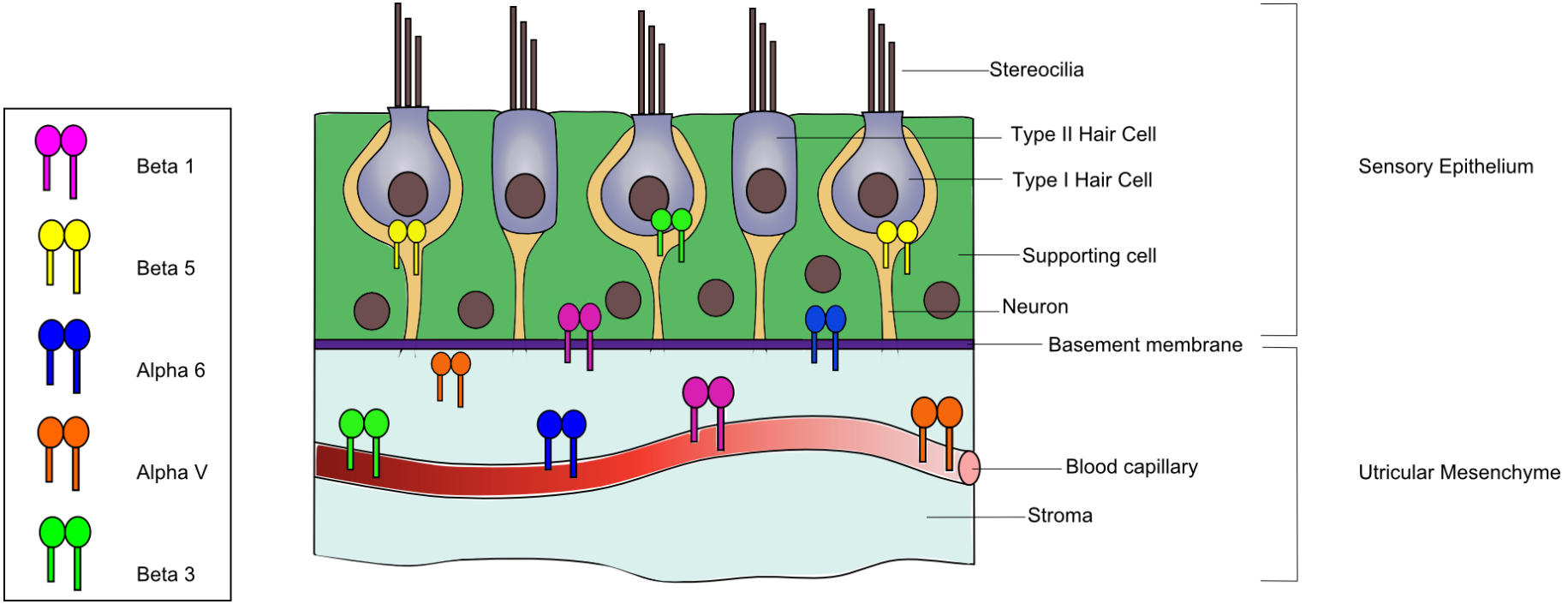

Figure 7-1 Integrin Expression in the Normal Adult Mouse Utricle

A summary of the integrin expression found in the normal, undamaged adult mouse utricle during this project through immunolabelling of utricular sections for five different α and β subunits. Integrins are present throughout the different structures of the tissue including the sensory epithelium, basement membrane and the underlying mesenchyme. Further work would be necessary to establish the α and β partners of each subunit detected and confirm which functional integrin heterodimers are present in this tissue.

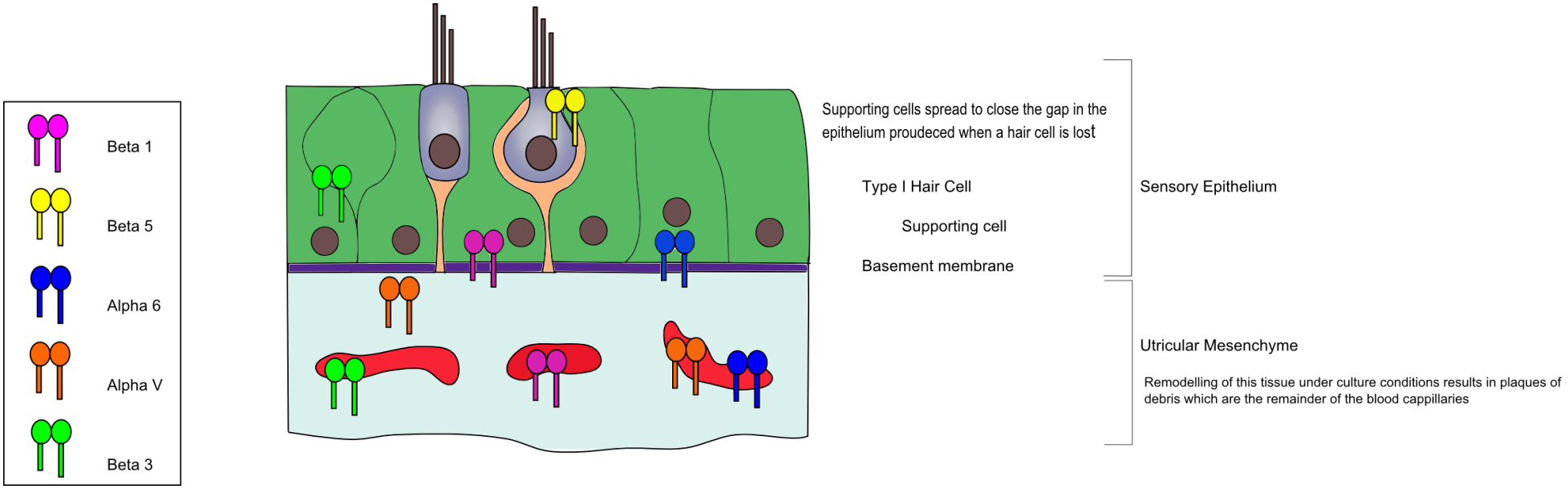

Figure 7-2 Integrin Expression at 4 Days Post-Gentamicin in Adult Mouse Utricles Maintained In Vitro

At 4 days post-gentamicin, the *in vitro* model of the response of adult mouse utricular tissue to the ototoxic aminoglycoside gentamicin shows a decrease in the number of vestibular hair cells labelled with myosin Viia. Integrin immunohistochemistry experiments suggest that expression of integrin β1 and α6 at the epithelial-basement membrane border remains unchanged from that observed in normal tissue, as does the localisation of integrin αV to the mesenchyme directly beneath the sensory epithelium. The structures of the mesenchyme i.e. blood vessels which expressed four integrin subunits in normal tissue, were labelled in a more 'plaque-like' manner, due to the remodelling of this region exhibited by tissue maintained in culture. Of the two integrins believed to be localised to vestibular hair cells in normal, undamaged utricles, β3 appeared to associate with regions of supporting cells where there had been an interface with a neuron, whilst β5 accumulated at the apical surface of the epithelium in response to the loss of hair cells.

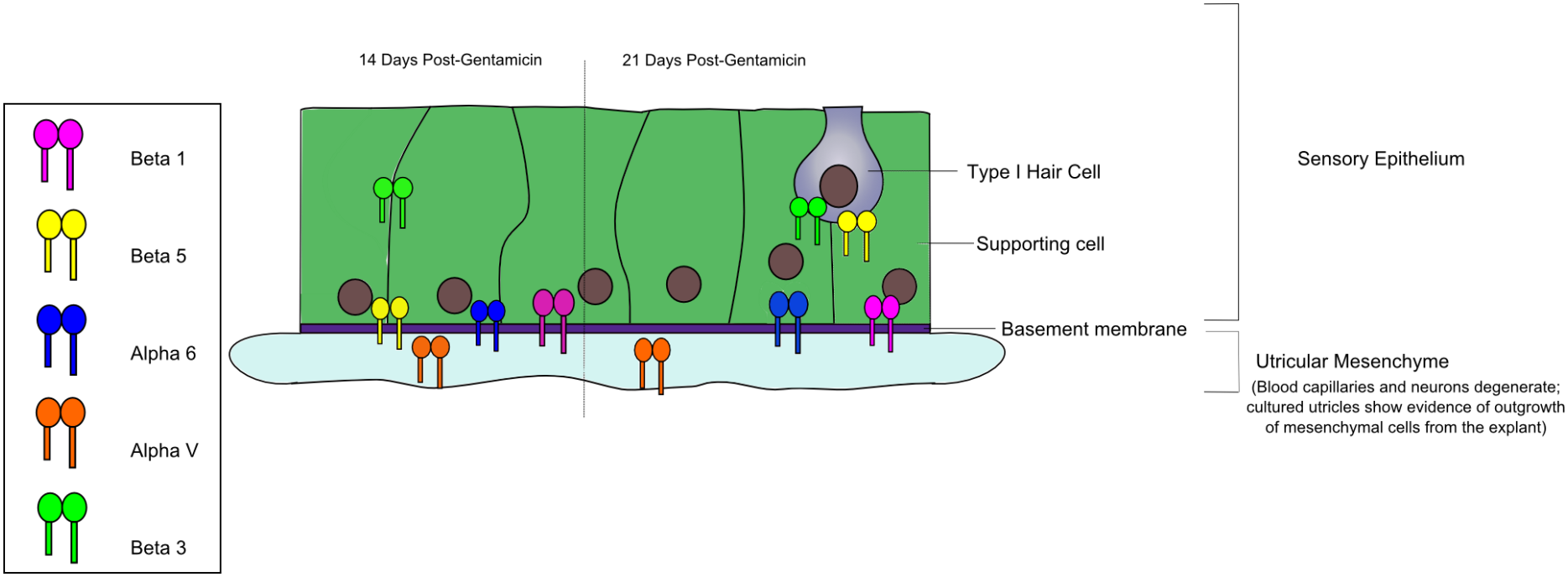

Figure 7-3 Integrin Expression at 14 and 21 Days Post-Gentamicin in Adult Mouse Utricles Maintained *In Vitro*

Based upon immunohistochemistry experiments on cultured tissue, the expression of integrin β1 an α6 at the epithelial-basement membrane border appears to persist at both 14 and 21 days post-gentamicin, as does the localisation of αV in the mesenchyme which lies directly beneath the basement membrane; the mesenchyme has undergone considerable remodelling by these time points and is very thin, therefore integrin labelling in this region also appears to have been lost with the disappearance of structures such as blood capillaries. At 14 days post-gentamicin, β3 remains associated with supporting cells, whilst β5 appeared to be redistributed to the basement membrane; by 21 days post-gentamicin, both β3 and β5 were observed at the interface between vestibular hair cells and the region where neural calyx interfaces would be expected in normal tissue.

whether their localisation was altered in response to hair cell loss. The majority of these subunits did not show any changes in their localisation pattern i.e. β1 expression was detected at the basement membrane across all three of the time points studied. Where integrins were detected in the underlying mesenchyme and the structures associated with this region of the tissue, there was loss of integrin expression, however this was attributed to the fact that the mesenchyme undergoes considerable degradation and remodelling whilst *in vitro*. Utricular cultures were observed to become thin and flattened during the course of the culture time period, as the mesenchymal cells migrated away from the sensory epithelium. The localisation of each of the integrin subunits investigated during this project across the three time points post-gentamicin studied is summarised in figures 7-2 and 7-3.

7.3.1.1 Limitations of Immunohistochemistry for the Detection of Utricular Integrins

Whilst the degenerate and quantitative PCR molecular biology techniques utilised in this project have the ability to detect the expression of integrin subunit genes within a given cDNA sample, they do not provide information as to the presence or location of translated integrin proteins within the adult mouse utricle. The cDNA samples used for PCR experiments in this work were obtained from the entire utricular sensory epithelium and its underlying mesenchyme; any integrin gene expression detected could therefore be attributed to any of a number of different cell types found within this tissue. Immunohistochemistry allows a protein of interest to be detected within a tissue sample, providing qualitative information regarding its localisation to a particular region or cell type.

This project investigated the expression pattern of five integrin subunits which had been positively detected by degenerate and quantitative PCR. Of the integrin antibodies used in this study, the integrin β1 and α6 antibodies could be described as providing the best quality immunolabelling of utricular cryosections i.e. showed the lowest level of background staining in conjunction with strong positive labelling. The immunohistochemistry experiments presented in this thesis encountered problems with excessive levels of background staining with some of the antibodies used. Background labelling may have a number of causes; these include non-specific binding of the

primary or secondary antibodies during incubation, hydrophobic protein interactions, cross-reactivity of secondary antibodies and the level of efficiency and epitope affinity of the primary antibody used. High levels of background labelling can obscure the 'true' signal, making it difficult to interpret the results of these qualitative experiments as what is background and what is positive labelling of the intended antigen is subjective to the visual interpretation of each individual observer. Background labelling can be reduced through the use of serum, as part of blocking solution during the experimental protocol, utilising the ability of the large serum proteins to 'block' sites within the tissue which would be potential sources of non-specific antibody binding. The use, however of both serum and L-lysine (an amino acid) as the blocking strategy for the immunohistochemistry experiments carried out during this project did not sufficiently reduce the background labelling observed for some of the integrin antibodies tested.

The labelling produced by the integrin αV antibody used in this study was improved by the use of a tyramide signal amplification (TSA) kit. This system allows for increased sensitivity (which may be of benefit where antigens are present at lower levels that might not be detected efficiently using a typical immunolabelling protocol, and which would also be masked by excess background staining). The nature of the tyramide radicals produced using the TSA system means that the signal enhancement it provides is restricted to regions in very close proximity to the sites of initial primary antibody binding; this attribute allowed the tendency for integrin αV to be localised to the mesenchyme directly beneath the basement membrane and within blood capillaries to be distinguished above the background labelling experienced. The results obtained with this integrin antibody are still limited by the level of background staining and could be subject to further analysis in order to determine the cause of this background in order to reduce or eliminate this problem. The use of negative control experiments, where the primary antibody is not used during the first incubation stage, would establish whether background staining could be attributed to non-specific binding or cross reactivity of the secondary antibody used. The affinity of the primary antibody for the intended epitope alone is also a potential cause of background staining. If a primary antibody shows affinity for other similar epitopes within other proteins, then the resulting immunolabelling experiments will not be specific for the protein e.g. integrin αV, which is being investigated. One method of confirming antibody specificity is via a peptide

competition assay; the primary antibody is incubated with an excess of the peptide which it was intended to recognise, resulting in the antibody being 'blocked.' Immunohistochemistry experiments may then be carried out, comparing the staining observed when sections of the tissue of interest are incubated with the normal primary antibody to that observed with the blocked antibody solution. Successfully block primary antibodies within the blocked solution which are specific for the intended recognition epitope will be unable to bind and label this epitope within the tissue sample, therefore, any labelling observed with the normal primary which is not present

Immunohistochemistry experiments used to investigate the expression pattern of integrin β3 utilised two different antibodies. The initial antibody used (CD61 monoclonal, BD Biosciences) produced a significant amount of background staining which made it impossible to distinguish the true signal from antibody bound to the correct epitope, which was not reduced despite the testing of serial dilutions of the primary and secondary antibodies. There did appear to be higher intensity labelling in the region of the neuronal structures within the underlying mesenchyme of normal utricles with this antibody. A second β3 antibody (polyclonal, Novus Biologicals) was therefore utilised in order to determine whether the background staining was attributable to the affinity of the antibody tested initially. This β3 antibody also showed neural localisation in normal, undamaged utricular tissue similar to that observed with the monoclonal β3 antibody, but also exhibited labelling which appeared to correspond with regions of type I hair cells in closest proximity to their neural calyces. That the two β3 antibodies tested show differences in their immunolabelling may be due to the different characteristics of monoclonal and polyclonal antibodies; polyclonal antibodies are more likely to produce non-specific binding, since they can recognise multiple epitopes on the target antigen. Correspondingly, the labelling shown by a monoclonal antibody can be affected as a result of these antibodies only recognising a single epitope – they can be 'too specific' and their binding efficiency may be adversely affected by the epitope they recognise being inaccessible due the conformational state of the protein. The immunogen of the polyclonal (Novus Biologicals) β3 antibody was within the C-terminal region of the integrin peptide; the supplier of the monoclonal β3 antibody (BD Biosciences) was not able to provide information on which region of the integrin peptide this antibody recognises, therefore differences in labelling exhibited by these

two antibodies may be as a result of a difference in accessibility of the epitopes they are able to recognise. Additional factors which may affect how well a primary antibody binds include the abundance of the antigen in the tissue studied i.e. antibodies against proteins expressed at low levels would likely require higher antibody dilutions to be used (which would carry the risk of causing an increase in the level of background staining) and the potential for the fixation process, in this case paraformaldehyde, to damage protein epitopes within the tissue sample.

The immunohistochemistry results presented here, in particular the labelling observed for integrin αV and β3, may be limited by some of the common difficulties encountered when carrying out these types of histological experiment. It must therefore be acknowledged that further work in order to reduce the level of background staining encountered would be beneficial and would improve the quality and reliability of the detection of these target antigens within the adult mouse utricle. Similar histology labelling techniques might also be carried out in order to obtain further information about expression patterns of integrins in the utricle i.e. in situ hybridisation of integrin subunits could be used to investigate whether mRNA distribution of these integrins corresponds to protein expression detected by immunohistochemistry.

7.3.2 Integrin Subunits Detected in the Normal Undamaged Adult Mouse Utricle

In this project, two PCR based approaches have been utilised, in addition to immunohistochemistry experiments, in order to identify which of the integrin α and β subunits are present in the tissue of interest in its normal, undamaged state. An initial screen of cDNA from the adult murine utricle was carried out by RT-PCR using a set of degenerate PCR primers, which detected the presence of a group of 5 subunits; α4, α9, β1, β5 and β8. The use of specific primers added a further 3 subunits to this group; α6, αV and β3.

A set of qPCR experiments required a ‘calibrator’ sample in order to carry out a relative quantification (RQ) study, using customised integrin gene expression array plates to investigate whether the expression level of integrins is altered in response to gentamicin-induced hair cell loss. This was achieved by running one array plate with cDNA from normal, uncultured utricles and thus provided an additional ‘screen’ of the tissue of interest in its undamaged state. The use of this sample as a calibrator allowed

the RQ study to investigate changes in integrin gene expression in comparison to the level present in normal tissue. The results of this qPCR study also indicate that β1, β5, β8, α6, αV and β3 (as identified by RT-PCR) are present in the normal mouse utricle. An additional 5 subunits; α3, α8, β4, β6 and β7 are also indicated as being expressed in this tissue. Of these subunits, antibodies against integrins β1, β3, β5, αV and α6 were successfully used to investigate the localisation of a subset of the integrin subunits detected in normal utricular tissue by PCR. It would be of interest to carry out similar immunohistochemistry experiments with antibodies against the remaining subunits detected by PCR in order to learn more about which region of this tissue, which contains a number of different and often highly specialised cell types, they are expressed within.

PCR-based methods using normal, uncultured utricular tissue cDNA have indicated the presence of 11 different integrin subunits in the utricle of the adult mouse. Since the tissue from which this cDNA sample was obtained consisted of the sensory epithelium (i.e. hair cells and supporting cells) and the underlying mesenchyme of the utricular macula, which would include the vasculature of this vestibular organ, in addition to some of the neurons which innervate this tissue, that as many as 11 integrins were detected is not surprising. It is highly likely that some of these integrins are restricted in their expression to one particular cell type i.e. endothelial cells, rather than being associated with the sensory epithelium directly. Immunolabelling of the tissue of interest with antibodies against some of the integrin subunits detected by molecular methods has provided additional information about the localisation of these proteins to particular regions of the utricle and these observations may be utilised in conjunction with degenerate and qPCR data in order to discuss potential functional roles for some of these integrins. As stated earlier in this chapter, the *in vitro* model of utricular response to gentamicin exposure is affected by the culture conditions in some aspects; the underlying mesenchymal tissue degrades and reduces in mass due to cellular migration away from the epithelium the longer the utricle is maintained *in vitro*. The utricular mesenchyme would not undergo the same reduction or remodelling in an *in vivo* mouse model. Integrins which may be present exclusively within the utricular mesenchyme might therefore still play a role in the cellular events triggered by damage to the sensory epithelium *in vivo*.

Two α subunits identified as being present by degenerate RT-PCR (and additionally confirmed by DNA sequencing), α4 and α9, were determined based on the analysis criteria described in chapter 5 as not being detected in the normal utricle by qPCR. The raw data from the '0 day' (normal, uncultured utricular tissue cDNA) gene expression array plate shows that α4 was only detected by one of the four replicate assays in normal utricular cDNA and α9 detected by two of the four replicates.

The discrepancy between these two PCR experiments over whether α4 and α9 are present in the tissue of interest may be due to the fact that the degenerate RT-PCR and the qPCR integrin assay were carried out using different cDNA samples. Yields of cDNA reverse transcribed from RNA extracted from pooled utricles (10 utricles dissected from 5 individual animals) were low in comparison to the amount of cDNA obtained from positive control tissues. Positive control tissue processed according to the RNeasy protocol, used 30mg of tissue; 10 utricles could not constitute anywhere near the same weight or number of cells. With the amount available it was not possible to use the same cDNA sample for the normal control qPCR array plate (which required a large volume of cDNA in order to distribute the sample across 96 wells) as had been used for the degenerate PCR experiments. It is therefore possible that integrin α4 and α9 were present in the cDNA sample used with the degenerate primers, but not in the second sample which was used for qPCR. If these experiments were repeated, it would be crucial to collect a greater number of cultured utricles at each time point in order to prevent the amount of cDNA being a limiting factor.

Integrin α4 is generally considered to be a leucocyte specific integrin subunit and is found in two known heterodimers; α4β1 and α4β7. Integrin α4β1 is able to interact with vascular cell adhesion molecule 1 (VCAM-1) and the endothelium in order to mediate the extravasation and trafficking of leucocytes during the inflammatory response (Postigo et al., 1993). Integrin α4β7 is described as having a similar role in terms of interaction with the endothelium (Berlin et al., 1995) but it has also been implicated as having a role in the recruitment of leucocytes specifically to gastrointestinal lymphoid tissue i.e. Peyer's patches (Ruegg et al., 1992).

Integrin α9 associates with only one of the β integrin subunits, to form the α9β1 heterodimer. This integrin has recently been implicated as having a key role in the

development of lymphatic valves (Bazigou et al., 2009). Earlier studies when this subunit was first discovered show that it is expressed in smooth and skeletal muscle in certain tissues, as well as within some epithelia e.g. airway epithelia and squamous epithelia, at cell-cell and cell-basement membrane contacts (Palmer et al., 1993). Although phylogenetic studies class α9 as being most closely related to the α4 subunit, α9 has only been described as being expressed on polymorphonuclear leucocytes (neutrophils) and not by any other types of leucocyte (Shang et al., 1999).

Based upon previous studies of the expression and function of these two α subunits, α4 would not be considered a subunit likely to be present in the mouse utricle, particularly not in terms of being associated with hair cells or supporting cells of the sensory epithelium. Integrin α9, having been described in some epithelia, at cell-cell contacts or in the region of the basement membrane, could be considered more likely to be found in the tissue of interest. In order to determine definitively whether α4 or α9 are present in the normal adult mouse utricle, further PCR replicates with several cDNA samples would be required (either using the degenerate primers or qPCR) in order to establish whether the detection of these subunits was due to a 'quirk' of the cDNA sample used for degenerate RT-PCR, or if this result is real. Immunofluorescent labelling of the utricle for these integrins would also potentially answer this question; however, there are only a limited number of primary antibodies raised against the murine integrin proteins which are commercially available.

The results of the qPCR integrin arrays using cDNA from utricles at 4 and 14 days post-gentamicin also indicate that integrin α4 and α9 are not present at these time points following gentamicin-induced hair cell loss. Although it would be required to repeat these qPCR experiments using several different samples of cDNA at each time point in order to confirm these results, for the purposes of this project, these two integrin subunits have not been considered for further discussion in terms of a potential role in the processes of hair cell loss and subsequent regeneration.

This chapter has discussed the limitations of the results presented in terms of the model system and experimental approaches used. In order to present the findings of the immunohistochemistry of integrins in the adult mouse utricle and the qPCR RQ analysis of changes in integrin gene expression following gentamicin treatment as being truly

representative of the behaviour of the vestibular sensory epithelium *in vitro*, it will be necessary to carry out the further which has been described e.g. replication of qPCR experiments in triplicate. With the acceptance that additional work is required to confirm the results suggested by experimental observations presented here, the following section of this discussion addresses the potential implications of these initial studies, suggesting potential functions for several integrin subunits believed to be present within the tissue of interest.

7.4 Changes in Integrin Subunit Expression Levels in Gentamicin Treated Utricular Tissue

Relative quantification studies comparing the results of integrin gene expression arrays run using cDNA from tissue at 4 and 14 days post-gentamicin, time points where hair cell loss would be occurring, to those of the normal '0 day' uncultured control array plate suggest that there are 10 integrin subunits which show different levels of expression across the 3 time points included in this study. A summary of the changes detected in these experiments is presented in table 7-1. However, the relative quantification of these gene expression levels indicates that not all of the changes observed (i.e. those shown in Figure 5-4) are significant. For the purposes of the work carried out during this project, this discussion focuses primarily upon those integrin subunits observed to show significant changes in their expression levels by relative quantification of qPCR results, in addition to those integrins for which antibodies were available in order to carry out immunofluorescent labelling of the utricle to localise integrin proteins.

All of the five integrin subunits for which immunohistochemistry experiments on cryosectioned utricular tissue were carried out were found to be expressed in samples from control adult mice which had not been maintained *in vitro*; each of these integrins was also detected by qPCR in cDNA samples from uncultured control utricles. Three of these integrins – namely β1, β3 and αV, were observed by RQ analysis of the qPCR data to show a significant increase in gene expression at 4 days post-gentamicin, compared to the control calibrator sample. In utricular sections immunolabelled for these integrins, however, there is no observable increase in the expression of these three integrin proteins. Immunohistochemistry evidence might actually suggest that there are

less of the integrin subunits which are found in the mesenchyme e.g. αV and β1, since this is the region of the tissue which has been shown to undergo extensive remodelling *in vitro*, resulting a loss of the structures to which these integrins were localised i.e. blood capillaries; by 14 and 21 days post-gentamicin, there is only a thin layer of mesenchyme remaining in these cultured utricles lying directly beneath the sensory epithelium. Integrins β3 and β5, which both appear to be localised to the region of vestibular hair cells which is in contact with neural calyces in the normal adult mouse utricle, can be observed to redistribute to other areas of the sensory epithelium following gentamicin treatment. Each of these subunits also demonstrated an increase in gene expression at 4 days post-gentamicin detectable by qPCR, although the increase shown by β5 was not calculated to be significant. Additionally, there are several discrepancies between the results of the immunolabelling and qPCR experiments; integrin α6 was not detected in the 4 days post-gentamicin cDNA sample used for qPCR analysis, but this subunit is clearly visible in immunolabelled utricular sections at this time point, remaining localised to the epithelial-basement membrane border. Integrin β3 was not detected at 14 days post-gentamicin in the qPCR experiments, whilst immunohistochemistry suggest that this integrin is in fact present at this time point within the remodelling mesenchyme and potentially at the former sites of supporting cell-neuron interfaces. These differences between the immunolabelling and qPCR experiments may be explained due to the fact that the qPCR gene expression assays were only run using a single pooled sample of cDNA for each time point studied; this cDNA might therefore not be truly representative of the gene expression of the tissue at each time point and result in some integrins being undetectable by qPCR at a given stage post-gentamicin, despite being localised in the tissue at that same time point by immunohistochemistry.

The immunohistochemistry time-series experiments presented here can only truly be said to provide qualitative information about the expression of a subset of integrin subunits in the normal adult mouse utricle and in gentamicin-treated tissue i.e. immunolabelling can detect the presence of a protein and its localisation within a tissue. However, it cannot be reliably used to ascertain whether the expression of the integrins in question is changing in terms of the amount present in response to gentamicin treatment. The qPCR data obtained in this study can provide quantitative information

about the expression of integrins in the tissue of interest at a mRNA level, relative to a chosen calibrator control sample. Changes in gene expression, such as those detected in these experiments, however, do not necessarily correspond to an equivalent increase or decrease in the amount of the protein encoded by that gene. Where integrin gene expression has been shown to increase e.g. integrin β1 at 4 days post-gentamicin, it may be the case that although more integrin β1 mRNA is present at this time point, there may not be a similar increase in the translation of this mRNA into the functional integrin β1 protein. Alternatively, the integrins which appear to be up-regulated in terms of gene expression based on qPCR data might be undergoing an increased rate of protein turnover as a response to the gentamicin treatment – thereby showing no visible difference by immunohistochemistry i.e. higher intensity staining, but manifesting as a detectable increase in gene expression in order to replenish these integrins as they turnover more rapidly. The qPCR data obtained in this work could be refined and focused on the sensory epithelium of the utricle to provide more specific insight into changes in integrin expression. Treatment of utricular tissue with thermolysin, to enable the removal of the sensory epithelium from the basement membrane and underlying mesenchyme would allow the qPCR gene assays to focus on integrin expression within supporting cells and hair cells only, and could yield different results to those presented in this thesis.

Integrin Subunit	Normal Utricular Tissue	4 Days Post-Gentamicin	14 Days Post-Gentamicin
Itga1	Not Detected	Not Detected	Not Detected
Itga2	Not Detected	Detected	Decreased **
Itga3	Detected	Increased *	Increased *
Itga4	Not Detected	Not Detected	Not Detected
Itga5	Not Detected	Not Detected	Not Detected
Itga6	Detected	Not Detected	Increased
Itga7	Not Detected	Not Detected	Not Detected
Itga8	Detected	Not Detected	Not Detected
Itga9	Not Detected	Not Detected	Not Detected
Itga11	Not Detected	Not Detected	Not Detected
Itgav	Detected	Increased *	Increased
Itgb1	Detected	Increased *	Increased *
Itgb3	Detected	Increased *	Not Detected
Itgb4	Detected	Increased *	Not Detected
Itgb5	Detected	Increased	Increased
Itgb6	Detected	Not Detected	Decreased
Itgb7	Detected	Not Detected	Not Detected
Itgb8	Detected	Increased	Increased

Table 7-1 Summary of Changes in Integrin Expression Detected by qPCR

This table summarises the results of the RQ analysis carried out on the qPCR data obtained during this project. Of the 18 integrin subunits screened for, six were not detected in either normal or gentamicin-treated utricular cDNA. Where an integrin subunit is referred to as 'increased' or 'decreased' refers to the level of gene expression detected at a given time pointe post-gentamicin in comparison to the calibrator control sample; the calibrator cDNA sample was obtained from normal utricles which had not been maintained *in vitro*.

* Denotes a change in expression which was calculated to be significant with 95% confidence based on the RQ max and min values across replicate assays.

** Since α2 was not detected in the calibrator sample, the decrease referred to at 14 DPG is in comparison to the level observed at 4 DPG

7.4.1 Limitations of Quantitative PCR Experiments

The data obtained through the qPCR screening experiments carried out in this project using customised TaqMan® Gene Expression assay plates is limited by the lack of replicate results. Although each gene assay included was replicated four times on each plate (with one plate being used per experimental condition investigated), only one pool of tissue was utilised and run as a qPCR experiment per time point. The data obtained for each culture incubation period post-gentamicin (plus the control calibrator sample) therefore represents an n number of 1. As a consequence of this, the changes in gene expression suggested by the results of RQ analysis of the qPCR data may not be truly representative of the typical behaviour exhibited by the tissue when maintained *in vitro*; cDNA from an individual utricle responding in a non-typical manner e.g. due to a lack of cellular nutrients required by the tissue during culture, could 'contaminate' a pooled cDNA sample. If the findings of these qPCR gene expression assays were to be published, and in order to ensure that any changes in integrin expression observed were representative of the normal response of the tissue to the experimental condition (gentamicin treatment) it would be necessary to repeat the experiments at least twice more in order to have assayed each gene of interest in triplicate at each experimental time point and in control tissue.

The qPCR experiments presented here were intended to serve as a preliminary screen of the tissue, due to the large number of integrin alpha and beta subunits found in mammals, in order to identify a subset of the integrins as being of particular interest and to focus subsequent further analysis by immunohistochemistry. Additionally, the financial implications of running these qPCR experiments also had to be taken into consideration; a set of 6 customised qPCR gene expression assay plates represented a cost of £1800, before the purchase of the additional reaction cocktail reagents. Replication of these qPCR experiments in triplicate would incur costs of at least £3600 for the TaqMan® assay plates alone, and due to the funding available for consumables used in this project, the financial costs of obtaining and running these plates was also a limiting factor in terms of repeating the qPCR experiments. The control sample plate which was used as the calibrator sample for the RQ analysis which was carried out on the data obtained from the qPCR gene expression assays consisted of cDNA obtained from utricles which had been dissected from adult mice and had been placed

immediately into RNAlater; these utricles had not been treated with gentamicin, nor had they been maintained *in vitro*. Immunostaining of mouse utricles maintained in culture revealed that this tissue undergoes cellular changes as a result of the *in vitro* experimental conditions; in particular the underlying mesenchyme shows evidence of considerable remodelling, cellular spreading and proliferation. The use of cDNA from control tissue which had not been subjected to culture conditions as the calibrator for the RQ study therefore means that it is not possible to ascertain whether the changes in expression levels of integrins and the other genes assayed for are a true representation of the effect of gentamicin treatment on gene expression, or whether some of these changes are a result of *in vitro* experimental conditions – this is particularly true of the comparison by RQ of utricular cDNA at 4 days post-gentamicin treatment to non-gentamicin treated, non-cultured utricular cDNA. In order to account for changes in gene expression which are purely a consequence of the tissue having been maintained in culture, it would be necessary to obtain cDNA samples from control tissue incubated *in vitro*, but which had not been exposed to the ototoxic aminoglycoside. It would be preferable, in order to account for all cellular changes in the tissue which occur due to *in vitro* conditions, to obtain a control counterpart cDNA sample for each of the post-gentamicin treatment time points (4, 14 and 21 days post-gentamicin) and to include these samples in the qPCR experiments carried out. However, as previously mentioned, the customised TaqMan® plates used in this project represent a considerable financial expense, and to both replicate the results of each cDNA sample in triplicate and include control counterpart cDNA samples for each time point would have raised the costs of this study yet further.

The results of the qPCR experiments presented in this thesis, although limited in terms of the control sample used as a calibrator and the lack of true replicates, serve as a further screen of the tissue of interest in its normal state and as an indication of the changes in integrin gene expression which may be occurring in response to gentamicin-induced hair cell loss. Whilst in order to be presented for publication as conclusive evidence that significant changes in integrin gene expression are taking place within the gentamicin-treated mouse utricle *in vitro*, the qPCR experiments discussed would require replication, they may be utilised to focus the attention of future work on

particular integrin subunits which this preliminary screen suggests are subject to up-regulation of gene expression.

7.4.2 Epithelial Integrins Appear to be Up-regulated in Utricular Tissue at 4 Days Post-Gentamicin

Several integrin subunits, namely α2, α3 and β4, which exhibit significant increases in their expression level at 4 days post-gentamicin, have been shown in previous studies to have a role in the processes involved in wound healing of epithelia such as the skin, cornea and airways. Although the cellular mechanisms involved in wound repair in these tissues involve migration of cells to the site of the lesion (a process which is not believed to be involved in scar formation in inner ear sensory epithelia) they also require proliferation in order to re-epithelialize the injury site. Wound healing in the skin involves migration of fibroblasts and re-organization of the extracellular matrix at the site of the lesion, whereas scar formation in the inner ear has been shown to involve myosin-based contractility of the actin cytoskeleton (Hordichok and Steyger, 2007) as well as supporting cell shape changes. In epithelia such as the skin, integrins such as α2β1, α3β1 and α6β4 are expressed in keratinocytes as cell adhesion molecules maintaining the integrity of the epithelium via cell-cell contacts.

Integrin α2 was not detected by qPCR in normal utricular cDNA, but was found to be present at both 4 and 14 days post-gentamicin. This α integrin only associates as a heterodimer with the β1 subunit. It is one of the major collagen binding integrins, having been shown in previous work to be able to interact with multiple types of this extracellular matrix molecule (Tuckwell et al., 1995). Integrin α2β1 has been described functionally as having a role in the wound healing process in terms of fibroblast migration and re-organisation of collagen (Tuckwell et al., 1995) in addition to being involved in platelet adhesion to collagen (Kunicki et al., 1993). Integrin β1, discussed in depth later in this chapter, also showed a significant increase in gene expression at 4 days post-gentamicin; it therefore might be suggested that expression of the integrin α2β1 heterodimer is being triggered in the utricle at this time point following gentamicin treatment. Although further confirmation that this observed change is truly representative of the behaviour of the tissue is required, through replication of the qPCR experiments, it would also be of interest to carry out immunolabelling of both normal

and gentamicin-exposed utricular tissue maintained *in vitro*. Labelling of the utricle with an antibody against α2, in conjunction with the antibody for β1 which has already been used successfully in this project, would have the ability to indicate the region of the tissue to which α2 localises, if it is indeed an integrin not present in normal tissue, and its expression is switched on as a result of aminoglycoside treatment.

Integrin α3, another α subunit which only forms one heterodimer, α3β1, is a known receptor for laminin-5, the major laminin isoform found in basement membranes. The only basement membrane protein positively identified in the tissue of interest in this project was collagen type IV. There is little previous work on the composition of the basement membrane of the murine utricle; it would be of interest in future studies to investigate this, since integrin expression is highly dependent upon expression of integrin ligands. Integrin α3 was detected in normal adult mouse utricular cDNA by qPCR and was detected at significantly higher levels at both 4 and 14 days post-gentamicin treatment.

Integrin β4 also shows a significant increase in expression at 4 days post-gentamicin compared to levels detected in normal utricular tissue. This subunit however was not detectable at 14 days post-gentamicin. Integrin β4 is only able to associate with the α6 subunit to form a functional heterodimer, however the RQ results for α6 differ from those of β4; α6 was found to be present in control utricular cDNA, but was then undetected at 4 days post-gentamicin. Unlike β4, α6 was detected at 14 days post-gentamicin at a higher level than that of normal tissue, although this difference was not calculated as being significant. In order to address whether these differences are real results, as discussed previously, further repeats of these qPCR gene expression assays are necessary, with different cDNA samples in order to rule out the possibility that these results are a product of one pooled sample containing tissue which is not truly representative of the utricle at each time point.

Integrin α6β4 is the only known integrin which is able to interact with intermediate filaments (most integrins interact with the cytoskeleton via actin filaments) and has been shown to be a component of hemidesmosomes and to be involved in the interaction of basal keratinocytes with the basement membrane upon which they sit. Integrin β4 has been implicated as playing a role in repair of lung epithelial damage,

since β4 positive alveolar epithelial cells (of which there are relatively few present in undamaged tissue) were shown to increase in number significantly following injury by bleomycin treatment (Chapman et al., 2011). It was suggested that these alveolar epithelial cells could represent a population of progenitors maintained in the tissue which are stimulated to proliferate in response to damage. Corneal epithelial wound healing studies have also shown that integrin β4 expression increases following damage, and that its localisation was also altered in healing cornea compared to its normal pattern of expression (Stepp et al., 1996).

Integrin α2, α3 and β4 have all been implicated in tissue repair in other epithelial organ systems, and have been suggested by the qPCR screen as showing changes in their expression level over time in utricular tissue damaged by gentamicin in culture. In order to further investigate these changes, it would be beneficial to carry out immunofluorescent labelling of utricular tissue with primary antibodies against these subunits to determine whether they show any visible alterations in their distribution i.e. re-localisation from cell-cell contacts or the epithelial-basement membrane border across the time points studied using the utricular organotypic culture model of hair cell loss and regeneration in the adult mouse.

The results of the immunohistochemistry and PCR based strategies employed in this study to identify the integrins which are present in the adult mouse utricle maybe utilised in conjunction with one another to propose potential functions for these cellular adhesion proteins within the tissue of interest, and whether they might be involved in the processes of gentamicin-induced hair cell loss and spontaneous vestibular hair cell regeneration. The following discussion sections investigate several integrin subunits for which both immunolabelling and qPCR data was obtained during this project and present potential functional roles for these adhesion molecules within the utricle, in addition to the future experiments which could be carried out in order to test these hypotheses.

7.4.3 Integrin β1 Expression in the Adult Mouse Utricle

The integrin β1 subunit is the most ‘promiscuous’ of the eight known mammalian β subunits; it is able to form functional heterodimers with almost all of the known integrin

α subunits. It could therefore be suggested that this would be the most probable integrin subunit to be found in the tissue of interest.

Immunohistochemistry experiments show evidence that in the normal adult mouse utricle, the integrin β1 subunit is present in several distinct regions of the tissue. Cryosections of utricular tissue labelled with an integrin β1 primary antibody in addition to the hair cell marker calretinin (Figure 6-1) reveal that this integrin subunit shows dense punctate expression at the border region between the sensory epithelium and the underlying connective tissue. Integrin β1 positive labelling is also present within the underlying mesenchyme which corresponds with the vascular network that exists in this region of the utricle.

In order to further explore the localisation of integrin β1 at the epithelial-mesenchymal border region, cryosections were co-labelled for integrin β1 and collagen type IV (Figure 6-2). Collagen type IV is the major constituent extracellular matrix protein of basement membranes (Kefalides, 1973) and was therefore selected to serve as a basement membrane marker. The results of these experiments indicate that integrin β1 is expressed in close proximity to the basement membrane which lies at the epithelial-mesenchymal border indicated by collagen type IV expression. Collagen type IV is also found in perivascular basement membranes (Colorado et al., 2000) and is observed to localise at regions corresponding with these structures, co-localising with integrin β1.

Integrin β1 expression does not appear to alter in response to gentamicin treatment in terms of its localisation within adult utricular tissue; integrin β1-positive labelling persists at the epithelial-mesenchymal border across all three post-gentamicin time points examined. Despite this lack of an obvious change in localisation pattern of integrin β1, the results of the initial qPCR screen are suggestive of a significant increase in the gene expression of this integrin subunit at 4 days post-gentamicin. Although β1 remains evident at the epithelial-mesenchymal border in a manner which does not appear to differ from immunolabelled control counterparts, integrin β1 is also found in mesenchymal blood capillaries in the tissue underlying the sensory epithelium, a feature which is observed to degenerate over time spent in culture (occurring in both control and gentamicin treated utricles) as the mesenchyme undergoes extensive remodelling. Given these observations, it might be expected that integrin β1 gene expression would

be decreased in cDNA obtained from gentamicin-treated utricles maintained *in vitro*, however, the results of the qPCR RQ analysis indicate that integrin β1 gene expression is significantly higher (approximately 10-fold) at 4 days post-gentamicin treatment, in comparison to the control, non-treated calibrator sample.

One of the few previous studies which investigated the presence of several integrin subunits within the murine utricle by *in situ* hybridisation, found that between the ages of E16 to P0, integrin β1 mRNA was distributed throughout the hair cell body in the sensory epithelial layer (Littlewood Evans and Muller, 2000). Although not mentioned specifically, observation of the *in situ* hybridization experiments carried out in this previous study using probes for α8 and β1 mRNA do appear to show that both are present at the epithelial-basement membrane border (the region at which the immunohistochemistry work carried out during this project has shown β1 expression to be localised), although mRNA localisation does not necessarily correlate with protein expression. This earlier study also identified a vestibular dysfunctional phenotype in mice deficient for integrin α8 which survived post-natally; many of these mice die a few days after birth due to severe kidney development defects (Muller et al., 1997). Immunohistochemistry localised this integrin α subunit to the apical surface of hair cells and to the developing stereocilia between the ages of E16 and P0. Since the integrin α8 subunit is only able to bind integrin β1 to form a functional heterodimer, then it would be suggested that integrin β1 protein is expressed in these regions of the immature mouse utricle also. Additional work was carried out in this previous study to localise several extracellular matrix proteins, including collagen type IV. In control tissue, collagen type IV was seen to be expressed at the apical surface of the vestibular hair cells; this is not seen in the immunohistochemistry co-labelling experiments of this project where utricular cryosections were labelled for collagen type IV to determine the location of basement membranes within the tissue, and showed this collagen isoform to be present at the border between the sensory epithelium and the underlying mesenchyme. This difference would suggest that there may be re-distribution of both the integrin β1 subunit and collagen type IV between P0 and adulthood in the mouse utricle.

Immunohistochemistry in this work on adult vestibular tissue does not suggest that integrin β1 is expressed in vestibular hair cells, nor in the stereocilia bundles of mature

utricular maculae. Since previous work has postulated a theory that the expression of integrin α8β1 is linked to development of the stereocilia (Littlewood Evans and Muller, 2000) then it may be the case that the expression of this particular integrin heterodimer is transient and once stereocilia development is complete, this protein is no longer required in this region. Since the previous study did not examine integrin α8 expression in animals older than P0, it might be anticipated that at some time point between birth and the animal being fully mature, an immunolabelling study, if conducted, would reveal at which point the stereocilia and hair cell apices cease to be integrin α8 positive.

Integrin β1 expression at the sub-epithelial basement membrane of the utricle would be expected based upon previous studies of the interaction of this integrin subunit with basement membranes and their major constituent, collagen type IV. This study has confirmed the presence of integrin β1 within the mouse utricle by both RT-PCR and qPCR, and has additionally localised this integrin to the epithelial-mesenchymal border of this tissue. Of the integrin heterodimers which are able to bind collagen extracellular matrix proteins, α1β1 and α2β1 are the two main integrins for which binding sites have been located within a triple helical region of the collagen type IV molecule (Eble et al., 1993) (Kern et al., 1993). It would therefore be considered likely that the integrin α subunit partner for integrin β1 at this basement membrane is either α1 or α2, however, integrin α1 was not detected in utricular cDNA from normal or gentamicin treated cultures by qPCR, and integrin α2 was only detected in cDNA from 4 and 14 days post-gentamicin utricles. On the basis of these results from this study, it is possible that one of the other α integrins which associates with β1 forms the integrin β1-containing heterodimer present at the basement membrane in the utricle.

The endothelial cells which form capillaries are known to interact with their extracellular matrix through several integrins which contain the β1 subunit; namely α1β1, α2β1, α3β1, α5β1 and α6β1 (Dejana et al, 1993). Work carried out in this project also identified integrin β1 as being expressed within the vasculature of the mature utricle within the underlying connective tissue and in some regions this co-localised with collagen type IV. Although this work does not confirm which β1-containing heterodimers are present in this tissue, it would be expected that the positive labelling for integrin β1 in the capillary network would be due to one or more of the known endothelial integrins, which play a key role in the adhesion of endothelial cells to the

perivascular basement membrane and extracellular matrix via binding of the ligands collagen type IV and laminin, which are the two major components of the basement membrane (Stupack and Cheresh, 2002).

Integrin β1 possesses the ability to form twelve functional integrin heterodimers in mammalian species. The work carried out during this project has identified integrin α6 as showing a similar localisation pattern by immunolabelling as that exhibited by integrin β1, suggesting that α6 might be a potential partner for β1 in this location. However, previous studies have identified the integrin α6β1 heterodimer as being the key laminin-binding integrin that is present on platelets and involved in the processes of platelet spreading and adhesion (Inoue et al., 2006); this would indicate that the integrin α6 and β1 subunits localised by immunohistochemistry are found in similar regions of the tissue, but are not present in the same heterodimer. The degenerate and qPCR experiments carried out in this work have each detected the presence of a number of the other potential alpha subunits which could associate with integrin β1: α3, α4, α8, α9 and αV. Immunolabelling of utricular sections for integrin αV indicates that this alpha subunit is restricted to the mesenchymal regions which lie directly beneath the sensory epithelium; it does not appear to be localised within either vestibular hair cells or the supporting cells. Based on these findings, it would seem less likely that αV is associating to form a heterodimer with β1 in this region of the utricle. In order to definitively identify which integrin alpha subunit or subunits make up the integrin β1-containing heterodimers present at the epithelial-mesenchymal border within the mouse utricle, it would be necessary to carry out co-immunoprecipitation experiments as part of future work. Co-immunoprecipitation using integrin β1 antibodies immobilised on agarose bead supports would be able to isolate β1-containing protein complexes from utricular tissue lysate, and allow subsequent analysis by SDS-PAGE and western blot in order to identify the co-precipitated proteins. In addition to identifying the heterodimeric partners for integrin β1, co-immunoprecipitation studies could also reveal the extracellular matrix ligands with which these integrins are binding, providing further insight into the function of these integrins in the tissue of interest.

Based on the location of integrin β1 and the potential alpha partners which this study has identified, integrin β1 could be anticipated as providing a typical adhesive role as is common to many integrin heterodimers. In order to provide structural integrity to the

utricle, the supporting cells must be sufficiently well anchored to the basement membrane upon which they are situated. It might therefore be speculated that integrin β1-containing heterodimers are responsible for the adhesive structures that would be expected to be present within any epithelial tissue, interacting with extracellular matrix proteins which are constituents of the basement membrane i.e. collagen type IV, as has been positively identified as being present in the basement membrane which underlies the sensory epithelium of the utricle.

In order to investigate this hypothesis, it would be of interest to examine what effect a lack of integrin β1 has upon the structure of the utricle. Integrin β1 deficient mice die very early on in development, so an experimental approach to investigate the effect of β1 deficiency in the utricle would require an inducible knockout system to overcome this problem. Producing a mutant mouse strain using the Cre/lox system, it would be possible to create an animal in which an integrin β1 deficiency could be induced through drug treatment e.g. by administering tamoxifen. Experiments with the intention of investigating the role of β1 in the utricle could potentially be carried out both *in vivo* and in vitro if necessary.Previous work on the development of Cre/lox mice strains for inducible β1 knockouts has encountered issue with lethality after induction, which might prove problematic if conducting long-term in vivo experiments e.g. looking at the effect of β1 knockout at 21 days-post gentamicin treatment. In non-gentamicin treated animals or control *in vitro* utricular tissue from Cre/lox β1 knockout mice, induction of the mutation would be used to investigate whether β1 is critical for the adhesion of supporting cells to the basement membrane. Previous work in other epithelial cells in vitro has shown that integrin β1 has a half-life of approximately 24 hours (Delcommenne and Streuli, 1995), although since no previous work has looked into integrin expression in depth within the inner ear, the level of integrin turnover in the utricle may differ from that observed in other tissue types. Testing a range of incubation time points following induction of the integrin knockout would therefore be required in order to examine whether a lack of new β1 protein affects the structure of the utricle; if the hypothesis that β1 is key for the adhesion of supporting cells to the basement membrane, it would be expected that the structural integrity of the tissue would be disrupted if deficient of this integrin subunit. This might result in the observation, by

immunolabelling of utricular sections with appropriate markers, of supporting cells which have become detached from the basement membrane.

Since the qPCR experiments carried out in this study suggest that β1 gene expression is significantly increased at 4 days post-gentamicin, there is the potential for a further role for this subunit in utricular tissue which has been exposed to ototoxic aminoglycosides. In gentamicin-damaged tissue, β1-containing heterodimers could be involved in cellular signalling stimulated by hair cell death or the reorganisation of the cytoskeleton and cellular spreading undergone by supporting cells as they change shape in order to close up holes left in the sensory epithelium where vestibular hair cells have been lost. The observed increase in integrin β1 at 4 days post-gentamicin could therefore be as a result of increased focal adhesion formation as the supporting cells undergo various morphological changes. These hypotheses could be investigated using the proposed inducible β1 knockout mouse – by treating with the aminoglycoside and then administering the tamoxifen required to induce the β1 deficiency. On examination of the utricular tissue at 4 days post-gentamicin by phalloidin labelling, it would anticipated that the supporting cell shape changes observed through the appearance of scars on the apical surface of the epithelium would be impaired if the tissue was unable to up-regulate β1; rather than the typical surface appearance at this stage post-gentamicin, it would be expected that the supporting cells would not be able to spread effectively, leaving gaps in the epithelial layer created by hair cell loss.

Integrin β1 has been previously shown to be involved in cutaneous wound healing; mice with a fibroblast-specific deletion of integrin β1 were observed to show delayed wound healing in comparison to wild-type control mice (Liu et al., 2010). Mice lacking β1 also displayed defects in the production of new extracellular matrix and reduced activation of latent TGF-β, a key signalling molecule known to be involved numerous cellular processes which occur during wound healing (Werner and Grose, 2003). Integrin β1 has also been shown to be critical for keratinocyte migration during re-epithelialisation of cutaneous wounds, since mice with a keratinocyte-specific deletion of β1 exhibited migration impairment and their wounds failed to close as did those of their control littermates (Grose et al., 2002).

Based upon both the results of experiments carried out in this project and the findings of previous studies regarding the numerous cellular processes in which this integrin has been shown to play a role, the integrin β1 subunit should be considered for further research into its function in the adult mouse utricle.

7.4.4 Integrin β3 and β5 Expression in the Adult Mouse Utricle is Associated with Vestibular Hair Cells

7.4.4.1 Integrin β3

Integrin β3 is one of two integrin subunits which have been identified as being associated with vestibular hair cells based upon the results of the immunohistochemistry experiments carried out during this study. The localisation pattern of integrin β3 in the utricle was also observed to change in response to gentamicin-induced hair cell loss; this subunit appears to be expressed within type I hair cells at the region in closest proximity to the neural calyx, but is redistributed at 4 days post-gentamicin to regions at which there would be an interface between supporting cells and neurons. Immunohistochemistry results suggest that this redistribution persists at 14 day-post gentamicin, however, at 21 days post-gentamicin β3 could be seen to localise within vestibular hair cells in a manner similar to that observed in normal utricular tissue.

Integrin β3 is able to associate with two α subunits to form the heterodimers αIIbβ3 and αVβ3. Whilst the αIIbβ3 integrin is specifically expressed on blood platelets, playing a critical role in the control of blood clot formation (Hodivala-Dilke et al., 1999), the αVβ3 heterodimer shows more widespread expression and is involved in many cellular processes, including angiogenesis (Brooks et al., 1994) and wound healing (Clark et al., 1996). A previous study demonstrated that integrin β3 null mice showed enhancement of the cutaneous wound healing process compared to their wild-type littermates (Reynolds et al., 2005). This enhanced wound closure (β3-deficient mice showed complete wound closure by day 5 after wounding, whereas wild-type controls had not completed the re-epithelialisation process until day 10) was found to be the result of increased levels of TGF-β1 in the platelets of mice which lack integrin β3. These previous findings highlight the ability of integrins to alter signalling pathways which regulate key cellular processes in addition to their cell-adhesion molecule properties.

With regards to the inner ear, integrin β3 has been implicated in previous work as having a role in the differentiation of hair cells through studies carried out on OC-2 cells (an immortalised cell line derived from the mouse inner ear). OC-2 cells can be maintained in a proliferative, undifferentiated state by incubation at 33°C, but can be induced to differentiate and express known hair cell markers such as myosin VI and myosin Viia by increasing the incubation temperature to 39°C (Rivolta et al., 1998). In this previous study, OC-2 cells were shown to increase surface levels of integrin β3 when switched to their differentiating state (Brunetta et al., 2012). This increase in β3 expression correlated with an increase in myosin VI and myosin Viia. This earlier study also showed that over-expression of β3 in undifferentiated OC-2 cells incubated at 33°C was able to produce an increase in myosin VI and myosin Viia that was comparable to levels seen in differentiated OC-2 cells.

That the work carried out in this project has detected β3 expression in vestibular hair cells supports the theory that integrins may play a role in the events of hair cell development, perhaps through facilitating the release of differentiated hair cells from the basement membrane. Myosin Viia expression was also investigated in cultured utricles at several time points by qPCR. Relative quantification of this data indicated that after being initially detected in normal, undamaged tissue, myosin Viia was undetectable at 4 days post-gentamicin treatment. Myosin Viia was detectable again by 14 days post-gentamicin, at a level that was significantly lower than that observed in normal tissue. That myosin Viia expression begins to re-emerge following a significant increase in β3 expression would support a potential role for this integrin in the differentiation of hair cells through transdifferentiation events triggered by gentamicin-induced hair cell loss in the mammalian utricle.

If integrin β3 is able to influence the expression of proteins such as myosin Viia (a key marker of hair cell differentiation) in the same manner observed in the OC-2 hair cell line in vestibular hair cells, i.e. via an integrin-mediated cell signalling pathway, this may indicate a role for integrin β3 in the spontaneous hair cell regeneration observed in the mammalian utricle. Based upon RQ analysis of the qPCR experiments carried out during this project, integrin β3 appears to show a significant increase in gene expression at 4 days post-gentamicin, which could also support a role for this integrin in phenotypic conversion of supporting cells to hair cells. In order to test the hypothesis

that integrin β3 has a functional role in spontaneous regeneration in the adult mouse utricle, it would be of interest to examine the effects of both a lack of integrin β3 and the over-expression of this integrin subunit. Integrin β3 knockout mice are viable, however, litter numbers are reduced due to placental defects and these animals remain susceptible post-natally to internal haemorrhaging, particularly of the gastrointestinal tract (Hodivala-Dilke et al., 1999).This is due to the fact that this integrin forms part of the αIIbβ3 heterodimer which is expressed on blood platelets and is critical for platelet aggregation following vascular injury. In order to study the effect of a lack of β3 on hair cell regeneration, it would therefore be preferable to either conduct the study *in vivo* using such β3 knockout animals, or alternatively, to develop an inducible β3 knockout strain via the Cre/lox recombinase system as described earlier in this chapter for integrin β1. Due to the long term nature of the experiments required to observe regeneration, there would be a risk of the knockout animals dying during the experimental time period - surgical administration of the aminoglycoside would also be extremely risky to such mice, due to their impaired blood clotting capabilities.

Using an *in vivo* model, with an inducible β3 knockout mouse strain, it would be possible to expose the vestibular epithelium to the aminoglycoside gentamicin, before administering tamoxifen to induce the gene disruption and knockout integrin β3. Whilst also running control experiments in parallel, the utricular tissue of mice unable to produce new integrin β3 protein would be examined at multiple time points post-gentamicin treatment by carrying out hair cell counts. If integrin β3 is required for the cellular processes which contribute to the phenotypic conversion of supporting cells to hair cells, then it would be expected that mice lacking this subunit would exhibit a reduction in the number of new hair cells produced following gentamicin treatment in comparison to control counterparts with the functional integrin β3 gene. A concomitant reduced level of gene expression of hair cell markers such as myosin Viia and myosin VI would also be expected if the tissue from these experiments was examined by qPCR. Conversely, if β3 was overexpressed within the utricle e.g. by transfection of this tissue with an appropriate integrin β3 adenoviral construct, following gentamicin treatment it would be expected that hair cell numbers in aminoglycoside treated tissue would be higher, in addition to an increase in hair cell markers detectable by qPCR, than in control utricular tissue. Over-expression of integrin β3 in normal, non-gentamicin

treated animals would be expected to produce an increase in the number of vestibular hair cells above the numbers which are normally found in the adult epithelium.

7.4.3.2 Integrin β5

The integrin β5 subunit was detected in this study by both immunohistochemistry and qPCR; this integrin appears to localise to the base of type I hair cells in the utricular epithelium in the region at which they associate with neural calyces, based upon immunolabelling of adult mouse utricular sections. However, the only known alpha integrin partner for β5 is the αV subunit, and the immunohistochemistry experiments carried out with an anti-integrin αV antibody indicated that this integrin subunit was not present at all in the sensory epithelium, only in the underlying mesenchymal tissue. These observations suggest that further experiments are required in order to confirm the presence of β5 in the sensory epithelium e.g. through additional immunohistological investigation (having made further attempts to reduce background labelling or through use of another αV primary antibody with greater efficacy and antigen specificity), *in situ* hybridisation or western blot. If the results of further work were to support the expression of the integrin αVβ5 heterodimer in vestibular type I hair cells, the localisation pattern of β5 observed might be indicative of a potential role for this integrin in the utricle. Numerous previous studies have shown that members of the integrin family are able to increase the regenerative capacity of adult neurons e.g. integrin α1 and α5 (Condic, 2001), enhancing the extension of neurites, required for the re-innervation of tissue. Changes in the expression of integrin α6 in the mouse inner ear during development have also been shown in previous work to be involved in neuronal outgrowth. Expression of α6 at E10.5 is restricted to the otic epithelium and the neuroblasts migrating out of this region by E12.5 were shown to be those cells which had lost expression of this integrin subunit. Instead, glial cells which interact with the developing neurons in the CVG were found to be α6-positive, indicating that integrins may be involved in the survival and organisation of auditory neurons during development (Davies, 2007).

One potential hypothesis for the presence of integrin β5 in proximity to the neural calyces of type I hair cells in the utricle is that this integrin functions as a target for neurons which innervate the vestibular hair cells. Within the *in vitro* model used in this

project, neurons of the utricular tissue degenerate as the mesenchymal tissue undergoes extensive remodelling – this process occurs in both control and gentamicin-treated tissue and is therefore a side effect of the culture conditions. A potential interaction between integrin β5 and vestibular neurons would therefore have to be tested *in vivo* where the neural processes have been observed to regrow from remnants of the neuronal architecture e.g. spiral ganglion cells, following hair cell loss, rather than being regenerated in their entirety (Strominger et al., 1995) . Integrin β5-null mice reproduce and develop normally (Huang et al., 2000b) , unlike other integrin knockout mice. It would therefore be of interest to examine the inner ears of these animals to investigate whether the formation of the utricle, in particular the innervation of the tissue i.e. through immunolabelling with markers such as myosin Viia and anti-neurofilament antibodies or calretinin to label the utricular neurons, is affected by a lack of β5 – at the time of writing this thesis, no reference to a vestibular phenotype was found in studies using β5-null mice to examine the role of this integrin in other organ systems. Several cellular processes thought to involve integrin β5 have been observed to be unaffected by a lack of this subunit in β5-null mice e.g. cutaneous wound healing; it may therefore be the case that if utricular tissue from these β5-deficient mice does not differ from that observed in normal animals, that other proteins, including other members of the integrin family, are able to compensate for a lack of integrin β5.

7.4.5 Integrin αV Expression in the Adult Mouse Utricle

The integrin αV subunit is the α integrin which is able to form the most functional heterodimers, being present in 5 of the 24 known mammalian integrins; αVβ3, αVβ5, αVβ6, αVβ8 and αVβ1. Alpha V integrins are commonly able to bind the ECM proteins vitronectin and fibronectin, with αVβ3 considered the 'classical vitronectin receptor.' Studies in the mouse have shown that αV integrins are predominantly expressed in the developing nervous system and skeletal muscle (Hirsch et al., 1994). αV integrins have also been implicated in vasculogenesis, angiogenesis (Brooks et al., 1994) and the activation of TGFβ1 (Li et al., 2010).

In this work, integrin αV appears to localise to the utricular mesenchyme which is in closest proximity to the basement membrane (Figure 6-7) as well as to the capillary network which is found within this tissue beneath the sensory epithelium. The only

previous study which shows any evidence of αV expression in the utricle indicates through *in situ* hybridisation that αV mRNA is distributed throughout vestibular hair cells in mice at P0 (Littlewood Evans and Muller, 2000), although this was not investigated further to establish whether the αV protein showed the same localisation pattern. Immunohistochemistry experiments carried out in this project did not detect any expression of integrin αV within the sensory epithelium in either normal utricular tissue, or in sections of utricular cultures damaged by gentamicin *in vitro*; αV expression was maintained in the mesenchyme at the region most proximal to the basement membrane at all three of the time points studied post-gentamicin exposure. The findings of this work suggest that like integrin β1, there may be redistribution of the integrin αV subunit during the maturation of the murine inner ear between P0 and the animal becoming an adult, possibly implicating that this integrin has a role in development of this sensory epithelium.

The integrin αV subunit showed a significant increase in gene expression at 4 days post-gentamicin in comparison to the level detected in normal utricular cDNA (Figure 5-4 A). Although the work completed during this project does not definitely identify which of the αV-containing integrins are present in the tissue of interest, of the 5 possible β subunits that αV can associate with, only integrin β1 and β3 demonstrate a similar significant increase in expression at 4 days post-gentamicin (Figure 5-5). Identification of the β subunit partner or partners for αV in the mouse utricle by co-immunoprecipitation would therefore be of benefit for future studies.

αV integrins, in particular αVβ5, have been previously identified as playing a vital role in the success of adenovirus infection (Summerford et al., 1999). αVβ5 has been shown to promote the internalisation of adenovirus particles and host-cell membrane permeablisation (Wickham et al., 1994). Due to this capability, αVβ5 expression on the cell surface has also been shown to correlate with greater efficacy of gene delivery using adenoviral vectors (Goldman and Wilson, 1995). That the αVβ5 integrin heterodimer is potentially expressed in the adult mouse utricle could be beneficial for treatment of vestibular disorders/damage by gene therapy. Previous studies using an adenoviral vector to transfect vestibular hair cells of cultured mouse utricles with *Atoh1* in order to enhance the regenerative capability of the tissue (Staecker et al., 2011), by directly inducing cells to become hair cells, show that the mouse utricle is able to

successfully internalise adenoviruses, and therefore it could be the presence of integrin αVβ5 that facilitates this process.

Integrin αVβ5 has also been shown to be involved in phagocytosis of apoptotic cells by amateur phagocytes in other organ systems such as the retina (Finnemann et al., 1997). That integrin αV has been shown to be significantly increased in the utricle at 4 days post-gentamicin, in comparison to normal tissue, might potentially be linked to supporting cells removing dying vestibular hair cells from the sensory epithelium by phagocytosis.

7.5 Future Work

The work presented in this thesis represents the first study to investigate the expression of the integrin family of cell-adhesion molecules in the adult mouse utricle. Having screened this tissue for the known α and β subunits, a subset of integrins has been identified as being expressed in utricular macula of adult mice within both the sensory epithelium and the underlying mesenchyme.

As addressed earlier in this discussion, there is some immediate future work which would be necessary in order to further corroborate the results obtained during this project. Although samples of utricular tissue used to produce cDNA for qPCR gene expression array experiments contained 8 to 10 individual utricles from several different animals, each 'pool' of tissue can only be technically classified as a single sample of cDNA for a particular time point. The qPCR array plates run with control utricular cDNA and cDNA from organotypic cultures maintained for three different time points post-gentamicin treatment represent an initial screen of the tissue for the majority of the known α and β integrins. Those integrins which have been highlighted as being present in this screen, and in particular, those which have shown significant expression level changes in response to hair cell damage and loss, would be candidates for replicate qPCR assays to be carried out with several different 'pooled' samples of cDNA for each time point. It was not possible to utilise the qPCR array plate data collected from the experiment run with cDNA from utricles at 21 days post-gentamicin treatment. This was due to the cDNA yield, despite using the same number of utricles as other time points, being significantly lower – possibly a consequence of the remodelling and migration of mesenchymal cells observed in long term cultures. This low cDNA yield

resulted in the integrin subunits detected only beginning to be amplified by the PCR reaction very late into the 50 cycle run of the experiment; the consistency of detection across replicate assays was also considerably reduced i.e. of the 4 replicate assays for each gene present on the plate, a given gene was often only detected by one or two of the replicates. Replication of these qPCR experiments in triplicate would increase the reliability of the results and the likelihood that they represent the true response of the tissue following gentamicin treatment.Since immunolabelling of utricles cultured for 21 days post-gentamicin treatment showed evidence of immature stereocilia bundles on the apical surface of the sensory epithelium, it would be of interest to be able to compare the expression levels of the integrins in tissue undergoing this kind of regenerative process, with their expression in normal, undamaged tissue. This would be particularly relevant where integrins such as α8β1 have been implicated by previous studies as having a role in the formation of stereocilia in vestibular hair cells (Littlewood Evans and Muller, 2000), as it might be anticipated based upon this work that expression of these two subunits would be up-regulated in the utricle if there are new apical hair bundles being produced in a manner similar to that which occurs during development.

A total of five integrin subunits were investigated further with immunohistochemistry in order to examine their localisation within the tissue, in addition to exploring the possibility of temporal-spatial changes in their expression pattern at several time points following gentamicin treatment. It would be of interest to obtain primary antibodies to allow the localisation of the remaining subunits detected by PCR in order to complete a full study of the expression pattern of these integrins, establishing which region of the tissue they are associated with i.e. are they linked to the mesenchyme or the sensory epithelium. Since functionally, the integrin subunits must exist as a heterodimer, it would be of interest to establish the pairings of α and β subunits which exist in the murine utricle. Although some of the subunits detected are only able to form a single heterodimer, and thus if they are present it must be inferred that this is the heterodimer present, in the case of the more 'promiscuous' α V and β 1 subunits, it might be possible that they are present in the utricle as part of several yet unknown pairings. Co-immunoprecipitation experiments could therefore be utilised in order to pull down particular integrins from utricular tissue cell lysate whilst still associated with their heterodimer partner. These experiments could also result in integrin-associated proteins

i.e. proteins through which integrins interact with the cytoskeleton being pulled down simultaneously, lending further insight into how the integrins which are present in the tissue are interacting with their intra and extracellular surroundings. Since the integrins expressed on any given cell type are directly influenced by the extracellular matrix ligands present in a particular tissue, identification and localisation of the integrin ligands present in the utricle would also be important for future investigation of the function of integrin heterodimers in the vestibular sensory epithelium.

The long-term culture model established during this project represents a successful method of inducing hair cell loss in the adult mouse utricle, in order to study the potential role of integrins in the repair and limited spontaneous regeneration which occurs in this tissue. However, it cannot be ruled out, as discussed earlier in this chapter, that the behaviour of the tissue *in vitro* in response to gentamicin treatment might differ from that which would occur *in vivo*. It would therefore be beneficial for future work to explore whether these differences i.e. the remodelling of the mesenchyme, have an influence on the expression and localisation of integrins by repeating both the immunohistochemistry experiments and the qPCR gene expression assays using an in vivo mouse model. The integrin subunits identified in this work as showing significant changes in expression level e.g. β3, β1 and αV would be candidates for further investigation using this culture model.

Inhibition of integrins has been the subject of numerous previous studies, with particular emphasis in the field of cancer research and their effect on tumour growth and angiogenesis. Integrin inhibitors, such as CNTO 95 (Trikha et al., 2004) an αV inhibitor antibody and LM609 (Brooks et al., 1995) an αVβ3 blocking monoclonal antibody, as well as small molecule (Kerr et al., 1999) and cyclic RGD-containing peptides i.e. cilengitide (Desgrosellier and Cheresh, 2010) have all been previously used to inhibit integrins and reduce tumour proliferation and angiogenesis. Utricular cultures incubated *in vitro* with a specific integrin inhibitor could be used in order to investigate whether some of the integrins highlighted by this project play a role in the cellular processes involved in hair cell loss and regeneration of the sensory epithelium. Immunolabelling of these cultured tissues for actin and myosin Viia could then be used to investigate whether blocking a particular integrin subunit has an effect upon the behaviour of the tissue of interest during a subsequent recovery period following gentamicin exposure

i.e. whether hair cell regeneration might be reduced or enhanced by inducing a loss of function of a particular integrin known to be present in normal tissue and up-regulated significantly following damage. Further *in vivo* based experiments were discussed at length in 7.4, describing the potential for the use of integrin knockout mice to explore the effect of deficiency in particular integrin subunits within both normal utricular tissue and in animals treated with an aminoglycoside to induce hair cell loss. This additional approach would provide a means of comparing the response of the utricle when lacking a given integrin subunit, when incubated in culture and when maintained *in vivo*.

The work carried out in this thesis has already begun to be applied to human vestibular epithelium within this research group. It will be of interest to observe how similar the integrin expression of the human tissue is in comparison to the mouse model used in this project and whether cultured utricles show similar changes in integrin expression level following gentamicin treatment. Mammalian vestibular epithelia are known to show limited regeneration of hair cells following damage, although not to the extent of the capabilities shown by birds and amphibians. The human organ of Corti is incapable of regenerating following the loss or damage of auditory hair cells. It would be of interest to explore the integrin expression of the mammalian organ of Corti and to compare this with that observed in the utricle. Although both epithelia contain hair cells which have a mechanosensory function, their arrangement and the supporting cells which surround them differ significantly. Recent studies on regeneration of auditory hair cells have demonstrated that treatment of noise-damaged mice *in vivo* with a γ-secretase inhibitor (producing an increase in Atoh1), was sufficient to induce phenotypic conversion of supporting cells into hair cells (Mizutari et al., 2013). However, despite being myosin Viia positive, these supporting cell-derived regenerated hair cells were still found to be attached to the basement membrane. It might be possible that integrins present in the utricle which could play a role in the processes of repair and regeneration are not found in the organ of Corti, and that the inability to replace auditory hair cells may be partially attributed to a lack of integrins which may potentially be involved in the utricle in the release of supporting cells which have converted to hair cells from their surface adhesions to the basement membrane.

7.6 Conclusion

The aim of this project was to investigate the integrin family of cell-surface adhesion molecules in an adult inner ear sensory epithelium that was known to undergo a degree of spontaneous regeneration following hair cell loss. Few previous studies had been conducted with regards to the presence of integrins in the inner ear, and those which existed had primarily been conducted on embryonic or very early postnatal animals.

The work presented in this thesis represents the first study of the integrin family in the adult mammalian utricle. A subset of the known mammalian integrin α and β subunits have been identified through a series of degenerate and quantitative PCR experiments as being present in the adult mouse utricle in its normal, undamaged state. Immunohistochemistry reveals the localisation of some of these subunits and demonstrates that they are present throughout the epithelial and mesenchymal structures of the utricle.

Through the use of an *in vitro* organotypic culture system as a model for the induction of damage responses and spontaneous regeneration in adult utricular tissue, qPCR and immunohistochemistry based experiments have been applied in order to investigate whether integrin expression is affected by the loss of vestibular hair cells. Several integrin subunits which have been previously described as being involved in tissue repair in other organ systems e.g. integrins β1, β3 and αV, have been shown in this project to demonstrate significant changes in gene expression level in tissue, in particular at 4 days post-gentamicin, when the utricle shows a large decrease in hair cell numbers, although further replicate qPCR experiments would be required to confirm that these results are a true representation of the typical behaviour of the utricle in terms of integrin expression. Immunofluorescent labelling of integrins in sectioned utricular tissue at three individual time points post-gentamicin treatment indicates that at least two of the integrin subunits studied in this project exhibited evidence of re-distribution following gentamicin treatment, suggesting that integrins might play a role in the cellular events of vestibular epithelial repair and regeneration.

The work described in this thesis represents a foundational study of the integrins of the adult mouse utricle and presents the integrin family as a group of cell-adhesion molecules which warrant further examination and research in order to learn more about

what their exact role might be in the vestibular sensory epithelium, and whether this might allow integrins to be manipulated in order to enhance the regenerative capabilities of the mammalian vestibular epithelium.

References

Adler, H.J., and Y. Raphael. 1996. New hair cells arise from supporting cell conversion in the acoustically damaged chick inner ear. *Neurosci Lett*. 205:17-20.

Al-Jamal, R., and D.J. Harrison. 2008. Beta1 integrin in tissue remodelling and repair: from phenomena to concepts. *Pharmacol Ther*. 120:81-101.

Ashmore, J.F. 1987. A fast motile response in guinea-pig outer hair cells: the cellular basis of the cochlear amplifier. *J Physiol*. 388:323-347.

Bagger-Sjoback, D., and M. Takumida. 1988. Geometrical array of the vestibular sensory hair bundle. *Acta Otolaryngol*. 106:393-403.

Baird, R.A., M.D. Burton, A. Lysakowski, D.S. Fashena, and R.A. Naeger. 2000. Hair cell recovery in mitotically blocked cultures of the bullfrog saccule. *Proc Natl Acad Sci U S A*. 97:11722-11729.

Baird, R.A., M.A. Torres, and N.R. Schuff. 1993. Hair cell regeneration in the bullfrog vestibular otolith organs following aminoglycoside toxicity. *Hear Res*. 65:164-174.

Barczyk, M., S. Carracedo, and D. Gullberg. 2010. Integrins. *Cell Tissue Res*. 339:269-280.

Bazigou, E., S. Xie, C. Chen, A. Weston, N. Miua, L. Sorokin, R. Adams, A.F. Muro, D. Sheppard, and T. Makinen. 2009. Integrin-alpha9 is required for fibronectin matrix assembly during lymphatic valve morphogenesis. *Dev Cell*. 17:175-186.

Beckingham, K.M., M.J. Texada, D.A. Baker, R. Munjaal, and J.D. Armstrong. 2005. Genetics of graviperception in animals. *Adv Genet*. 55:105-145.

Belkin, A.M., and M.A. Stepp. 2000. Integrins as receptors for laminins. *Microsc Res Tech*. 51:280-301.

Berggren, D., W. Liu, D. Frenz, and T. Van De Water. 2003. Spontaneous hair-cell renewal following gentamicin exposure in postnatal rat utricular explants. *Hear Res*. 180:114-125.

Berlin, C., R.F. Bargatze, J.J. Campbell, U.H. von Andrian, M.C. Szabo, S.R. Hasslen, R.D. Nelson, E.L. Berg, S.L. Erlandsen, and E.C. Butcher. 1995. alpha 4 integrins mediate lymphocyte attachment and rolling under physiologic flow. *Cell*. 80:413-422.

Bermingham, N.A., B.A. Hassan, S.D. Price, M.A. Vollrath, N. Ben-Arie, R.A. Eatock, H.J. Bellen, A. Lysakowski, and H.Y. Zoghbi. 1999. Math1: an essential gene for the generation of inner ear hair cells. *Science*. 284:1837-1841.

Bird, J.E., N. Daudet, M.E. Warchol, and J.E. Gale. 2010. Supporting cells eliminate dying sensory hair cells to maintain epithelial integrity in the avian inner ear. *J Neurosci*. 30:12545-12556.

Bolz, H., B. von Brederlow, A. Ramirez, E.C. Bryda, K. Kutsche, H.G. Nothwang, M. Seeliger, C.S.C.M. del, M.C. Vila, O.P. Molina, A. Gal, and C. Kubisch. 2001. Mutation of CDH23, encoding a new member of the cadherin gene family, causes Usher syndrome type 1D. *Nat Genet*. 27:108-112.

Brooks, P.C., R.A. Clark, and D.A. Cheresh. 1994. Requirement of vascular integrin alpha v beta 3 for angiogenesis. *Science*. 264:569-571.

Brooks, P.C., S. Stromblad, R. Klemke, D. Visscher, F.H. Sarkar, and D.A. Cheresh. 1995. Antiintegrin alpha v beta 3 blocks human breast cancer growth and angiogenesis in human skin. *J Clin Invest*. 96:1815-1822.

Brunetta, I., S.O. Casalotti, I.R. Hart, A. Forge, and L.E. Reynolds. 2012. beta3-integrin is required for differentiation in OC-2 cells derived from mammalian embryonic inner ear. *BMC Cell Biol*. 13:5.

Cavalcanti-Adam, E.A., T. Volberg, A. Micoulet, H. Kessler, B. Geiger, and J.P. Spatz. 2007. Cell spreading and focal adhesion dynamics are regulated by spacing of integrin ligands. *Biophys J*. 92:2964-2974.

Cavani, A., G. Zambruno, A. Marconi, V. Manca, M. Marchetti, and A. Giannetti. 1993. Distinctive integrin expression in the newly forming epidermis during wound healing in humans. *J Invest Dermatol*. 101:600-604.

Chapman, H.A., X. Li, J.P. Alexander, A. Brumwell, W. Lorizio, K. Tan, A. Sonnenberg, Y. Wei, and T.H. Vu. 2011. Integrin alpha6beta4 identifies an adult distal lung epithelial population with regenerative potential in mice. *J Clin Invest*. 121:2855-2862.

Chen, H.C., P.A. Appeddu, J.T. Parsons, J.D. Hildebrand, M.D. Schaller, and J.L. Guan. 1995. Interaction of focal adhesion kinase with cytoskeletal protein talin. *J Biol Chem*. 270:16995-16999.

Clark, R.A. 1990. Fibronectin matrix deposition and fibronectin receptor expression in healing and normal skin. *J Invest Dermatol*. 94:128S-134S.

Clark, R.A., M.G. Tonnesen, J. Gailit, and D.A. Cheresh. 1996. Transient functional expression of alphaVbeta 3 on vascular cells during wound repair. *Am J Pathol*. 148:1407-1421.

Cluzel, C., F. Saltel, J. Lussi, F. Paulhe, B.A. Imhof, and B. Wehrle-Haller. 2005. The mechanisms and dynamics of (alpha)v(beta)3 integrin clustering in living cells. *J Cell Biol*. 171:383-392.

Colombatti, A., P. Bonaldo, and R. Doliana. 1993. Type A modules: interacting domains found in several non-fibrillar collagens and in other extracellular matrix proteins. *Matrix*. 13:297-306.

Colorado, P.C., A. Torre, G. Kamphaus, Y. Maeshima, H. Hopfer, K. Takahashi, R. Volk, E.D. Zamborsky, S. Herman, P.K. Sarkar, M.B. Ericksen, M. Dhanabal, M. Simons, M. Post, D.W. Kufe, R.R. Weichselbaum, V.P. Sukhatme, and R. Kalluri. 2000. Anti-angiogenic cues from vascular basement membrane collagen. *Cancer Res*. 60:2520-2526.

Condic, M.L. 2001. Adult neuronal regeneration induced by transgenic integrin expression. *J Neurosci*. 21:4782-4788.

Corwin, J.T. 1981. Postembryonic production and aging in inner ear hair cells in sharks. *J Comp Neurol*. 201:541-553.

Corwin, J.T. 1985. Perpetual production of hair cells and maturational changes in hair cell ultrastructure accompany postembryonic growth in an amphibian ear. *Proc Natl Acad Sci U S A*. 82:3911-3915.

Corwin, J.T., and D.A. Cotanche. 1988. Regeneration of sensory hair cells after acoustic trauma. *Science*. 240:1772-1774.

Cotanche, D.A. 1987. Regeneration of hair cell stereociliary bundles in the chick cochlea following severe acoustic trauma. *Hear Res*. 30:181-195.

Cunningham, L.L. 2006. The adult mouse utricle as an in vitro preparation for studies of ototoxic-drug-induced sensory hair cell death. *Brain Res*. 1091:277-281.

Cunningham, L.L., A.G. Cheng, and E.W. Rubel. 2002. Caspase activation in hair cells of the mouse utricle exposed to neomycin. *J Neurosci*. 22:8532-8540.

Davies, D. 2007. Temporal and spatial regulation of alpha6 integrin expression during the development of the cochlear-vestibular ganglion. *J Comp Neurol*. 502:673-682.

Davies, D., and M.C. Holley. 2002. Differential Expression of α3 and α6 Integrins in the Developing Mouse Inner Ear. *The Journal of Comparative Neurology*. 445:122-132.

Davies, D., C. Magnus, and J.T. Corwin. 2007. Developmental Changes in Cell-Extracellular Matrix Interactions Limit Proliferation in the Mammalian Inner Ear. *European Journal of Neuroscience*. 25:985 - 998.

Delcommenne, M., and C.H. Streuli. 1995. Control of integrin expression by extracellular matrix. *J Biol Chem*. 270:26794-26801.

Denman-Johnson, K., and A. Forge. 1999. Establishment of hair bundle polarity and orientation in the developing vestibular system of the mouse. *J Neurocytol*. 28:821-835.

Desgrosellier, J.S., and D.A. Cheresh. 2010. Integrins in cancer: biological implications and therapeutic opportunities. *Nat Rev Cancer*. 10:9-22.
Dohlman, G.F. 1969. The shape and function of the cupula. *J Laryngol Otol*. 83:43-53.
Dohlman, G.F. 1981. Critical review of the concept of cupula function. *Acta Otolaryngol Suppl*. 376:1-30.
Dupuy, A.G., and E. Caron. 2008. Integrin-dependent phagocytosis: spreading from microadhesion to new concepts. *J Cell Sci*. 121:1773-1783.
Eble, J.A., R. Golbik, K. Mann, and K. Kuhn. 1993. The alpha 1 beta 1 integrin recognition site of the basement membrane collagen molecule [alpha 1(IV)]2 alpha 2(IV). *EMBO J*. 12:4795-4802.
Erkman, L., R.J. McEvilly, L. Luo, A.K. Ryan, F. Hooshmand, S.M. O'Connell, E.M. Keithley, D.H. Rapaport, A.F. Ryan, and M.G. Rosenfeld. 1996. Role of transcription factors Brn-3.1 and Brn-3.2 in auditory and visual system development. *Nature*. 381:603-606.
Ewan, R., J. Huxley-Jones, A.P. Mould, M.J. Humphries, D.L. Robertson, and R.P. Boot-Handford. 2005. The integrins of the urochordate Ciona intestinalis provide novel insights into the molecular evolution of the vertebrate integrin family. *BMC Evol Biol*. 5:31.
Fincham, V.J., V.G. Brunton, and M.C. Frame. 2000. The SH3 domain directs acto-myosin-dependent targeting of v-Src to focal adhesions via phosphatidylinositol 3-kinase. *Mol Cell Biol*. 20:6518-6536.
Finnemann, S.C., V.L. Bonilha, A.D. Marmorstein, and E. Rodriguez-Boulan. 1997. Phagocytosis of rod outer segments by retinal pigment epithelial cells requires alpha(v)beta5 integrin for binding but not for internalization. *Proc Natl Acad Sci U S A*. 94:12932-12937.
Fitzpatrick, R.C., and B.L. Day. 2004. Probing the human vestibular system with galvanic stimulation. *J Appl Physiol*. 96:2301-2316.
Flock, A., and H.C. Cheung. 1977. Actin filaments in sensory hairs of inner ear receptor cells. *J Cell Biol*. 75:339-343.
Forge, A., and L. Li. 2000. Apoptotic death of hair cells in mammalian vestibular sensory epithelia. *Hear Res*. 139:97-115.
Forge, A., L. Li, J.T. Corwin, and G. Nevill. 1993. Ultrastructural evidence for hair cell regeneration in the mammalian inner ear. *Science*. 259:1616-1619.
Forge, A., L. Li, and G. Nevill. 1998. Hair cell recovery in the vestibular sensory epithelia of mature guinea pigs. *J Comp Neurol*. 397:69-88.
Gale, J.E., W. Marcotti, H.J. Kennedy, C.J. Kros, and G.P. Richardson. 2001. FM1-43 dye behaves as a permeant blocker of the hair-cell mechanotransducer channel. *J Neurosci*. 21:7013-7025.
Gale, J.E., J.R. Meyers, and J.T. Corwin. 2000. Solitary hair cells are distributed throughout the extramacular epithelium in the bullfrog's saccule. *J Assoc Res Otolaryngol*. 1:172-182.
Germain, E.C., T.M. Santos, and I. Rabinovitz. 2009. Phosphorylation of a novel site on the {beta}4 integrin at the trailing edge of migrating cells promotes hemidesmosome disassembly. *Mol Biol Cell*. 20:56-67.
Goldman, M.J., and J.M. Wilson. 1995. Expression of alpha v beta 5 integrin is necessary for efficient adenovirus-mediated gene transfer in the human airway. *J Virol*. 69:5951-5958.
Grinnell, F. 1994. Fibroblasts, myofibroblasts, and wound contraction. *J Cell Biol*. 124:401-404.
Grose, R., C. Hutter, W. Bloch, I. Thorey, F.M. Watt, R. Fassler, C. Brakebusch, and S. Werner. 2002. A crucial role of beta 1 integrins for keratinocyte migration in vitro and during cutaneous wound repair. *Development*. 129:2303-2315.

Groves, A.K. 2010. The challenge of hair cell regeneration. *Exp Biol Med (Maywood)*. 235:434-446.

Hackney, C.M., and D.N. Furness. 1995. Mechanotransduction in vertebrate hair cells: structure and function of the stereociliary bundle. *Am J Physiol*. 268:C1-13.

Hanks, S.K., and T.R. Polte. 1997. Signaling through focal adhesion kinase. *Bioessays*. 19:137-145.

Hasson, T., M.B. Heintzelman, J. Santos-Sacchi, D.P. Corey, and M.S. Mooseker. 1995. Expression in cochlea and retina of myosin VIIa, the gene product defective in Usher syndrome type 1B. *Proc Natl Acad Sci U S A*. 92:9815-9819.

Hertle, M.D., M.D. Kubler, I.M. Leigh, and F.M. Watt. 1992. Aberrant integrin expression during epidermal wound healing and in psoriatic epidermis. *J Clin Invest*. 89:1892-1901.

Hildebrand, J.D., M.D. Schaller, and J.T. Parsons. 1995. Paxillin, a tyrosine phosphorylated focal adhesion-associated protein binds to the carboxyl terminal domain of focal adhesion kinase. *Mol Biol Cell*. 6:637-647.

Hirsch, E., D. Gullberg, F. Balzac, F. Altruda, L. Silengo, and G. Tarone. 1994. Alpha v integrin subunit is predominantly located in nervous tissue and skeletal muscle during mouse development. *Dev Dyn*. 201:108-120.

Hodivala-Dilke, K.M., K.P. McHugh, D.A. Tsakiris, H. Rayburn, D. Crowley, M. Ullman-Cullere, F.P. Ross, B.S. Coller, S. Teitelbaum, and R.O. Hynes. 1999. Beta3-integrin-deficient mice are a model for Glanzmann thrombasthenia showing placental defects and reduced survival. *J Clin Invest*. 103:229-238.

Holmes, R.S., and U.K. Rout. 2011. Comparative Studies of Vertebrate Beta Integrin Genes and Proteins: Ancient Genes in Vertebrate Evolution. *Biomolecules*. 1:3-31.

Hordichok, A.J., and P.S. Steyger. 2007. Closure of supporting cell scar formations requires dynamic actin mechanisms. *Hear Res*. 232:1-19.

Huang, C., Q. Zang, J. Takagi, and T.A. Springer. 2000a. Structural and functional studies with antibodies to the integrin beta 2 subunit. A model for the I-like domain. *J Biol Chem*. 275:21514-21524.

Huang, X., M. Griffiths, J. Wu, R.V. Farese, Jr., and D. Sheppard. 2000b. Normal development, wound healing, and adenovirus susceptibility in beta5-deficient mice. *Mol Cell Biol*. 20:755-759.

Hudspeth, A.J. 2001. How the ear's works work: mechanoelectrical transduction and amplification by hair cells of the internal ear. *Harvey Lect*. 97:41-54.

Hughes, A.L. 2001. Evolution of the integrin alpha and beta protein families. *J Mol Evol*. 52:63-72.

Huhtala, M., J. Heino, D. Casciari, A. de Luise, and M.S. Johnson. 2005. Integrin Evolution: Insights from Ascidian and Teleost Fish Genomes. *Matrix Biology*. 24:83-95.

Hynes, R.O. 2004. The emergence of integrins: a personal and historical perspective. *Matrix Biol*. 23:333-340.

Inoue, O., K. Suzuki-Inoue, O.J. McCarty, M. Moroi, Z.M. Ruggeri, T.J. Kunicki, Y. Ozaki, and S.P. Watson. 2006. Laminin stimulates spreading of platelets through integrin alpha6beta1-dependent activation of GPVI. *Blood*. 107:1405-1412.

Jiang, H., S.H. Sha, A. Forge, and J. Schacht. 2006. Caspase-independent pathways of hair cell death induced by kanamycin in vivo. *Cell Death Differ*. 13:20-30.

Johnson, M.S., N. Lu, K. Denessiouk, J. Heino, and D. Gullberg. 2009. Integrins during evolution: Evolutionary trees and model organisms. *Biochemica et Biophysica Acta*. 1788:779-789.

Jonkman, M.F., H.H. Pas, M. Nijenhuis, G. Kloosterhuis, and G. Steege. 2002. Deletion of a cytoplasmic domain of integrin beta4 causes epidermolysis bullosa simplex. *J Invest Dermatol*. 119:1275-1281.

Jorgensen, J.M., and C. Mathiesen. 1988. The avian inner ear. Continuous production of hair cells in vestibular sensory organs, but not in the auditory papilla. *Naturwissenschaften*. 75:319-320.

Kachar, B., M. Parakkal, and J. Fex. 1990. Structural basis for mechanical transduction in the frog vestibular sensory apparatus: I. The otolithic membrane. *Hear Res*. 45:179-190.

Kanazashi, S.I., C.P. Sharma, and M.A. Arnaout. 1997. Integrin-ligand interactions: scratching the surface. *Curr Opin Hematol*. 4:67-74.

Kashyap, T., E. Germain, M. Roche, S. Lyle, and I. Rabinovitz. 2011. Role of beta4 integrin phosphorylation in human invasive squamous cell carcinoma: regulation of hemidesmosome stability modulates cell migration. *Lab Invest*. 91:1414-1426.

Kawamoto, K., M. Izumikawa, L.A. Beyer, G.M. Atkin, and Y. Raphael. 2009. Spontaneous hair cell regeneration in the mouse utricle following gentamicin ototoxicity. *Hear Res*. 247:17-26.

Kefalides, N.A. 1973. Structure and biosynthesis of basement membranes. *Int Rev Connect Tissue Res*. 6:63-104.

Kern, A., J. Eble, R. Golbik, and K. Kuhn. 1993. Interaction of type IV collagen with the isolated integrins alpha 1 beta 1 and alpha 2 beta 1. *Eur J Biochem*. 215:151-159.

Kerr, J.S., R.S. Wexler, S.A. Mousa, C.S. Robinson, E.J. Wexler, S. Mohamed, M.E. Voss, J.J. Devenny, P.M. Czerniak, A. Gudzelak, Jr., and A.M. Slee. 1999. Novel small molecule alpha v integrin antagonists: comparative anti-cancer efficacy with known angiogenesis inhibitors. *Anticancer Res*. 19:959-968.

Kieffer, N., and D.R. Phillips. 1990. Platelet membrane glycoproteins: functions in cellular interactions. *Annu Rev Cell Biol*. 6:329-357.

Kim, M., C.V. Carman, and T.A. Springer. 2003. Bidirectional transmembrane signaling by cytoplasmic domain separation in integrins. *Science*. 301:1720-1725.

Kimura, R.S. 1966. Hairs of the cochlear sensory cells and their attachment to the tectorial membrane. *Acta Otolaryngol*. 61:55-72.

Koster, J., D. Geerts, B. Favre, L. Borradori, and A. Sonnenberg. 2003. Analysis of the interactions between BP180, BP230, plectin and the integrin alpha6beta4 important for hemidesmosome assembly. *J Cell Sci*. 116:387-399.

Kramer, R.H., G.M. Fuh, and M.A. Karasek. 1985. Type IV collagen synthesis by cultured human microvascular endothelial cells and its deposition into the subendothelial basement membrane. *Biochemistry*. 24:7423-7430.

Kunicki, T.J., R. Orchekowski, D. Annis, and Y. Honda. 1993. Variability of integrin alpha 2 beta 1 activity on human platelets. *Blood*. 82:2693-2703.

Lang, H., and C. Liu. 1997. Apoptosis and hair cell degeneration in the vestibular sensory epithelia of the guinea pig following a gentamicin insult. *Hear Res*. 111:177-184.

Lapeyre, P., A. Guilhaume, and Y. Cazals. 1992. Differences in hair bundles associated with type I and type II vestibular hair cells of the guinea pig saccule. *Acta Otolaryngol*. 112:635-642.

Lee, J.O., P. Rieu, M.A. Arnaout, and R. Liddington. 1995. Crystal structure of the A domain from the alpha subunit of integrin CR3 (CD11b/CD18). *Cell*. 80:631-638.

Li, J., Y. Qu, X. Li, D. Li, F. Zhao, M. Mao, D. Ferriero, and D. Mu. 2010. The role of integrin alpha(v)beta (8) in neonatal hypoxic-ischemic brain injury. *Neurotox Res*. 17:406-417.

Li, L., and A. Forge. 1997. Morphological evidence for supporting cell to hair cell conversion in the mammalian utricular macula. *Int J Dev Neurosci*. 15:433-446.

Li, L., G. Nevill, and A. Forge. 1995. Two modes of hair cell loss from the vestibular sensory epithelia of the guinea pig inner ear. *J Comp Neurol*. 355:405-417.

Lim, D.J. 1972. Fine morphology of the tectorial membrane. Its relationship to the organ of Corti. *Arch Otolaryngol*. 96:199-215.

Lim, D.J. 1986. Functional structure of the organ of Corti: a review. *Hear Res*. 22:117-146.
Lin, V., J.S. Golub, T.B. Nguyen, C.R. Hume, E.C. Oesterle, and J.S. Stone. 2011. Inhibition of Notch activity promotes nonmitotic regeneration of hair cells in the adult mouse utricles. *J Neurosci*. 31:15329-15339.
Litjens, S.H., J.M. de Pereda, and A. Sonnenberg. 2006. Current insights into the formation and breakdown of hemidesmosomes. *Trends Cell Biol*. 16:376-383.
Littlewood Evans, A., and U. Muller. 2000. Stereocilia defects in the sensory hair cells of the inner ear in mice deficient in integrin alpha8beta1. *Nat Genet*. 24:424-428.
Liu, S., D.A. Calderwood, and M.H. Ginsberg. 2000. Integrin cytoplasmic domain-binding proteins. *J Cell Sci*. 113 (Pt 20):3563-3571.
Liu, S., S.M. Thomas, D.G. Woodside, D.M. Rose, W.B. Kiosses, M. Pfaff, and M.H. Ginsberg. 1999. Binding of paxillin to alpha4 integrins modifies integrin-dependent biological responses. *Nature*. 402:676-681.
Liu, S., S.W. Xu, K. Blumbach, M. Eastwood, C.P. Denton, B. Eckes, T. Krieg, D.J. Abraham, and A. Leask. 2010. Expression of integrin beta1 by fibroblasts is required for tissue repair in vivo. *J Cell Sci*. 123:3674-3682.
Lo, S.H., P.A. Janmey, J.H. Hartwig, and L.B. Chen. 1994. Interactions of tensin with actin and identification of its three distinct actin-binding domains. *J Cell Biol*. 125:1067-1075.
Lopez, I., V. Honrubia, S.C. Lee, G. Schoeman, and K. Beykirch. 1997. Quantification of the process of hair cell loss and recovery in the chinchilla crista ampullaris after gentamicin treatment. *Int J Dev Neurosci*. 15:447-461.
Ma, Y.Q., J. Qin, C. Wu, and E.F. Plow. 2008. Kindlin-2 (Mig-2): a co-activator of beta3 integrins. *J Cell Biol*. 181:439-446.
Marchisio, P.C., S. Bondanza, O. Cremona, R. Cancedda, and M. De Luca. 1991. Polarized expression of integrin receptors (alpha 6 beta 4, alpha 2 beta 1, alpha 3 beta 1, and alpha v beta 5) and their relationship with the cytoskeleton and basement membrane matrix in cultured human keratinocytes. *J Cell Biol*. 112:761-773.
Marcotti, W., S.M. van Netten, and C.J. Kros. 2005. The aminoglycoside antibiotic dihydrostreptomycin rapidly enters mouse outer hair cells through the mechano-electrical transducer channels. *J Physiol*. 567:505-521.
Marcus, D.C., T. Wu, P. Wangemann, and P. Kofuji. 2002. KCNJ10 (Kir4.1) potassium channel knockout abolishes endocochlear potential. *Am J Physiol Cell Physiol*. 282:C403-407.
Martin, P. 1997. Wound healing--aiming for perfect skin regeneration. *Science*. 276:75-81.
Matsui, J.I., A. Haque, D. Huss, E.P. Messana, J.A. Alosi, D.W. Roberson, D.A. Cotanche, J.D. Dickman, and M.E. Warchol. 2003. Caspase inhibitors promote vestibular hair cell survival and function after aminoglycoside treatment in vivo. *J Neurosci*. 23:6111-6122.
Matsui, J.I., J.M. Ogilvie, and M.E. Warchol. 2002. Inhibition of caspases prevents ototoxic and ongoing hair cell death. *J Neurosci*. 22:1218-1227.
Meiteles, L.Z., and Y. Raphael. 1994. Scar formation in the vestibular sensory epithelium after aminoglycoside toxicity. *Hear Res*. 79:26-38.
Mercurio, A.M., I. Rabinovitz, and L.M. Shaw. 2001. The alpha 6 beta 4 integrin and epithelial cell migration. *Curr Opin Cell Biol*. 13:541-545.
Meyers, J.R., and J.T. Corwin. 2007. Shape change controls supporting cell proliferation in lesioned mammalian balance epithelium. *J Neurosci*. 27:4313-4325.
Mitra, S.K., D.A. Hanson, and D.D. Schlaepfer. 2005. Focal adhesion kinase: in command and control of cell motility. *Nat Rev Mol Cell Biol*. 6:56-68.
Miyamoto, S., S.K. Akiyama, and K.M. Yamada. 1995a. Synergistic roles for receptor occupancy and aggregation in integrin transmembrane function. *Science*. 267:883-885.

Miyamoto, S., H. Teramoto, O.A. Coso, J.S. Gutkind, P.D. Burbelo, S.K. Akiyama, and K.M. Yamada. 1995b. Integrin function: molecular hierarchies of cytoskeletal and signaling molecules. *J Cell Biol*. 131:791-805.

Mizutari, K., M. Fujioka, M. Hosoya, N. Bramhall, H.J. Okano, H. Okano, and A.S. Edge. 2013. Notch inhibition induces cochlear hair cell regeneration and recovery of hearing after acoustic trauma. *Neuron*. 77:58-69.

Montcouquiol, M., and J.T. Corwin. 2001. Intracellular Signals That Control Cell Proliferation in Mammalian Balance Epithelia: Key Roles for Phosphatidylinositol-3 Kinase, Mammalian Target of Rapamycin, and S6 Kinases in Preference to Calcium, Protein Kinase C, and Mitogen-Activated Protein Kinase. *The Journal of Neuroscience*. 21:570-580.

Moser, M., B. Nieswandt, S. Ussar, M. Pozgajova, and R. Fassler. 2008. Kindlin-3 is essential for integrin activation and platelet aggregation. *Nat Med*. 14:325-330.

Mould, A.P., J.A. Askari, and M.J. Humphries. 2000. Molecular basis of ligand recognition by integrin alpha 5beta 1. I. Specificity of ligand binding is determined by amino acid sequences in the second and third NH2-terminal repeats of the alpha subunit. *J Biol Chem*. 275:20324-20336.

Muller, U., D. Wang, S. Denda, J.J. Meneses, R.A. Pedersen, and L.F. Reichardt. 1997. Integrin alpha8beta1 is critically important for epithelial-mesenchymal interactions during kidney morphogenesis. *Cell*. 88:603-613.

Murakami, J., T. Nishida, and T. Otori. 1992. Coordinated appearance of beta 1 integrins and fibronectin during corneal wound healing. *J Lab Clin Med*. 120:86-93.

Nakagawa, T., T.S. Kim, N. Murai, T. Endo, F. Iguchi, I. Tateya, N. Yamamoto, Y. Naito, and J. Ito. 2003. A novel technique for inducing local inner ear damage. *Hear Res*. 176:122-127.

Niessen, C.M., M.H. van der Raaij-Helmer, E.H. Hulsman, R. van der Neut, M.F. Jonkman, and A. Sonnenberg. 1996. Deficiency of the integrin beta 4 subunit in junctional epidermolysis bullosa with pyloric atresia: consequences for hemidesmosome formation and adhesion properties. *J Cell Sci*. 109 (Pt 7):1695-1706.

Nishikawa, S., and F. Sasaki. 1996. Internalization of styryl dye FM1-43 in the hair cells of lateral line organs in Xenopus larvae. *J Histochem Cytochem*. 44:733-741.

O'Toole, T.E., Y. Katagiri, R.J. Faull, K. Peter, R. Tamura, V. Quaranta, J.C. Loftus, S.J. Shattil, and M.H. Ginsberg. 1994. Integrin cytoplasmic domains mediate inside-out signal transduction. *J Cell Biol*. 124:1047-1059.

Oesterle, E.C., T.T. Tsue, T.A. Reh, and E.W. Rubel. 1993. Hair-cell regeneration in organ cultures of the postnatal chicken inner ear. *Hear Res*. 70:85-108.

Palmer, E.L., C. Ruegg, R. Ferrando, R. Pytela, and D. Sheppard. 1993. Sequence and tissue distribution of the integrin alpha 9 subunit, a novel partner of beta 1 that is widely distributed in epithelia and muscle. *J Cell Biol*. 123:1289-1297.

Peltonen, J., H. Larjava, S. Jaakkola, H. Gralnick, S.K. Akiyama, S.S. Yamada, K.M. Yamada, and J. Uitto. 1989. Localization of integrin receptors for fibronectin, collagen, and laminin in human skin. Variable expression in basal and squamous cell carcinomas. *J Clin Invest*. 84:1916-1923.

Phillips, D.R., I.F. Charo, and R.M. Scarborough. 1991. GPIIb-IIIa: the responsive integrin. *Cell*. 65:359-362.

Pickles, J.O., S.D. Comis, and M.P. Osborne. 1984. Cross-links between stereocilia in the guinea pig organ of Corti, and their possible relation to sensory transduction. *Hear Res*. 15:103-112.

Postigo, A.A., J. Teixido, and F. Sanchez-Madrid. 1993. The alpha 4 beta 1/VCAM-1 adhesion pathway in physiology and disease. *Res Immunol*. 144:723-735; discussion 754-762.

Pulkkinen, L., V.E. Kimonis, Y. Xu, E.N. Spanou, W.H. McLean, and J. Uitto. 1997. Homozygous alpha6 integrin mutation in junctional epidermolysis bullosa with congenital duodenal atresia. *Hum Mol Genet*. 6:669-674.

Pytela, R., S. Suzuki, J. Breuss, D.J. Erle, and D. Sheppard. 1994. Polymerase Chain Reaction Cloning with Degenerate Primers: Homology-Based Identification of Adhesion Molecules. *Methods in Enzymology*. 245:420 - 451.

Reynolds, L.E., F.J. Conti, M. Lucas, R. Grose, S. Robinson, M. Stone, G. Saunders, C. Dickson, R.O. Hynes, A. Lacy-Hulbert, and K. Hodivala-Dilke. 2005. Accelerated re-epithelialization in beta3-integrin-deficient- mice is associated with enhanced TGF-beta1 signaling. *Nat Med*. 11:167-174.

Richardson, G.P., I.J. Russell, V.C. Duance, and A.J. Bailey. 1987. Polypeptide composition of the mammalian tectorial membrane. *Hear Res*. 25:45-60.

Rivolta, M.N., N. Grix, P. Lawlor, J.F. Ashmore, D.J. Jagger, and M.C. Holley. 1998. Auditory hair cell precursors immortalized from the mammalian inner ear. *Proc Biol Sci*. 265:1595-1603.

Roberson, D.F., C.S. Kreig, and E.W. Rubel. 1996. Light microscopic evidence that direct transdifferentiation gives rise to new hair cells in regenerating avian auditory epithelium. *Aud. Neurosci.* 2:195-205.

Roberson, D.F., P. Weisleder, P.S. Bohrer, and E.W. Rubel. 1992. Ongoing production of sensory cells in the vestibular epithelium of the chick. *Hear Res*. 57:166-174.

Rubel, E.W., L.A. Dew, and D.W. Roberson. 1995. Mammalian vestibular hair cell regeneration. *Science*. 267:701-707.

Ruegg, C., A.A. Postigo, E.E. Sikorski, E.C. Butcher, R. Pytela, and D.J. Erle. 1992. Role of integrin alpha 4 beta 7/alpha 4 beta P in lymphocyte adherence to fibronectin and VCAM-1 and in homotypic cell clustering. *J Cell Biol*. 117:179-189.

Ruoslahti, E., and M.D. Pierschbacher. 1987. New perspectives in cell adhesion: RGD and integrins. *Science*. 238:491-497.

Ryals, B.M., and E.W. Rubel. 1988. Hair cell regeneration after acoustic trauma in adult Coturnix quail. *Science*. 240:1774-1776.

Saito, K. 1983. Fine structure of the sensory epithelium of guinea-pig organ of Corti: subsurface cisternae and lamellar bodies in the outer hair cells. *Cell Tissue Res*. 229:467-481.

Schaapveld, R.Q., L. Borradori, D. Geerts, M.R. van Leusden, I. Kuikman, M.G. Nievers, C.M. Niessen, R.D. Steenbergen, P.J. Snijders, and A. Sonnenberg. 1998. Hemidesmosome formation is initiated by the beta4 integrin subunit, requires complex formation of beta4 and HD1/plectin, and involves a direct interaction between beta4 and the bullous pemphigoid antigen 180. *J Cell Biol*. 142:271-284.

Schlecker, C., M. Praetorius, D.E. Brough, R.G. Presler, Jr., C. Hsu, P.K. Plinkert, and H. Staecker. 2011. Selective atonal gene delivery improves balance function in a mouse model of vestibular disease. *Gene Ther*. 18:884-890.

Schwartz, M.A., and R.K. Assoian. 2001. Integrins and Cell Proliferation: Regulation of Cyclin-Dependent Kinases via Cytoplasmic Signalling Pathways. *Journal of Cell Science*. 114:2553-2560.

Seiler, C., and T. Nicolson. 1999. Defective calmodulin-dependent rapid apical endocytosis in zebrafish sensory hair cell mutants. *J Neurobiol*. 41:424-434.

Sekerkova, G., C.P. Richter, and J.R. Bartles. 2011. Roles of the espin actin-bundling proteins in the morphogenesis and stabilization of hair cell stereocilia revealed in CBA/CaJ congenic jerker mice. *PLoS Genet*. 7:e1002032.

Shang, T., T. Yednock, and A.C. Issekutz. 1999. alpha9beta1 integrin is expressed on human neutrophils and contributes to neutrophil migration through human lung and synovial fibroblast barriers. *J Leukoc Biol*. 66:809-816.

Singer, A.J., and R.A. Clark. 1999. Cutaneous wound healing. *N Engl J Med*. 341:738-746.
Sobkowicz, H.M., B.K. August, and S.M. Slapnick. 1996. Post-traumatic survival and recovery of the auditory sensory cells in culture. *Acta Otolaryngol*. 116:257-262.
Spinardi, L., Y.L. Ren, R. Sanders, and F.G. Giancotti. 1993. The beta 4 subunit cytoplasmic domain mediates the interaction of alpha 6 beta 4 integrin with the cytoskeleton of hemidesmosomes. *Mol Biol Cell*. 4:871-884.
Staecker, H., M. Praetorius, and D.E. Brough. 2011. Development of gene therapy for inner ear disease: Using bilateral vestibular hypofunction as a vehicle for translational research. *Hear Res*. 276:44-51.
Stepp, M.A., S. Spurr-Michaud, and I.K. Gipson. 1993. Integrins in the wounded and unwounded stratified squamous epithelium of the cornea. *Invest Ophthalmol Vis Sci*. 34:1829-1844.
Stepp, M.A., S. Spurr-Michaud, A. Tisdale, J. Elwell, and I.K. Gipson. 1990. Alpha 6 beta 4 integrin heterodimer is a component of hemidesmosomes. *Proc Natl Acad Sci U S A*. 87:8970-8974.
Stepp, M.A., and L. Zhu. 1997. Upregulation of alpha 9 integrin and tenascin during epithelial regeneration after debridement in the cornea. *J Histochem Cytochem*. 45:189-201.
Stepp, M.A., L. Zhu, and R. Cranfill. 1996. Changes in beta 4 integrin expression and localization in vivo in response to corneal epithelial injury. *Invest Ophthalmol Vis Sci*. 37:1593-1601.
Stone, J.S., and E.W. Rubel. 2000. Cellular studies of auditory hair cell regeneration in birds. *Proc Natl Acad Sci U S A*. 97:11714-11721.
Strominger, R.N., B.A. Bohne, and G.W. Harding. 1995. Regenerated nerve fibers in the noise-damaged chinchilla cochlea are not efferent. *Hear Res*. 92:52-62.
Stupack, D.G., and D.A. Cheresh. 2002. ECM remodeling regulates angiogenesis: endothelial integrins look for new ligands. *Sci STKE*. 2002:pe7.
Stupack, D.G., X.S. Puente, S. Boutsaboualoy, C.M. Storgard, and D.A. Cheresh. 2001. Apoptosis of adherent cells by recruitment of caspase-8 to unligated integrins. *J Cell Biol*. 155:459-470.
Summerford, C., J.S. Bartlett, and R.J. Samulski. 1999. AlphaVbeta5 integrin: a co-receptor for adeno-associated virus type 2 infection. *Nat Med*. 5:78-82.
Takagi, J., B.M. Petre, T. Walz, and T.A. Springer. 2002. Global conformational rearrangements in integrin extracellular domains in outside-in and inside-out signaling. *Cell*. 110:599-511.
Takeuchi, S., M. Ando, and A. Kakigi. 2000. Mechanism generating endocochlear potential: role played by intermediate cells in stria vascularis. *Biophys J*. 79:2572-2582.
Takumida, M. 2001. Functional morphology of the crista ampullaris: with special interests in sensory hairs and cupula: a review. *Biol Sci Space*. 15:356-358.
Tamura, R.N., C. Rozzo, L. Starr, J. Chambers, L.F. Reichardt, H.M. Cooper, and V. Quaranta. 1990. Epithelial integrin alpha 6 beta 4: complete primary structure of alpha 6 and variant forms of beta 4. *J Cell Biol*. 111:1593-1604.
Tasaki, I., and C.S. Spyropoulos. 1959. Stria vascularis as source of endocochlear potential. *J Neurophysiol*. 22:149-155.
Taylor, R.R., and A. Forge. 2005. Hair cell regeneration in sensory epithelia from the inner ear of a urodele amphibian. *J Comp Neurol*. 484:105-120.
Thornberry, N.A., and Y. Lazebnik. 1998. Caspases: enemies within. *Science*. 281:1312-1316.
Tilney, L.G., D.J. Derosier, and M.J. Mulroy. 1980. The organization of actin filaments in the stereocilia of cochlear hair cells. *J Cell Biol*. 86:244-259.

Tilney, M.S., L.G. Tilney, R.E. Stephens, C. Merte, D. Drenckhahn, D.A. Cotanche, and A. Bretscher. 1989. Preliminary biochemical characterization of the stereocilia and cuticular plate of hair cells of the chick cochlea. *J Cell Biol*. 109:1711-1723.

Towers, E.R., J.J. Kelly, R. Sud, J.E. Gale, and S.J. Dawson. 2011. Caprin-1 is a target of the deafness gene Pou4f3 and is recruited to stress granules in cochlear hair cells in response to ototoxic damage. *J Cell Sci*. 124:1145-1155.

Trikha, M., Z. Zhou, J.A. Nemeth, Q. Chen, C. Sharp, E. Emmell, J. Giles-Komar, and M.T. Nakada. 2004. CNTO 95, a fully human monoclonal antibody that inhibits alphav integrins, has antitumor and antiangiogenic activity in vivo. *Int J Cancer*. 110:326-335.

Tsuprun, V., and P. Santi. 1999. Ultrastructure and immunohistochemical identification of the extracellular matrix of the chinchilla cochlea. *Hear Res*. 129:35-49.

Tuckwell, D., D.A. Calderwood, L.J. Green, and M.J. Humphries. 1995. Integrin alpha 2 I-domain is a binding site for collagens. *J Cell Sci*. 108 (Pt 4):1629-1637.

Vahava, O., R. Morell, E.D. Lynch, S. Weiss, M.E. Kagan, N. Ahituv, J.E. Morrow, M.K. Lee, A.B. Skvorak, C.C. Morton, A. Blumenfeld, M. Frydman, T.B. Friedman, M.C. King, and K.B. Avraham. 1998. Mutation in transcription factor POU4F3 associated with inherited progressive hearing loss in humans. *Science*. 279:1950-1954.

van der Flier, A., and A. Sonnenberg. 2001. Function and interactions of integrins. *Cell Tissue Research*. 305:285-298.

Vinogradova, O., J. Vaynberg, X. Kong, T.A. Haas, E.F. Plow, and J. Qin. 2004. Membrane-mediated structural transitions at the cytoplasmic face during integrin activation. *Proc Natl Acad Sci U S A*. 101:4094-4099.

Vinogradova, O., A. Velyvis, A. Velyviene, B. Hu, T. Haas, E. Plow, and J. Qin. 2002. A structural mechanism of integrin alpha(IIb)beta(3) "inside-out" activation as regulated by its cytoplasmic face. *Cell*. 110:587-597.

Wang, G.P., I. Chatterjee, S.A. Batts, H.T. Wong, T.W. Gong, S.S. Gong, and Y. Raphael. 2010. Notch signaling and Atoh1 expression during hair cell regeneration in the mouse utricle. *Hear Res*. 267:61-70.

Wang, J.H. 2012. Pull and push: Talin activation for integrin signaling. *Cell Res*.

Warchol, M.E., and J.T. Corwin. 1996. Regenerative proliferation in organ cultures of the avian cochlea: identification of the initial progenitors and determination of the latency of the proliferative response. *J Neurosci*. 16:5466-5477.

Warchol, M.E., P.R. Lambert, B.J. Goldstein, A. Forge, and J.T. Corwin. 1993. Regenerative proliferation in inner ear sensory epithelia from adult guinea pigs and humans. *Science*. 259:1619-1622.

Wegener, K.L., A.W. Partridge, J. Han, A.R. Pickford, R.C. Liddington, M.H. Ginsberg, and I.D. Campbell. 2007. Structural basis of integrin activation by talin. *Cell*. 128:171-182.

Weil, D., S. Blanchard, J. Kaplan, P. Guilford, F. Gibson, J. Walsh, P. Mburu, A. Varela, J. Levilliers, M.D. Weston, and et al. 1995. Defective myosin VIIA gene responsible for Usher syndrome type 1B. *Nature*. 374:60-61.

Weisleder, P., and E.W. Rubel. 1993. Hair cell regeneration after streptomycin toxicity in the avian vestibular epithelium. *J Comp Neurol*. 331:97-110.

Werner, M., T.R. Van De Water, T. Andersson, G. Arnoldsson, and D. Berggren. 2012. Morphological and morphometric characteristics of vestibular hair cells and support cells in long term cultures of rat utricle explants. *Hear Res*. 283:107-116.

Werner, S., and R. Grose. 2003. Regulation of wound healing by growth factors and cytokines. *Physiol Rev*. 83:835-870.

Wersall, J. 1956. Studies on the structure and innervation of the sensory epithelium of the cristae ampulares in the guinea pig; a light and electron microscopic investigation. *Acta Otolaryngol Suppl*. 126:1-85.

Wickham, T.J., E.J. Filardo, D.A. Cheresh, and G.R. Nemerow. 1994. Integrin alpha v beta 5 selectively promotes adenovirus mediated cell membrane permeabilization. *J Cell Biol*. 127:257-264.

Wu, W.J., S.H. Sha, J.D. McLaren, K. Kawamoto, Y. Raphael, and J. Schacht. 2001. Aminoglycoside ototoxicity in adult CBA, C57BL and BALB mice and the Sprague-Dawley rat. *Hear Res*. 158:165-178.

Xiang, M., L. Gan, D. Li, Z.Y. Chen, L. Zhou, B.W. O'Malley, Jr., W. Klein, and J. Nathans. 1997. Essential role of POU-domain factor Brn-3c in auditory and vestibular hair cell development. *Proc Natl Acad Sci U S A*. 94:9445-9450.

Xiang, M., W.Q. Gao, T. Hasson, and J.J. Shin. 1998. Requirement for Brn-3c in maturation and survival, but not in fate determination of inner ear hair cells. *Development*. 125:3935-3946.

Xiong, J.P., T. Stehle, S.L. Goodman, and M.A. Arnaout. 2003. New insights into the structural basis of integrin activation. *Blood*. 102:1155-1159.

Xiong, J.P., T. Stehle, R. Zhang, A. Joachimiak, M. Frech, S.L. Goodman, and M.A. Arnaout. 2002. Crystal structure of the extracellular segment of integrin alpha Vbeta3 in complex with an Arg-Gly-Asp ligand. *Science*. 296:151-155.

Zahreddine, H., H. Zhang, M. Diogon, Y. Nagamatsu, and M. Labouesse. 2010. CRT-1/calreticulin and the E3 ligase EEL-1/HUWE1 control hemidesmosome maturation in C. elegans development. *Curr Biol*. 20:322-327.

Appendix

Gel Images for Restriction Digests of Degenerate PCR Products

The results of the restriction digests carried out on cloned degenerate RT-PCR products are illustrated by the images of agarose gels on which restriction digest products were run. As described in 2.8.4,these digests were used to identify which of the potentially detected amplicons were present in the PCR products for each degenerate primer pair. Table A-1 summarises the integrin subunits each restriction digest was intended to distinguish between, and the expected banding patterns for each restriction digest.

Figure	Integrins to be Identified	Restriction Digest	Expected Bands
A	αX, αM, αE & αD	BglI	αX/αD = 1766, 1763, 1318 & 206 bp bands
			αM/αE = 1447, 1318, 289, 286 & 206 bp bands
B	α1, α2, α10 & α11	BamHI	α1 = linearised plasmid, does not cut other amplicons/the vector
C	α1, α2, α10 & α11	XhoI	α2 = linearised plasmid, does not cut other amplicons/the vector
D	α1, α2, α10 & α11	RsaI	Cuts all amplicons once (linearises), except α10
E	α5, αV, αIIb & α8	HaeII	αV/αIIb = 1990, 906, 370 & 8 bp bands
			α5/ α8 = 1990, 476, 433, 370 & 8 bp bands
F	αV & αIIb	ApaI	Linearises if αV. αIIb = 3071 & 212 bp bands
F	α5, αV, αIIb & α8	PstI	Linearises if α8. α5 = 3142 & 138 bp bands
G	α3, α6 & α7	EcoRV	α7 = linearised plasmid, does not cut other amplicons/the vector
H	α6 & α3	TaqI	α3 = 1444, 576, 434, 82 & 80 bp bands
			α6 = 1444, 576, 434 & 165 bp bands
I	β1, β4 & β7	HindIII	β7 = linearised, does not cut other amplicons/the vector
J	β1, β4 & β7	TaqI	β1 = 1444, 576, 526, 434 & 377 bp bands
			β4 = 1444, 576, 526, 434 & 368 bp bands
			β7 = 1444, 576, 526, 434, 273 & 107 bp bands
K	β3, β5 & β6	TaqI	β3 = 1444, 576, 526, 434, 309 & 75 bp bands
			β5 = 1444, 576, 526, 434, 266 & 121 bp bands
			β7 = 1444, 576, 526, 434 & 381 bp bands
L	β2 & β8	NcoI	β2 = linearised, plasmid, β8 = 3108 & 255 bp bands

Table A-1 Restriction Digest Figures Reference Table

Summary of the restriction digests used to identify integrin amplicons from degenerate PCR products. References are provided for gel photo images which show representative results of each of the digests carried out.

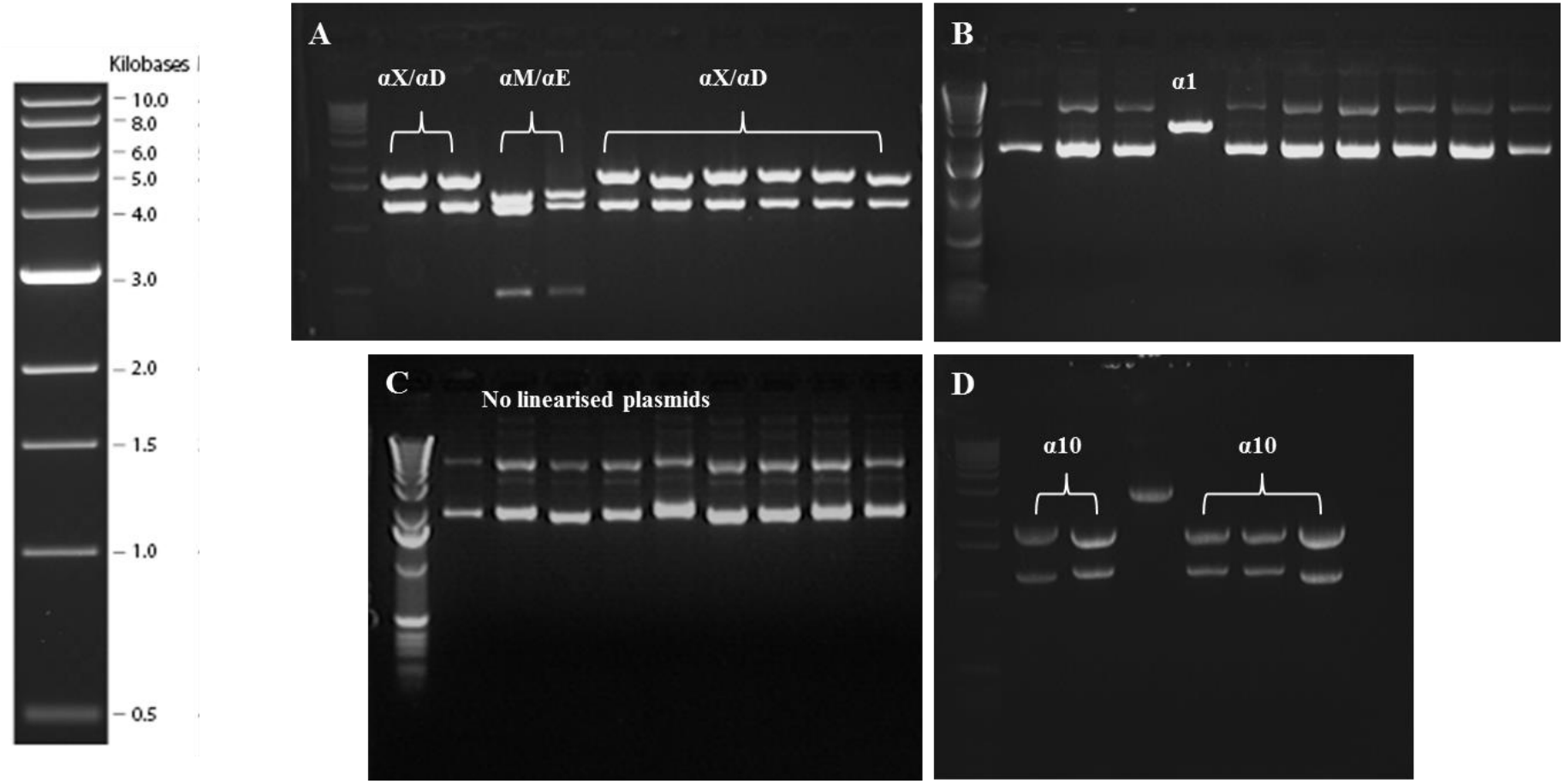

Figure A-1 Restriction Digests of Cloned Degenerate PCR Products

Images of restriction digest products run on an appropriate weight agarose gel. A 1kb DNA ladder (NEB) was used to determine the size of the digest products.

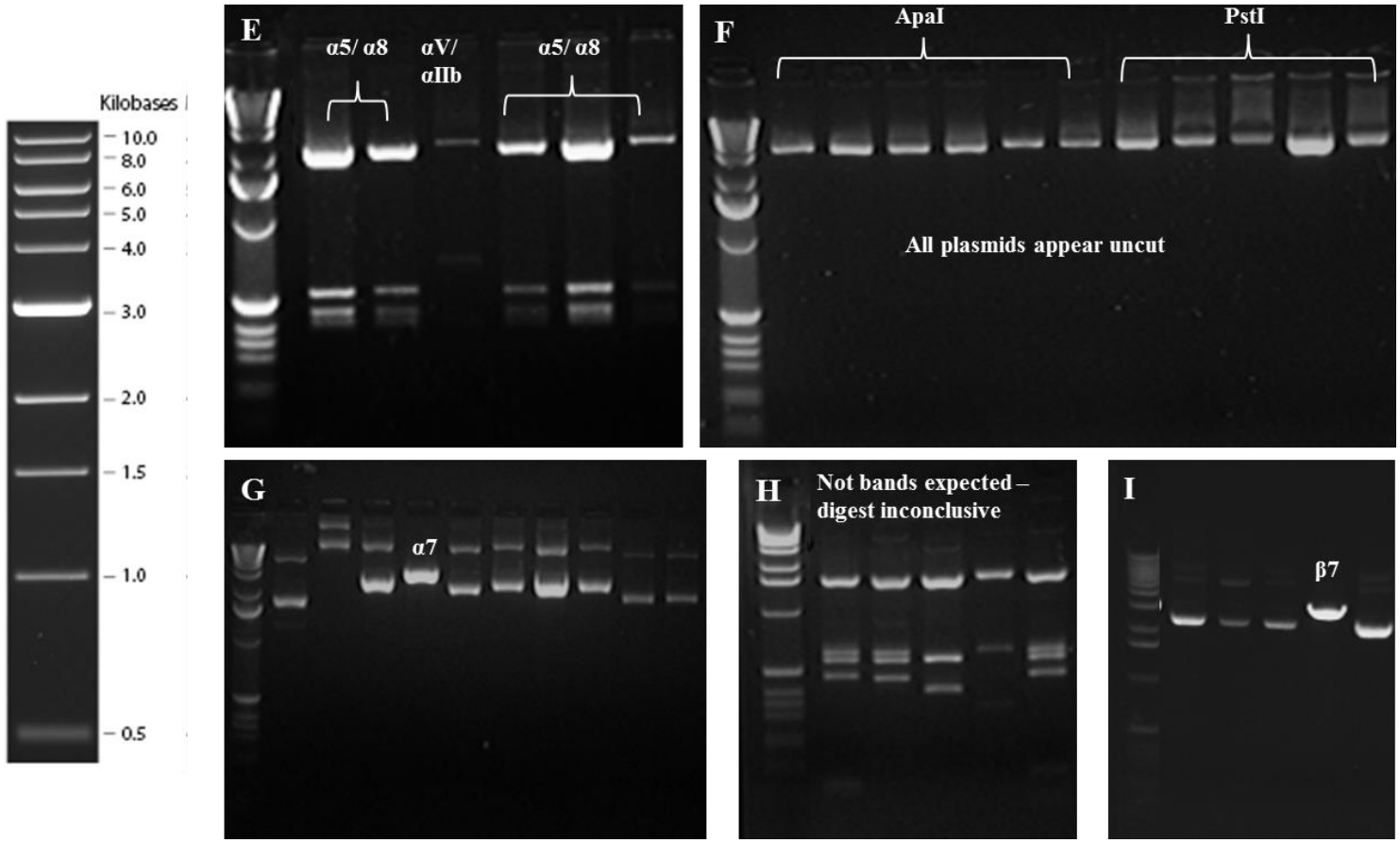

Figure A-2 Restriction Digests of Cloned Degenerate PCR Products

Images of restriction digest products run on an appropriate weight agarose gel. A 1kb DNA ladder (NEB) was used to determine the size of the digest products.

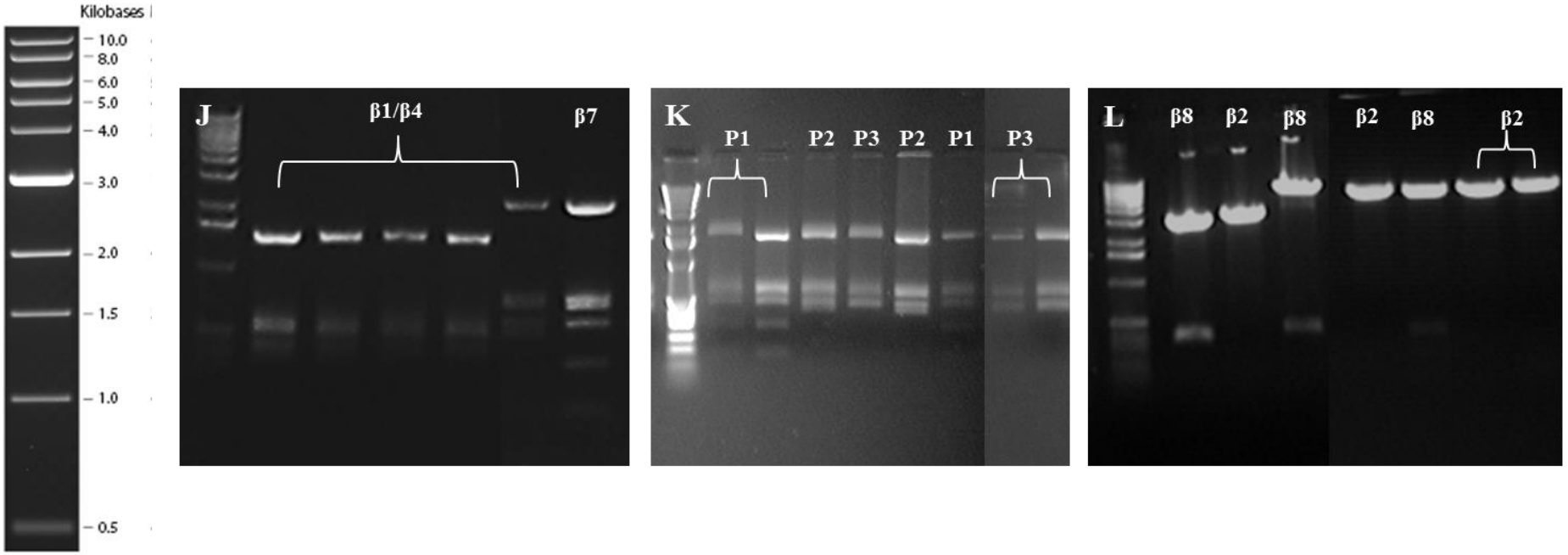

Figure A-3 Restriction Digests of Cloned Degenerate PCR Products

Images of restriction digest products run on an appropriate weight agarose gel. A 1kb DNA ladder (NEB) was used to determine the size of the digest products. (K) P1, P2 & P3 indicate the three different banding patterns detected in restriction digests produced – a sample of each was sent for DNA sequencing to confirm the identity of the integrin subunit amplified.

One-way ANOVA with Tukey's Test

The following data represents the full output generated by the GraphPad software used to analyse hair cell count data by one-way ANOVA with the post hoc Tukey's Test. The summary data from this statistical analysis is shown in table 4-1.

One-way Analysis of Variance (ANOVA)

The P value is 0.0012, considered very significant.
Variation among column means is significantly greater than expected by chance.

Tukey-Kramer Multiple Comparisons Test
If the value of q is greater than 4.508 then the P value is less than 0.05.

Comparison	Mean Difference	q		P value
Control (2 D) vs Gent (2 DPG)	2.530	3.239	ns	P>0.05
Control (2 D) vs Gent (14 DPG)	4.761	6.095	**	P<0.01
Control (2 D) vs Control (28 D)	1.080	1.312	ns	P>0.05
Control (2 D) vs Gent (28 DPG)	5.116	6.550	**	P<0.01
Gent (2 DPG) vs Gent (14 DPG)	2.231	3.498	ns	P>0.05
Gent (2 DPG) vs Control (28 D)	-1.449	2.104	ns	P>0.05
Gent (2 DPG) vs Gent (28 DPG)	2.586	4.055	ns	P>0.05
Gent (14 DPG) vs Control (28 D)	-3.681	5.343	*	P<0.05
Gent (14 DPG) vs Gent (28 DPG)	0.3551	0.5568	ns	P>0.05
Control (28 D) vs Gent (28 DPG)	4.036	5.858	**	P<0.01

Difference	Mean Difference	95% Confidence Interval From	To
Control (2 D) - Gent (2 DPG)	2.530	-0.9915	6.051
Control (2 D) - Gent (14 DPG)	4.761	1.240	8.282
Control (2 D) - Control (28 D)	1.080	-2.631	4.792
Control (2 D) - Gent (28 DPG)	5.116	1.595	8.638
Gent (2 DPG) - Gent (14 DPG)	2.231	-0.6440	5.106
Gent (2 DPG) - Control (28 D)	-1.449	-4.555	1.656
Gent (2 DPG) - Gent (28 DPG)	2.586	-0.2889	5.462
Gent (14 DPG) - Control (28 D)	-3.681	-6.786	-0.5751
Gent (14 DPG) - Gent (28 DPG)	0.3551	-2.520	3.230
Control (28 D) - Gent (28 DPG)	4.036	0.9302	7.141

Assumption test: Are the standard deviations of the groups equal?

ANOVA assumes that the data are sampled from populations with identical
SDs. This assumption is tested using the method of Bartlett.

Bartlett's test can only be performed when every column has at least five values.

Assumption test: Are the data sampled from Gaussian distributions?

ANOVA assumes that the data are sampled from populations that follow
Gaussian distributions. This assumption is tested using the method Kolmogorov and Smirnov:

Group	KS	P Value	Passed normality test?
Control (2 D)	Too few values to test.		
Gent (2 DPG)	Too few values to test.		
Gent (14 DPG)	Too few values to test.		
Control (28 D)	Too few values to test.		
Gent (28 DPG)	Too few values to test.		

Intermediate calculations. ANOVA table

Source of variation	Degrees of freedom	Sum of squares	Mean square
Treatments (between columns)	4	60.050	15.013
Residuals (within columns)	12	19.526	1.627
Total	16	79.576	

F = 9.226 =(MStreatment/MSresidual)

Summary of Data

Group	Number of Points	Mean	Standard Deviation	Standard Error of Mean	Median
Control (2 D)	2	5.988	0.6571	0.4646	5.988
Gent (2 DPG)	4	3.458	1.185	0.5927	2.946
Gent (14 DPG)	4	1.227	0.4745	0.2373	1.170
Control (28 D)	3	4.907	2.578	1.489	5.755
Gent (28 DPG)	4	0.8714	0.5501	0.2750	0.7836

Group	Minimum	Maximum	95% Confidence Interval From	To
Control (2 D)	5.523	6.452	0.08409	11.891
Gent (2 DPG)	2.714	5.224	1.572	5.344
Gent (14 DPG)	0.7252	1.842	0.4715	1.982
Control (28 D)	2.012	6.955	-1.498	11.313
Gent (28 DPG)	0.3275	1.591	-0.003768	1.747